University of Sunderland

Usage guidelines

SEAWATER INTAKE RISERS FOR
FLOATING LIQUEFIED NATURAL GAS (FLNG) VESSELS

IAN CRAIG

A doctoral report and portfolio submitted in partial fulfilment of the requirements
of the University of Sunderland for the degree of
Professional Doctorate

September 2018

CONFIDENTIALITY

This Doctoral Report and accompanying Portfolio contains information that is both commercially confidential and also commercially advantageous to the proprietary owner.

Consequently, this report and accompanying portfolio shall not be placed into public domain for a minimum of 5 years from the submission date and thereafter, only with express permission in writing from the Author who will seek the relevant approvals.

ABSTRACT

As the world energy demand increases, and the desire for cleaner fuels strengthens, a number of major oil and gas companies are developing Floating Liquefied Natural Gas (FLNG) vessels to harvest natural gas 'stranded' in reservoirs that have previously been considered too uneconomic to develop. A key requirement for this new generation of vessels is a high volume of low temperature seawater for process cooling.

The aim of this research is to investigate whether the concepts underpinning free hanging cantilever seawater intake risers used on Floating, Production, Storage and Offloading (FPSO) vessels can be extended to the design of seawater intake risers for FLNG vessels in order to reach and import colder seawater from depths greater than has so far been achieved with these systems. The research focusses on establishing the physical, mechanical and fatigue properties of a number of material elements under consideration for this application and then investigates a number of combinations to determine the optimum configuration for a hybrid deep seawater intake riser.

To demonstrate the strength and fatigue capabilities of the hybrid riser, the selected configuration is then subject to a more detailed analysis with consideration of a number of key aspects such as vessel motion, marine growth, vortex induced vibration, stability due to internal flow and excursion due to external fluid. A number of sensitivities are also performed with respect to riser damping, riser length, vessel size and geographical location. Additionally, the flow characteristics in terms of pressure loss and temperature gain are examined and a number of sensitivities performed to show that the cold seawater can be imported effectively. Finally, using published data for FLNG vessels currently under construction, an economic argument is presented to highlight the potential cost advantage of reaching and importing colder seawater by means of a deep seawater intake riser.

As a result of this research, the solution being presented offers a significant technological advantage for these systems in the field enabling high volumes of seawater to be imported from greater depths whilst accommodating the loads induced by the environmental conditions and minimising the loads induced into the hull of the vessel. Furthermore, the solution is based on the concepts of a field proven system, thereby limiting the risks associated with untested technological advancements. The findings of this research enable the process efficiencies of FLNG vessels to be greatly enhanced thus contributing to the more efficient

extraction of a cleaner fuel which, in a world with ever increasing energy demands, is critical to the global economy.

The novelty of the research is demonstrated by two successful patent applications, one in relation to the improved features of existing seawater intake riser systems and the other in relation to the use of multiple material elements for a hybrid seawater intake riser. Both patents have been examined and granted in five jurisdictions, namely, Europe, Japan, China. South Korea and the USA.

ACKNOWLEDGEMENTS

TABLE OF CONTENTS

LIST OF FIGURES

LIST OF TABLES

ABBREVIATIONS & ACRONYMS

API	American Petroleum Institute
ASME	American Society of Mechanical Engineers
ASTM	American Society for Testing and Materials
BTU	British Thermal Unit
CAPEX	Capital Expenditure
CI	Cast Iron
CO_2	Carbon Dioxide
DNV	Det Norske Veritas
DAF	Drag Amplification Factor
ESDU	Engineering Sciences Data Unit
FEA	Finite Element Analysis
FEED	Front End Engineering Design
FLNG	Floating Liquefied Natural Gas
FPSO	Floating Production Storage & Offloading
GFRP	Glass Fibre Reinforced Plastic
HDPE	High Density Polyethylene
LNG	Liquefied Natural Gas
MGPS	Marine Growth Protection System
MTPA	Million Tonnes per Annum
NB	Nominal Bore
OTEC	Ocean Thermal Energy Conversion
PE	Polyethylene
PPI	Plastics Pipe Institute
PTFE	Polytetrafluoroethylene
RAO	Response Amplitude Operators
RB	Rotational Bending
ROV	Remote Operated Vehicle
RPN	Risk Priority Number
SCG	Slow Crack Growth
SCR	Steel Catenary Riser
SDR	Standard Dimension Ratio
SDSS	Super Duplex Stainless Steel
SEN	Single Edge Notch
SG	Specific Gravity
SIF	Stress Intensification Factor

SPM	Single Point Mooring
SSHR	Self-Standing Hybrid Riser
SWIR	Seawater Intake Riser
SWLP	Seawater Lift Pump
tcf	Trillion Cubic Feet
TPA	Tonnes per Annum
TTR	Top Tensioned Riser
VIV	Vortex Induced Vibration
3PB	Three Point Bending

FOREWORD BY THE AUTHOR

Real-world: *"in, from or having to do with actual experience or practice, rather than being theoretical, idealistic or impractical"*

(Websters New World College Dictionaries, 2014)

During the course of this research, I have been asked on a number of occasions why I selected to undertake the professional doctorate programme to study the research subject as opposed to a traditional PhD. My summary response to this has been that the research subject, i.e. investigating the advancement of an existing system in the field, is a real-world problem and is more suited for study in the workplace. However, a more in-depth explanation is offered here.

According to Bourner et al (2001), the first professional doctorate was awarded in the USA in 1921 but, having gained its impetus in Australia during the 1980s (Maxwell, et al., 2004), it did not arrive in England until the early 1990s.

Around the same time, the UK governments white paper 'Realising our potential' (Office of Science and Technology (OST), 1993) expressed concern that "the traditional PhD does not always match up to the needs of a career outside research in academia….".

Research by Bourner et al (2001) shows that, since the early 1990s and the publication of the white paper, there has been a growth in professional doctorates in a wide range of subjects and goes on to identify twenty ways in which the professional doctorate differs from a traditional PhD, including;

- Integration between theory and practice, stating *"The PhD is concerned with making a contribution to theory per se whereas the professional doctorate is concerned with making a research-based contribution to practice"*:

- -Breadth of studies, stating *"… the universities stressed the greater breadth of professional doctorates compared with the traditional PhD"*

These differences are supported by the British School of Osteopathy (BSO, 2017);

"Because professional doctorates focus on professions and practices, the emphasis is not just on understanding a theoretical body of knowledge, but on the nature of practice itself, including required skills and awareness of necessary processes. By their nature, professional doctorates are broader and more holistic, blending knowledge and skills with professional competence".

Maxwell (2008) illustrates the professional doctorate concept as shown in Fig. I below.
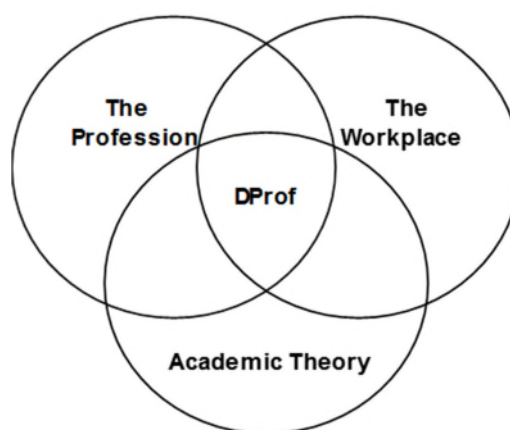
Fig. i: The Professional Doctorate Concept (Maxwell, 2008)

From a professional perspective, I began my career in 1979 as an apprentice draughtsman at the shipyards on the River Tyne and have since worked in the Offshore and Marine industries for in excess of 35 years gaining an HNC, HND and BEng(Hons). I have held various positions during the course of my career, progressing from draughtsman to design engineer to project engineer, then as project manager to technical director and currently as a consultant engineer. It is a career that has taken me to engineering offices, manufacturing facilities, fabrication yards and offshore installations worldwide. Furthermore, I have been registered as a professional engineer with the Engineering Council for nearly 20 years, firstly as an Incorporated Engineer and now as a Chartered Engineer. In summary, it is the only profession I have known and a profession in which I am demonstrably competent.

Within the workplace, I have been directly involved with the design and supply of the system that forms the subject of this research since circa 2002. During this time, I have acquired a wealth of experience with these systems ranging from preparation of project specifications with the client, component design and system analysis, project delivery, including inspection and testing, through to supervision of system installation offshore. I am currently engaged as a consultant by a leading supplier of these systems which I continue to work with on a daily basis. More recently, there has been interest from the stakeholders in a new generation of vessels as to whether these systems that are currently in operation, can be advanced to suit the increased functional requirements of this new generation of vessels. This presents a real-world problem from which the starting point is a known and proven existing system,

therefore, given my experience and daily involvement with these systems, the workplace is ideal position from which to address this problem.

It can be seen that, by applying academic theory to this real-world problem, the three constituent parts of the model in Fig. i are fulfilled making the professional doctorate (DProf) an ideal programme for this study, or as Lester (2004) describes it *"a vehicle for self-managed development as a leading professional taking forward an area of practice"* My Reflective Account of the Professional Doctorate Programme can be found in the accompanying Portfolio [Section 1.0].

Finally, as required by the professional doctorate programme specification (University of Sunderland, 2015), *"Collaboration with professional colleagues and the profession in the course of the studies and the conduct of the research is essential"*, therefore to clearly identify the work undertaken by the author and the work performed collaboratively, the introductory chapter includes a Thesis Outline which describes the content of each chapter and defines my contribution to the research.

CHAPTER 1.0

INTRODUCTION

1. INTRODUCTION

As the world energy demand increases, and the desire for cleaner fuels strengthens, a number of major oil and gas companies are developing Floating Liquefied Natural Gas (FLNG) vessels to harvest natural gas 'stranded' in reservoirs that have previously been considered too uneconomic to develop due to their geographical location in terms of water depth or distance from shore which makes the construction of an export pipeline and/or a receiving terminal prohibitively expensive. Several of these vessels are currently under construction, the first of which became operational in late 2016 (Petronas, 2016).

An FLNG vessel liquefies the harvested natural gas using the on-board processing facilities and then stores the liquefied natural gas (LNG) in tanks until such time that it can be offloaded and transported onshore via a sea going vessel. Liquefication is achieved by cooling the natural gas to approximately -162°C, which due to cost, complexity and efficiency of the process, requires large volumes of seawater and for which it is beneficial to reach and import water of as low temperature as practical from below sea level.

Similarly, Floating, Production, Storage and Offloading (FPSO) vessels have been used for many years to recover oil from remote reservoirs, or where the water depth makes a fixed leg platform impractical. To increase the efficiency of the utility and process systems on board these vessels, particularly in equatorial waters, they often have seawater intake risers (SWIR) installed enabling them to obtain colder and cleaner seawater from below sea level. The SWIR systems installed on FPSO vessels are field proven and as such, the same concept is under consideration for the importation of higher volumes of seawater from greater depths to meet the increased functional requirements of an FLNG vessel.

1.1. Research Aims & Objectives

The aim of this research project is to develop an innovative riser system for the high volume and low temperature seawater requirements of FLNG vessels, using prior knowledge and experience gained in the field from similar systems on FPSO vessels.

Specific objectives are to:

i) Perform a state-of-the-art review of systems currently operating in the field on FPSO vessels.

ii) Undertake a literature review to explore and summarise current work, in order to provide a context for this study, identify gaps in existing research, and demonstrate how this project relates to the challenges in the field.

iii) Design an appropriate research methodology to ensure that the research is accomplished in a systematic and reliable manner.

iv) Collect and critically appraise field data from systems in operation on FPSO vessels to evaluate if current system designs can be enhanced.

v) Identify the physical and mechanical properties of the materials under consideration so that the analysis of the proposed solution and its component parts return realistic and justifiable data.

vi) Determine the optimum configuration for the system and analyse the strength and fatigue capabilities, and the flow assurance characteristics, of the proposed solution.

vii) Compare the system costs against the efficiency gains, so that an economic argument can be made for the proposed solution.

1.2. State of the Art Technology

As the onshore, shallow water and more easily accessible oil reserves become depleted, oil companies are taking oil exploration and production to deeper and less accessible locations. This has seen an emergence of floating oil production installations, often referred to as FPSO (Floating Production Storage and Offloading) vessels, where the water depth makes a fixed leg platform impractical or where the reservoir location is too remote from a pipeline infrastructure. As the acronym suggests, an FPSO is a ship shape vessel that is moored to the seabed over the oil reservoir from which oil is delivered to the FPSO via flexible riser pipes. The oil is treated through an on-board process or 'production' facility and then stored in the tanks of the vessel. A sea going 'shuttle' tanker comes alongside and is connected to the FPSO, so that the stored oil can be transferred to the tanks of the shuttle tanker via an offloading system. The shuttle tanker then transports the oil onshore. Fig.1-1 shows the quantity and location of FPSO vessels currently in operation.

Fig.1-1: Worldwide Distribution of FPSO Vessels

(Nutter, 2014)

In many locations, particularly the warm water locations such as West Africa and Brazil, process engineers have found it beneficial to use cooler, cleaner and less oxygenated seawater from below sea level for the vessel's cooling, process, utility and water injection systems. This is achieved using a Seawater Intake Riser (SWIR) system, the utilization of which is fairly recent in the industry, with the first systems being installed circa. 2000. To date there are estimated to be approximately 150 FPSO vessels in operation of which approximately 60 are in deep water locations (Nutter, 2014) and likely to have a

SWIR system installed, the functional requirements of each being similar in terms of volumetric flow and depth from which water is imported. While the system design has been refined over the years, the basic concept of the systems has not changed indicating that the current technologies are proven and industry accepted.

A SWIR system is effectively a number of flexible pipe sections connected together and suspended from the underside of the FPSO at the seawater inlets in the form of a free-hanging cantilever, enabling the seawater pumps to draw seawater from a specified depth below sea level. Each SWIR system is bespoke to each installation, designed accordingly and subject to a hydrodynamic analysis which considers the vessel response characteristics, the field specific environmental conditions and the flexible hose string properties which can be optimised to suit the required configuration.

The length of each SWIR system is also field specific but to date, the maximum depths achieved have been approximately 120-130m. Consequently, the SWIR system cannot be installed at the onshore location during the vessel construction and must be deployed once the vessel has been moored over the reservoir, which creates a number of limitations to its design, most notably the weight restriction.

The SWIR system is generally deployed using a similar technique to a drill string, that is, the first flexible pipe section is held in a vertical position while the next section is lowered into place by the on-board vessel crane and connected to the first section. The two connected sections are then lowered into the water by the vessel crane until the second section can be held to enable a third section to be connected, and so on until the desired length is achieved. It is desirable to utilise the on-board vessel crane for the installation (and recovery for maintenance and inspection) of the system as opposed to an external heavy lift crane which can be expensive to charter. Therefore, the capacity of the on-board vessel crane can limit the installation weight of the SWIR which is a function of the diameter and quantity of flexible pipe sections.

A typical configuration for a SWIR system installed on an FPSO would consist of three 20"NB SWIR, 50-100m in length, with a flow rate of 2000m^3/hr per SWIR. Each SWIR is normally fitted with a coarse strainer at the lower end to prevent the ingress of debris or sea life similar to that shown in Fig.1-2.

A marine growth protection system (MGPS) is normally installed in the system which consists of a small-bore sodium hypochlorite line attached to the flexible

pipe sections, to enable sodium hypochlorite to be injected into the seawater via a dispersion ring fitted inside the strainer.
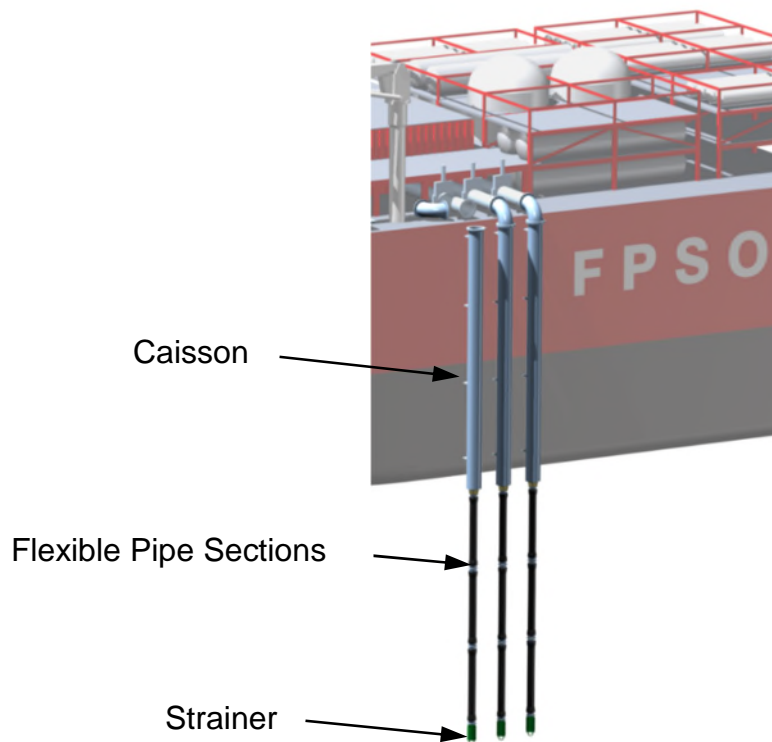
Fig.1-2: Typical SWIR System on an FPSO (External Caisson)

The main components that make up the Seawater Intake Risers can be summarised as follows:

- Riser Hang Off Arrangement (Riser Seat & Riser Head)
- Flexible hose Sections
- Strainer
- Sodium Hypochlorite Injection Line

A more detailed description of the components and systems variants is presented in the Portfolio [Section 3.0].

1.3. Research Question

The main research question explored in this work is as follows:

"Can the concepts underpinning seawater intake systems on FPSO vessels be extended to the design of intake systems with the high volume and low temperature seawater requirements of FLNG vessels?"

This can be divided into the following sub-questions:

- ❖ *What are the additional seawater requirements of FLNG vessels?*
- ❖ *What is the optimum configuration for the proposed solution?*
- ❖ *Does the proposed solution have sufficient strength and fatigue capabilities?*
- ❖ *Are the flow characteristics of the proposed solution fit for purpose?*
- ❖ *Is the proposed solution economically viable?*

1.4. Thesis Outline

In **Chapter 1**, the author uses his experience and knowledge as an active practitioner in the field to introduce the research subject, present the research aims and objectives, describe the state of the art technology associated with the system under consideration and establish the research question and sub-questions.

The Author undertakes a literature review in **Chapter 2** to explore and summarise the current work around the research subject in order to provide a context for this study, identify gaps in the existing research and demonstrate how this project relates to the challenges in the field.

A suitable research methodology is developed by the Author in **Chapter 3** that is used for the execution of the project to ensure that the that the research is accomplished in a cautious, systematic and reliable manner by using proven research techniques from existing literature.

The Author uses his knowledge of the research subject and contacts within the industry in **Chapter 4** to collect field data from existing SWIR systems currently operating in the field. The collected data is analysed by the Author to determine if there are any common themes and how the data may be used to improve or enhance the system. Using his knowledge of the research subject and the field

data obtained, the Author proposes a marine growth mitigation philosophy for consideration with the proposed solution.

In **Chapter 5**, the Author uses his knowledge and experience of the research subject to investigate and identify the physical and mechanical properties of the materials under consideration for the proposed solution. The Author uses his knowledge of bonded rubber flexible pipe design and construction to direct a third-party analyst (with appropriate software and experience) to generate a realistic FEA model so that the behaviour of the composite structure can be accurately predicted. To assist with this, the Author uses his knowledge of bonded rubber flexible pipe design to direct third party test facilities to perform material testing, which includes;

- compression testing of rubber compounds so that separate and realistic elastic modulus for tension and compression can be applied to the FEA model.
- cyclic testing of the reinforcement materials, from which, the Author performs a statistical analysis of the raw test data obtained so that usable SN data can be applied to realistically predict the service life of the composite structure.

The Author also investigates the use of thick walled HDPE pipes for water transportation, including the use and limitations of butt fusion welding for joining HDPE, and collates and compares relevant strength and fatigue data. For the raw test data obtained, the Author uses an industry recognised technique to perform a statistical analysis so that usable SN data can be applied to realistically predict the service life of the HDPE.

In **Chapter 6**, the Author uses his knowledge and experience of the research subject and Orcaflex software to investigate the mechanics of the riser concept under consideration. The Author investigates riser natural frequency and analyses multiple configurations of the concept to determine the optimum solution and then uses Orcaflex software to perform further analysis to determine the strength of the selected configuration and fatigue damage induced by waves and current. The effect that internal and external flow has on the riser is also investigated by the Author and sensitivity studies of the system are performed and compared with respect to riser damping, riser length, vessel size and geographical location. Additionally, the flow characteristics in terms of pressure loss and temperature gain are examined and a number of sensitivities performed to show that the cold seawater can be imported effectively.

Using his knowledge and experience from practice in **Chapter 7**, the Author reviews the potential redundancy requirements of the seawater intake system and perform an analysis of the potential failure modes of the proposed solution, the mitigation measures and the cost impact. The Author then uses his involvement with the tendering process of the three live FLNG projects to assess the cost advantage of the SWIR systems specified for each project which is then compared against the potential advantage of using the proposed solution on the same projects. This analysis is based on the Authors direct involvement with live projects and published literature to make an economic argument for the proposed solution.

1.5. Summary

This chapter has presented an introduction to the research subject, defined the aims and objectives of the study and addressed the first objective by performing a state-of-the-art review of systems currently operating in the field on FPSO vessels. The research question has been established, which has then been broken down into several sub-questions, and an outline of the thesis presented.

A literature review in the next chapter will address the second objective which is to explore and summarise current work in order to provide a context for this study, identify gaps in existing research, and demonstrate how this project relates to the challenges in the field

CHAPTER 2.0

LITERATURE REVIEW

2. LITERATURE REVIEW

2.1. Search Criteria

The following literature review was undertaken utilising a number sources with the following key words:

FLNG, Seawater, Intake, Riser, Cantilever, Aspirating, VIV

OnePetro is a unique library of technical documents and journal articles serving the oil and gas exploration and production industry with an advanced search function.

Offshore Engineer is an industry publication that provides a monthly update on Projects, Products and States of the Industry and has a digital website with a search function.

Discover is a site accessible through the University of Sunderland library services that can be used to search for good quality, academic information across all subject areas from academic sources such as journals, databases, reviews, magazines, and conference proceedings.

Google is an internet search engine that enables a generic internet search to be undertaken.

2.2. Natural Gas

The global demand for energy continues to increase and it is estimated that by the middle of this century, the increase could by as much as 80% from its level at 2000 (Shell Global, 2014).
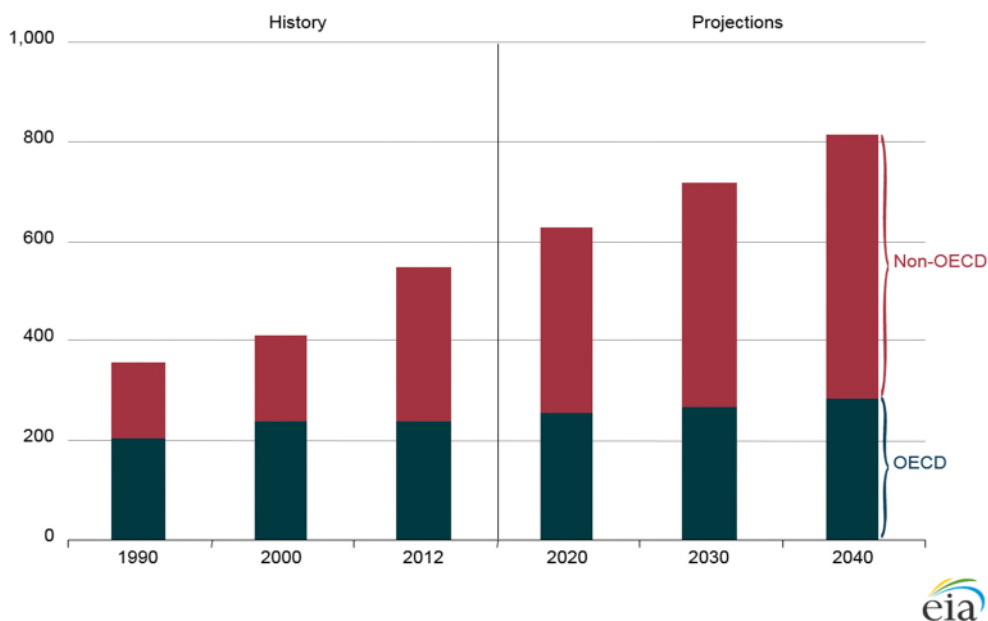
Fig.2-1: World energy consumption, 1990 – 2040

(EIA, 2016)

The US Energy Information Administration provide the projection shown in Fig.2-1 which suggests similar levels of growth in demand.

Similarly, due to increasing environmental concerns, cleaner fuels are continually being sought in order to reduce CO_2 emissions. Of the fossil fuels, Natural Gas is the cleanest burning, and therefore the most desirable, having 29% less CO_2 emissions than Oil and 44% less than Coal (Energy Information Administration, 1999).

The published natural gas reserves, excluding North America, at the beginning of 2008 were 6,230 trillion cubic feet (tcf) which represents approximately 55 years of global gas consumption at the current rate (Attanasi & Freeman, 2013), although it is forecast that the annual consumption will increase from 124tcf in 2015 to 177tcf by 2040 (Baraniuk, 2018). However, of these published reserves, approximately 17.5%, or 9.6 years' global demand, is categorised as Offshore Stranded Gas.

Stranded Gas is a term used to define offshore natural gas reserves that are considered uneconomic to develop due to their geographical location in terms of water depth or distance from shore which makes the construction of an export pipeline prohibitively expensive.

The graph in Fig.2-2 illustrates the quantity and locations of the known Stranded Gas Reserves.
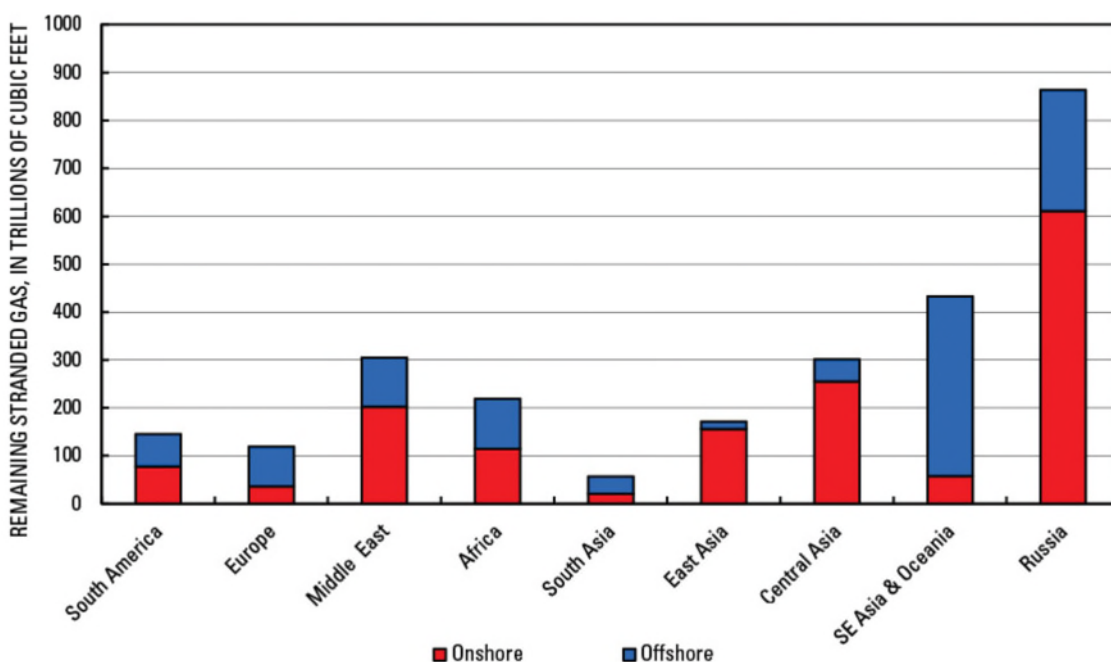
Fig.2-2: Bar Graph showing volume of Stranded Gas by Location
(Attanasi & Freeman, 2013)

2.3. FLNG Vessels

To meet the increasing global energy demand and the desire for cleaner fuels, a number of major oil and gas companies are developing Floating Liquefied Natural Gas (FLNG) vessels (Rangel, 2016), the function of which is to harvest offshore stranded gas, liquefy it using the on-board processing facilities and then store the liquefied natural gas (LNG) in tanks until such time that it can be offloaded and transported onshore via a sea going vessel.

Consequently, there is a significant Investment into FLNG vessels and the independent business information provider Visiongain estimate that in 2014 alone, the global FLNG market is valued at US$11.845 billion (OE, 2014) whereas Douglas-Westwood, a market research group to the Energy Sector, forecast that between 2014 to 2020 the total expenditure will be US$64.4 billion (OE, 2014) with a number of major oil and gas companies already developing Floating Liquefied Natural Gas (FLNG) vessels (Rangel, 2016).

One of the first FLNG vessels, currently under construction, is the Shell Prelude FLNG vessel, as illustrated in Fig.2-3, which expected to be producing gas by the end of 2018.

Fig.2-3: Prelude FLNG: Largest Ship Hull in the World
(Interesting Engineering, 2014)

In late 2016, the Petronas PFLNG1 vessel was the first FLNG vessel to produce gas, but due to its the shallow water location (approx. 75m), the

installation of a deep SWIR system was not possible and the system installed is typical of the SWIR installed on FPSO vessels, extending to approximately 50m below sea level. Fig.2-4 shows the installation of this system for which the author was the project manager and was on board to provide supervision during installation.

Fig.2-4: Installation of PFLNG1 Seawater Intake Riser

2.4. Ocean Thermoclines

A key requirement for the FLNG vessel processing facilities is the high volume of cooling water which is taken from the surrounding seawater, and the deeper the seawater the colder it is, as illustrated in Fig.2-5.

Typical Temperature Profiles
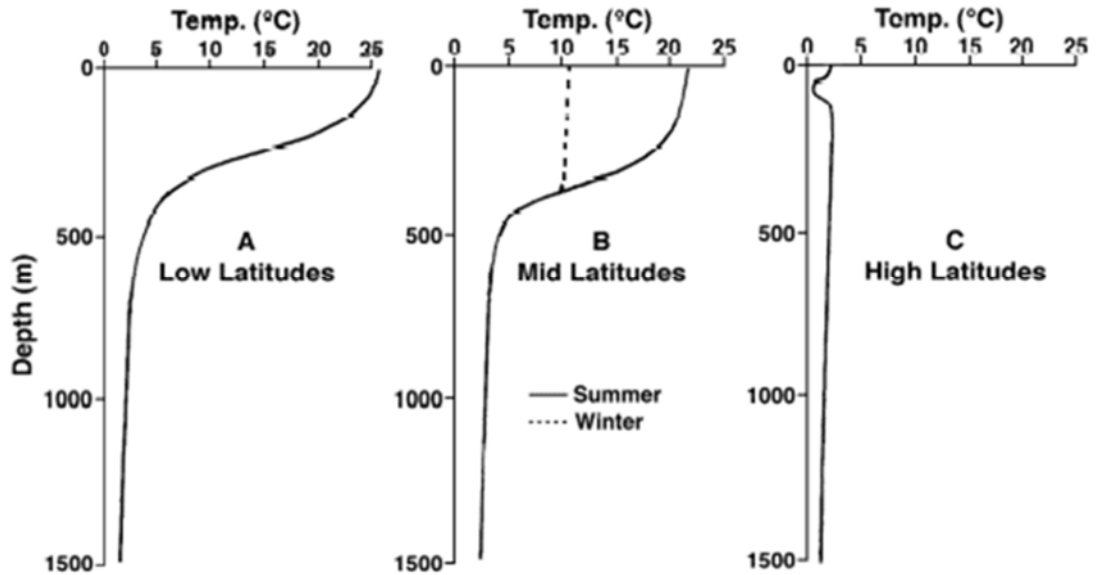
Fig.2-5: Typical Ocean Temperature Profiles

(Earthguide, 2013)

The low latitudes relate to equatorial bodies of water whereas the mid latitude relates to bodies of water between the tropics and the Arctic and Antarctic circles, the high latitudes are within the Arctic and Antarctic circles.

It can be seen that for the low and mid latitude profiles, there is a dramatic temperature transient between the depths of 100m-400m which is known as a thermocline. Energy from the sun is absorbed within the first few centimetres of the surface, but the turbulence created by the waves mixes and distributes the heat to form a fairly uniform temperature profile down to approximately 100m.

However, beyond the depth of this effect, the seawater temperature decreases rapidly and from the above graphs, it can be seen that at around 400m-500m depth, the temperature profile regains its uniformity. Consequently, obtaining seawater from below the thermocline is of interest to process engineers who estimate that a seawater temperature reduction of 15-20°C corresponds to 15-20% increased production capacity of the liquefication process (Pettersen, et al., 2013).

2.5. Riser Configurations

Traditionally, the term Riser is used in the offshore and marine industry to describe a conduit that connects an offshore installation to a subsea system and that is used to either deliver or export media to or from that installation or else for reservoir drilling and completion purposes. There are several types of rigid and flexible riser configurations commonly used in the industry, for example, a Top Tensioned Riser (TTR) where the rigid riser is held under tension by the platform, a Self-Standing Hybrid Riser (SSHR) which consists of a rigid vertical riser fixed to the seabed and connected to the platform by a flexible riser section or Steel Catenary Riser (SCR) which is made up from steel tube in a catenary configuration as shown in Fig.2-6.
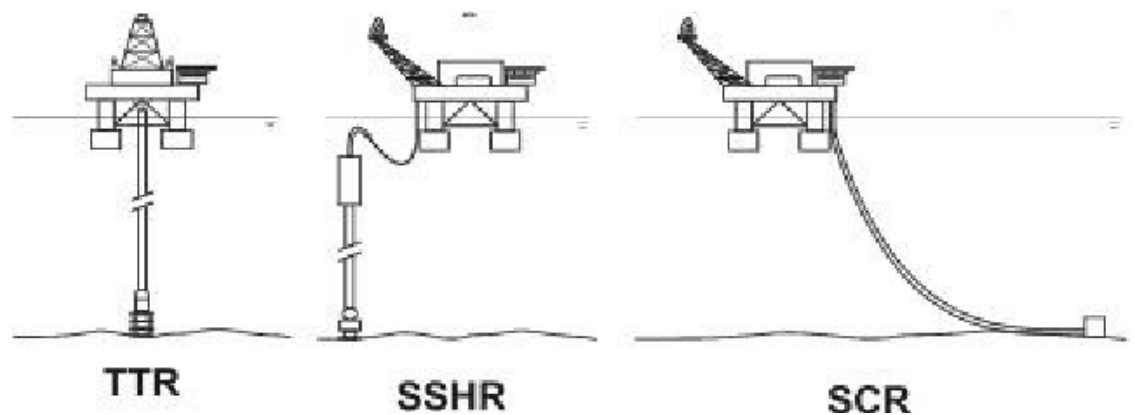
Fig.2-6: Riser Configurations

(Brandt, et al., 2008)

Similarly, there are several types of configuration used for flexible risers as shown in Fig.2-7.
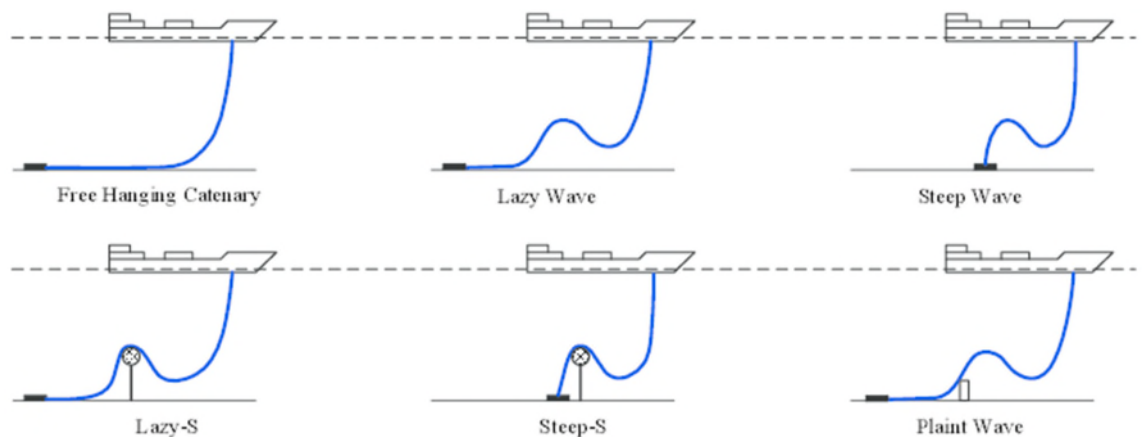
Fig.2-7: Flexible Riser Configurations

(Jahanshahi, 2013)

The term Riser has also been used to describe the system currently used for importation of seawater onto an offshore installation such as an FPSO, and as the Riser is not connected to the seabed, it can be more specifically described as a free hanging cantilever riser. As the riser is in a suction application, in the literature, this configuration is also referred to as an Aspirating Cantilever (Paidoussis & Tetreault-Friend, 2009).
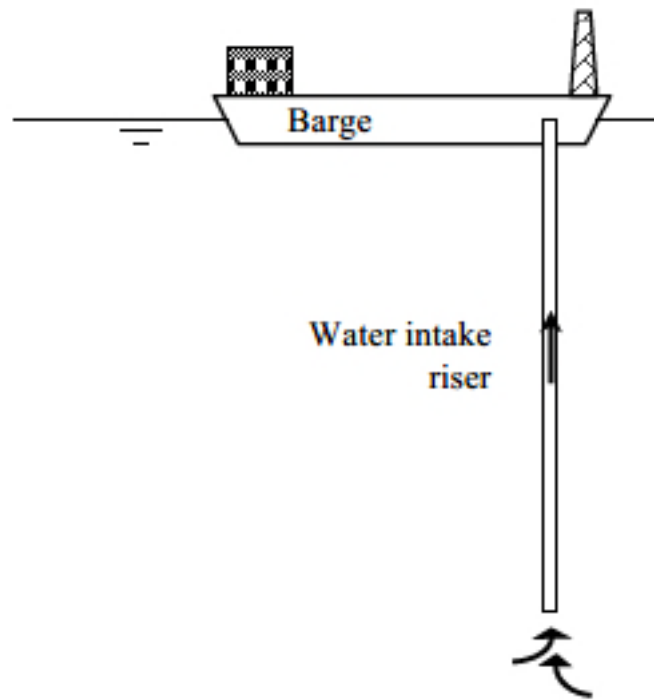
Fig.2-8: Free Hanging Aspirating Cantilever Riser
(Kuiper & Metrikine, 2005)

Other applications that adopt a free hanging 'aspirating' cantilever riser configuration include, Deep Water Mining Systems and Ocean Thermal Energy Conversion (OTEC) processes.
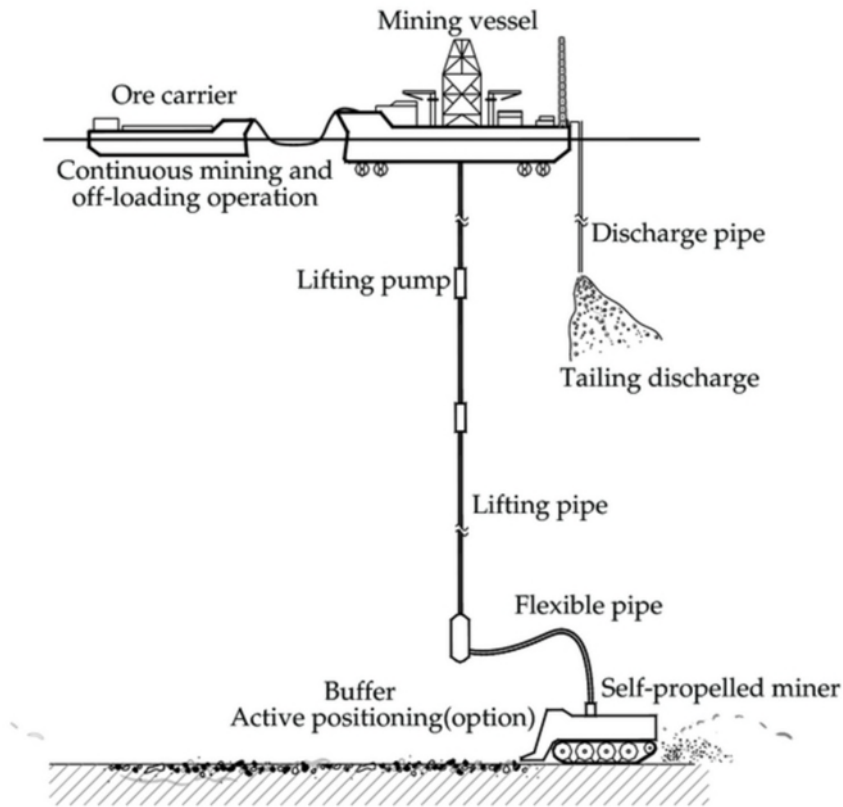
Fig.2-9: Deep Sea Mining System

(Lee, et al., 2012)

In a deep-sea mining system, a free hanging lifting pipe (or 'aspirating cantilever') is lowered to the sea floor where is transfers the mined products up to the mining vessel from which a free hanging cantilever discharge pipe returns the tailings to the mining site.
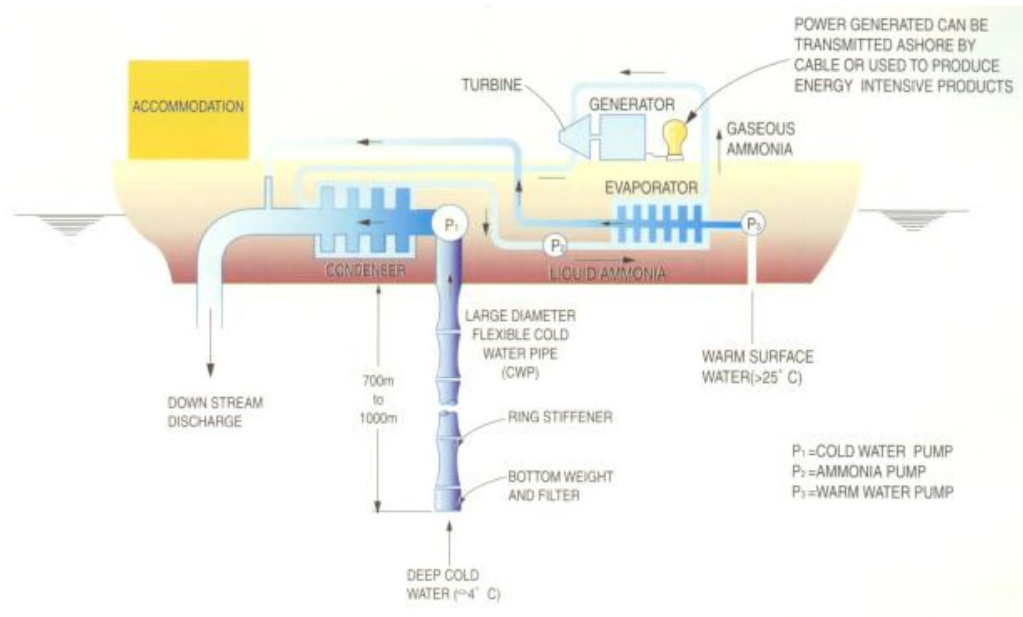
Fig.2-10:   OTEC System

(Brown, 1998)

An OTEC system uses thermodynamic principles such as the Rankine cycle to convert heat energy into mechanical work, by using the warm surface seawater to vaporize and expand a low boiling point fluid (e.g. ammonia) to drive an electricity producing generator. A free hanging 'aspirating' cantilever riser is used to obtain cold seawater which cools the vapour to a liquid form, creating a continuous generating cycle (Bharathan, 2011).

Although not 'aspirating', other applications that adopt a free hanging cantilever configuration include towing lines for geological sonar equipment and also drilling risers during installation or hang-off operations.
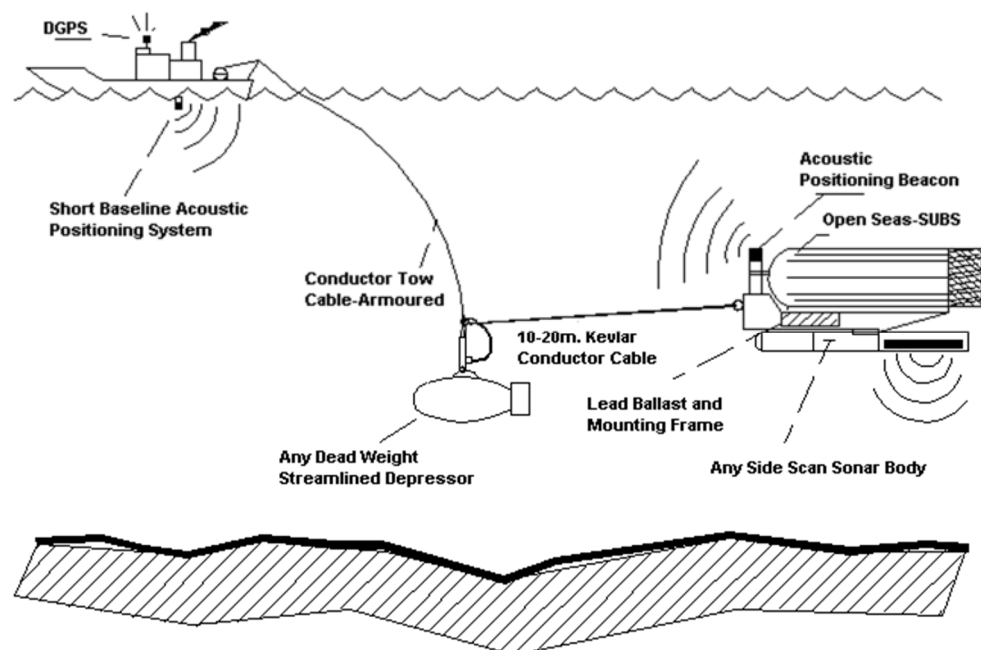
Fig.2-11:   Sonar Tow Cable Arrangement
(Open Seas Instrumentation, 2014)

Geological survey vessels suspend sonar equipment using a towing cable, which is also used to transmit data back to the vessel, creating a free hanging cantilever configuration.
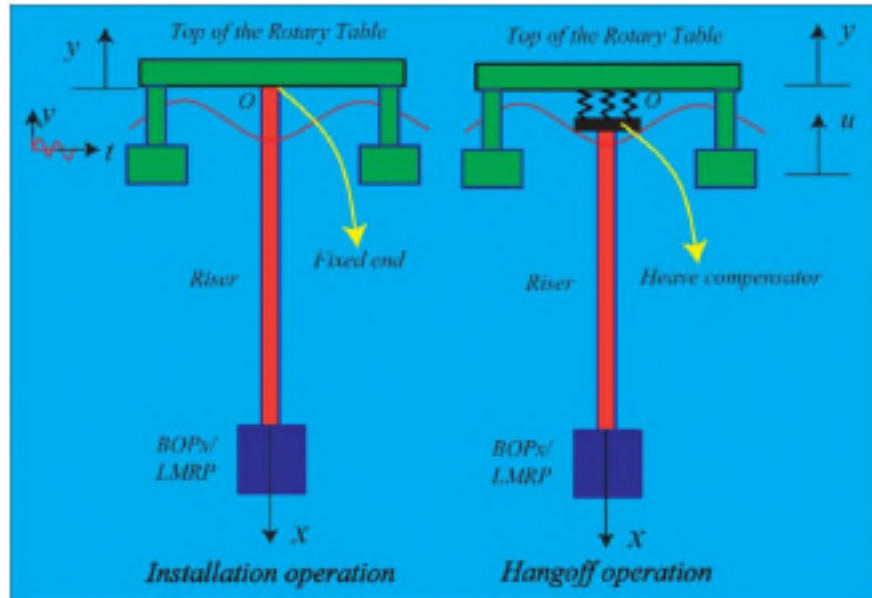
Fig.2-12:   Drilling Riser Installation and Hang Off

(Wang, et al., 2016)

During storm conditions, it is common practice for Drilling Platforms to suspend operations and hang-off the drilling riser from the underside of the vessel, which temporarily creates a free hanging cantilever riser, a configuration which is also created during the installation of the drilling riser equipment. Sparks (2007) reviews some of the problems related to hung-off risers but concludes that there are still some unanswered questions in relation to effect axial resonance has on the longitudinal behaviour.

2.6. Aspirating Cantilevers

Fluid flow inside a pipe can cause vibrations and instability and, using a garden hose for an analogy, it is known that when a flexible pipe with a free end discharges (or conveys) fluid the pipe end becomes unstable once a critical velocity is reached and has a seemingly erratic dynamic response. This phenomenon was observed as far back as 1885 by Brillouin (Bourrieres, 1939) with a more serious and remarkably accurate study being undertaken by Bourrieres in 1939 (Paidoussis, 2014). Ibrahim (2010) provides a comprehensive overview of the research into the mechanics of pipes conveying fluids and some of the related problems. His conclusions refer to Paidoussis (2005) who addresses three unresolved or partly resolved issues in this field, one of which is the stability of the aspirating cantilever pipe.

The stability of an aspirating cantilever has been studied for many years and is linked to the Feynman reverse sprinkler question of whether a lawn sprinkler

head would rotate if the water was sucked into the sprinkler head by the hose, and if so, in which direction. This issue is discussed by Paidoussis and Tetreault-Friend (2009) and Jenkins (2011) who make the comparison to the behaviour of an aspirating cantilever.

Paidoussis first attempted to understand the dynamics of an aspirating cantilever in 1966 (Giacobbi, et al., 2012) but it wasn't until the mid-eighties when a practical application in deep ocean mining prompted a further analytical study by Paidoussis and Luu (1985) which concluded that an aspirating cantilever loses stability at very low flow velocities, although, as explained by Giacobbi, et al (2012), at the time, practical experiments to validate this theory were unsuccessful.

Since then, numerous analytical and experimental studies have been undertaken by Paidoussis (1998) (1999), Kuiper and Metrikine (2005) (2008), Kuiper et al (2007), Giacobbi (2007) (2010), Giacobbi et al (2008) (2012) and Rinaldi (2009) in an attempt to fully understand the behaviour of the aspirating cantilever and the effect of various aspects such as the inlet profile, fluid flow at the inlet and effect of surrounding fluid damping.

More recently, Paidoussis (2014) consolidates the previous research and attempts to provide a contemporary theory on this phenomenon which he sums up by arguing that instability, in the form of flutter, does occur in aspirating pipes but energy is transferred at such a modest rate that it may be dissipated in the surrounding fluid making the critical flow velocity for the onset of flutter unattainable. Indeed, his concluding remark is:

"The conclusion therefore is that the last word on whether or how aspirating pipes flutter has not yet been written".

2.7. Vortex Induced Vibration

A phenomenon known as Vortex Induced Vibration (VIV) is another key aspect of Riser design. VIV occurs when a steady flow of air or water passes a slender structure and forms vortices downstream of the structure. If these vortices become regular and periodic and are close to the natural frequency of the structure, the structure can become excited leading to accelerated fatigue. This effect is famously demonstrated by the Tacoma Narrows bridge incident (Billah & Scanian, 1991).

The phenomena of VIV due to ocean waves and currents on submarine structures has been studied for many years the findings of which have been

incorporated into several industry recommended practices such as DNV-RP-F203 (DNV, 2009) Riser Interference, DNV-RP-F204 (DNV, 2010) Riser Fatigue, and DNV-RP-C205 Environmental Conditions and Environmental Loads (DNV, 2014).

Although the aforementioned literature is primarily concerned with fixed structures and risers supported at both ends, there having been several studies specifically related to the effect of VIV on a submerged flexible cantilever. Fujarra at el (2001) found that the VIV response of a cantilever behaves similar to that of an elastically restrained cylinder while experiments by Prastianto et al (2009) found that the response was strongly influenced by the 'reduced velocity' parameter. A further study by Prastianto (2009) investigated the effect cross flow currents on two free hanging cantilevers in tandem and found that, while the upstream cantilever behaved similar to a single cantilever, the response of the downstream cantilever was dependent the distance between the two cantilevers and uses the term Wake Induced Vibrations (WIV) to explain this effect. Meng and Kajiwara (2013) investigated the VIV response of a cantilever pipe in the form of a disconnected drilling riser discharging fluid into the sea and developed a mathematical model giving good agreement with previous work by Fujarra et al (2001). Blevins (2001) is a classic text on this subject and provides examples of how to estimate the VIV response of a typical marine riser and a towed hydrophone.

There are also a number of bespoke software packages available that are used to model the effects of VIV, among these are SHEAR7 developed by the MIT and VIVA distributed by JD Marine. Orcaflex software also includes tools for modelling VIV including two Wake Oscillator Models, namely the Milan model (Falco, et al., 1999) and the Iwans and Blevins model (Iwan & Blevins, 1974) , specifically selected by Orcina for Orcaflex through literature review and model testing.

2.8. Seawater Intake Risers for FLNG Vessels

A number of recent studies (Rogez, 2012) (Pettersen, et al., 2013) (Chaudhury & Chakkarapani, 2014) (Luppi, et al., 2014), have identified free hanging cantilever seawater intake risers (SWIR), similar to those currently employed on FPSO vessels as a means for FLNG vessels to obtain seawater from below the ocean surface.

A free hanging SWIR refers to a single pipe string that is connected to the underside of a vessel, not joined to another pipe string or structure, and is free to move independently.

An alternate concept to the free hanging SWIR has been considered for the Shell Prelude FLNG project (Pipeline & Gas Journal, 2014), whereby the SWIR are connected to one another and a central structure in a bundle, the conceptual feature of the bundle being to ensure that the individual risers do not collide with one another as shown in Fig.2-13.

FLNG Cooling Water Intake Risers:

- Eight 42"-risers delivering 50,000 m^3/h from 150m water depth
- One 30" central pipe to carry spacers
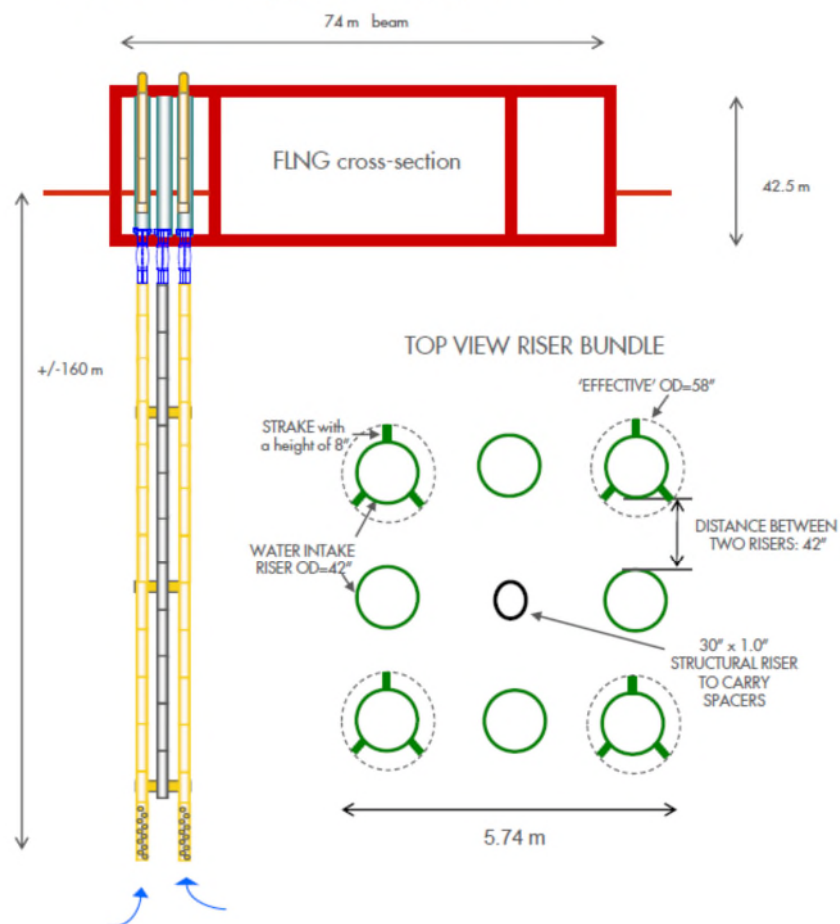
Fig.2-13: Shell Prelude FLNG Seawater Intake Riser (SWIR) Bundle (Project Connect, 2011)

Although there are no known bundled pipe configurations currently in operation, the SWIR bundle for the Shell Prelude FLNG (still under construction at time of writing), has been designed to deliver 50,000m^3/hr of sea water from a depth of approximately 160m (Pipeline & Gas Journal, 2014). During the Front

End Engineering Design (FEED) phase of this project, the author was involved with the SWIR system proposals and performed some preliminary analysis of the bundled concept for comparison against the single pipe concept. The author was invited to a workshop with the Shell personnel to present the findings of this comparative study, an extract of which is presented in the Portfolio [Section 11.0].

Pettersen et al (2013) have indicated that Statoil, the majority state owned Norwegian energy company, were in the process of technical qualification of water intake from 400-1000m. (Note: The author was engaged by a supplier of such systems as the principle researcher for a feasibility study commissioned by Statoil in respect of this requirement).

Chaudhury & Chakkarapani (2014) have investigated the FLNG seawater intake requirement and proposed a free hanging SWIR for this application, citing volume requirements of 30,000-60,000m^3/hour from depths of 500-1000ft as a basis for their study, whereas Luppi et al (2014) have also presented a free hanging SWIR proposal for an FLNG requiring 51,960m^3/hr from 139m depth.

Jung et al (2010) investigated the dynamics of a large diameter riser pipe (~3m diameter) to obtain water from a depth of 300m for an OTEC application and a common solution for both the FLNG and OTEC application was investigated by Rogez (2012), and which was partly sponsored by the Total (the French energy company), which studied free hanging risers of ~1.6m diameter for a volume requirement of 30,000m^3/hour from a depth of 800-900m.

Table 2-1 summarizes these most recent studies:

Study	Water Volume	Water Depth	FLNG or OTEC
Jung et al (2010)	Not specified	300m	OTEC
Shell Prelude FLNG (2011)	50,000m^3/hr	160m	FLNG
Rogez (2012)	30,000m^3/hr	800-900m	FLNG / OTEC
Pettersen et al (2013)	Not specified	400-1000m	FLNG
Chaudhury & Chakkarapani (2014)	30,000-60,000m^3/hr	500-1000ft (150-300m)	FLNG
Luppi et al (2014)	51,960m^3/hr	139m	FLNG

Table 2-1: Summary of subject studies

A typical configuration for a SWIR installed on an FPSO vessel would consist of 3-off free hanging SWIR risers, providing a total seawater flow rate of 6,000m^3/hr from depths of between 40-120m depth.

The diameter of the SWIR is general selected based on a maximum allowable velocity, for example, the Norwegian NORSOK standard P-001 (NORSOK, 2006) specifies a maximum velocity of 3 metres per second (m/s) for untreated seawater through carbon steel pipes. Similarly, the Plastic Pipe Institute (PPI, 2000) give a general design velocity of 5-10 feet per second (1.52 – 3.04 m/s) for water flow through plastic pipe, both of which are in line with the general design parameter accepted for sizing SWIR. Based on a velocity of 3m/s, a single 20"NB (500mm dia.) SWIR would accommodate a flow rate of approximately 2,100m^3/hr whereas a single 60"NB (1500mm dia) SWIR would accommodate a flow rate of 19,000m^3/hr.

Table 2-2 compares the typical seawater requirements of an FPSO and FLNG vessel which contextualises the scaling adaptation:

Requirement	FPSO	FLNG
Volumetric Flow Rate	6,000m^3/hr	50,000m^3/hr
Depth	<100m	>500m
Configuration	3 x Ø 500mm SWIR	3 x Ø 1500mm SWIR

Table 2-2: Comparison of Typical FPSO & FLNG SWIR Requirements

Recognising the increasing interest in large diameter SWIR, Cao et al (2015) performed some large scale model testing of an aspirating cantilever arrangement. A cantilever was submerged in water and subjected to varying frequencies of horizontal and vertical sinusoidal motion at the upper end to simulate vessel motion combined with various internal flow rates. The main findings were that the arrangement could be accurately modelled in current commercial software provided that the calibration is correct and offers drag coefficient and added mass coefficient ranges to achieve this. The tests also reveal a coupling effect between the SWIR and the entrained water when the subjected to vertical oscillations, increasing the tension into the connection point. The study concludes that the dynamic characteristics of a SWIR design needs to be optimised by balancing the effect of bending stiffness, length and tension. The study also presents the flow chart, shown in Fig.2-13, on how such a design might be achieved with consideration for the field and project

specifications on the strength, fatigue, interference and installation aspects of the SWIR.
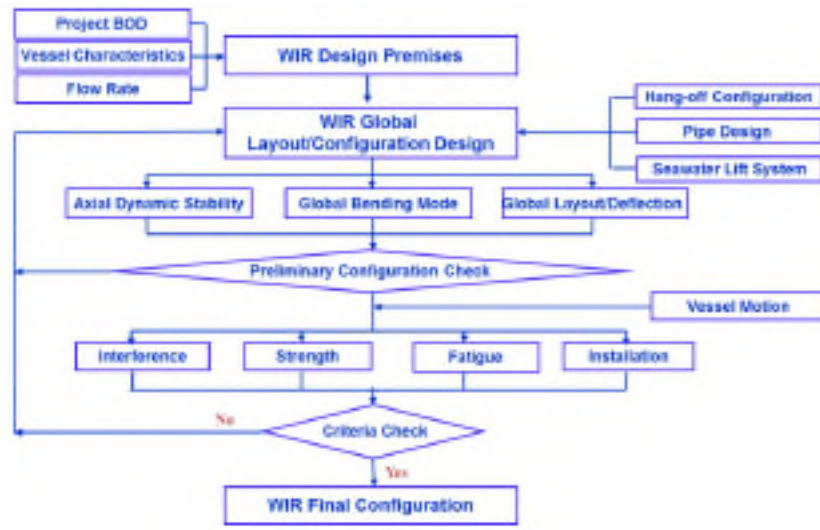
Fig.2-14:   SWIR Design Flow Chart

(Cao, et al., 2015)

2.9. Mooring Arrangements

Each of the above studies provide varying depths of detail with some focussing on different aspects. One consideration in developing a SWIR system is the possible interference with the vessel mooring lines. Like an FPSO, an FLNG vessel is a floating vessel that is moored to the seabed, and for which there are two main mooring concepts, namely Spread Moored and Turret Moored.

A Spread Moored vessel is one where the vessel is anchored by a four-group arrangement of mooring lines at the bow and stern and which enables the vessel to maintain a fixed orientation in global coordinates (Howell, et al., 2006), as shown in Fig.2-15.
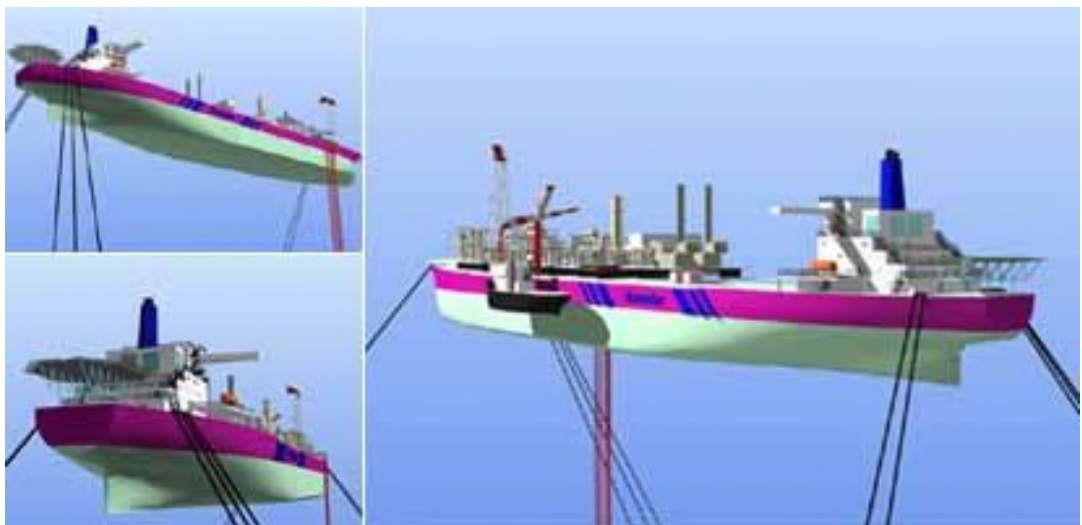
Fig.2-15:   Spread Moored Vessel

(Ice Engineering, 2009)

A Turret Moored FPSO is designed with a single point mooring (SPM) system consisting of a swivel stack which allows the vessel to rotate so that it can weathervane about the mooring system. Within the turret are rotary interfaces consisting of toroidal swivels which allow the reservoir fluids to be transferred from the turret across to the vessel whilst it is weathervaning.

This concept enables the FPSO to change its heading into the prevailing environmental conditions which reduces the load on the mooring and provides a more optimum offloading orientation (Howell, et al., 2006) as shown in Fig.2-16.
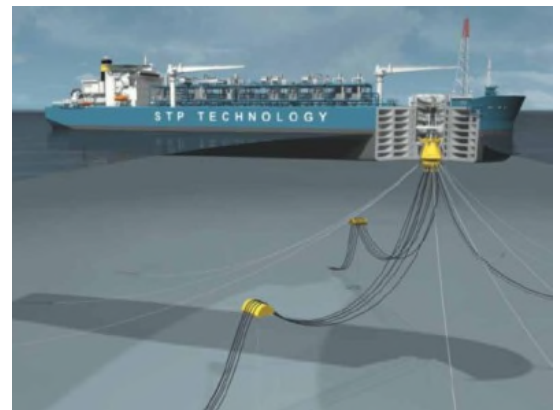
(Bluewater, 2013)   (Delft University of Technology, 2014)

Fig.2-16:   Turret Moored Vessels

The preference of one concept over another is dependent upon field specific considerations such as, vessel response, environmental conditions, subsea field architecture, layout of processing equipment on the vessel, and the cargo offloading requirements (Howell, et al., 2006).

Consequently, a free hanging SWIR connected to the hull of a turret moored vessel will rotate about the mooring lines and so consideration must be given to possible interference and given the potential length of the SWIR, the stability and behaviour of the SWIR under environmental forces of waves and current is a key aspect.

To date SWIR systems installed on FPSO vessels have been relatively short in length, (max 120m) and so potential interference with the mooring lines has not been problematic.

2.10. Material Selection

A key consideration for the SWIR design is the weight of the installed system in relation to the loads transferred into the floating structure and also installation capabilities and limitations. Both the stability and weight characteristics of a potential SWIR are directly linked to the material selection, and a number of options have been considered by the studies to date.

In the study by Luppi et al (2014), Rubber Hoses were selected for the FLNG vessel but given that the length under consideration in their study (139m) is not dissimilar to the lengths already in the field, the stability and weight characteristics are not dissimilar to systems already in the field.

The Shell Prelude FLNG has specified steel risers for its bundled concept (Project Connect, 2011), and steel risers are also considered in the study by Chaudbury & Chakkarapani (2014).

However, Jung et al (2010) and Rogez (2012) favour more lightweight materials of Glass Fibre Reinforced Plastic (GFRP) and High Density Polyethylene (HDPE) respectively, although it is noted that Jung et al (2010) discounts HDPE due to insufficient strength but this was on the assumption that a buffer (or ballast weight) of 5000tons would need to be added to the lower end of the riser.

The materials currently being considered for seawater intake systems can be broadly split into two material groups, namely, homogenous pipe elements and composite pipe elements.

A homogenous material is one which has uniform composition throughout and is generally isotropic in behaviour, that is, the material has the same property values in all directions, for example steel pipe and HDPE pipe.

A composite material is one constructed from two or more materials, each with different properties which, when combined, create a material with different characteristics from the component materials. These materials are generally anisotropic in behaviour, that is having different properties values in each direction, for example bonded rubber flexible pipes.

Thilmany (2009) identifies Olgierd Cecil Zienkiewicz as an early pioneer of the finite element method, a technique first developed in the 1940's for the numerical solution of complex problems in structural mechanics outside the scope of the classic beam theory. From the 1960's the finite method was extended to other engineering disciplines such as fluid dynamics, heat transfer, soil mechanics, wave propagation and electromagnetics. Until recently, finite

element analysis (FEA) had only been performed by highly qualified and specialised analysts. Due to the rapid advancement of computer technology over the last 20 years, high end FEA software packages are readily available and engineers can use personal computers to obtain accurate FEA results and, as reported in the Bloomberg Businessweek (Vance, 2013), FEA software packages such as ANSYS, allows engineers to test designs without building prototypes. Such is the confidence in FEA software, that some design codes accept FEA as proof of design. An example of this is the design code for Piping Components, ASME B31.3 (ASME, 2010), Para 304.7.2, which states that the pressure design of components can be substantiated by "(d) detailed stress analysis (e.g. finite element method)…".

FEA is achieved by breaking down a component into a number of small regular elements that can be more easily expressed by equations from physical theory. When combining the mathematical models of these elements into an overall model, approximate solutions of various physical problems such as stress analysis, heat transfer etc. can be obtained for more complex components (Lloyd's Register, 2014).

With modern FEA software, it is possible to model and analyse both isotropic and anisotropic structures although, generally, due to the characteristics of each component material and the interaction between them, a composite material is more complex to model.

Flexible pipes are an example of composite materials, and in the offshore and marine industry, these can be sub-divided into two main groups, Unbonded Flexible Pipes (API, 2017) and Bonded Flexible Pipes (API, 2018). In a bonded flexible pipe, the elastomers, textiles and steel reinforcements materials are bonded together by a vulcanisation process whereas in an unbonded flexible pipes, the composite material layers are usually independent of one another.

Due to the increasing demand of subsea equipment and the use of extra-long risers in deep water applications (Bahtui, 2008), there have been several studies related to the numerical analysis and FEA of unbonded flexible pipes in order to predict their in-service behaviour, including those by Bahtui (2008), Saevik (2011) and Rahmati et al (2017). One of the characterising features of these studies is how the boundary conditions for the contact, friction and slipping between the individual layers are addressed. Due to the bonding process through vulcanisation, this feature is not as relevant for bonded flexible pipes.

However, there have been several studies related to the numerical analysis of bonded flexible pipes such as that by McIver (1995), and more recently (Li, 2015) and Tonatto et al (2017) and although these studies address different applications, they do suggest that FEA modelling of bonded flexible pipes can provided realistic outputs.

2.11.   Marine Growth

Another factor in assessing the stability of the SWIR is the effect of Marine Growth attachment.

Marine growth is known to attach itself to subsea structures although the depth to which this occurs and the types of marine growth vary geographically. However, attached marine growth changes the surface roughness of the SWIR, increasing the drag factor, which can have a significant effect on the behaviour due to ocean currents (which also vary significantly with geographical location). With the exception of the study by Luppi et al (2014), who indicates the marine growth cases to be the most critical, the effect of marine growth has not been considered by the above studies.

Marine growth profiles vary from region to region but examples of profiles are shown in Tables 2-3 & 2-4.

Table 3 – Thickness of marine growth [a]

Water depth m	56° to 59° N mm	59° to 72° N mm
Above + 2	0	0
+2 to - 40	100	60
Under - 40	50	30

[a] The water depth refers to mean water level

The thickness of marine growth may be assumed to increase linearly to the given values over a period of 2 years after the structure has been placed in the sea.

Unless more accurate data are available, the roughness height may be taken as 20 mm below + 2 m. The roughness should be taken into consideration when determining the coefficients in Morison's equation.

Table 2-3:   NORSOK Marine Growth Profile

(NORSOK, 2007)

The NORSOK standard N-003 (NORSOK, 2007) provides the above marine growth profile to be used in the absence of any field specific data between the latitudes of 56° - 72°, primarily intended for the Norwegian Continental Shelf whereas the below marine growth profile is provided by Statoil (Statoil, 2010) for a field in offshore Tanzania.

Table 8.1	Marine growth profile estimates. Data are obtained from [8].			
Level	**Thickness**	**Roughness**	**Weight in air**	**Weight in seawater**
m below MSL	mm	mm	kg/m^2	kg/m^2
+2	100	50	9.5	3.2
-10	100	50	9.5	3.2
-65	25	18	2.4	0.8
Below -65	0	3	0.0	0.0

Table 2-4:   Marine Growth Profile

(Statoil, 2010)

The profile in Table 2-4 suggests that for deep water locations, marine growth is minimal below a certain depth, however further research in respect of marine growth, identifies the mesopelagic zone, often referred to as the 'twilight' zone and operationally defined as the region between 200m-1000m depth of the world's oceans. This region is characterised by increased hydrostatic pressure, diminished light, high inorganic nutrient concentrations and episodic food supply (Robinson, et al., 2010). A study by Robinson et al (2010) confirms that marine organisms do exist at these depths and describes the known ecology within the twilight zone.

Direct correspondence with the prime author of the study, Dr Carol Robinson, also describes how marine growth attachment may occur at these depths.:

"…there are definitely organisms living at 500m and most organisms prefer to be attached to something than floating around as often the thing they're attached to becomes a hot spot of food / prey. The first thing that will happen is the pipes will get covered with bacterial slime, then microzooplankton, then anything larger. I think as a rule of thumb, anything put into the sea will foul it just depends on the timescale. The timescale may also depend on which ocean at 500m since some waters have higher surface plankton productivity than others which rains down to the depths when the plankton die providing a food source for the organisms at depth."

This is further corroborated by Stanczak (2004), who describes that the growth of a biofilm can be such that it provides a foundation for the growth of seaweed, barnacles and other organisms although the conditions and substrate have a significant impact on the marine growth attachment. Lebret et al (2009) describes how biofilm attachment begins to occur within seconds or minutes of a substrate submersion into seawater.

Stanczak (2004) indicates certain types of biofilm favour a water velocity of 1m/s for maximum development but mussels will not occur at velocities greater than 2m/s whereas Powell and Webster (Powell & Webster, 2012) suggest that marine fouling is usually more prevalent in warm waters with velocities of less than 1m/s as, above this, most fouling organisms find it difficult to attach themselves.

- *Current Anti-Fouling Techniques*

The technique most commonly used to prevent marine growth from entering the SWIR and vessel is the injection of a sodium hypochlorite solution into the seawater at the intake points. The principle is that the sodium hypochlorite is injected and mixed into the seawater at the SWIR intake point to kill any marine organisms prior to entry to the on-board seawater system. A further sodium hypochlorite injection point is often provided at the pump intake to provide further anti-fouling measures. The sodium hypochlorite can be injected either as a continuous dose or a higher shock dose.

As the sodium hypochlorite solution has a specific gravity (SG) of 1.157 (Powell, 2002, p. 10) which is higher than the ~1.025 SG of seawater (ITTC, 2011), the limitation of this technique is that, when injected at the SWIR intake point, the sodium hypochlorite is only effective when the system is operational, i.e. drawing in seawater. When the system is idle, the injected sodium hypochlorite will gravitate downwards and out of the strainer. Furthermore, injecting sodium hypochlorite from within the strainer does not provide any anti-fouling benefits to the outer surface of the strainer.

The technique most commonly used to prevent marine growth from forming on the surfaces of the strainer and other metallic components is the use of polymeric foul-release paint systems such as PTFE based systems. Foul-release paint systems differ from anti-fouling paint systems in as much as they do not contain biocides, instead they provide the substrate with a slippery, low friction surface onto which fouling organisms have difficulty attaching (International Paint Ltd, 2010) and any which do will be loosely adhered and are removed from the surface by water movement or by its own weight (International Paint Ltd, 2014). Whereas the biocide within an anti-fouling paint system depletes over a relatively short period, the foul-release paint does not have a depletion rate, however, correspondence with a leading supplier of this type of paint system, International Paints, advise:

"We recommend an Intersleek re-coat every 5 years. This is due to micro-abrasions that occur on the surface of the coating caused by sand, grit or whatever else is floating about in the sea during the in-service period of the coating. These micro abrasions become more pronounced over time and will eventually compromise the anti-fouling performance of the coating…. A re-coat every 5 years ensures the highest possible performance of the Intersleek system."

As a part of this research, International Paints agreed to perform tests to see if their Intersleek paint system could be applied to flexible pipe elements. A series of samples were provided to International who performed a number of test applications, which yielded mixed results, details of which can be found in Portfolio [Section 5.0]. In summary, the tests indicated potential for this solution but further testing would be required before it could be applied with commercial confidence.

One of the most effective metallic materials to resist adherence of biofouling are high copper based alloys such as the 90-10 copper nickel alloy which has been used in several applications that benefit from its combined good corrosion and biofouling resistance properties including water intakes. The release of free copper ions provides this biofouling resistance although it is thought that the nature of the surface film also contributes to this effect (Powell & Webster, 2012, p. 26).

Harder and Lee (Harder & Lee, 2009) also indicate that the surface energy of the material can influence the bio-adhesion capability and make reference to the Baier Curve which provides a generalised relationship between the surface energy of a material and its resistance to bio-adhesion. Lines (2012) indicates that HDPE has a low surface energy and specifies a surface energy value consistent with weak bio-adhesion according to the Baier curve, and as such resists marine growth attachment.

2.12. Discussion

From the literature review, it can be seen that there is substantial interest in the development of FLNG vessels, although currently there is only one operational vessel and this is located in shallow water and so cannot benefit from a deep SWIR. Consequently, there is no empirical data for SWIR systems of the magnitude under consideration.

It can also be seen that a large proportion of the offshore stranded gas reserves are located in the warm water locations of South East Asia & Oceania, South America, Middle East and Africa where the thermoclines are more dramatic and therefore the ability to import seawater from greater depths more attractive.

There are a number of parallel fields that use a similar arrangement to that being considered for the SWIR, in particular the deep mining systems which were the catalyst behind the further research and interest in aspirating cantilevers. Similarly, the towed hydrophone and disconnected drilling riser arrangements have led to further research in regards to the VIV response of such arrangements. In general, the vast amount of literature on the subject and advances in simulation software have made it possible to predict the VIV response of riser systems with some accuracy.

The review of marine growth literature has shown that, over time, marine growth will attach itself to any object placed in seawater, regardless of the depth. It has highlighted the marine growth formation mechanism and the conditions which certain marine organisms prefer and also that the normal operating velocity of seawater through the seawater intake system makes it difficult for marine growth to attach. Marine growth is a known and considered design consideration, however, to date there is no known data available from the FPSO systems in the field to corroborate the design data or indicate how the current marine growth mitigation measures are performing.

The materials currently in the field, and also considered by the other studies in this research area, are predominantly; bonded rubber flexible pipes, HDPE pipe sections and steel pipe sections. Again, with advancements in FEA simulation software, it is possible to model both homogenous and composite structures with some degree of accuracy to predict the strength and fatigue capabilities of these systems.

Only limited research has been undertaken in the development of a suitable SWIR for FLNG vessels and, although the required volumetric flow rates are

similar, the detail of the research that has been undertaken is varied in terms of material selection, consideration of marine growth and the assessment of VIV.

With the exception of the Shell Prelude, the studies that have been undertaken each consider the single pipe concept, which has been proven on FPSO vessels. Although each of the studies considers the effect of VIV, except Luppi (2014) who acknowledges this, they conclude that the phenomenon is unlikely, while none of the studies address the instability of an SWIR due to internal aspirating flow nor the pressure loss or temperature gain characteristics of the SWIR.

It is also noted that none of the previous studies put forward an economic argument for the advantages of these systems, however, given the huge investment into the system currently under development for the Shell Prelude project and also the 'short' system installed on the PFLNG1 vessel, it would suggest that the stakeholders have evidence that these systems are economically advantageous.

Nonetheless, these studies are the emergent body of literature around the research subject to which this study will contribute.

2.13.   Summary

So, summarising the literature review, it can be seen that there are no deep water SWIR currently in operation therefore there is a knowledge gap around the optimum material selection and configuration for this application. From the limited number of studies that have been undertaken, it can be seen that there are also some knowledge gaps around the stability due to internal flow and the VIV response of an aspirating cantilever, both of which may have an impact on the fatigue life of the structure. It is also noted that the pressure loss and temperature gain characteristics of the SWIR have not previously been addressed nor has an economic argument been made as to the advantages of such a system.

As the bundled concept is as yet unproven in the field, this research will focus on the single pipe concept and will aim to address each of the above areas.

The next chapter will address the third objective which is to design an appropriate research methodology to ensure that the research is accomplished in a systematic and reliable manner

CHAPTER 3.0

METHODOLOGY

3. METHODOLOGY

3.1. Research Objectives

To design a research process that will fulfil the remaining research objectives identified in section 1.1, it is first necessary to address each objective individually.

iv) *Collect and critically appraise field data from systems in operation on FPSO vessels to evaluate if current system designs can be enhanced.*

To date, minimal installation or operational data has been collated for the SWIR systems currently installed in the field which may be due to a number of factors. For example, it is generally found that, due to the potential loss of production, offshore engineers are very resourceful and if a system develops a fault, they would endeavour to correct it without contacting the system supplier unless absolutely necessary. A further factor may be that, as the SWIR system is connected to the underside of the vessel, it is not readily visible to on-board personnel and the condition of the system can only be properly assessed during routine maintenance and inspection, making general observations of the system impractical.

Nonetheless, to ensure that the functionality and in-service life of the SWIR systems are maintained, it is essential that the systems are inspected periodically and any maintenance work undertaken where necessary. Furthermore, to create a body of knowledge around the performance and design of the SWIR, it is desirable that vessels operating with these systems undertake an inspection regime and document the findings to build up a statistical data base. This field data can then be used to re-evaluate the design of the systems in-service and will be invaluable in the design of new systems, ensuring the continued development and advancement of these systems.

v) Identify the physical and mechanical properties of the materials under consideration so that the analysis of the proposed solution and its component parts return realistic and justifiable data.

For the existing SWIR systems in the field, there are only a limited number of materials used for the flexible riser elements which suggests that they are proven in the field and accepted by the industry for this application. The physical and mechanical properties of these materials will be established and documented so that the analysis of the system in the subsequent objective can be undertaken with a confidence that the outputs are realistic and the results are justifiable, with the aim of demonstrating to the industry that these materials are suitable for SWIR installed on FLNG vessels.

vi) Determine the optimum configuration for the system and analyse the strength and fatigue capabilities, and the flow assurance characteristics, of the proposed solution.

The main geometrical differences between the systems installed in the field on FPSO vessels and those required to meet the increased functional demands of an FLNG vessel are the diameter and length of the SWIR, both of which will increase the weight of the system. The weight is an important consideration for a number of reasons such as the installation philosophy as, on FPSO vessels, the installation is normally achieved using an on-board crane therefore increasing the weight of the system would mean increasing the capacity of the on-board crane, installing a dedicated pull-in winch or else chartering a heavy lift vessel, all of which have financial implications. Once installed, the increased weight of the system induces greater loads into the hull of the vessel which means additional strengthening at the connection point. The increase in diameter and length of the system increases the area subject to drag forces induced by the ocean currents, which can also generate increased loads into the vessel. At the same time, the system needs to have a certain amount of weight to maintain stability in ocean currents so that the lower end excursions do not interfere with surrounding risers and structures. The increase in length will also affect the natural frequency and thus the stability of the SWIR due to vortex induced vibration from the ocean currents, which when excited, can cause fatigue damage and thus reduce the life of the SWIR.

The optimum SWIR in terms of materials and configuration, that will provide the best weight versus stability relationship needs to be established. Once this

optimum configuration has been identified, a more detailed analysis needs to be performed which will demonstrate to the industry that the strength and fatigue capabilities of the selected materials are adequate for the application.

The effect that aspirating flow has on the stability of the SWIR will also be investigated.

The increase in length of the SWIR will also increases the flow path of the seawater, therefore, in addition to the structural characteristics of the SWIR, the flow assurance characteristics in terms of pressure loss and temperature gain also need to be demonstrably suitable for the application.

vii) Compare the system costs against the efficiency gains, so that an economic argument can be made for the proposed solution.

The main purpose of the SWIR is to provide cooler seawater to the process facilities and thus improve the efficiency of the production plant for which the stakeholders of these vessels need to have evidence that the efficiency gains from these systems outweigh the cost to supply, install and maintain them. Therefore, using available data, an economic argument needs to be made to this effect.

3.2. Research Design

3.2.1. Research Approach

The selected research approach is one of mixed methods, utilising both qualitative and quantitative approaches.

The type of field data to be collated is expected to be qualitative in nature in the form of reports containing observations and photographs as well as subjective opinion from the responsible personnel. Therefore, a qualitative evaluation is the selected approach for this element of the research. The purpose of the evaluation is to determine the technical and operational implications of the collected data and how this may be applied to the improvement of the system. As Robson (2002, p. 205) suggests, "Evaluation is often concerned not only with assessing the worth or value, but also with seeking to assist in the improvement of whatever is being evaluated".

Robson (2002, p. 207) goes on to list some of the purposes of evaluation research, such as:

- To find out what the client needs are
- To improve the innovation
- To assess the outcome of the innovation
- To find out how the innovation is operating
- To assess the efficiency of the innovation
- To understand why the innovation works (or doesn't work)

The other objectives will take the form of a quantitative study. The research is expected to numerically determine the physical and mechanical properties of materials and if they can accommodate the loads induced into them by the systems, in terms of terms of strength and fatigue. Likewise, the flow assurance characteristics will be quantifiably established as will the economic argument. The selected approach for these objectives will use the scientific method, which as suggested by Marczyk (2005, p. 5) is characterised by the elements:

- Empirical approach
- Observations
- Questions
- Hypotheses
- Experiments
- Analyses
- Conclusions
- Replication

3.2.2. Research Methods

Whereas a traditional survey may appear to be the obvious method for collecting field data, it is unlikely that a survey in this instance would be effective. Instead, the data collection will follow the form of Field Research. Schatzman and Strauss describe the field researcher as "… a methodological pragmatist. He sees any method of enquiry as a system of strategies and

operations designed – at any time – for getting answers to certain questions about event which interest him." (Schatzman & Strauss, 1973, p. 7).

Using a list of systems supplied into the field the objective is to firstly identify the Maintenance Supervisor on duty during the relevant activities and contact them directly via e-mail with a request to provide any reports or field data relating to the SWIR. It is envisaged that direct contact as such will enable a dialogue to be established. It is anticipated that the Field Research will form a continuous process during the course of the project, as and when personnel are identified or are available for contact.

A documentary analysis will be undertaken to investigate the materials considered for the SWIR system and examine the strength and fatigue characteristics when used in a submerged dynamic application. Various data sources will be investigated, however, Blaxter et al (2001, p. 208) highlight two key points in documentary analysis, which are that, documents cannot be taken at face value as they are artificial and partial accounts which need to be critically assessed for research purposes and, much of the significance of documents is revealed when they are considered in relation to one another through comparative analysis. Depending upon the availability of data for the materials under consideration, physical testing of materials may also form part of the research which would also align with the Scientific Method

Due to the scale of the system under consideration, prototype testing is impractical therefore computer simulation of the system is the selected methodology for the strength and fatigue assessment. This element of research would be reiterative and would form the experiment part of the Scientific Method.

3.2.3. Data Collection Tools

Having established contact with the relevant personnel in the field, it is anticipated that direct contact as such will enable a dialogue to be established which can then be focussed on areas of interest and which may yield otherwise unrequested data. Additionally, pending on time zones and availability, telephone interviews may be established. This technique is based around an unstructured interview which is described as "The interviewer has a general area of interest and concern but lets the conversation develop within this area. It can be completely informal" (Robson, 2002, p. 270). Burgess (1990, p. 102)

suggests that Field Researchers prefer this strategy as it gives informants the opportunity to develop their responses outside of a structured format.

The data will be recorded using a Field Notes pro-forma, Burgess (1990) refers to these as Substantive Fieldnotes which "consist of a continuous record of situations, events and conversations in which the research participates" (Burgess, 1990, p. 167). It is anticipated that the Field Research will form a continuous process during the course of the project, as and when personnel are identified or are available for contact.

The characteristics of the selected materials will be recorded from the documentary analysis and, if data is unavailable, it may be necessary to perform physical testing or else further modelling with the use of an FEA software package.

Orcaflex (Orcina, 2014) is a hydrodynamic software package based upon the finite element method and will be used for the computer simulation. This package enables a flexible pipe system to be modelled with consideration given to environmental data, vessel response characteristics and the physical properties of the SWIR to provide predicted behaviour of the system. Other aspects of the system that can modelled and investigated are the effects of marine growth and the phenomena of vortex induced vibration (VIV).

3.2.4. Data Analysis

The data harvested from the field research will be subject to a thematic analysis which Boyatzis (1998, p. vii) describes as a process of "encoding qualitative information". A thematic analysis requires that the data is coded into relevant themes and cross referenced where applicable. Each theme can then be analysed and evaluated and the findings fed into the relevant aspect of the second objective.

The outputs from the computer simulation will be subject to a documentary analysis and will be cross-referenced with the industry standard recommended practices to determine if the strength and fatigue limits of the selected materials are acceptable.

3.3. Summary

In summary, the research methodology for the collection and analysis of field data will be a qualitative evaluation from a field research method using a form of unstructured interview and field notes as the data collection tools which will then be evaluated using thematic analysis.

The remaining objectives will be a quantitative approach using the scientific method consisting of computer simulation and documentary analysis. The outputs will be cross referenced with relevant industry recommended practices for comparison.

The methodology chosen for this research project can be illustrated as follows:
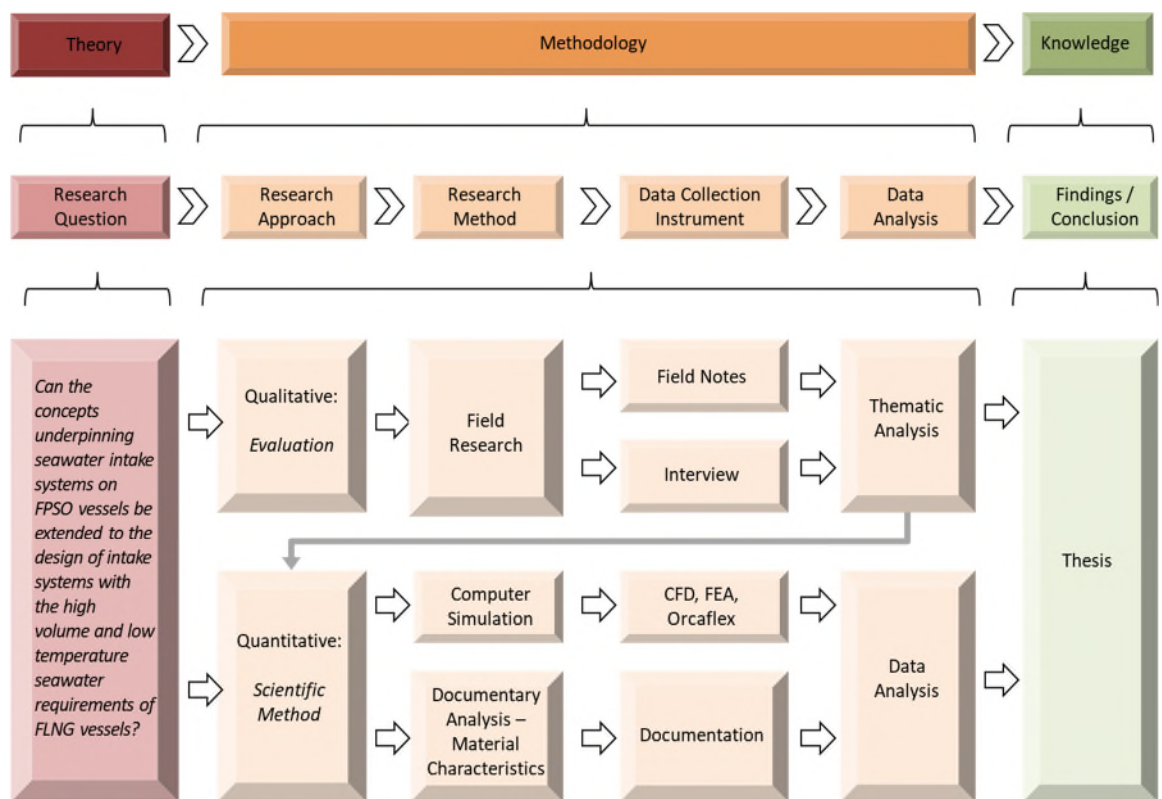
Fig.3-1: Representation of the Research Design
(Developed by Ian Craig 2015.)

The next chapter will address the fourth objective which is to collect and critically appraise field data from systems in operation on FPSO vessels to evaluate if current system designs can be enhanced

CHAPTER 4.0

FIELD DATA & MARINE GROWTH MITIGATION

4. FIELD DATA & MARINE GROWTH MITIGATION

The value of field data from existing Seawater Intake Risers (SWIR) in the field is important to create a body of knowledge around the performance and design of these systems, not only to re-evaluate the design of the systems in-service but also for the design of new systems, ensuring their continued development and advancement of these systems.

As described in Section 3.2.3, the selected data collection tool for the field data is the use of Field Notes to record any data received from the field through established contact with the relevant personnel.

The vessels targeted, the introductory e-mail and the responses received are presented in the Portfolio [Section 4.0].

Any field data received has been recorded on a field note pro-forma, which are also presented in the Portfolio [Section 4.0], and from which the main themes are summarised and the key words identified to enable a thematic analysis of the data.

4.1. Field Note Summary

Each of the keywords from the Field Notes was assigned one of the following main themes:

- Flexible Element
- Corrosion
- Marine Growth
- Maintenance

and the data summarised as follows;

Keyword	Theme	Vessel			
		Golfinho	MV23	Kizomba	MV21
Rubber Hose Damage	Flexible Element	X			
HDPE	Flexible Element	X			
Ballast Weight	Corrosion	X			
Failure	Corrosion	X			
Pump Blockage	Marine Growth		X		
Pump Failure	Marine Growth		X		
Hypochlorite Damage	Marine Growth		X		
Caisson Failure	Corrosion			X	
Galvanic Corrosion	Corrosion			X	
Dissimilar Metals	Corrosion			X	
Installation Tools	Maintenance				X
Maintenance	Maintenance				X
Strainer	Marine Growth				X
Corrosion	Corrosion				X

Table 4-1: Field Note Summary

The main themes were then given sub-themes and the findings synthesised.

Theme	Sub Themes	
Flexible Element	Rubber Pipe	HDPE
Corrosion	Galvanic	Oxidations
Marine Growth	Internal	External
Maintenance	System	Frequency
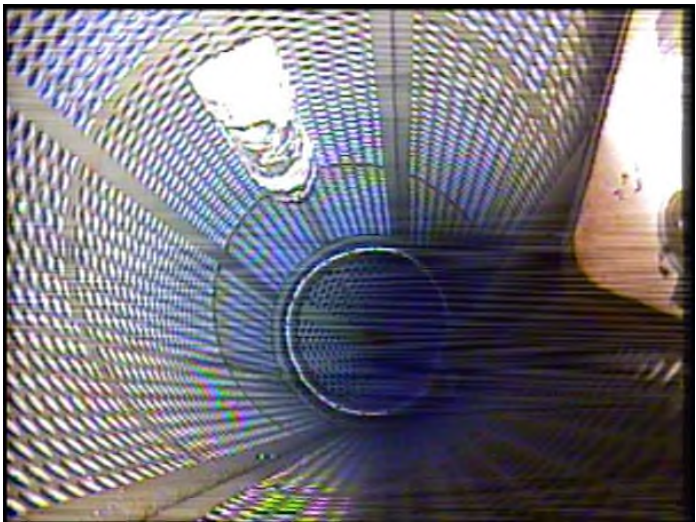
Table 4-2: Field Note Themes & Sub-Themes

4.2. Thematic Analysis
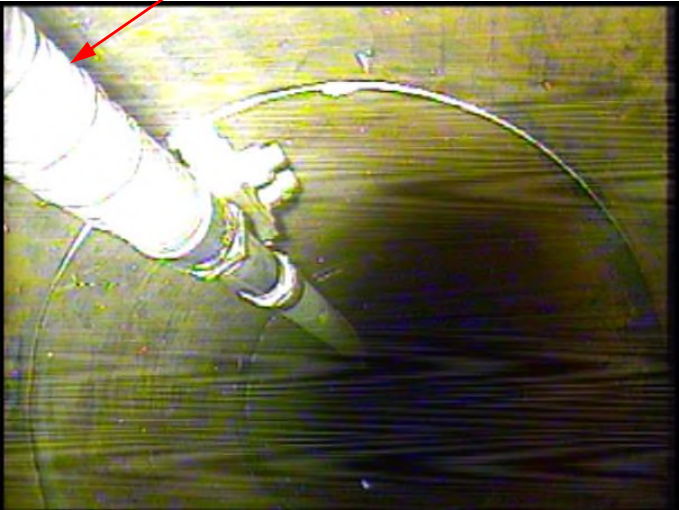
Theme	Sub-theme	Findings
Flexible Element	Rubber Pipe	The damage to the rubber pipe on the Golfinho vessel was due to a wear point from contact with the adjacent SWIR. Contact between flange and adjacent SWIR Damage to Flexible Rubber Pipe outer cover and reinforcement layer Although this was an 'abnormal' condition due to the loss of the ballast weight, and DNV Recommended Practice, RP F203 Riser Interference (DNV, 2009) does permit collisions in certain circumstance, e.g. temporary and extreme conditions, subject to the consequences being evaluated and found acceptable, this does highlight that prolonged contact between SWIR can cause damage, therefore, consideration should be given to the potential collision with adjacent SWIR and possibility of wear points during the system design.
	HDPE	The HDPE sections on the Golfinho were inspected and no signs of any damage reported. This system had been operating for approx. 5 years prior to this inspection which suggests that the HDPE sections are suitable for the application.
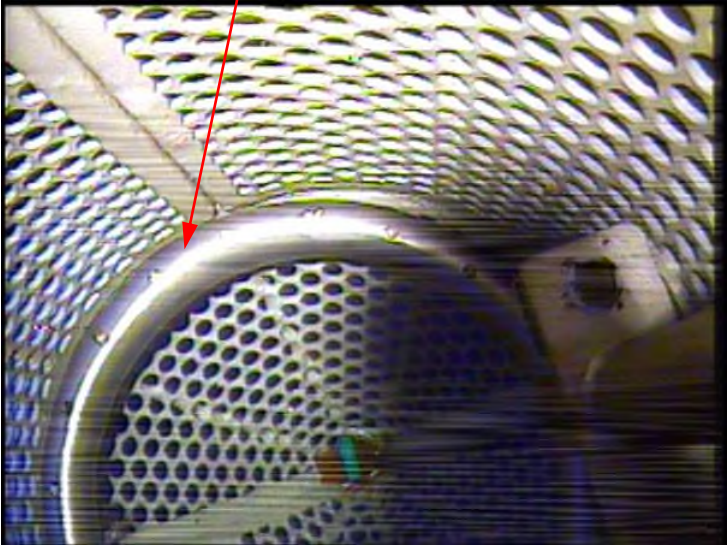
Theme	Sub-theme	Findings
Corrosion	Galvanic	The ballast weight attached to one of the Golfinho SWIR became detached. The ballast weight was manufactured from Cast Iron (CI) and was fixed to the HDPE strainer using stud bolts and nuts manufactured from super duplex stainless steel (SDSS). To prevent galvanic corrosion, isolation bushes were supplied to isolate the CI from the SDSS. The photographs show that the bolts and nuts are still in place, as are some of the isolation bushes. This suggests that the holes in the CI ballast weight corroded significantly and became larger than the nuts used for the joint, allowing the ballast weight to slip over the bolting.

Theme	Sub-theme	Findings
Corrosion (Contd.)	Galvanic (Contd.)	As this only occurred on one of the three SWIR, it must be assumed that the isolation bushes were either incorrectly fitted during assembly or else failed during service. This provides a good indication of the aggressive nature of galvanic corrosion in these conditions and should be given serious consideration during design and where possible, avoided. Break off point and Water pump Caisson Pump Inlet The photographs from the Kizomba SWIR caisson show that the caisson corroded circumferentially until the complete caisson broke away, taking the SWIR with it to the seabed. It would appear that a circumferential weld failed but reference to the design drawing shows that there was not a weld at this location. It is understood that this corrosion is due to galvanic corrosion between the carbon steel caisson and the super duplex stainless steel pump stack. Although this was not a failure of the SWIR, it further highlights the aggression of galvanic corrosion in these conditions and further research suggests that this is not an uncommon problem with seawater intake caissons as identified by Heselmans et al (Heselmans, et al., 2011)
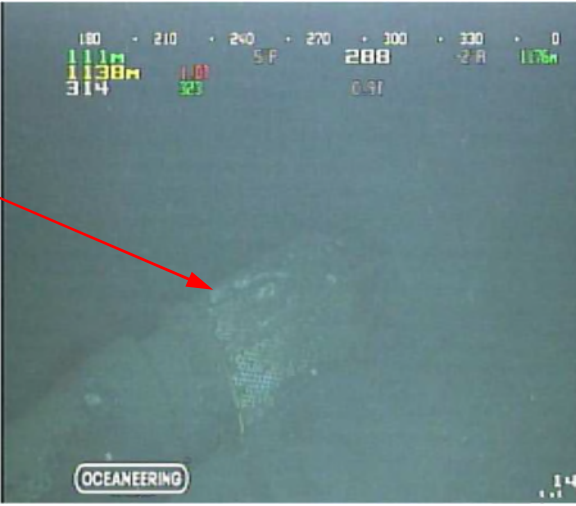
Theme	Sub-theme	Findings
Corrosion (Contd.)	Oxidation	The Riser Heads on the Golfinho SWIR showed little sign of corrosion, the coating system was generally intact and the anodes showed minimal depletion. Before Cleaning After Cleaning The boroscope inspection of the MV23 SWIR shows that the anode within the strainer is showing little sign of depletion despite being operation for around 5 years. This suggests that the coating system and cathodic protection measures are providing good protection against corrosion.
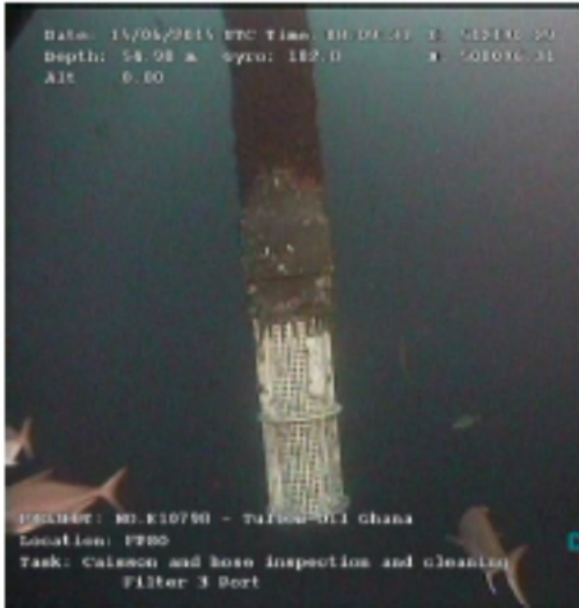
Theme	Sub-theme	Findings
Corrosion (Contd.)	Oxidation (Contd.)	Likewise, the subsea photographs of the MV21 strainers after cleaning show the strainers and flange stud bolts to be in good condition and the anodes with minimal depletion despite also being in operation for approx. 5 years operation. Before Cleaning After Cleaning This provides further evidence that the coating systems and cathodic protection measures are appropriate for the service.

Theme	Sub-theme	Findings
Marine Growth	Internal	The internal bores of the rubber hose and HDPE section on the Golfinho SWIR showed a small amount of marine growth but nothing significant. This is particularly interesting as the Golfinho SWIR was not fitted with a hypochlorite injection facility inside the strainer, although there is a hypochlorite injection point at the pump intake. From the boroscope examination of the MV23 SWIR, it can be seen that the internal bore of the SWIR has a thin covering of marine growth in places Hypochlorite Line This SWIR was fitted with a hypochlorite dosing line and dispersion ring, which can be seen in the photographs, but due to the problems encountered with the pump, it is most likely that this layer formed during the time that the pump was idle.

Theme	Sub-theme	Findings
Marine Growth (Contd.)	Internal (Contd.)	Hypochlorite Dispersion Ring It is noted that the internal surface of the strainer does not have any marine growth formation even though this strainer did not have a foul release coat applied.

Theme	Sub-theme	Findings
Marine Growth (Contd.)	External	Marine Growth on HDPE Sections It was noticeable from the photographs and the underwater footage that there was more marine growth on the rubber hose section than the HDPE section. Although the marine growth thickness was not reported, it appears to be no more than 10mm thick at the worst areas. This suggest that the marine growth profiles specified during design are conservative. Strainer upper holes clear Marine Growth formation on strainer lower holes The strainer section did show some signs of marine growth at the lower holes, this suggests that the flow through the lower part of the strainer is lower than the flow nearer the top of the strainer.

Theme	Sub-theme	Findings
Marine Growth (Contd.)	External (Contd.)	Photographs from the Kizomba SWIR lying on the seabed show that the marine growth on the external surface of the flexible hoses is minimal, even at the upper more 'active' zone.

Flexible Rubber Pipe

Detached Caisson

This SWIR was installed around 2004 without any reported inspection activities which again suggest that the marine growth profiles provided during design stage are conservative.

Strainer upper section clear

The strainer does show marine growth formation at the lower part but again is clear at the upper part indicating that this is where the main flow path is concentrated.

Theme	Sub-theme	Findings
Marine Growth (Contd.)	External (Contd.)	The MV21 subsea photographs show a marine growth formation on the upper flexible rubber pipes. Although difficult to assess the thickness, the surface roughness appears to be significant whereas the marine growth at the lower sections appears to be less significant, suggesting a gradient profile. Marine Growth on upper flexible pipe sections Marine Growth on lower flexible pipe sections

Theme	Sub-theme	Findings
Marine Growth (Contd.)	External (Contd.)	The marine growth formation on the MV21 strainers also indicates that the main flow path is at the upper part of the strainer.

Date: 15/06/2015 UTC Time: 05:37:58 E: 512192.82
Depth: 54.67 m   Gyro: 223.7
Alt   0.00

PROJECT: NO.E10798 – Tullow Oil Ghana
Location: FPSO
Task: Caisson and hose inspection and cleaning

Theme	Sub-theme	Findings
Maintenance	System	Photographs from of the installation tool on the MV21 vessel show it to be in poor condition. Current Condition (2016) During installation (2010) This tool was used to install this SWIR in 2010, which suggests that, once installed, little importance is given to future retrieval or maintenance of the system although an in-situ inspection and cleaning of the strainers was performed after approx. 5 years' operation.
	Frequency	The Golfinho project was the only known vessel to have retrieved the SWIR and this was a 'forced' inspection due to an identified problem. This suggests that the recommended inspection frequency of 3-5 years is not generally being adhered to although an in-situ inspection and cleaning of the MV21 strainers was performed after approx. 5 years. From the poor responses received from the other vessels contacted, it appears that very little inspection and maintenance of the systems in service has been undertaken.

From the data collected, it can be seen that one of the main areas of interest is marine growth. Marine growth in relation to SWIR can be broadly separated into two distinct areas, external and internal. By attaching itself to the outer surfaces of the SWIR, external marine growth alters the behaviour of the SWIR by increasing the diameter and creating a rougher surface, both of which increase the drag when subject to the ocean current. Furthermore, the weight of the marine growth increases the loads into the hull and also the increases the crane hook load should the system be retrieved. This is generally considered during the design of the systems, however, mitigating the marine growth can only improve the efficiency of the SWIR.

For the efficient operation of the vessel processing systems, it is desirable that marine growth does not form on the internals of the equipment such as the heat exchangers as this will at best reduce the efficiency or worst case corrode or block the equipment which may in turn result in a costly shutdown of production. In relation to the SWIR, marine growth on the internal surface of the system will increase the surface roughness and therefore the drag which increases the pressure losses through the system and therefore the pump efficiency. Therefore, internal marine growth can affect the whole operation of the facility and so prevention is arguably more important than external marine growth and thus mitigation measures are essential.

4.3. Proposal for Anti-Fouling Philosophy

With consideration of the above and the literature review in section 2.11, a marine growth mitigation philosophy is proposed based on the following rationale:

During the installation and pre-commissioning phase of the SWIR system, that is when the system is submerged but not operational, a biofilm may begin to form on the internal and external surfaces of the components.

A strainer fabricated from a 90-10 copper nickel alloy would resist the formation of the biofilm during this phase. The HDPE components have a relatively low surface energy and would also resist the formation of the biofilm at this phase. The steel pipe and riser head would be coated internally and externally with a PTFE based foul-release fouling paint system which would also resist the formation of the biofilm. The external surface of the flexible hose elements could be coated with a low surface energy material, such as polyurethane, or a copper impregnated coating to resist the attachment of marine growth.

However, it is assumed that a biofilm may begin to form on the flexible pipe string elements.

The sodium hypochlorite injection point would be located at the upper end of the SWIR, for example within the riser head.

Prior to start-up of the system, a shock dose of sodium hypochlorite would be injected into the SWIR which would gravitate downwards through the string attacking any biofilm that may have formed on the inside of the flexible pipe string elements. It is known that one operator pours a solution of sodium hypochlorite directly into the caisson during idle periods to achieve this effect.

When the system is in operation, the water velocity through the SWIR is generally between 2-3m/s which is higher than the preferred velocity for biofilm formation. Any organisms within the seawater would be treated by the sodium hypochlorite injection at the riser head and also by the injection point at the pump intake system, thus protecting the vessel processing equipment. The flow velocity through the strainer is typically in the region of 0.5m/s which is within preferred velocities of biofilm formation, however, a strainer fabricated from 90-10 copper nickel will resist formation even at this velocity.

Over time, the external surface of the system may begin to allow marine growth formation, although this will be mitigated by foul-release paint on the steel pipe sections, the low surface energy of the HDPE sections and by either a polyurethane or copper impregnated coating on the rubber hose section. Regular inspection by Remote Operated Vehicle (ROV) may be performed to assess the marine growth on the system, and if problematic, may be water jetted by ROV if a full system retrieval is not preferred.

One area of caution would be the connection between the copper nickel strainer and the steel pipe section as the field data discussed in section 4.2 highlights the aggressive nature of galvanic corrosion where dissimilar metals are connected. Instead of isolations bushes, a more robust solution to this would be to encapsulate the lower steel pipe section in rubber.

The benefits of the above philosophy are that the optimum and known anti-fouling measures are applied plus the internal hypochlorite line is not installed within the full length of the SWIR, providing improved pressure loss characteristics and reduced weight. Furthermore, any possible degradation of the sodium hypochlorite line over the life of the system, and the potential replacement costs are eliminated. Any maintenance to the hypochlorite system

would be at the upper end of the string which is more easily accessible and achievable without a full system retrieval.

4.4. Summary

In summary, it has been found that, there is very little field data available to substantiate the design and performance of the SWIR systems in the field although the field data that has been obtained as a part of this research has provided an insight into the design and performance of the seawater intake systems. The marine growth distribution observed on the strainer unit on several systems indicates that the flow path through the strainer unit is concentrated at the upper area of the strainer and not evenly distributed across the open area. This suggests that, increasing the open area by simply lengthening the strainer will not reduce the pressure losses through the strainer.

The field data has indicated that the current corrosion protection measures are operating satisfactorily, although in terms of galvanic corrosion, it has highlighted the aggressive nature of dissimilar metal corrosion and the significant effects it can have.

The field data also shows that the marine growth protection system is operating satisfactorily on the internal bore of the system although, externally, it shows that marine growth will readily attach itself, in particular at the irregular surfaces such as the flange connections. It does however indicate that marine growth does not attach itself to the HDPE sections as readily.

However, it has also highlighted that unintended contact between adjacent SWIR's can establish wear points which in turn can cause damage.

The fifth objective is addressed in the next chapter which is to identify the physical and mechanical properties of the materials under consideration so that the analysis of the proposed solution and its component parts return realistic and justifiable data.

CHAPTER 5.0

MATERIALS

5. MATERIALS

This Chapter investigates the property characteristics of the materials under consideration for the Sea Water Intake Risers (SWIR).

As described in Section 1.2, the SWIR installed on FPSO vessels generally consist of a series of bonded rubber flexible pipe sections connected together, however, it is known that there are at least three vessels currently operating in the field that include High Density Polyethylene (HDPE) pipe sections in the SWIR. As it is the upper section of the SWIR that is exposed to the main environmental loads and loads induced from the vessel motion, in these systems a section (or sections) of bonded rubber flexible pipe is connected to the vessel and forms the top part of the SWIR with the HDPE forming the lower part of the SWIR. Although not as flexible as a bonded rubber flexible pipe, HDPE pipe sections provide sufficient flexibility for the less onerous loadings in the lower sections of the SWIR.

There are several advantages in using HDPE pipe sections for this application, but most notably it is the comparative low weight of HDPE that is considered most advantageous. HDPE has a specific gravity (SG) of <1 therefore, when submerged in sea water, it becomes positively buoyant, which reduces the required crane capacity during installation of the system and also reduces the loads into the hull of the vessel once the system is installed. To provide stability to these SWIR systems, a ballast weight is connected to the lower end of the SWIR and for the known SWIR systems in the field that utilise HDPE sections, various ballast weight solutions are employed such as cast iron, concrete and chain links contained in a basket.

It is because of the weight saving advantages that HDPE is under consideration for this project, and preliminary analysis by the author (Craig, 2014) examined a number of SWIR configurations which indicated that the use of steel pipe sections as ballast at the lower end of the SWIR is a possible solution in terms of weight versus stability with the advantage that it also forms a part of the flow path.

Consequently, this chapter characterises three SWIR material elements, namely, bonded rubber flexible pipes, HDPE pipes and steel pipes.

5.1. Bonded Rubber Flexible Pipes

5.1.1. Design Codes & Guidelines

There are a number of industry Design Codes & Guidelines associated with the design and manufacture of bonded rubber flexible pipes. Craig (2016) identifies the industry codes and guidelines associated with the design and manufacture of bonded rubber flexible pipes and determines those most

appropriate for a SWIR application to assure the satisfactory operation and life in field. The associated design codes and guidelines are compared and contrasted to the requirements of a SWIR application and then critically appraised to determine which provide the most relevant verification and validation criteria for the design and manufacture of bonded rubber flexible pipes used in a SWIR application with due consideration given to the specific requirements of these bonded rubber flexible pipes.

Craig (2016) concludes that there are a number of design codes and guidelines related to the design and manufacture of bonded rubber flexible pipes and whilst there are criteria from several of these design codes and guidelines that may be applied, the design and manufacture of bonded rubber flexible pipes for a SWIR application is not specifically covered by the scope of any one of the documents reviewed. Consequently, the most relevant criteria from the reviewed documents is identified and a methodology proposed to verify and validate the design and manufacture of a flexible pipe in a SWIR application, the design element of which is summarized below and used within this study:

Item	Description	Input Data	Process	Output	Acceptance Criteria
1	Flexible Hose Design	Design Specification Component Properties	Build FEA Model Simulate Axial & Bending Loading Extract Results	Axial & Bending Stiffness Reinforcement Stress Factors	Within strength and fatigue requirements of application
2	Hydrodynamic Analysis	Vessel RAO Data Meteocean Data Riser Properties	Build Model Establish Design & Survival Load Case Combinations Run Analyses Extract Results	Hose Maximum Tension Hose MBR	Hose allowable tension not exceed Hose MBR not exceed
3	Hose Fatigue Analysis	Vessel RAO Data Meteocean Data SN Data	Establish Hs / Tz Occurrences Define Fatigue Bins Run Orcaflex wave scatter tool Extract fatigue load cases Run Analyses Extract Results	Bending Moment & Tension ranges	Predicted fatigue of Hose Reinforcement Materials within S-N allowable (DFF = 3)

Table 7: Seawater Intake Riser Flexible Pipe Proposed Design Methodology

Table 5-1: Flexible Pipe Design Methodology

(Craig, 2016)

5.1.2. Composite Structure Modelling

- *Methodology*

To characterise and predict the behaviour of the bonded rubber flexible pipe considered in this study, the following methodology was applied:

Data was collated for a 40"NB flexible rubber pipe section that had previously been manufactured for a SWIR application.

The data set consisted of material and dimensional properties and also results from physical testing of the finished product including elongation under pressure and the measured stiffness during bending.

Using this data set, a digital model of the flexible pipe was created in recognised FEA software and then tuned it so that the simulated behaviour of the flexible pipe was as close as practicable to the actual measured behaviour of the flexible pipe.

A separate model was established for the flanged joint and subject to FEA to determine the stress factors of the flange construction and the stud bolts used to connect the flanges.

Once satisfied that the digital model was an accurate representation of the actual flexible pipe, stress factors were extracted from the simulations which were then used to predict the fatigue life of the flexible pipe and flange connection.

Based on real world data, these modelled characteristics of the 40"NB bonded rubber flexible pipe section formed the 'control' data in the subsequent analyses and were used as the basis for determination of the 60"NB hose characteristics.

- *Finite Element Analysis*

The bonded rubber flexible pipe is a composite structure meaning it is constructed from a number of material types and forms. A detailed description of the flexible pipe construction is presented in the Portfolio [Section 7.0] (PDL, 667-003:2015, p. 6), but in summary the structure consists of;

- Hose End Steel Nipples (with flanges)
- Rubber Inner Liner
- Circumferential Steel Rings embedded in Rubber
- Textile Reinforcement Plies (wrapped helically) embedded in Rubber
- Rubber Outer Cover

As such, the flexible pipe construction is not homogenous and empirical data for bonded rubber flexible pipes is varied and not as readily available as it is for homogeneous materials such as steel.

Therefore, to characterise the bonded rubber flexible pipe under consideration and perform a fatigue assessment, an independent analyst was directed by the author to perform an FEA of the flexible pipe using real world data (PDL, 667-003:2015) as described in the above methodology.

To compare the behavioural properties and fatigue capabilities of textile reinforced flexible pipe versus a steel cord reinforced flexible pipe, a 'like for like' exercise was undertaken, whereby the same flexible pipe digital model was modified to replace the textile reinforcement layers with steel cord reinforcement layers. It should be noted that, to achieve the same tensile strength, fewer layers of steel cord were required, resulting in a small geometric change in terms of the outside diameter of the flexible pipe.

During the execution of this comparative FEA, the software utilised for the analysis became unstable due to problems with the compression of steel cord, which was resolved by applying a 'smeared' reinforcement element, details of which are presented by PDL (727-001:2015, p. 11).

Consequently, the FEA of the textile reinforced flexible pipe was revisited and the 'smeared' element applied, together with the results of the subsequent material tests presented in the section 5.1.3, details and results of this updated data on the textile reinforced pipe are presented by PDL (727-002:2015).

- *Fatigue Assessment*

To compare the fatigue behaviour of the textile reinforced flexible pipe and the steel cord reinforced flexible pipe, a fatigue assessment, based on a live project, was performed using the data obtained from the FEA, details of which are presented by PDL (667-002:2015) and (727-002:2015) for the textile reinforced flexible pipe and the steel cord reinforced flexible pipe respectively.

The load path of the flexible pipe is through the flanged end and into the reinforcement layers which are the most likely points of fatigue failure and therefore the main area of focus for the fatigue assessment. The reinforcement layers for the textile reinforced flexible pipe were in the form of a polyester textile yarn, and although there was test data available for the

strength of the textile yarn, it was found that limited fatigue data existed for this material.

Fatigue data presented by Lechat et al (2010) and Davies (Davies, et al., 2010) was used as a basis for the initial fatigue assessment although an additional standard deviation was applied to this data for added conservatism, further detail regarding the application of this data is presented by PDL (667-002:2015, p. 13).

Due to the limited availability of textile yarn fatigue data, an independent test facility was directed by the author to perform cyclical load tests on samples of the actual textile yarn used in the flexible pipe construction, details of these tests are described in section 5.1.3, the results of which were then used for a further fatigue assessment of the textile reinforced flexible pipe as discussed in (PDL, 727-002:2015) Appendix A.

For the steel cord reinforced flexible pipe, the steel cord SN data was obtained from the American Petroleum Institute (API) document API-RP-2SK (API, 2005), further detail regarding the application of this data is presented by PDL (727-002:2015, p. 11). API is a recognised authority whose codes and guidelines are also widely accepted within the industry.

The fatigue properties of steel are well documented, however, as the application for the SWIR is an offshore and marine environment, the fatigue data and assessment techniques within Det Norske Veritas (DNV) recommended practice DNV-RP-0005 (DNVGL, 2016) were used for the fatigue assessment of the steel flange connection. DNV is a recognised classification society whose codes and guidelines are widely accepted by the industry.

- *Findings*

In terms of the increase in diameter and elongation under pressure, as well as the bending stiffness, the results from the FEA of the textile reinforced flexible pipe section provide a good correlation with the actual test results from the flexible pipe testing.

To achieve the same tensile strength in the steel cord reinforced flexible pipe, fewer layers of steel cord were required, resulting in a small geometric reduction of the outside diameter of the flexible pipe, meaning less rubber compound is used in the construction.

The model enhancements applied to the model of the steel cord reinforced flexible pipe section, i.e. the non-linear stress-strain curve for rubber (ref. section 5.1.3) and application of smeared element type, provided a more robust model for the software to simulate and the results indicated that the compression stiffness of the rubber compound on the inside of the bend, was a dominant feature of the bending stiffness of the flexible pipe. As the steel cord reinforced flexible pipe has a smaller outside diameter and therefore less rubber compound, this may explain why the bending stiffness is approximately 10% less and the weight is approximately 5% less than the textile reinforced flexible pipe.

The data obtained from both the textile reinforced and the steel cord reinforced flexible pipe FEA were applied to the same global analysis parameters for an existing project in order that the fatigue capabilities of the flexible pipe sections could be compared. It was found that the textile reinforced pipe section did provide a better fatigue life than the steel cord reinforced pipe, primarily due to the amount of textile cords rather than the properties of the textile cord, although both flexible pipes sections exceeded the required life in field of the application considered. This sample fatigue assessment indicated that the likely point of failure would be in the weld of the flange at the flexible pipe end.

The stress factors from the textile reinforced flexible pipe FEA are used for the analysis presented in Chapter 6.

5.1.3. Material Testing

- *Reinforcement Material*

As discussed above, during the FEA of the bonded rubber flexible pipe, there were a number of apparent knowledge gaps in relation to the materials under consideration, most notably, the fatigue data for the textile yarn. Although data was obtained from Lechat et al (2010) and Davies et al (2010) for the initial analysis, an independent test facility was directed by the author to perform cyclical load tests on samples of the actual textile yarn used in the flexible pipe construction.

It should be noted that, during the manufacture of the bonded rubber flexible pipe section, part of the process requires that the complete flexible pipe construction is vulcanised, meaning that it is placed in an autoclave and subject to heat for a period of time. This process modifies the polymer

by forming cross-links between individual polymer chains, however, being an integral part of the construction, the textile (polyester) yarns are also subject to this process.

Although polyester is a thermoplastic, it is known from tensile testing performed on the textile yarn before and after the vulcanisation process that the tensile strength of the yarn is reduced due to this process, as presented in the Portfolio [Section 5.0], which is thought to be caused by heat degradation of the outer filaments of the yarn. Therefore, to obtain realistic fatigue data for the yarn, the samples provided for cyclical load test were firstly calendered in rubber and then subject to the vulcanisation process so that they were a realistic representation of the yarn in service.

The samples of yarn were subjected to tensile cycling at various loads relating to the measured ultimate tensile strength of the yarn. The number of cycles to failure were recorded for each loading as shown in Fig. 5-1, details of the testing are presented in the Portfolio [Section 5.0] (Intertek, 2015).
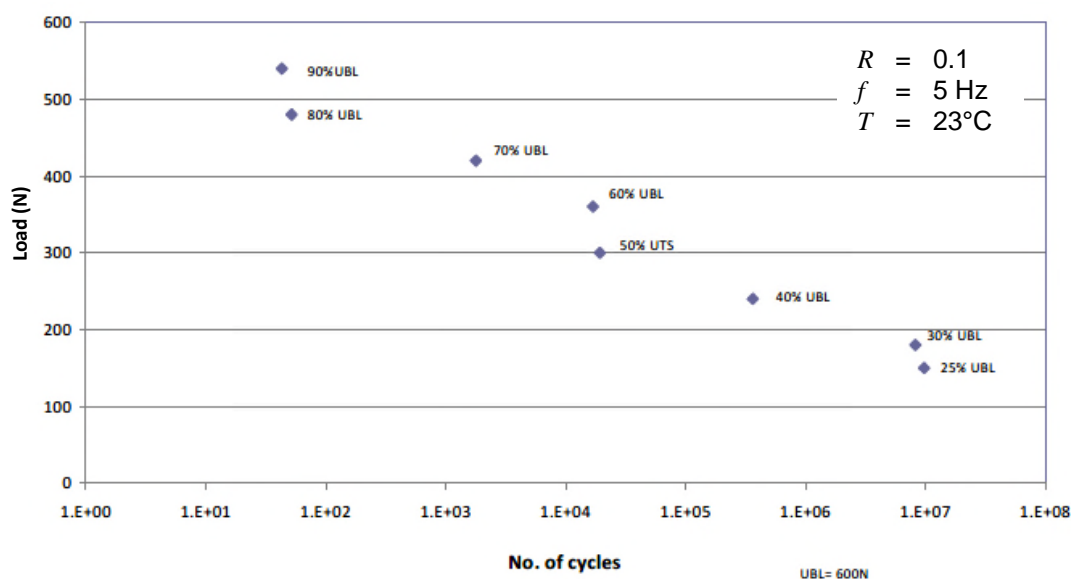
Fig.5-1: Textile Reinforcement Raw Test Data

A statistical analysis of the raw test data was performed in accordance with the industry recognised standard ASTM E739 (ASTM, 2015) details of which are presented in the Portfolio [Section 6.0].

This produced the usable SN Curve shown in Fig.5-2 from which the -95% Confidence band is used.
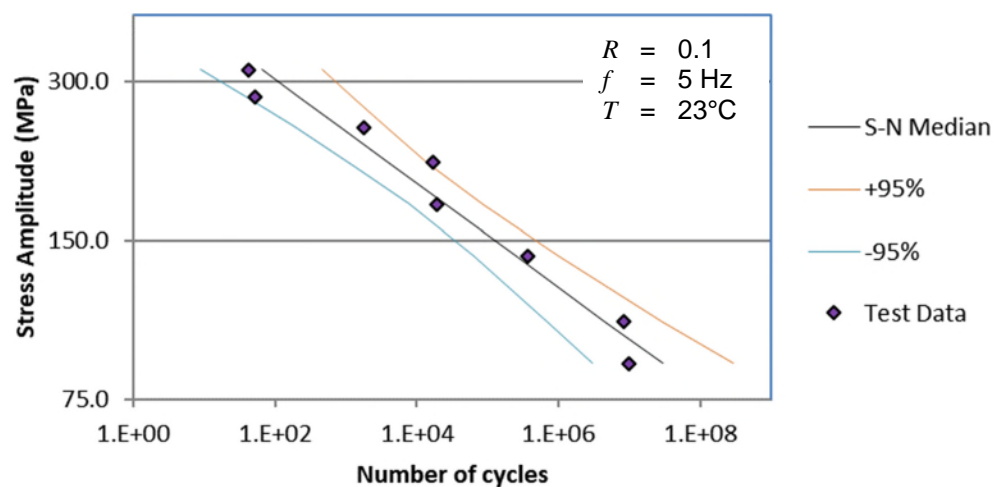
Fig.5-2: Textile Reinforcement SN Curve

It should be noted that, due to the characteristics of the yarn, the cyclic testing was undertaken with a stress ratio of R=0.1, (where R = Min Stress / Max Stress) therefore the SN Curve shown in Fig.5-2 represents the actual stress amplitude during testing and has a positive mean stress.

- *Rubber Compound*

Another knowledge gap identified was in relation to the 'stiffness' of rubber under compression. During the bending of a bonded flexible rubber pipe, the rubber pipe section is in tension on the outside of the neutral axis and is under compression on the inside of the neutral axis.

For the FEA of the textile reinforced flexible pipe, material data for the actual rubber compound was available in terms of shore hardness and elongation under tension. Using this data, and as suggested in ASTM D1415 (ASTM, 1999) for well-vulcanised rubbers, a linear modulus of elasticity was assumed. To verify (or otherwise) this assumption, an independent test facility was directed to perform compressive tests on rubber samples, the results of which indicated that the rubber compound was in fact stiffer in compression than in tension and are presented in the Portfolio [Section 5.0], (SGS, 2015).

Using this data, a non-linear stress-strain curve was developed and applied for the FEA of the reinforced flexible pipes, details of which are presented in by PDL (727-001:2015, p. 8).
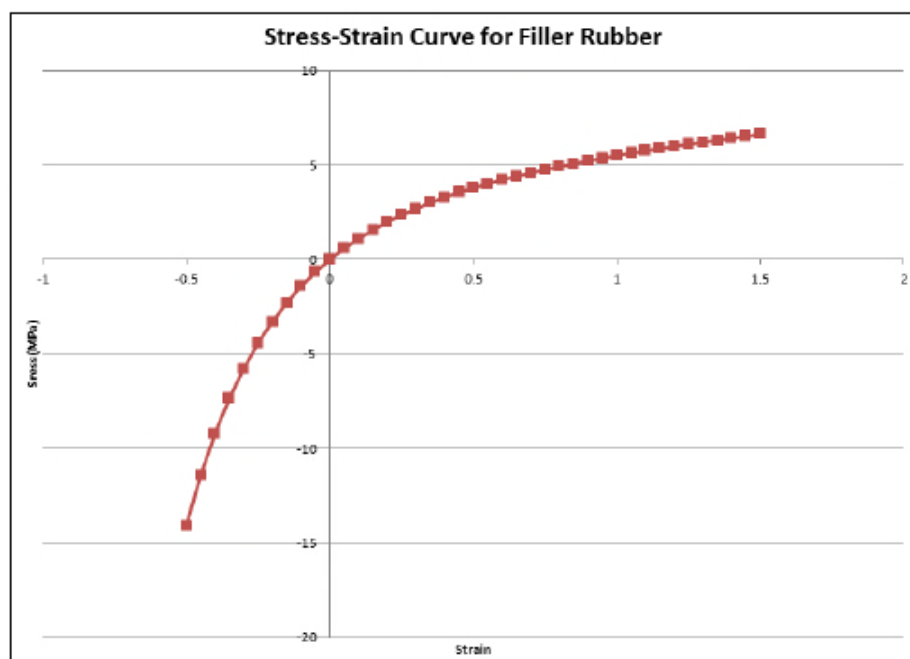
Fig.5-3: Rubber Compound Stress-Strain Curve

5.1.4. Material Properties considered in this study

For the analyses performed in Chapters 6 of this report, the following material properties for the bonded rubber flexible pipe are considered.

- *Physical Properties*

Description	Bonded Rubber Flexible Pipe	
	40"NB[1]	60"NB[2]
Outside Diameter (m)	1.220	1.760
Inside Diameter (m)	1.0	1.5
Section Length (m)	11.5	11.5
Section weight [in air] (kg)	6,400	11,990
Section weight [in water] (kg)	2,200	4,145

Table 5-2: Bonded Flexible Rubber Pipe – Physical Properties

1) Data based on previously manufactured flexible pipe (Emstec, 2013)

2) Data based on information received from hose manufacturer (Emstec, 2014)

- *Mechanical Properties*

Description	Bonded Rubber Flexible Pipe	
	40"NB[1]	60"NB[2]
Bending Stiffness (kN.m^2) [3]	2,129	9,122
Axial Stiffness (kN)	17,000	25,500
Axial Strength (kN) [4]	3,141	7,068
Minimum Bend Radius (m)	4.0	6.0

Table 5-3: Bonded Flexible Rubber Pipe – Mechanical Properties

1) Data based on previously manufactured flexible pipe (Emstec, 2013)

2) Data based on information received from hose manufacturer (Emstec, 2014)

3) Average value. Bending stiffness modelled as a variable in accordance with outputs obtained from the FEA (PDL, 727-002:2015)

4) Value based on theoretical burst pressure

- *Fatigue Properties*

Flexible Pipe Section

Description	Bonded Rubber Flexible Pipe	
	40"NB[1]	60"NB[2]
Tensile Stress Factor (MPa/kN)	0.02765	0.00686
Curvature Stress Factor (MPa/Rad/m)	640	1099
Ultimate Tensile Strength (MPa)	369	369
SN Curve Parameters	Ref. Fig. 5-2 (-95% Conf Band)	

Table 5-4:   Bonded Flexible Rubber Pipe – Fatigue Properties

1) Data based on FEA output (PDL, 727-002:2015)

2) Scaled up based on data from 40"NB

Flange Weld

Description	Bonded Rubber Flexible Pipe	
	40"NB[1]	60"NB[2]
Tensile Stress Factor (MPa/kN)	0.154	0.0689
Curvature Stress Factor (MPa/Rad/m)	0.520	0.1788
SN Curve Parameters [3]: log a1 =	12.164	12.164
log a2 =	15.606	15.606
m1 =	3	3
m2 =	5	5
Fatigue Limit @ 10^7 cycles (MPa)	52.63	52.63

Table 5-5: Bonded Flexible Rubber Pipe Flange Weld – Fatigue Properties

Stud bolts

Description	Bonded Rubber Flexible Pipe	
	40"NB[1]	60"NB[2]
Tensile Stress Factor (MPa/kN)	0.012	0.01714
Curvature Stress Factor (MPa/Rad/m)	0.046	0.0321
SN Curve Parameters [4]: log a1 = log a2 = m1 = m2 =	10.570 13.617 3 5	10.570 13.617 3 5
Fatigue Limit @ 10^7 cycles (MPa)	21.05	21.05

Table 5-6:   Bonded Flexible Rubber Pipe Stud bolts – Fatigue Properties

1)   Data based on FEA output (PDL, 727-002:2015)

2)   Scaled up based on data from 40"NB

3)   DNVGL-RP-C203 Table 2-1 Curve D (DNVGL, 2016)

4)   DNVGL-RP-C203 Table 2-2 Curve W3 (DNVGL, 2016)
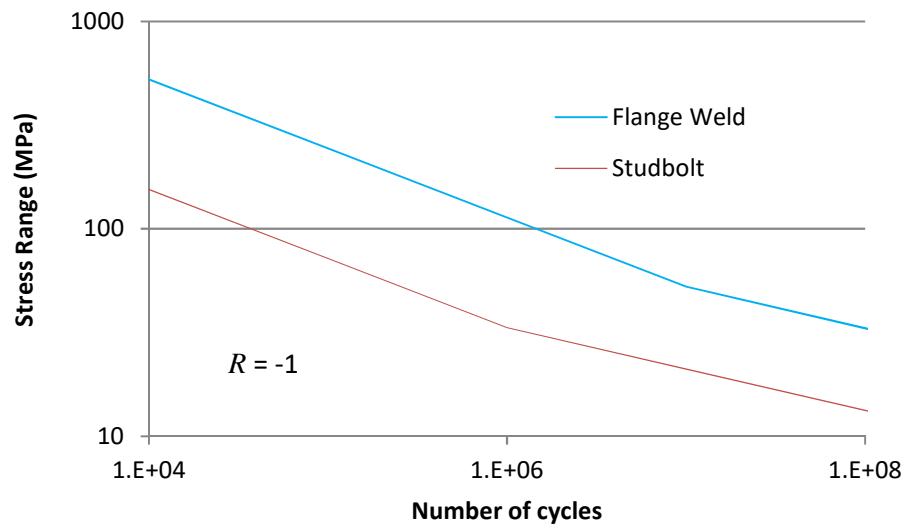
Fig.5-4: SWIR Connection SN Curves

It should be noted that, as indicated in section 5.1.3, the testing of the textile reinforcement was undertaken with a stress ratio of R=0.1 therefore the SN data generated has a positive mean stress.

However, for the flange weld and studbolts, the SN data has a stress ratio of R=-1 which is a full reversal and therefore has zero mean stress. As the system under consideration will always have a positive stress, it is necessary allow for a positive mean stress.

The fatigue results tool within Orcaflex has a number of models for the mean stress effects, one of which is the commonly used Goodman model:

$$\sigma_e \ = \ \frac{\sigma_r}{\left[1-\left(\frac{\sigma_m}{SMTS}\right)\right]} \qquad\qquad \text{(Orcina, 2014)}$$

where: σ_e = Equivalent Stress

   σ_r = True Stress Range

   σ_m = Mena Stress

   $SMTS$ = Ultimate Tensile Strength

For the flange weld and studbolt fatigue calculations, the Goodman correction will be selected.

5.2. HDPE Pipe Sections

5.2.1. Design Codes & Guidelines

High Density Polyethylene (HDPE) pipe sections are readily available in diameters from 25mm to 2000mm and are extruded from HDPE granules and are generally supplied in lengths of 12m sections for ease of handling and transportation. The individual pipe sections are often connected using fusion welding, that is, the ends of each pipe are heated to a prescribed temperature and then butted together under pressure and allowed to cool. This enables the polymer links to fuse with one another forming a continuous joint.

There are a number of standards associated with the design and manufacture of HDPE sections, but the most common standards adopted by the industry are the design standard DVS 2205 (DVS, 2015), the manufacturing standard DIN 8075 (DIN, 2012), the dimensional standard ASTM F714 (ASTM, 2013) and the butt fusion welding standard WIS-4-32-08 (Water UK, 2016) which will be used as the basis for this research study.

5.2.2. Polyethylene Piping Systems

Polyethylene (PE) is classified as a polyolefin and is produced by polymerizing the olefin ethylene. It belongs to the thermoplastics group of plastics, which when heated above a certain temperature, become soft and mouldable but then solidify again once cooled.

Within the thermoplastics group, materials can be separated into two further categories, i.e. amorphous and semi-crystalline. PE belongs to the semi-crystalline category which are characterised by having an amorphous phase and a crystalline phase known as spherulites. The amorphous phase provides the material with its strength while the semi-crystalline phase provides the ductility.

The molecular structure and weight distribution obtained through the production process provide a range of PE grades, categorised by density, e.g.;

- VLDPE (Very Low Density PE)
- LDPE (Low Density PE)
- MDPE (Medium Density PE)
- HDPE (High Density PE)
- UHMWPE (Ultra High Molecular Weight PE)

(Krishnaswamy, 2007)

Of these categories, HDPE has been used successfully for over 50 years in piping systems in various applications such as Water and Natural Gas Distribution, Sewer Network, Petrochemical Piping and Nuclear Power Plants. In 2007 it was estimated that there were approx. 3.6 million tonnes of HDPE piping used worldwide in outdoor applications (Krishnaswamy, 2007). HDPE grade PE100 has been used in these applications since 1988 (PPI, 2014).

A particular subset of HDPE resins is commonly used for piping systems which are 'bimodal' in as much as they have two peaks in the molecular weight distribution giving the optimum balance of mechanical properties for high performance piping systems, as illustrated below in Fig.5-5.
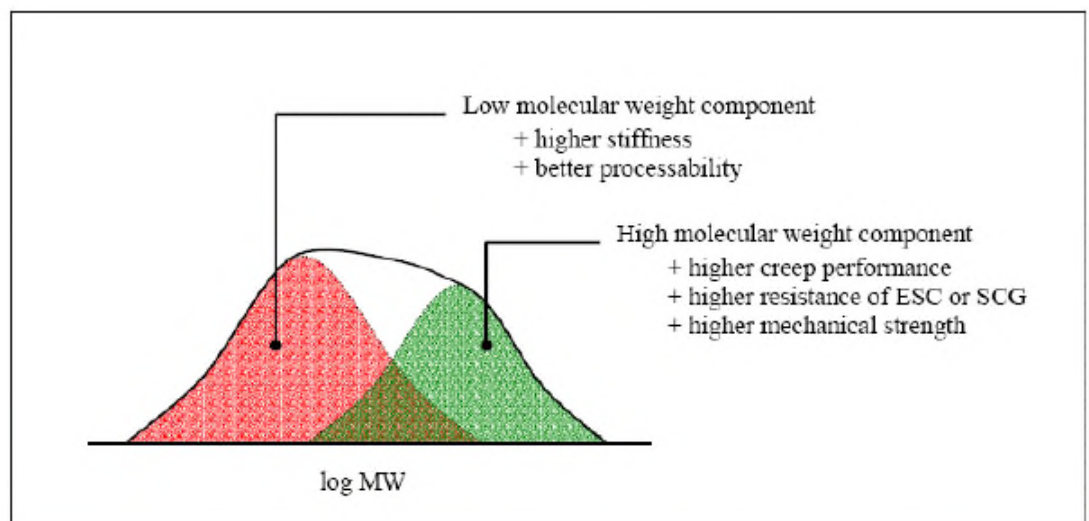
Figure 4   **Schematic of molecular weight distribution of bi-modal HDPE materials [MW = Molecular Weight; ESC = Environmental Stress Cracking and SCG = Slow Crack Growth]**

Fig.5-5: Molecular Weight Distribution of Bi-Modal HDPE Material (Krishnaswamy, 2007)

Brogden (2000) argues that it is the ductility of these modern HDPE materials that add to the good fatigue properties as cracks quickly become blunted due to the large amount of energy absorbed by the deformation around the crack tip which only allows the crack to grow a short distance before having to be re-initiated.

This subset of resins is often referred to as PE4710 or PE100, which are references from a more precise method of classifying PE materials

PE4710 is a grade designated by the Plastics Pipe Institute (PPI) which is a trade association of resin manufacturers and suppliers to the plastic pipe industry. The PPI evaluate resin data provided by the manufacturers and

assign it an appropriate designation of which PE4710 may be interpreted as shown in Table 5-7:

PE 4710	4	Density cell class 4 per D3350, 0.948 - 0.955 gm/cc (59.182 to 59.618 lbs/ft^3);
	7	SCG cell class 4 per D3350, PENT value > 500 hours
	10	1000 psi (6.89 MPa) hydrostatic design stress for water at 73 °F (23 °C)

Table 5-7: Interpretation of PE4710 Designated Pipe
(Krishnaswamy, 2007)

PE100 is a grade designated by the European system which specifies the pipe by its minimum required strength (MRS) in accordance with ISO Standard 12162 (ISO, 2009) and for which PE100 has an MRS of 10MPa.

The American Society for Testing of Materials (ASTM) provide a further methods of classifying PE materials with ASTM D3350 Standard Specification for Polyethylene Plastics Pipe and Fittings Materials (ASTM, 2014) which provides a seven digit reference for specifying grades by density, melt index, tensile strength etc.

In this system, reference 445474C is within the bimodal subset with the cell classification shown in Table 5-8.

Cell No.	Description
4	Density Range 0.948 to 0.955 gm/cc (59.182 to 59.618 lbs/ft^3) per ASTM D1505
4	Melt index of < 0.15 gm/10 min (0.00529 oz/10 min) per ASTM D1238
5	Flexural Modulus between 110 and 160 ksi (0.758 to 1.103 MPa) per ASTM D790
4	Tensile Strength between 3500 to 4000 psi (24.1 to 27.6 MPa) per ASTM D638
7	PENT Test Failure Time of > 500 hours per ASTM D 1473
4	Hydrostatic Design Basis of 1600 psi (11.03 MPa) per ASTM D2837
C	Black with 2% minimum carbon black

Table 5-8: Interpretation of HDPE 445474C Cell Classification
(Krishnaswamy, 2007)

For the purposes of this research PE grades PE4710, PE100 and HDPE 445474C will be considered as equivalents, but will be primarily referred to by the European reference PE100 unless specifically referenced otherwise by the literature.

5.2.3. HDPE Pipe

High Density Polyethylene (HDPE) pipe sections are extruded from HDPE granules, generally supplied in lengths of 12m for ease of handling and transportation and are readily available in diameters from 25mm to 2000mm.

For large diameter HPDE pipes, the wall thickness t is generally expressed as a ratio with the outside diameter D_o (i.e. D_o/t). ASTM refer to this as the

Standard Dimension Ratio (SDR) and the convention in PE pipe standards such as ASTM F714 (ASTM, 2013) is to limit these a few standard ratios (PPI, 2008, p. 132), for example:

SDR 11, SDR 13.5, SDR 17, SDR21, SDR 26 & SDR32.5.

For the diameter of HDPE pipes under consideration within this research, the above SDR's would equate to wall thicknesses as shown in Table 5-9.

Outside Diameter *(mm)*	Wall Thickness *(mm)*					
	SDR 11	**SDR 13.5**	**SDR 17**	**SDR 21**	**SDR 26**	**SDR 32.5**
1067	97	79	63	51	41	33
1600	145	118	94	76	61	49

Table 5-9: HDPE Wall Thicknesses

HDPE pipes with wall thicknesses <25mm are generally considered as 'thin walled' whereas HDPE pipes with wall thicknesses >25mm are considered 'thick walled' (Wilson, 1995) so it can be seen from Table 5-9 that the HDPE pipes considered for this research are all 'thick walled'.

There are a number of techniques currently used for joining HDPE pipe sections such as saddle fusion, socket fusion and electro-fusion, however, the most reliable, and most dominant, method for joining medium and large diameter HDPE pipes is Butt Fusion Welding (Hill, et al., 2001). This technique can be used either to connect sections of HDPE pipe directly to one another in the field, or else to connect HDPE flanges to each end of the HDPE pipe sections in the factory to enable mechanical joining in the field. The latter of these options is considered from hereon in as it is desirable to enable the HDPE pipe sections in the SWIR to be disassembled, inspected and reinstalled.

The next section investigates butt weld fusion of thick walled (>25mm) HDPE pipes.

5.2.4. Butt Weld Fusion of HDPE Pipe

Butt fusion welding is the dominant method of jointing for large PE pipe sizes and although there are a number of international standards relating to the method, the principle of the technique is the same. With reference to the jointing cycle shown in Figs 5-6 and 5-7, the two pipe ends are pressed against a heater plate with a fixed temperature and a bead allowed to form (initial bead up), the pressure is reduced and the pipe ends are held against the heater plate for a specified period of time (heat soak) after which the heater plate is removed. Once removed the hot pipe ends are immediately pressed together at a specified pressure (fusion pressure), so that the fused material 'rolls' back (bead roll over) and then allowed to cool for a specified period of time (cooling time).
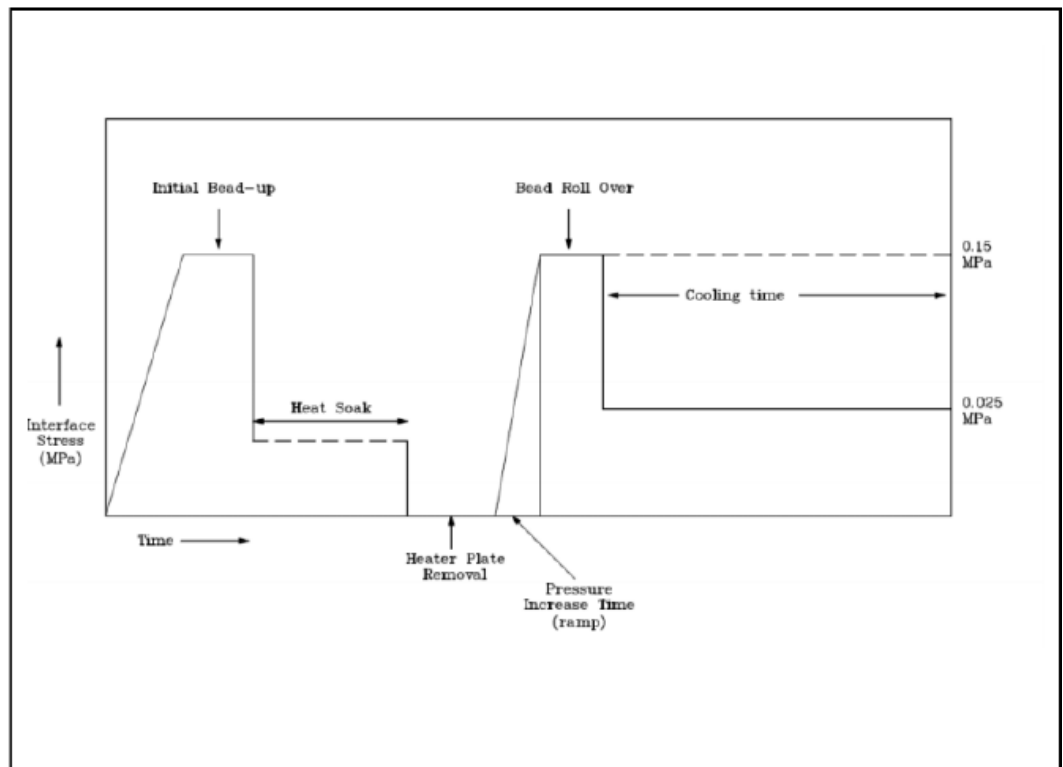
(Water UK, 2016)

Fig.5-6:   Butt Fusion Jointing Cycle (not to scale)
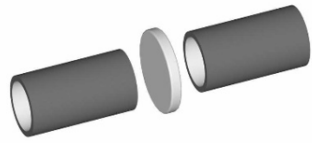
Heater Plate placed between pipe ends
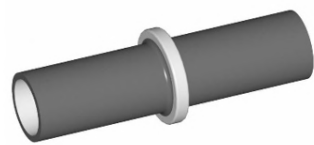
Initial Bead Up & Heat Soak
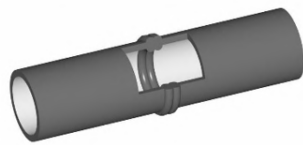
Fusion Pressure, Bead Roll Over & Cooling

(Marley, 2016)   (Marley, 2010)

Fig.5-7: Stages of PE Butt Fusion Process

Cross Sections through various completed HDPE Butt Fusion Welds are shown in Fig.5-8 below:
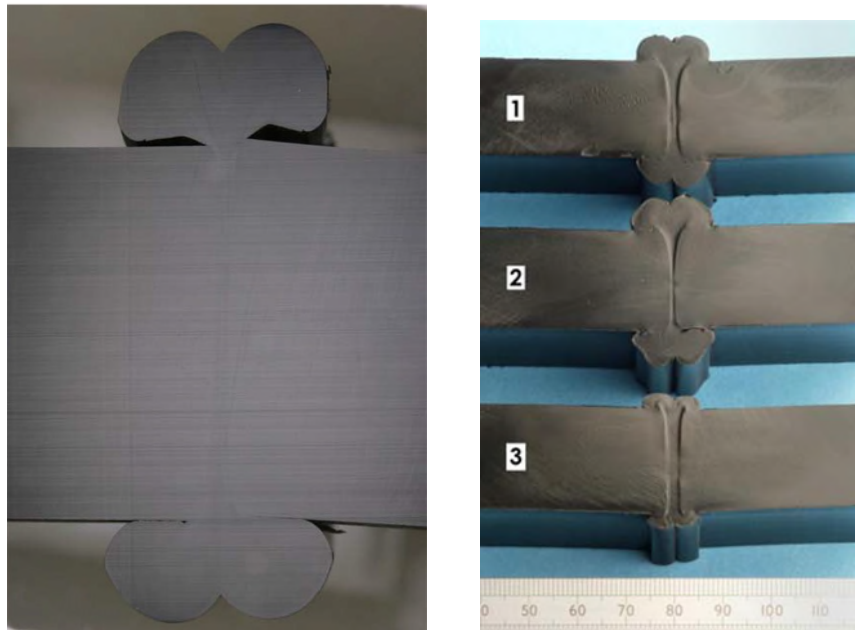
Fig.5-8: Cross Section through HDPE Butt Fusion Weld

Hill et al (2001) argue that the success of Butt Fusion Welding is dependent upon three main factors, namely;

- Absence of Contamination
- Sufficient Heat Input
- Good final morphology

According to Hill et al (2001), contamination of the weld during the fusion process is one of the causes of brittle failure. On thin walled pipes, a relatively large area of the pipe end surface is expelled into the weld bead during the bead up phase, taking with it most of the contamination, therefore thin walled pipes do not often exhibit brittle failure due to contamination. Thick walled pipes however, are more prone to contamination and tensile tests often show ductile failure at the middle of the section but brittle failure near the pipe surface. This suggests that any contamination is expelled from the centre of the pipe wall during bead up but does not move completely into the bead. While butt fusion welds in the field are more prone to contamination, welds performed in controlled factory conditions are less likely to be contaminated by dust (Hill,

et al., 2001). As the butt weld fusion process under consideration for the SWIR would be carried out in factory conditions, weld failure through contamination will not be explored further in this study.

With regard to heat input and final morphology, Hill et al (2001) identify a number of international standards for the butt welding of thick walled PE pipes and compare the heat soak times, cooling times and fusion pressure requirements of each (some of which show consistency while others differ widely from the majority) and investigates the effect that each of these factors has on the final morphology of the butt fusion weld. It is argued that during the fusion process, there must be a mixing of the PE molecules at each pipe end which forms a strong joint through the co-crystallisation during cooling. However, during this phase of the jointing cycle, the material will not have sufficient time to become perfectly mixed to the same degree as the parent material, thus giving it the behaviour of a PE with a lower apparent chain entanglement. The mechanical properties of the weld interface will therefore be representative of a PE with a lower molecular weight which, for PE100, results in a lower interface toughness compared to the parent pipe (and which has been verified through Charpy impact testing of the weld). It is therefore suggested by Hill et al (2001) that, to substantiate the success of the butt weld fusion process, it is necessary to monitor one of the PE properties affected by the lower apparent chain entanglement such as ductility.

Wilson (1995) investigated the quality of butt weld fusion in large diameter PE100 pipes by comparing the strength, ductility and toughness of the welds against the parent pipe. Using the weld process specified in the UK Water Industry Specification (WIS) for the fusion welding of PE100, WIS 4-32-08 (Water UK, 1994) it was found that, by optimising the weld test specimen, acceptable weld quality of thick walled pipes could be achieved. The tests showed that the tensile strength of the weld was comparable to the tensile strength of the parent pipe, i.e. approx. 26-28MPa, whereas the ductility, although consistent, was found to be in the range of 464-503kJ/m^2, less than the parent pipe which was in the range of 723-1103kJ/m^2. These findings were corroborated through further testing by Hill et al (2001) which provided consistently average ductility values at the weld interface of between 500-600kJ/m^2 and which correlated well with impact test results of the weld area, with values in the range of 8.4-11.5kJ/m^2 being recorded compared to the parent pipe level of 16kJ/m^2. Welding and testing trials by Lowe et al (2006),

which looked at varying welding conditions, indicated that if the minimum energy recorded during the tensile test was greater than 300kJ/m^2 then the failure would be ductile in nature.

The above values are tabulated in Table 5-10 below for comparison;

Property	Weld	Parent Pipe
Tensile Strength (MPa)	26-28	26-28
Ductility (kJ/m^2)	464-503	723-1103
Toughness (kJ/m^2)	8.4-11.5	16

Table 5-10:   HDPE Butt Fusion Weld v Parent Pipe Properties

The current revision of the UK Water Industry Specification (WIS) for the fusion welding of PE100, WIS 4-32-08 (Water UK, 2016) references the work undertaken by Wilson (1995), Hill et al (2001) and Lowe et al (2006), and includes requirements for testing of joints and states that no joint should fail in a brittle manner and that all test samples must exhibit ductile failure to pass, for which a value above 300kJ/m^2 is considered satisfactory. It should be noted that additional measures have recently been introduced to this standard in relation to thick walled pipes to ensure realistic assessment of the ductility test.

So, in conclusion, in the absence of contamination and when welded in accordance with the WIS 4-32-08 (Water UK, 2016), a butt fusion weld in thick walled HDPE pipe exhibits a tensile strength equivalent to that of the parent pipe but the ductility and toughness of the joint are lower than that of the parent pipe yet sufficient that, when tested destructively, the weld fails in ductile mode as opposed to brittle failure.

The next section looks at the life prediction of HDPE parent pipe and butt weld fusion joints in the field.

5.2.5. Fatigue Data

- *Test Conditions*

When establishing test data for materials, it is important to consider the conditions under which the data is obtained as this will be relevant to the applicability of the data when it is used in assessing the capabilities of the subject component.

Brogden (2000) investigated the effect of many variables when fatigue testing PE100 used in piping systems for water transportation with specific consideration for the frequency, R ratio, waveform and test method which were considered to have important implications on the fatigue life of water pipes.

The R ratio is the minimum peak stress over the maximum peak stress of the test piece, so for example, where the minimum test stress is 0, the R ratio would be R=0. It was found that for PE100, the fatigue life showed little difference for R ratios between 0 and 0.3.

Of the three test methods considered by Brogden (2000), rotational bending (RB), three-point bending (3PB) and single edge notch (SEN) it was found that the RB testing gave a reduced life compared to 3PB and SEN. RB testing gives a full stress reversal, i.e. R=-1, and this reduction in life was attributed to a lower modulus under compression.

Testing by Brogden (2000) showed no effect for test frequencies of between 0.1 – 1.1 Hz which was in agreement with Channell & Cawood (1989) who found no effect for test frequencies of between 0.1 – 10Hz. However, it was found that RB tests at low frequencies of 0.001 Hz showed a slightly reduced lifetime for PE100 and, although the effect was small, was attributed to the duration that the test piece was placed under compressive load and also to toughening of PE100 at higher frequencies due to a higher strain rate.

Of the three Waveforms considered; sinusoidal, square and triangular, it was found that these had little effect on the fatigue life of PE100.

The failure mode for the test pieces were primarily ductile, the exception being the 3PB of thick walled PE100 at high stress levels which exhibited brittle failure. It was noted that the fatigue limit for PE80 in low stress levels exceed 7 million cycles.

Brogden (2000) references several publications that all indicate a decrease in fatigue life with an increase test temperature with the lower test temperature generally being the ambient laboratory temperature of approximately 22°C. However, tests in water by Takahara et al (1981) gave increased lifetimes which indicates that good heat transfer to the surroundings improves fatigue life.

- *Parent Pipe*

Using samples from a 200mm dia x 12.7mm wall thickness PE100 pipe, Djelbi et al (2014) perform uniaxial loaded fatigue testing at a frequency of 2Hz and a stress ratio of R=0 at room temperature. From these tests, and using two methods, two SN curves are presented in the form of Basquins equation:

$$S_{max} = 32.46 * N^{-0.067}$$

$$S_{max} = 32.24 * N^{-0.068}$$

Using the same conditions, further testing by Djelbi et al (2015) provides a further SN curve for HDPE under two block loading in the form of Basquins equation, which is commonly used to model the SN curve of HDPE:

$$S_{max} = 33.5 * N^{-0.0728}$$

This SN curve was then used to perform damage calculations using three different techniques, from which Miners method is deemed to be a good predictive tool.

The three SN curves presented in the above references are plotted in Fig. 5-9 below and show similar characteristics.
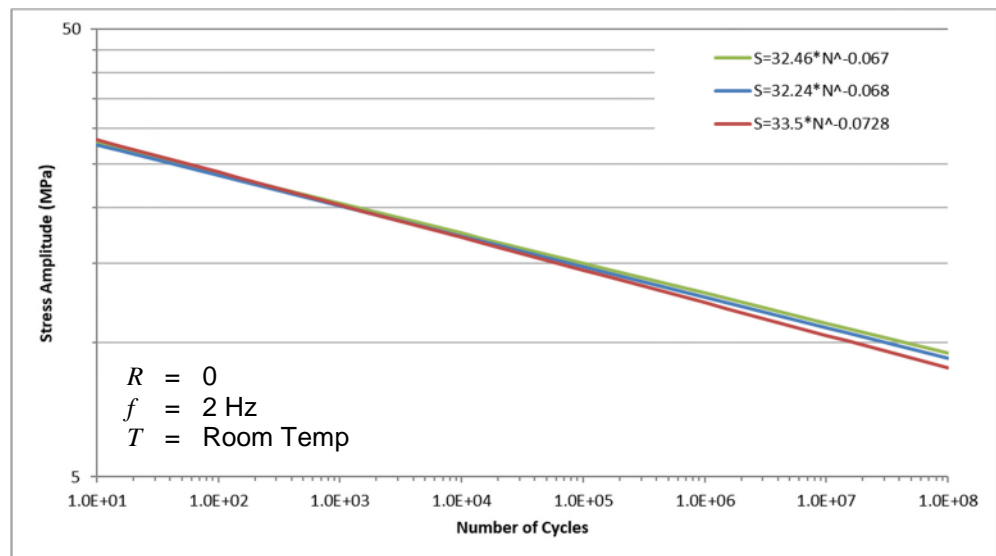
Fig.5-9: SN Curves for PE100 Pipe (Djelbi et al)

Samples from a of 125mm dia. x 11.5mm wall thickness PE100 pipe were used to develop the Wohler curve presented by Intec (Intec Engineering BV, 2008) as shown in Fig. 5-10.
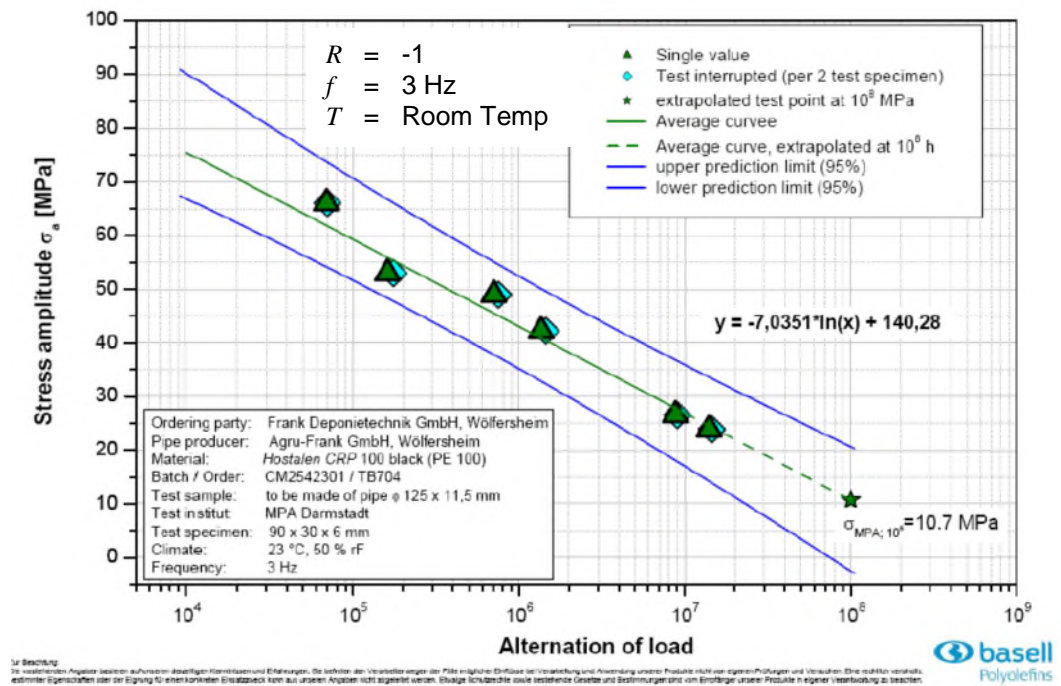
Fig.5-10:   Wohler Curve for PE100 Pipe (Intec)
(Intec Engineering BV, 2008)

These fatigue tests were conducted at 23°C at a frequency of 3Hz and a stress ratio of R=-1.

From the Wohler Curve shown in Fig.5-10, the lower prediction limit (-95%) is presented by Intec Engineering (2010) as the minimum SN Curve for PE100 as shown below in Fig.5-11.
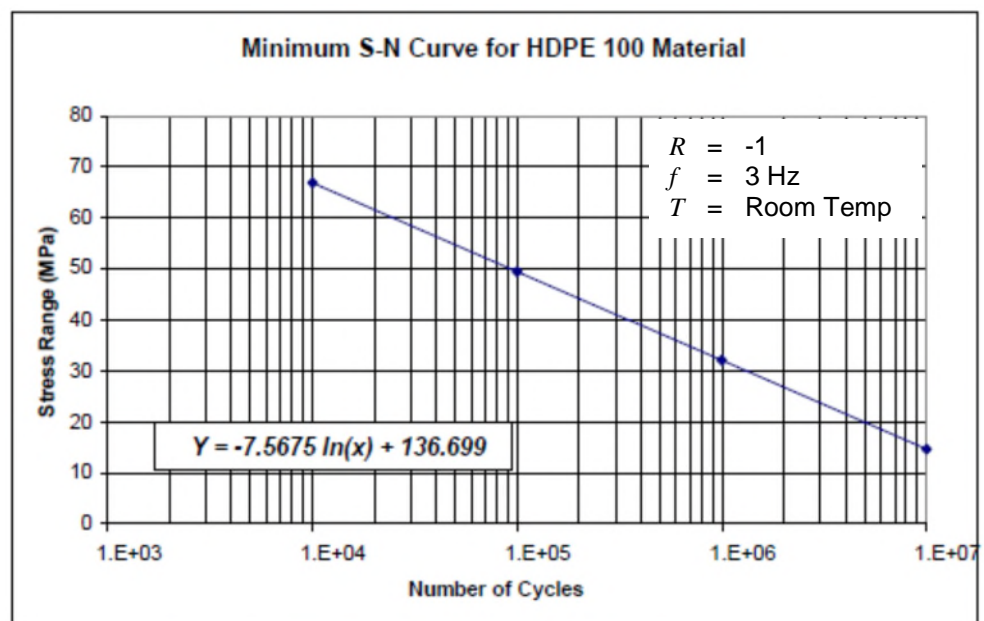
Fig.5-11:   SN Curve for PE 100 Pipe (Intec)
(Intec Engineering BV, 2010)

By expressing the Intec SN curve in Fig.5-10 as 'Stress Amplitude', i.e. R=0, and comparing it with the Djelbi SN Curves, it can be seen from Fig.5-12 that, Intec data is more onerous at the region below the PE100 design stress (<10MPa) and therefore a more conservative selection for the fatigue assessment.
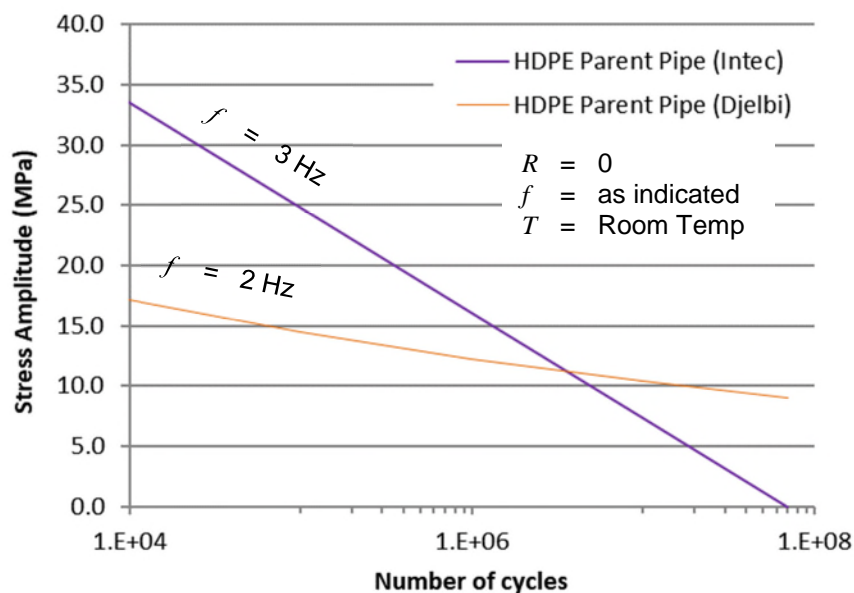
Fig.5-12:   PE100 Pipe SN Curve Comparison

Note that the difference in test frequency f is unlikely to contribute to the difference in test data as demonstrated by Channell & Cawood (1989).

- *Butt Weld*

As described in the previous paragraph, during the butt weld fusion process of HDPE pipes, a weld bead is formed on the inside and outside surfaces of the pipe as shown in Fig. 5-8.

Bergstrom et al (2004) identified from tensile creep tests that weld failure is nearly always initiated from the outside of the pipe wall at one of the weld beads and consequently performed further testing of welds, with and without beads, to determine the effect of this on the time to failure. The results from these tests indicated that, by removing the inner and outer weld beads, the time to failure was significantly increased by a factor of approximately 10, however, this was still only in the region of 20-40% of the time to failure of the parent material.

Although Bergstrom et al (2004) concluded that the exact mechanism for the increased time to failure due to weld bead removal is not clear, the butt weld fusion standard WIS 4-32-08 (Water UK, 2016) has adopted this practice and states that the outer bead must be removed after cooling of the weld.

Becetel (2009) performed fatigue testing on samples from PE 100 pipe 1200mm dia. x 70mm wall thickness (similar in size to that under consideration for this research study). These test samples included a circumferential fusion butt weld within each test piece from which the weld bead was removed.

The tests were conducted at 23°C with a stress ratio R=0 and at a test frequency of 1.05Hz, except the test at 1MPa which was at a frequency of 9Hz, but still within the range of no effect demonstrated by Channell & Cawood (1989).

The test data is reproduced in Table 5-11 below:

Stress (MPa)	Number of Cycles to Failure
8.5	203,818
6.4	541,485
3.8	2,302,195
3.0	5,413,974
2.0	13,896,106
1.0*	>180,000,000**

*Test Frequency 9Hz (all other tests at 1.05Hz)

**Sample was still running at end of test period

Table 5-11:   HDPE Fatigue Test Results (Becetel)

A statistical analysis of the raw test data was performed in accordance with the industry recognised standard ASTM E739 (ASTM, 2015) details of which are presented in the Portfolio [Section 6.0].

This produced the usable SN Curve as shown in Fig.5-13.
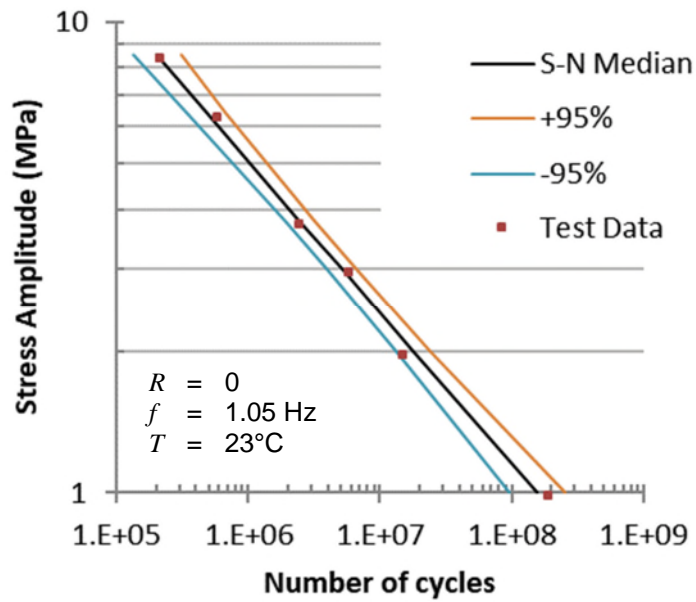
Fig.5-13:   PE100 Butt Fusion Weld SN Curve (Becetel)

During the Becetel testing, two samples were tested with the weld bead left in place and the cycles to failure recorded as shown in Table 5-12.

Stress (MPa)	Number of Cycles to Failure
9.0	24,571
6.0	132,297

Table 5-12:   HDPE Fatigue Test Results – Beaded Weld (Becetel)

Although only two samples were tested, an SN curve can be established for comparison purposes by determination of the material constants for Basquins equation as follows:

Basquins Equation:

$S = A*N^b$ (Stephens, et al., 2001, p. 84)   eq.1

and by taking logs:

$$log\ (S_{max}) = log\ A + b\ log(N) \qquad\qquad\qquad eq.2$$

and substituting upper and lower values from test data:

$log\ (9) = log\ A + b\ log(24{,}571)$ so;

$$log\ (9) = log\ A + 4.39*b \qquad\qquad\qquad eq.3$$

$log\ (6) = log\ A + b\ log(132{,}297)$ so;

$$log\ (6) = log\ A + 5.12*b \qquad\qquad\qquad eq.\ 4$$

then subtracting eq.4 from eq.3 and simplifying:

$$b = \frac{log\ (6) - log\ (9)}{0.7311}$$

therefore: $\boldsymbol{b = -0.2408}$

and from eq. 4: $A = \dfrac{6}{10^{5.12*b}}$

therefore $\boldsymbol{A = 102.66}$

$$\boldsymbol{S_{max} = 102.66*N^{-0.240891}}$$

which can be plotted with the unbeaded weld as shown below in Fig.5-14.
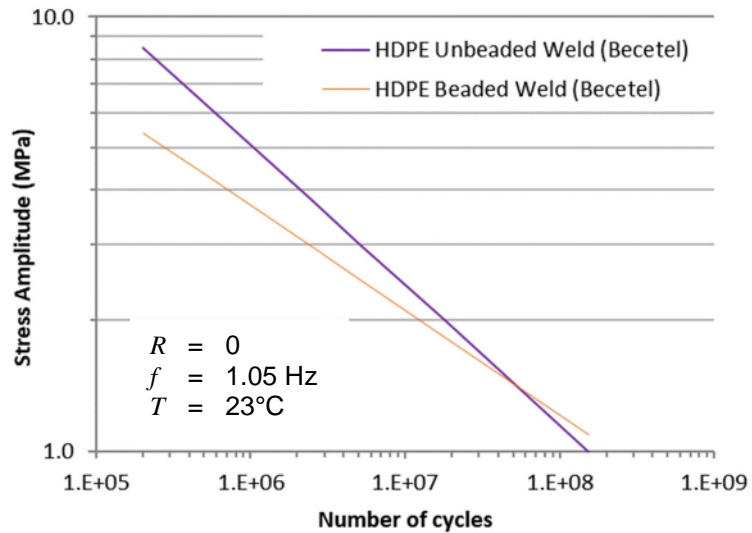
Fig.5-14:   Beaded v Unbeaded Weld SN Curve (Becetel)

The convergence between the two sets of data at the lower stress levels may be partly explained by the non-completion of the Unbeaded Weld test at 1MPa and the limited number samples for the Beaded Weld tests, nonetheless this does agree with the previous discussion whereby the removal of weld beads improves the fatigue life.

Testing of butt fusion welds by Adams et al (2014) included a traditional and a new transition joint, for components with different wall thicknesses. The design of the new transition joint was such that it was representative of a weld between pipes of the same wall thickness (as opposed to the traditional design where the weld was between a parallel wall pipe and a tapered wall pipe) as shown in Fig. 5-15.

Traditional Transition Joint
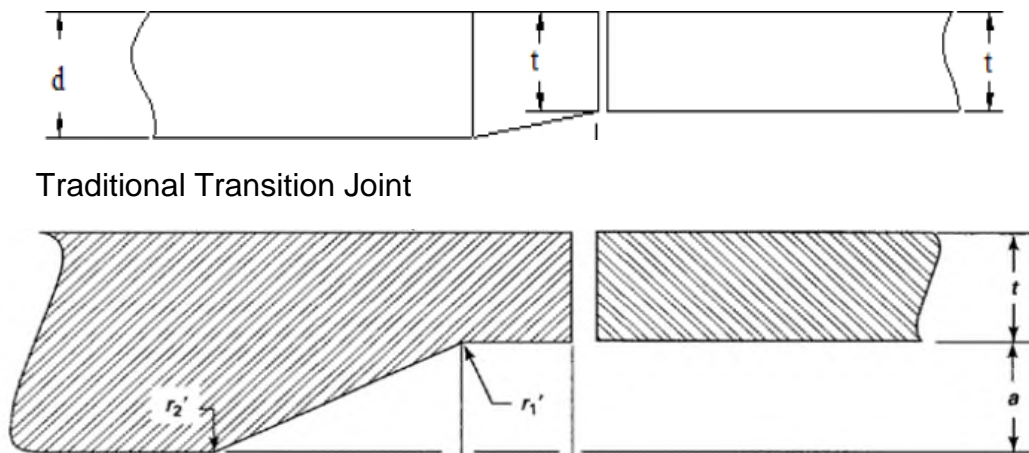
New Transition Joint   (Adams, et al., 2014)

Fig.5-15:   Traditional & New HDPE Weld Transition Joint

These tests were performed with a stress ratio R=0 and at a temperature of 70°F (~21°C), and although not stated, the test setup uses a hydraulic actuator to displace the test sample so it is assumed the test frequency is relatively low.

The results of these indicated that time to weld failure for both types of transition joints was similar, and the following SN curves were produced from the testing:

New Transition: $S_{max} = 11659 * N^{-0.149}$ (where S_{max} is in psi)

Old Transition: $S_{max} = 8420 * N^{-0.12}$ (where S_{max} is in psi)

which can be plotted as shown below in Fig. 5-16
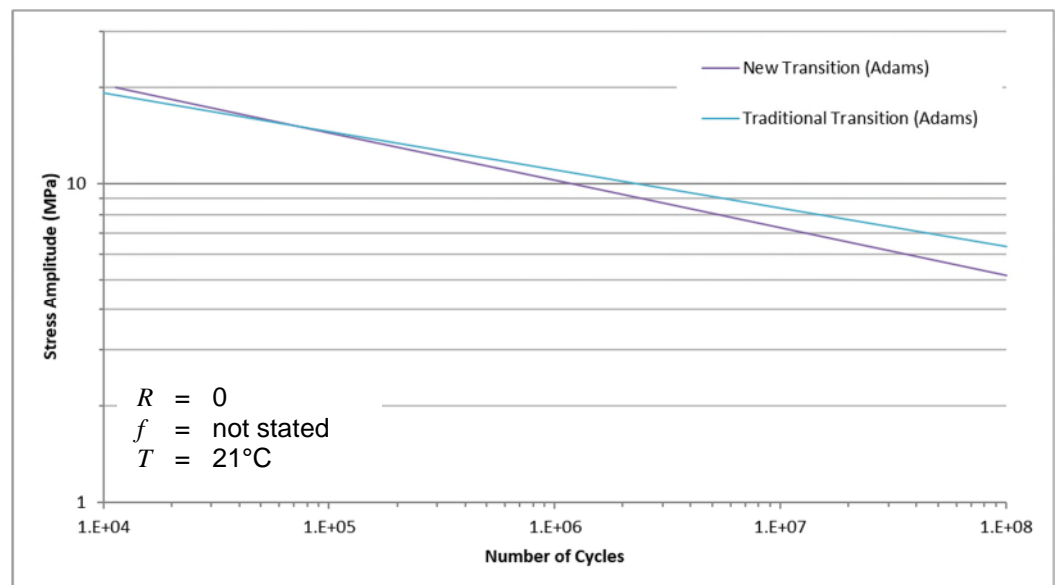
Fig.5-16:   SN Curves for Traditional & New HDPE Weld Transition Joint

It was observed that for the new transition joint, the failure point moved from the fusion joint into the parent pipe. From this Adams et al (2014) conclude that the Stress Intensification Factor (SIF) for these fusion joints will be 1.0. It should be noted that this testing was performed on thin walled pipe and although not stated, from the photographic evidence, the welds beads were left intact on the fusion joints

- *Stress Intensification Factors*

By comparing the parent pipe weld SN data against the butt fusion weld SN data, it can be seen that the butt fusion weld generally has lower fatigue life prediction, especially at the upper stress ranges, as illustrated below in Fig. 5-17
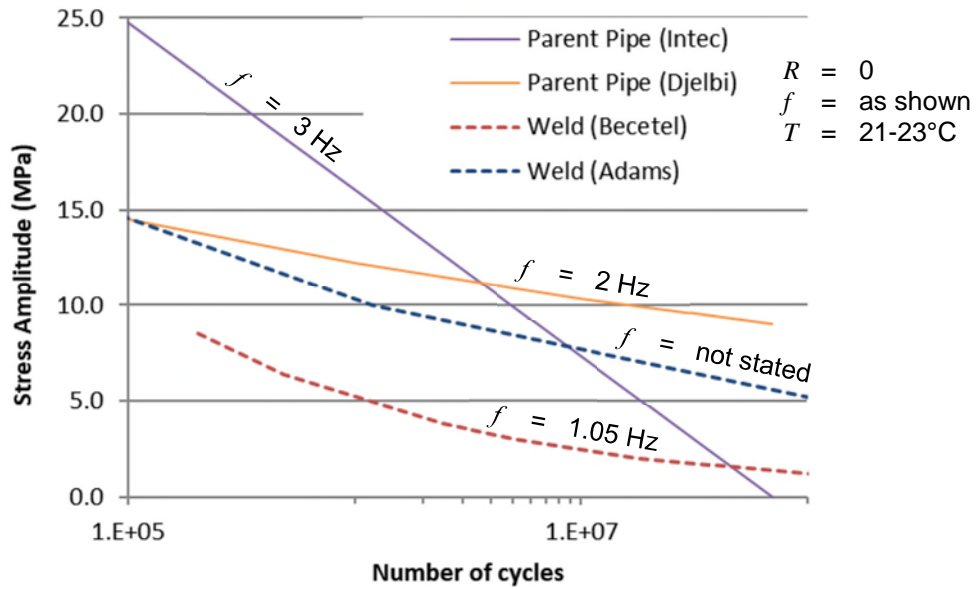
Fig.5-17:   Comparison of SN Curves for Parent Pipe v Butt Fusion Weld

Some points to note when comparing the above SN data, the Weld (Adams) is obtained from thin walled HDPE pipe, whereas the Weld (Becetel) is obtained from thick walled HDPE pipe. Also, the Parent Pipe (Djelbi) is obtained by uniaxial loading, whereas the Parent Pipe (Intec) is obtained by stress reversal through bending.

Although Adams (2014) concludes that the SIF for the fusion joints is 1.0 when compared to the parent pipe, the above comparison suggests that this is very much dependent upon the test conditions.

Kalyanam et al (2015) indicate that a well-known failure mode in HDPE piping is slow crack growth (SCG) which occur from flaws under sustained stresses and when the flaw is in a butt fusion joint, the time to failure is markedly different than when located in the parent material. Further work by Kalyanam et al (2016) compares the SCG of parent and joint HDPE materials through experimental analysis concludes that in the modern bimodal HDPE materials (such as PE100) lower SCG resistance of the joint

material persists and that the failure time (in creep tests) is two orders of magnitude smaller in the butt fusion joint than that of the parent material.

By comparing the predicted life of the parent pipe and butt fusion weld, it is possible to illustrate the SIF for the butt fusion weld.

Using the SN data from the Becetel tests (unbeaded and beaded samples) and the Adams tests (traditional and new transition joints), a stress factor is applied so that the predicted number of cycles equates to the non-factored predicted number of cycles of the parent pipe SN data presented by Djelbi.

These stress intensification factors (SIF) can be plotted for each data set against the stress amplitude to show the trend of the butt fusion weld against the parent pipe, as shown in Fig.5-18.
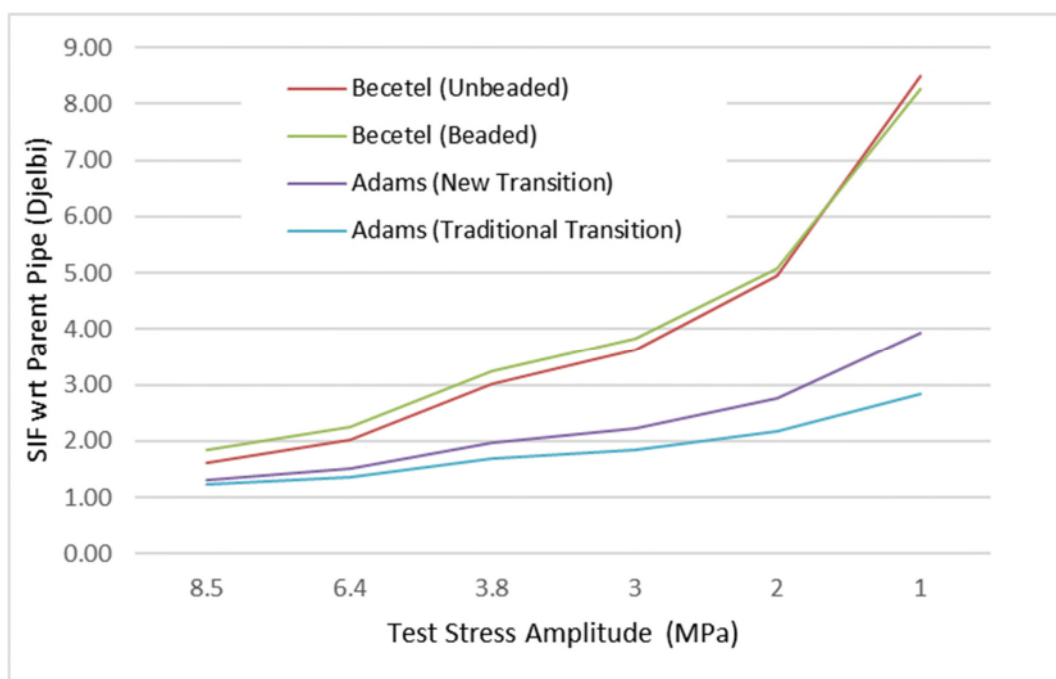
Fig.5-18:   SIF Butt Fusion Welds v Parent Pipe (Djelbi)

It can be seen that the general trend is that the SIF increases as the test stress amplitude decreases, with the Becetel tests (on thick walled pipes) increasing more severely.

The same data was then compared against the parent pipe SN data presented by Intec and is presented below in Fig.5-19.
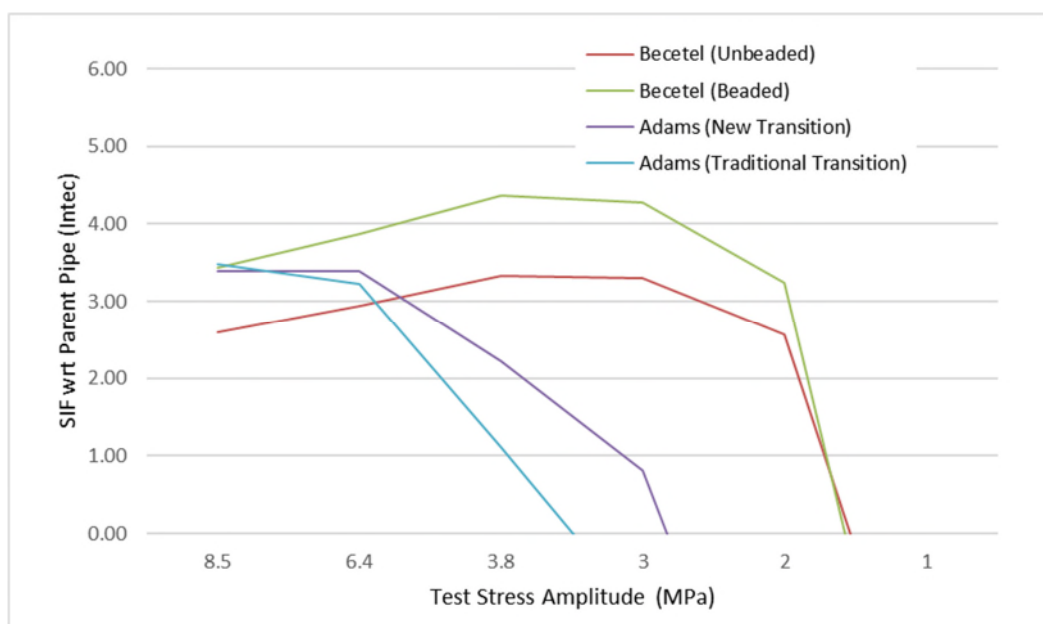
Fig.5-19:   SIF Butt Fusion Welds v Parent Pipe (Intec)

It can be seen that the trend here is the opposite of the previous data set, where the SIF generally decreases as the test stress amplitude decreases. This suggests that butt fusion welds subject to bending tend towards a similar fatigue lift as parent pipe subject to bending at lower stress amplitudes. Conversely, when compared against butt fusion welds subject to bending, the fatigue life of parent pipe subject to axial loading increase significantly at lower stress amplitudes. This highlights the importance of test conditions when selecting SN data for fatigue assessment.

Due to the bending of SWIR in operation, it is considered that the Becetel weld data and the Intec parent pipe data are more aligned with the characteristics and behaviour of the HDPE pipe application in this study.

5.2.6. Material Properties considered for this study

- *Physical Properties*

Description	HDPE Pipe	
	40"NB[1]	60"NB[1]
Outside Diameter (m)	1.067	1.600
Inside Diameter (m) [2]	0.985	1.478
Section Length (m)	11.5	11.5
Section weight [in air] (kg) [3]	1,451	3,239
Section weight [in water] (kg) [3]	-107	-237

Table 5-13:   HDPE Pipe – Physical Properties

1) Dimensions in accordance with ASTM F714 (ASTM, 2013)

2) Wall thickness ratio DR26

3) Based on SG of 0.955 (PPI, 2004)

- *Mechanical Properties*

Description	HDPE Pipe			
	40"NB		60"NB	
	Short Term	*Long Term*	*Short Term*	*Long Term*
Creep Modulus (N/mm^2) [1]	800	239	800	239
Allowable Stress (N/mm^2) [2]	9	6.15	9	6.15
Poisson's Ratio [3]	0.40		0.40	
Minimum Bend Radius (m) [4]	36.28		54.40	

Table 5-14:   HDPE Pipe – Mechanical Properties

1) Values in accordance with DVS 2205 (DVS, 2015)

2) Values determined from (DVS, 2015) as follows:

Allowable Stress $\quad K_d = \dfrac{K_k * f}{y_M * A1 * A2} \quad$ (DVS, 2015) eq. 3

where: $\quad K_k$ (short term)   = 13 N/mm^2

$\quad K_k$ (long term)   = 10 N/mm^2

$\quad$ f (short term)   = 0.9

$\quad$ f (long term)   = 0.8

$\quad y_M$ = 1.3

$\quad$ A1 = 1

$\quad$ A2 = 1

3) Value from Plastic Pipe Institute (PPI, 2004)

4) Calculated using 34 x OD (PPI, 2009)

- *Fatigue Properties*

Description	HDPE Pipe	
	40"NB	**60"NB**
Parent Pipe:	Ref. Fig.5-12 (Intec)	
Butt Fusion Weld:	Ref. Fig. 5-13 (-95% Conf Band)	

Table 5-15: HDPE Pipe – Fatigue Properties

It should be noted that the testing of the HDPE butt fusion weld was undertaken with a stress ratio of R=0 therefore the SN data generated has a positive mean stress.

However, for the parent pipe, the SN data has a stress ratio of R=-1 which is a full reversal and therefore has zero mean stress. As the system under consideration will always have a positive stress, it is necessary allow for a positive mean stress.

As described in section 5.1.4, the Goodman correction will be selected for the parent pipe in the Orcaflex fatigue results tool to allow for the mean stress effects.

5.3. Steel Pipe

5.3.1. Industry Codes & Guidelines

Steel pipe is used extensively in the offshore and marine industry for low pressure and high pressure applications. There are many different standards relating to steel pipe, mainly in relation to material grades, but a commonly used carbon steel grade is ASTM A106 (ASTM, 2015), whereas the most common dimensional standard is ASME B36.10 (ASME, 2004).

Steel pipe according to the above standards is readily available in diameters from 1/8"NB to 48"NB, and for sizes above 48"NB, material specification API 5L (API, 2013) is normally considered.

The pipe sections are generally supplied in lengths of 12m sections, for ease of handling and transportation, and can be connected together by welding directly to one another or else flanges can be welded to each pipe section end and the sections connected using stud bolts and nuts. Commonly used standards for carbon steel flanges are the dimensional standard ASTM B16.47 (ASME, 2011) and material grade ASTM A105 (ASTM, 2002).

For the purposes of this project, the above standards and specifications will be considered.

5.3.2. Fatigue Data

Fatigue data for carbon steel is readily available, and a number of industry codes provide SN curves for carbon steel in offshore and marine applications.

One such document is DNVGL-RP-C203 (DNVGL, 2016) which is an industry accepted recommended practice and provides a range of SN curves for steel (including steel submerged in seawater) and a methodology for fatigue damage calculations.

5.3.3. Material Properties considered in this study

The physical properties of carbon steel are widely documented although for the purposes of this project, the properties provided in the standards described in the above paragraph will be considered. Furthermore, the industry adopted standard for piping design is ASME B31.3 (ASME, 2014), which provides allowable design parameters for a range of piping components, will also be considered.

- *Physical Properties*

Description	Steel Pipe	
	40"NB[1]	60"NB[1]
Outside Diameter (m)	1.016	1.524
Inside Diameter (m) [2]	0.978	1.486
Section Length (m)	11.5	11.5
Section weight [in air] (kg)	5,386	8,130
Section weight [in water] (kg)	4,683	7,070

Table 5-16: Steel Pipe – Physical Properties

1) Dimensions in accordance with ASME B36.10 (ASME, 2004)
2) Wall thickness 19.05mm

- *Mechanical Properties*

Description	Steel Pipe	
	40"NB	60"NB
Young's Modulus (N/mm^2) [1]	203,450	203,450
Allowable Stress (N/mm^2) [1]	137.9	137.9
Poisson's Ratio [1]	0.3	0.3
Minimum Bend Radius (m) [2]	749	1124

Table 5-17: Steel Pipe – Mechanical Properties

1) Value from ASME B31.3 (ASME, 2014)
2) Calculated using maximum bending stress of 137.9 N/mm^2

- *Fatigue Properties*

Description	Steel Pipe	
	40"NB[1]	60"NB[1]
Parent Pipe SN Curve [Category C] [2]:		
log a1 =	12.192	12.192
log a2 =	16.320	16.320
m1 =	3.0	3.0
m2 =	5.0	5.0
Fatigue Limit @ 10^7 cycles (MPa)	73.10	73.10
Butt Weld SN Curve [Category D] [2]:		
log a1 =	11.764	11.764
log a2 =	15.606	15.606
m1 =	3.0	3.0
m2 =	5.0	5.0
Fatigue Limit @ 10^7 cycles (MPa)	52.63	52.63

Table 5-18: Steel Pipe – Fatigue Properties

1) Value from DNVGL-RP-C203 Table 2-2 (DNVGL, 2016)
2) Category selected as per DNVGL-RP-C203 Table A-9 (DNVGL, 2016)
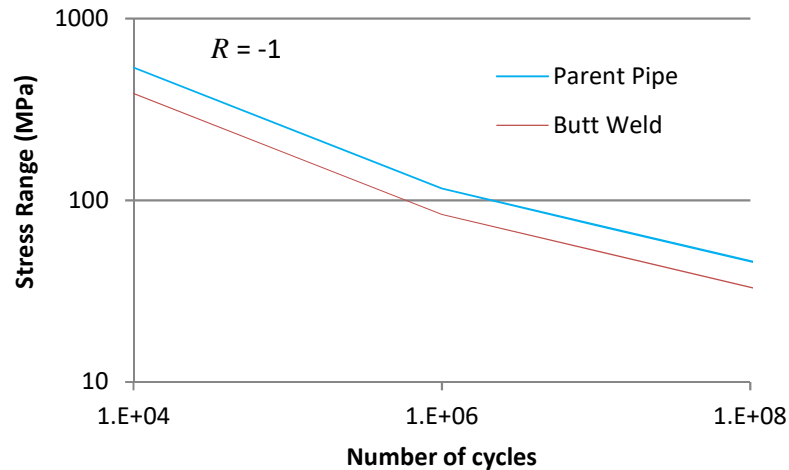
Fig.5-20:   Steel Pipe SN Curves

It should be noted that the SN data has a stress ratio of R=-1 which is a full reversal and therefore has zero mean stress. As the system under consideration will always have a positive stress, it is necessary allow for a positive mean stress.

As described in section 5.1.4, the Goodman correction will be selected for the parent pipe and butt welds in the Orcaflex fatigue results tool to allow for the mean stress effects.

5.4. Summary

The above review has demonstrated that for flexible rubber pipes and HDPE pipes, there is limited data available, particularly in regard to fatigue capabilities.

For the flexible rubber pipe section, a Finite Element Analysis (FEA) was undertaken to obtain further data concurrent with the physical testing of the reinforcement material to determine its fatigue characteristics. Similarly, compression testing and tensile testing of the rubber compound was performed to determine its stiffness characteristics. The FEA highlighted that the bending stiffness of the flexible rubber pipe was dominated by the rubber stiffness. It also highlighted that a flexible rubber pipe with textile reinforcement had better fatigue characteristics than the same flexible rubber pipe reinforced with steel cord.

It was found that, for the grade of High Density Polyethylene (HDPE) under consideration, the availability of fatigue data for the parent pipe, and more specifically for butt fusion welds, was also limited. However, available fatigue

data sets for parent pipe were compared with each other and it was found that the fatigue test method contributed to the fatigue life predictions of the HDPE parent pipe. This was also the case for the available fatigue data for the butt fusion welds. The effect of various test conditions for HDPE pipe were reviewed which indicated that the test frequency, the R ratio and the test temperature of the fatigue data obtained had limited effect on the outcome of the test data. A review of the butt fusion jointing process found that, generally, the butt fusion weld has the same tensile strength as the parent pipe but has lower fatigue life. The relevant data sets were compared and trends for the Stress Intensifications Factors (SIF) of butt fusion welds established.

For the steel pipe, and also the steel components of the flexible rubber pipe, it was found that recognised industry codes and guidelines provided comprehensive material and fatigue data.

For each of the materials reviewed, the appropriate physical, mechanical and fatigue properties were established and will be used for the analysis of the system under consideration.

The next chapter will determine the optimum configuration for the system and analyse the strength and fatigue capabilities, and the flow assurance characteristics, of the proposed solution which is the sixth objective of the study.

CHAPTER 6.0

RISER MECHANICS

6. RISER MECHANICS

6.1. SWIR Configuration Selection

Using the materials detailed in Chapter 5, this Chapter investigates a number of SWIR configurations and identifies the most optimum solution which is then subject to a more detailed analysis in terms of strength and fatigue capabilities. A number of sensitivity studies are then undertaken on the selected configuration. This approach is generally in line with the preliminary configuration check in the WIR design flow chart presented by Cao et al (2015) as shown in Fig.2-13.

The following considerations are taken into account for the preliminary configuration check;

6.1.1. Function

From previous analyses of SWIR systems by the author, it is known that the highest bending is induced at the upper end of the flexible pipe string. This is primarily due to the ocean current profiles, which are highest at the surface and reduce with depth. Furthermore, the loads induced by the vessel motion are also primarily absorbed at the upper end of the flexible pipe string. Consequently, it is common practice to install a stiffer, more robust flexible rubber pipe section as the first section to accommodate the greater loads seen at the upper end of the flexible pipe string. Below this, a less stiff flexible pipe section is generally installed as there is less bending induced by the current and thus lower loads incurred. On a number of systems supplied into the field, these lower hoses have been manufactured from HDPE which is less flexible than a flexible rubber pipe but flexible enough to absorb the bending from the currents. On these systems, and due to the positive buoyancy of HDPE, it has been necessary to add ballast weight at the lower end of the flexible pipe string to ensure that the string maintains a positive load onto the riser seat and also to maintain the stability of the string in the ocean currents.

Using the above rationale and building on previous work undertaken by the author (Craig, 2014), the configurations for a 40"NB x 500m long SWIR shown below in Fig.6-1 are considered.
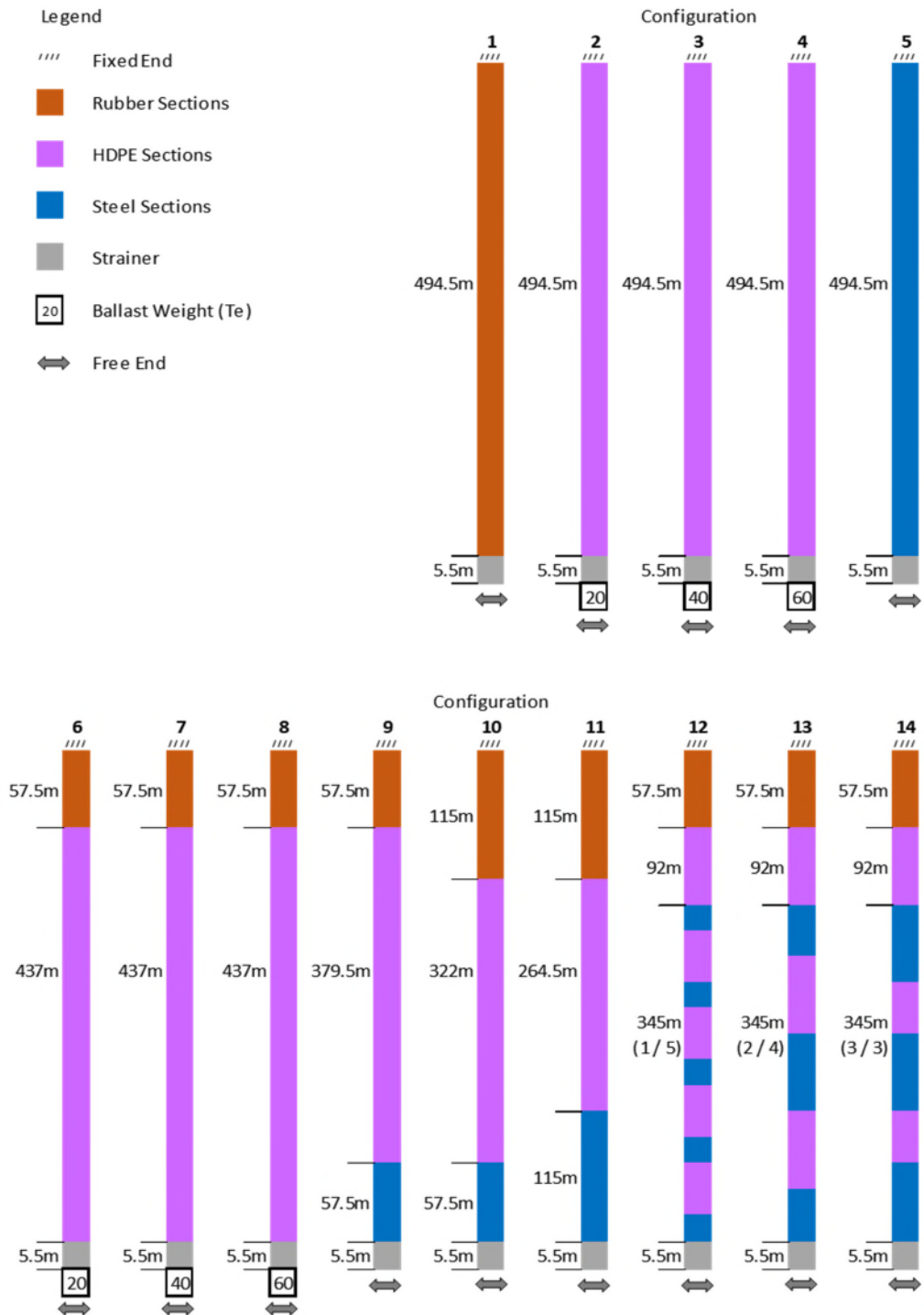
Fig.6-1: SWIR Configurations

Configurations 1 to 5 are uniform cantilevers, that is the material is the same for the complete length of the SWIR, and are included in the preliminary analysis primarily for comparison against the non-uniform configurations 6 to 14. The non-uniform configurations consist of a combination of materials to form the SWIR. It should be noted that configurations 2, 3 and 4 are all HDPE uniform risers but with differing ballast weights attached at the lower end. HDPE has positive buoyancy therefore a ballast weight is required to prevent the SWIR from 'floating' to the surface.

Configuration 6 to 14 all consist of flexible rubber sections at the upper end as, from the authors experience of systems on FPSO vessels, this is where the largest axial and bending loads occur.

For configurations 12, 13 and 14, the lower section consists of alternating steel and HDPE sections in the ratios shown (e.g. 1/5 = 1 Steel section after every 5 HDPE sections).

6.1.2. Stability

Two aspects are considered in terms of stability, namely impact of vortex induced vibration (VIV) and lower end excursion.

- *Vortex Induced Vibration*

As described in Section 2.7, VIV is induced by the ocean current flowing around the SWIR and which can lead to accelerated fatigue damage. It is therefore desirable to minimise the magnitude and frequency of the oscillation of the SWIR due to this phenomenon.

- *Natural Frequency of the SWIR*

The SWIR is in the form of a free hanging cantilever, fixed at the upper end and free at the lower end and for cantilevers with uniform properties, the natural frequencies can be determined using the empirical equation:

$$f_n = \frac{K_n}{2\pi}\sqrt{\frac{EIg}{wl^4}}$$

(Young, 1989) Table 36 Case 3

where f_n = Natural frequency

K_n = Constant for mode n of vibration

E = Modulus of Elasticity

I = area moment of inertia

g = gravitational acceleration

w = load per unit length (inc beam weight)

l = length of cantilever

The natural frequency of a cantilever is a function of its stiffness (EI) over its length (l), therefore, the stiffer the cantilever, the higher the natural frequency and the longer the cantilever, the lower the natural frequency.

Using the above equation for the materials under consideration, this relationship is illustrated in Fig. 6.2. It can be seen that a 100m long cantilever from steel has higher natural frequencies than the less stiff 100m HDPE cantilever, which in turn has higher natural frequencies than the least stiff 100m Bonded Rubber Pipe cantilever.
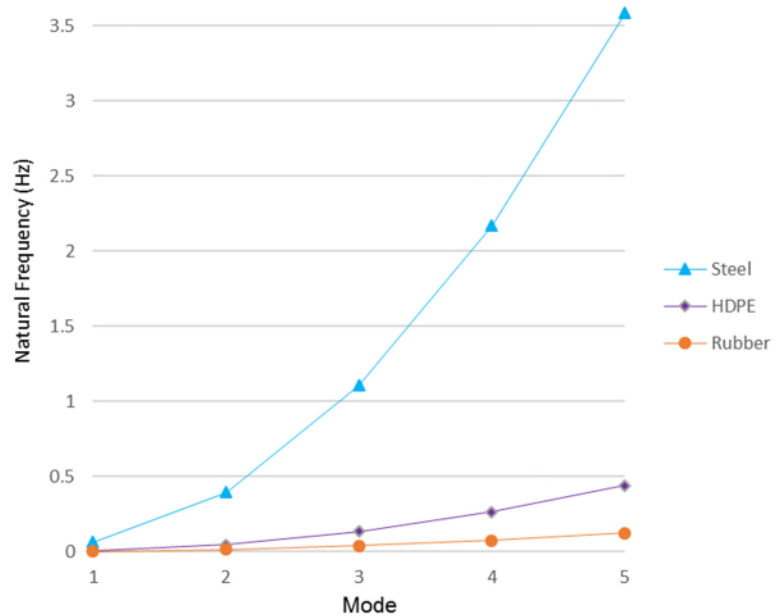
Fig.6-2: Natural Frequencies of 100m Cantilever

Fig.6-3 shows that for the Bonded Rubber Pipe cantilever, the natural frequency reduces as the length of the cantilever increases.
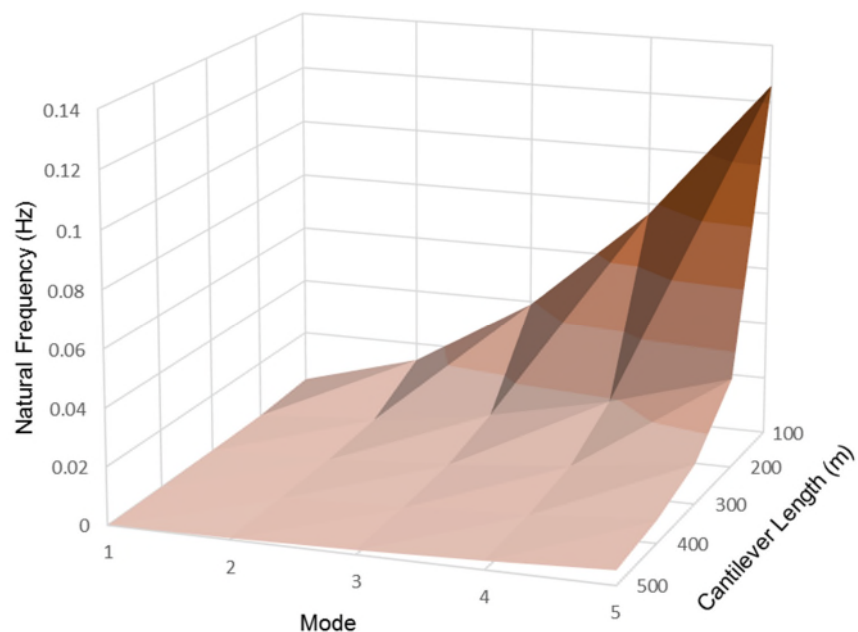
Fig.6-3: Natural Frequencies of Rubber Cantilever

Whereas, this empirical equation can be applied to uniform cantilevers with constant stiffness and mass, it cannot be applied to a non-uniform cantilever with varying stiffness and mass, such as the hybrid SWIR configurations under consideration and as shown in Fig.6-1.

Determination of the natural frequencies for a non-uniform cantilever is much more complex for which a number of techniques are available, for example, Abdelghany et al (2015) has presented a technique using differential transformation method whereas Al-Ansari (2012) identifies the modified Rayleigh model as a suitable method.

The Orcaflex software developed by Orcina (Orcina, 2014) derives the natural frequencies for uniform and non-uniform cantilevers by solving the static equation for the cantilever and creating the mass and stiffness matrices which are then solved using either the Lanczos algorithm or a tridiagonal matrix diagonalization method depending upon the number of nodes and degrees of freedom.

The cantilevers considered in Fig.6-2 were modelled in Orcaflex and the natural frequencies extracted and compared against those determined using the empirical equation and are shown in Fig.6-4.
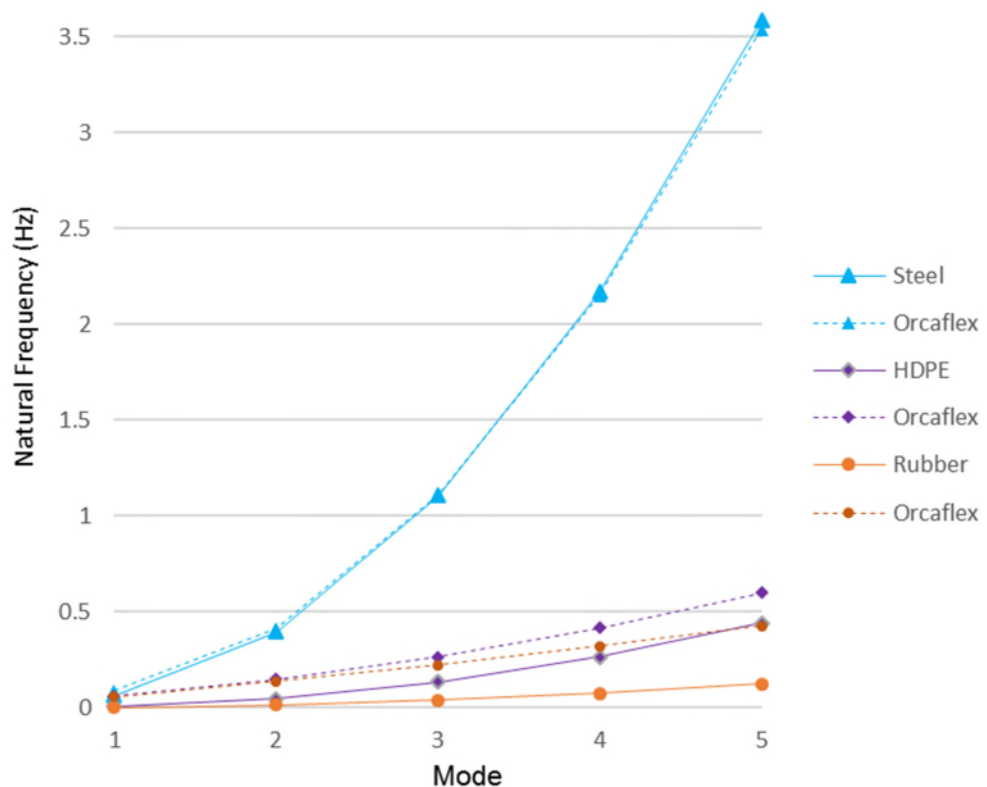
Fig.6-4: Comparison of Natural Frequencies of 100m Cantilever

It can be seen from the above figure that for the stiffest cantilever, there is good correlation between Orcaflex and the empirical equation. However, for the less stiff cantilevers, although the tendency of the natural frequencies is similar, the correlation is not as accurate especially for the higher modes.

However, this study does not intend to evaluate the accuracy of the various techniques and will use the industry accepted Orcaflex software tool to determine the natural frequencies for the hybrid SWIR.

- *Lower End Excursion*

It is generally desirable to minimise the excursion of the free end of the flexible pipe string for two main reasons. Firstly, to avoid any potential interference with mooring lines or other riser systems and secondly, the further the lower end excursion, the higher the intake point and thus an increase in water.

6.1.3. Loads induced by the SWIR

The loads induced into the vessel hull are a major consideration when optimising the SWIR. The vessel hull at the connection location needs to be designed with sufficient strength to accommodate tensile loads and bending moments induced by the SWIR, and the higher these loads, the stronger the structure needs to be, which generally means more steel and thus more weight.

It is therefore desirable to keep the induced loads as low as practicable into the hull structure, which is a function of the weight and flexibility of the SWIR, i.e. the lower the weight the lower the tensile load and the greater the flexibility the lower the bending moment.

Weight saving on any equipment package is advantageous to the global weight of the vessel, but an additional advantage in minimising the weight is the installation of the system. To minimise the costs of a high capacity lifting device or an external crane barge for installation (and retrieval for maintenance and inspection), it is desirable to keep the installation weight as low as is reasonably practicable.

6.1.4. Preliminary Analysis

The SWIR configurations shown in Fig.6-1 were modelled in Orcaflex and a static analysis performed so that the natural frequency of each SWIR configuration could be obtained by a modal analysis of the results.

Then a dynamic analysis of these configurations was performed to identify the stability of the line in terms of vortex induced vibration (VIV) response and lower end excursion due to current plus the comparable loadings into the vessel connection point.

A series of uniform currents from 0.1m/s to 1.5m/s were simulated for 500s to ensure that the VIV response became settled. The Orcaflex 'Milan Wake Oscillator' tool was selected for each configuration as this has shown good correlation with experiments for uniform currents.

6.1.5. Results

- *Natural Frequency*

The natural frequency of each configuration was extracted from the static analysis and are plotted below in Figs.6-5 & 6-6. As the natural frequency of configuration 5 (uniform steel SWIR) is exceptionally high, it is omitted from Fig.6-6 for clarity.
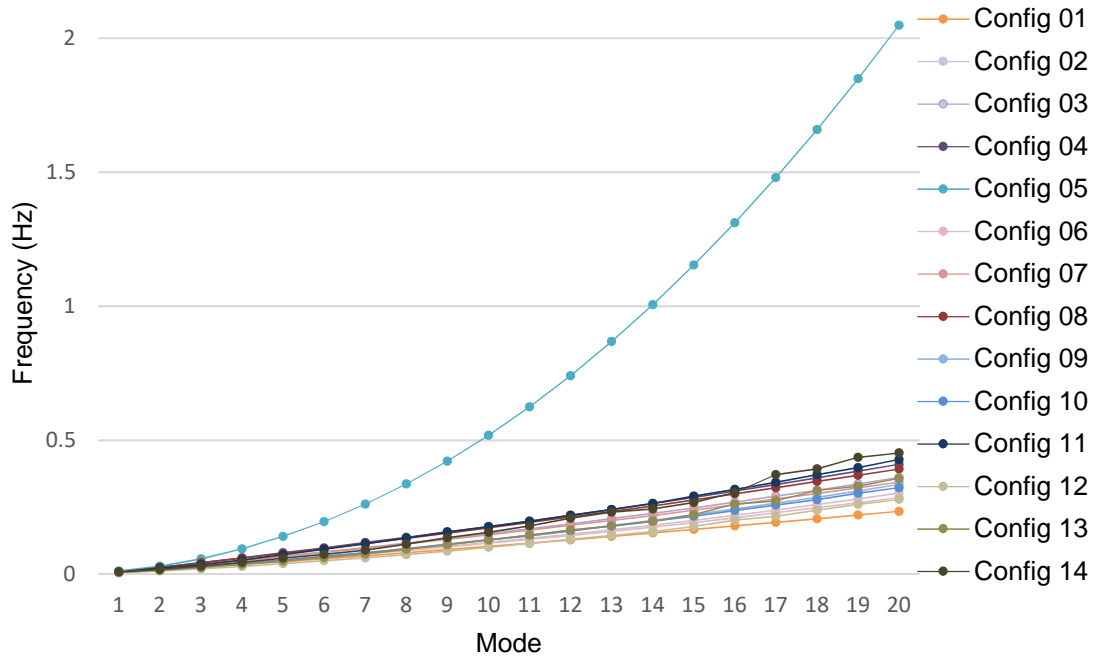
Fig.6-5: Natural Frequency of SWIR Configuration
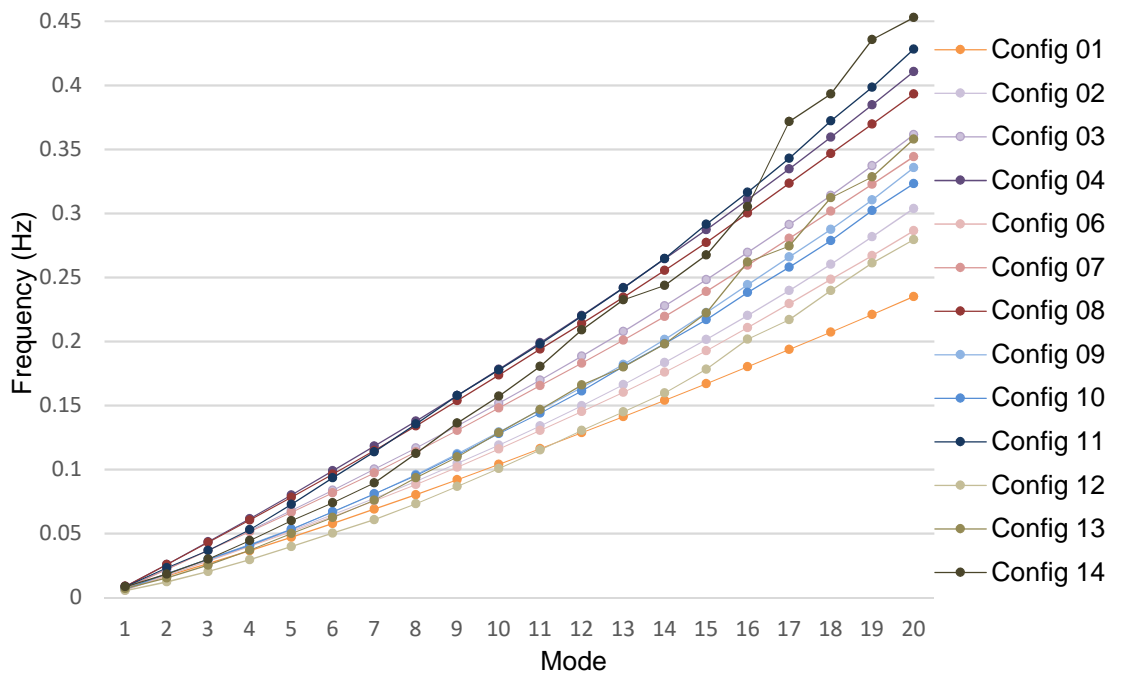
Fig.6-6: Natural Frequency of SWIR Configuration (excl. 5)

- *VIV Response*

The VIV response of each configuration was extracted from the dynamic simulations in the form of maximum VIV offset amplitude and maximum VIV offset curvature and are plotted below in Figs.6-7 and 6-8 respectively:
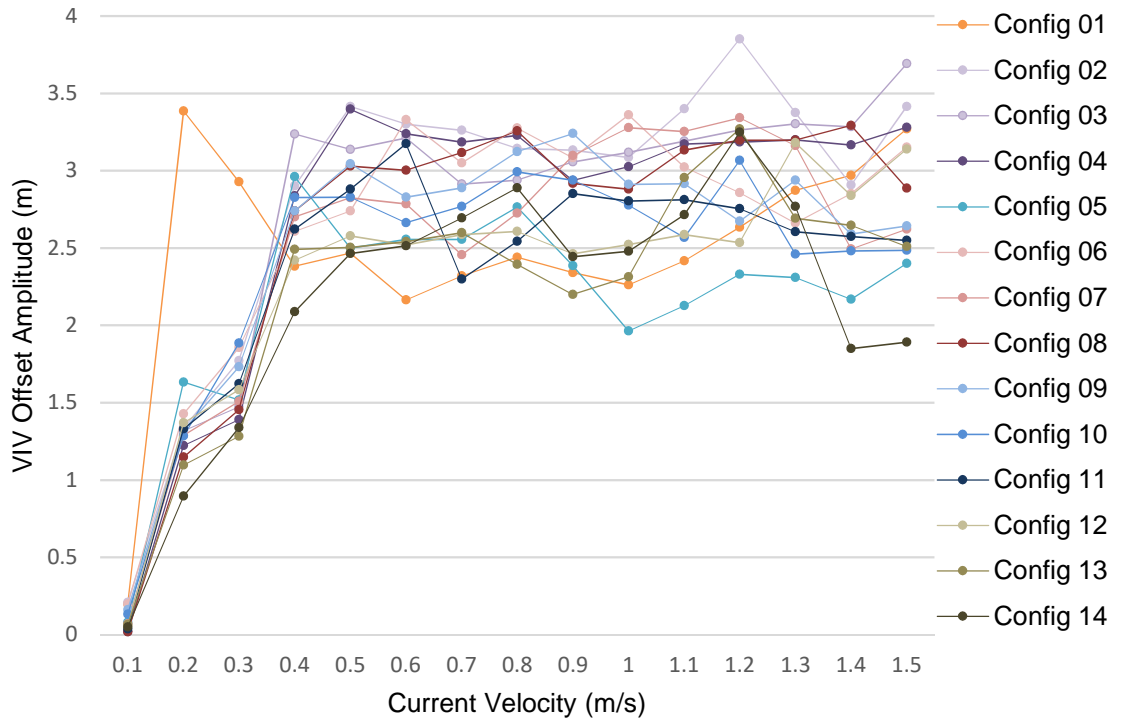
Fig.6-7: Maximum VIV Offset Amplitude of SWIR Configurations
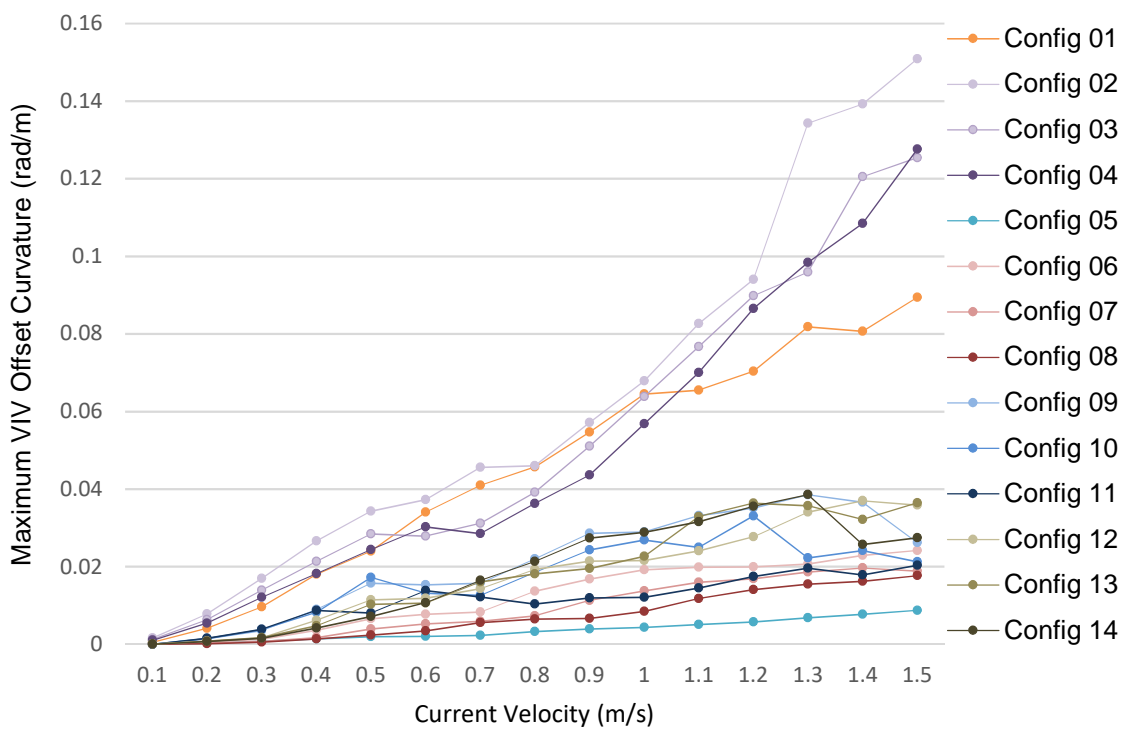
Fig.6-8: Maximum VIV Offset Curvature of SWIR Configurations

- *Lower End Excursion*

The maximum lower end excursion in metres was extracted from each of the dynamic simulations and are plotted below in Fig.6-9.
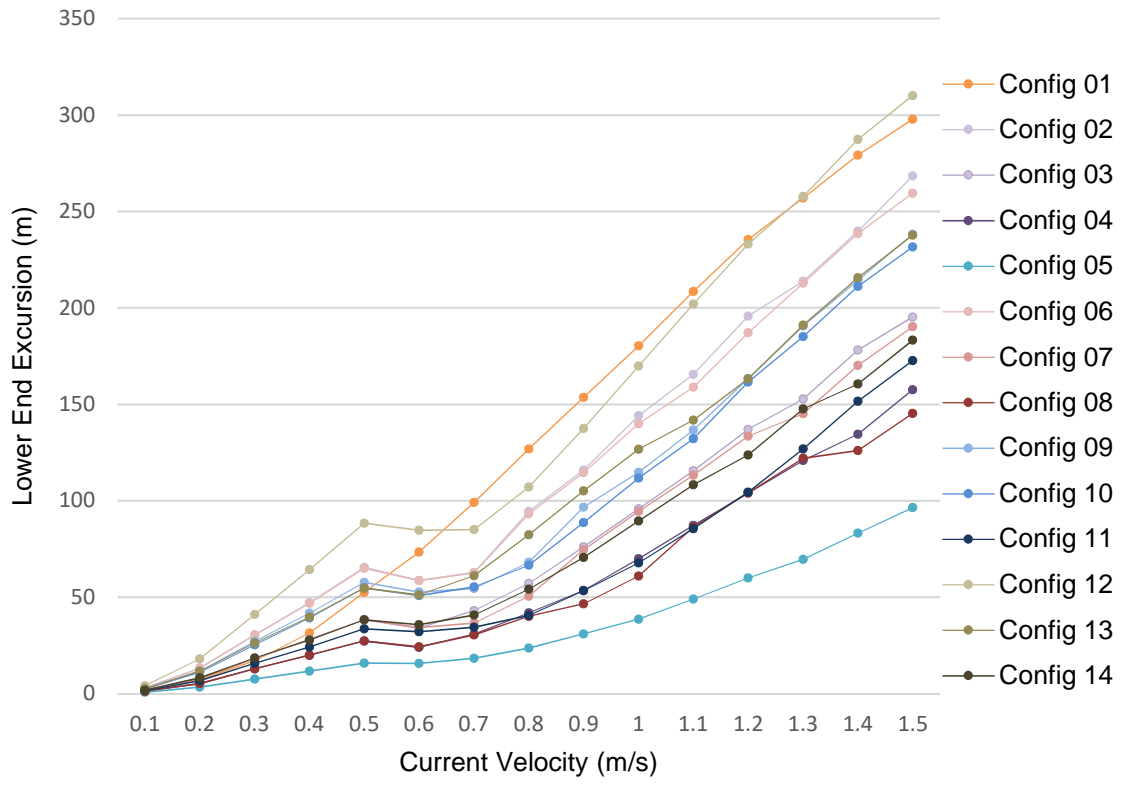
Fig.6-9: Maximum Lower End Excursion of SWIR Configurations

- *Loading into Connection Point*

The maximum loads into the hull connection point in terms of tension and bending moment were extracted from the dynamic analysis for each configuration and are plotted below in Figs.6-10 thru 6-13. As the loads from configuration 5 (uniform steel SWIR) are exceptionally high, they are omitted from Figs.6-11 and 6-13 for clarity.
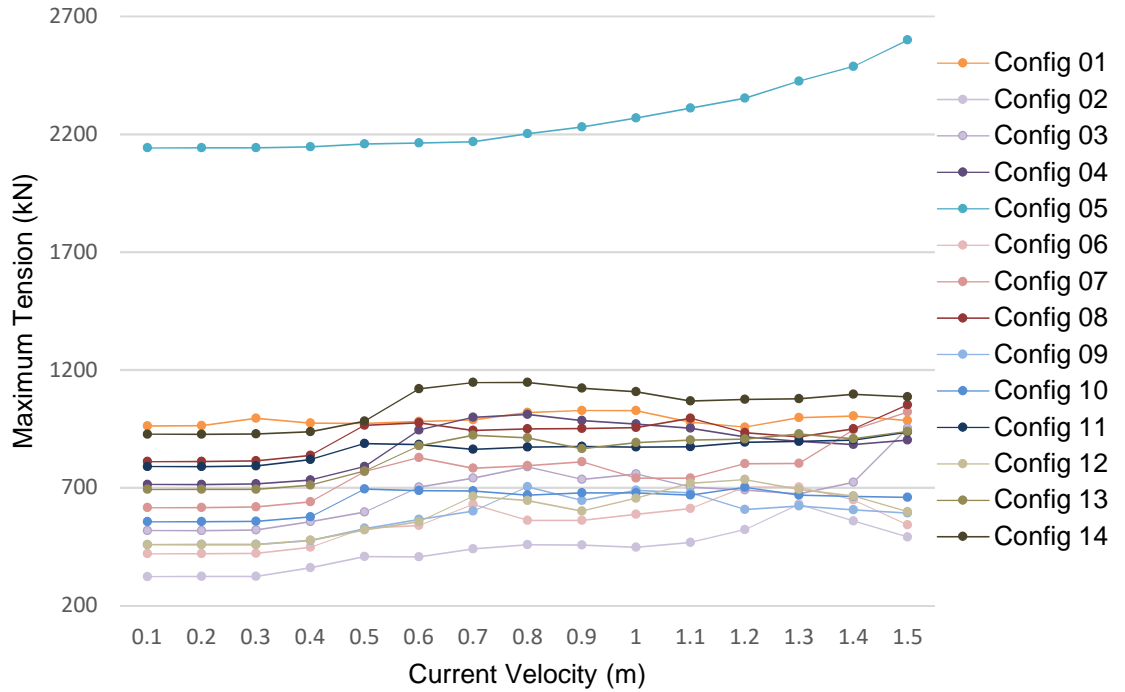
Fig.6-10:   Maximum End Tension of SWIR Configurations
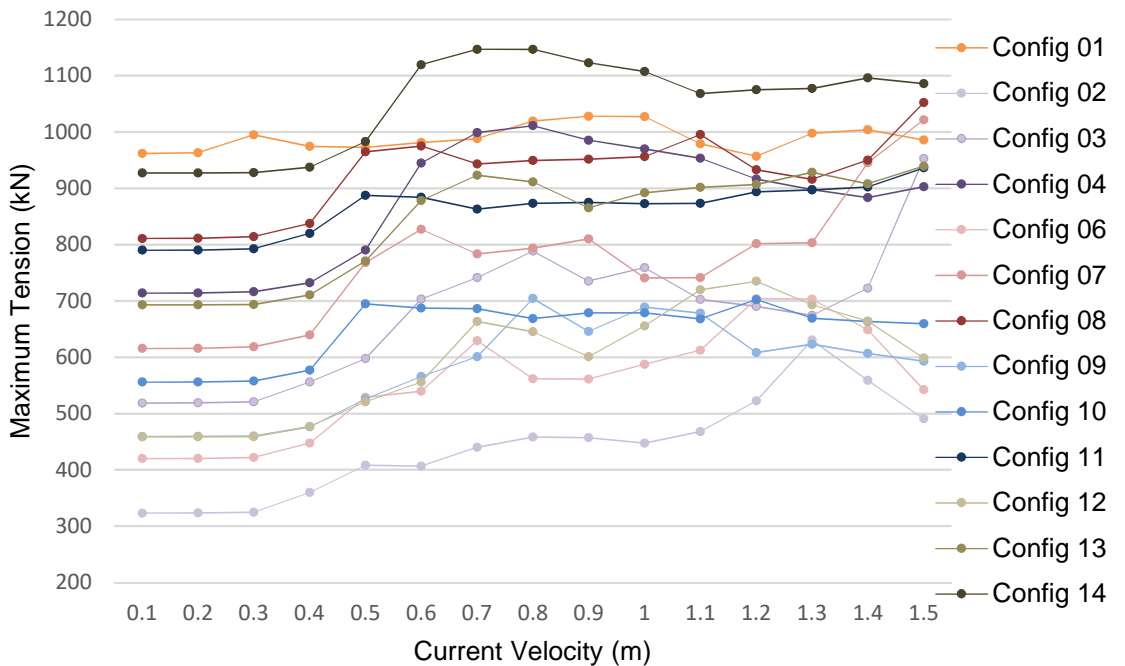
Fig.6-11:   Maximum End Tension of SWIR Configurations (excl. 5)
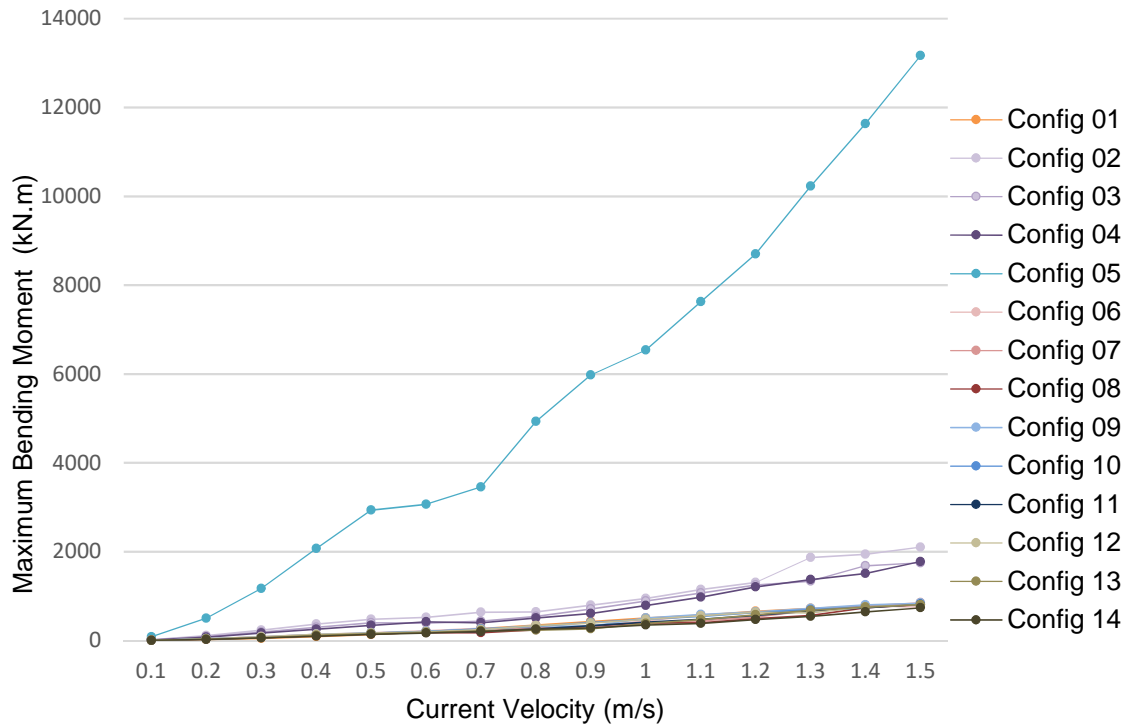
Fig.6-12:   Maximum Bending Moment of SWIR Configurations
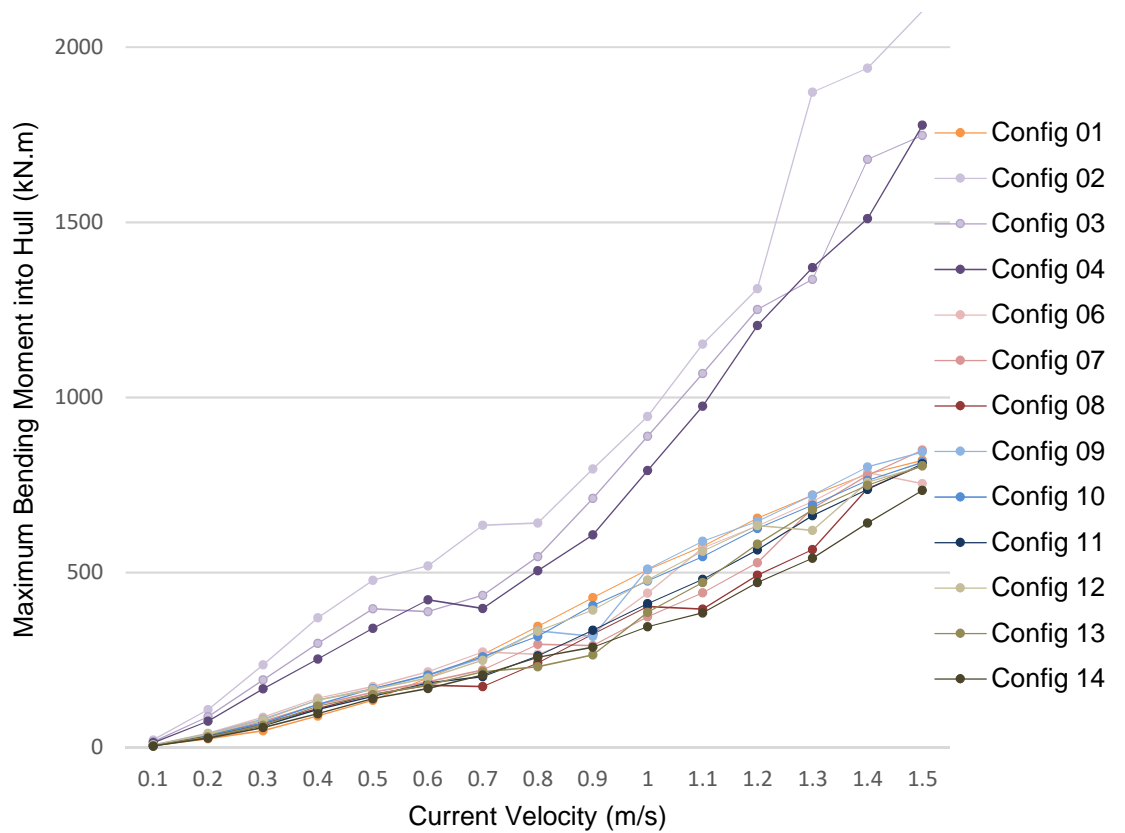
Fig.6-13:   Maximum Bending Moment of SWIR Configurations (excl. 5)

6.1.6. Discussion

From the above analyses the following observations can be made. With the exception of configuration 5 (uniform steel SWIR), the natural frequencies of each of the configurations are in a similar range but can be sub-divided into three groups, where configuration 01 has the lowest natural frequencies then configurations 2, 3, 6, 7, 9, 10, 12, and 13 in the mid-range and with configurations 4, 8, 11 and 14 having the highest natural frequencies. Configuration 1 (uniform rubber SWIR) is the most flexible riser so would expect to have the lowest natural frequency. It can also be seen from configurations 2, 3 and 4 and also 6, 7 and 8 that, as more weight is added, the riser becomes stiffer and the natural frequencies increase accordingly which is also expected. Generally, the lower the natural frequency, the lower the number of oscillations if the SWIR is excited and theoretically lower cyclical damage, therefore a low natural frequency would be preferred.

From the VIV response plots, it can be seen, for current velocities above 0.4m/s, the VIV offset amplitudes range from 2m – 3.5m for nearly all of the configurations, and apart from configuration 5 (lowest) and configuration 2 (highest) the varying offsets of the remaining configurations means they cannot be easily sub-grouped. However, from the VIV offset curvature plot, it can be seen that configuration 5 (uniform steel SWIR) has the lowest curvature which, being the most rigid, would be expected. After that, configurations 6, 7, 8 and 11 have the next lowest VIV offset curvatures with configurations 10, 12, 13 and 14 slightly higher. Configurations 1, 2, 3 and 4 have the highest range of VIV offset curvatures. The curvature is examined because, for a common VIV offset amplitude, the lower the curvature, the lower excitation mode of the riser, so theoretically, if the SWIR is excited, the lower the cyclical damage due to bending. Therefor a lower VIV offset curvature would be preferred.

The lower end excursion plots again show that configuration 5 (uniform steel SWIR) has the lowest excursion which being the most rigid would be expected. After that, the configurations can be divided into three sub-groups, with configurations 3, 4, 7, 8, 11 and 14, having the lowest excursions, then configurations 2, 6, 10 and 13 in the middle group with configurations 1 and 12 having the highest excursions. To reduce the possibility of the SWIR interfering with other risers and mooring lines, a minimal lower end excursion is preferred.

From plots showing the loadings into the connection point, it can be seen that configuration 5 (uniform steel SWIR) has values significantly higher than the

other configurations which due to its weight and rigidity would be expected. For the tension into the connection point, with the exception of configuration 2 (lowest) and configuration 14 (highest), the remaining configurations can be sub-divided into two groups. Configurations 3, 6, 7, 9, 10 and 12 having lower tensions (although configurations 3 and 7 increase dramatically at the highest current velocities) and configurations 1, 4, 8, 11, and 13 having higher tensions into the connection point. For the bending moments into the connection point, with the exception of configurations 2, 3 and 4 which have the highest values, the remaining configurations all have similar values and cannot be readily divided into sub-groups.

6.1.7. Summary

In summary, the most optimum configuration is determined as follows. Due to the excessive loads into the connection point configuration 5 can be discounted.

Configurations 3, 4, 7 8 11 and 14 have the lowest lower end excursion and from these configurations 7, 8 and 11 have the lowest VIV offset curvatures suggesting lower cyclical damage. Configuration 7 does have a lower tension into the connection point, but this does increase dramatically at the higher current velocities suggesting erratic stability.

This leaves configurations 8 and 11 which both have natural frequencies in the same range but which are still comparatively low. Due to the practicalities of incorporating and handling 60 tonnes of ballast weight offshore in addition to the pipe sections that would be necessary for configuration 8, configuration 11 is selected as the most optimum solution.

When building the model of the selected Configuration 11 for a more detailed analysis, a number of test runs were undertaken to verify the accuracy and robustness of the model. These test runs included some fatigue simulations which highlighted a 'weak' area at the connection between the lower end of the HDPE and the upper end of the steel pipe sections. This was attributed to the high bending moments from the rigid steel sections being transmitted into the less rigid HDPE sections.

To overcome this, the last HDPE section and the first steel pipe section were replaced by bonded flexible rubber pipe sections which provided a more

flexible transition between the HDPE and steel pipe sections. The resulting Configuration 11a being as shown in Fig.6-14 below:
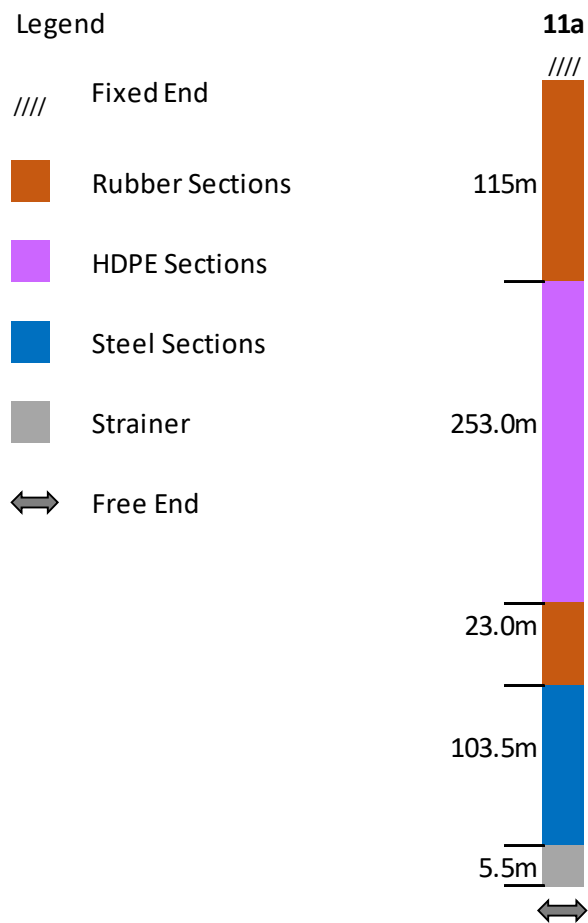
Fig.6-14:   SWIR Configuration 11a

To validate this modification, the amended configuration 11a was analysed as described in Section 6.1.4 and the outputs compared to the original configuration 11 as shown below in Figs.6-15 thru' 6-20.
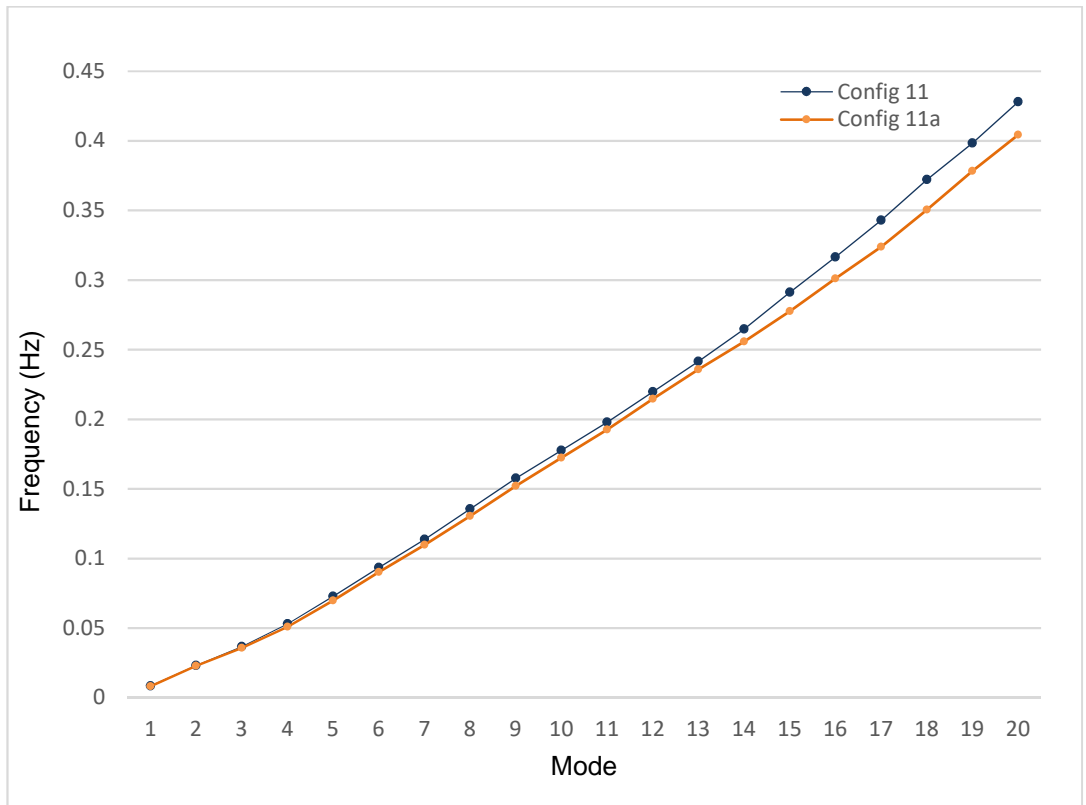
Fig.6-15:   Natural Frequency of SWIR Config. 11 v 11a
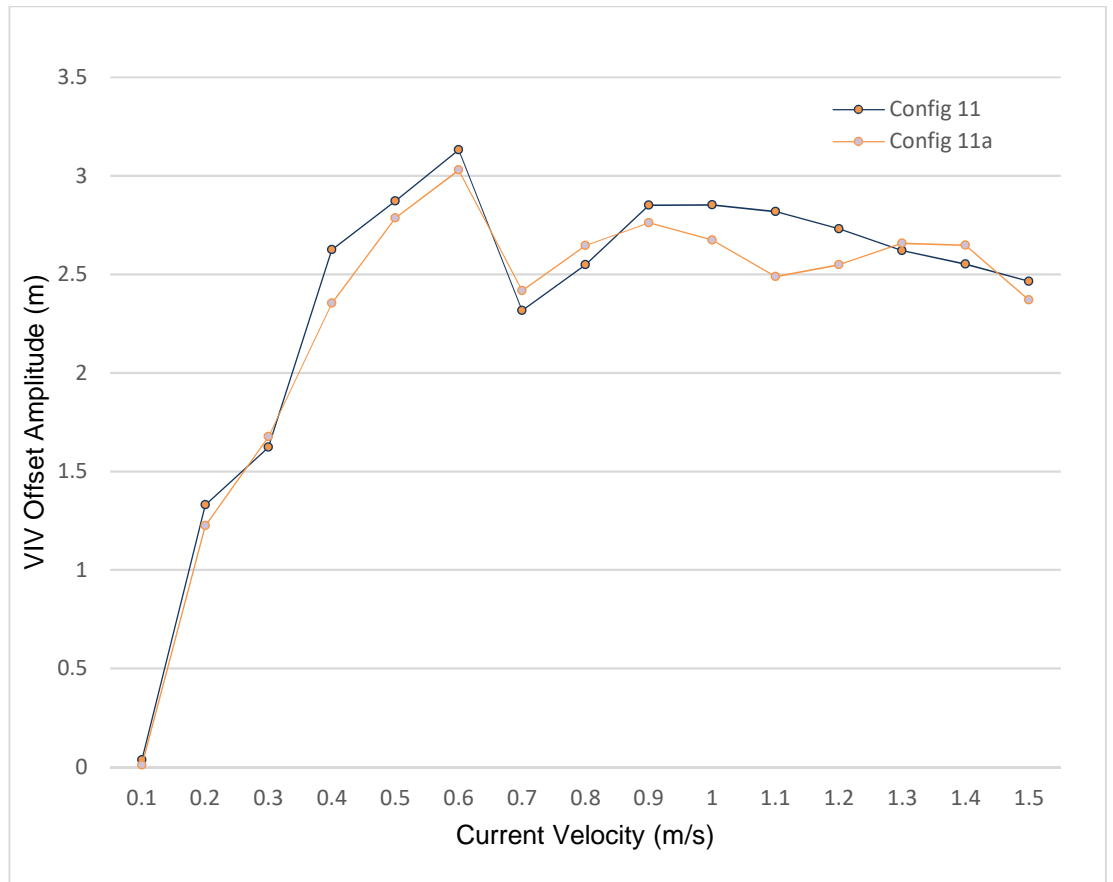
Fig.6-16:   Maximum VIV Offset Amplitude of SWIR Config. 11 v 11a
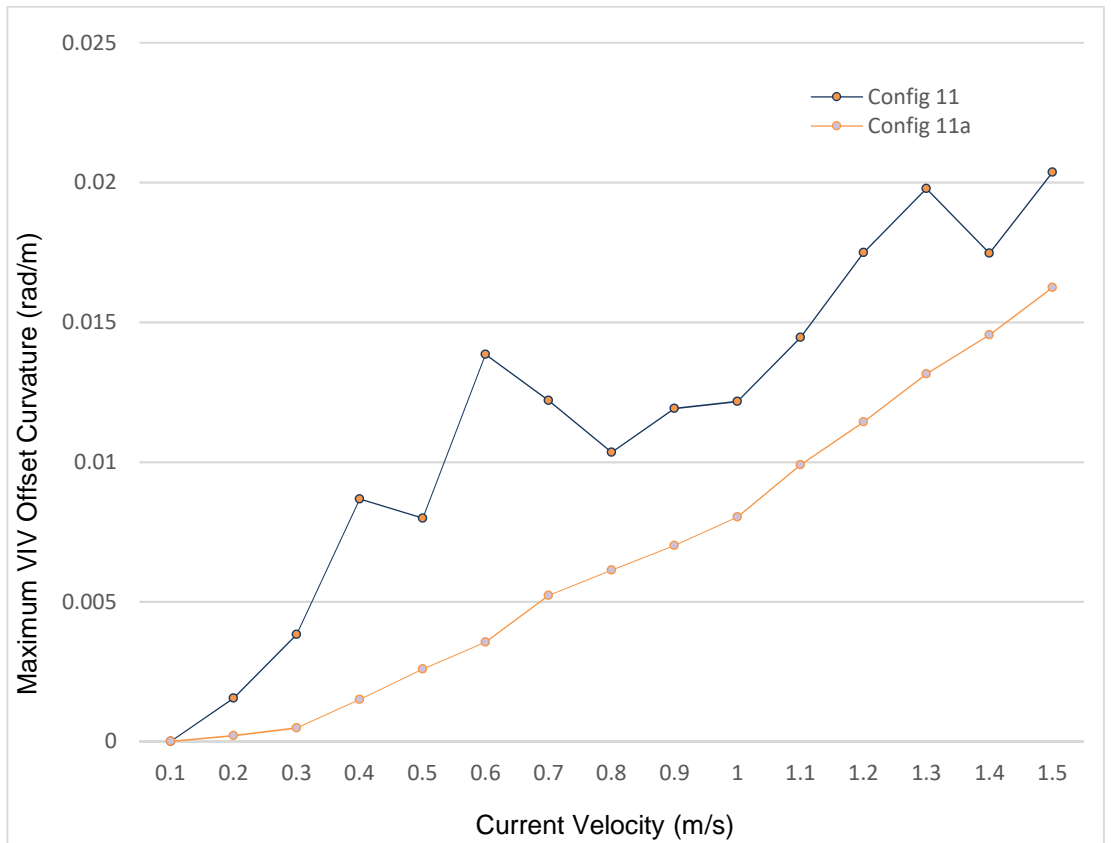
Fig.6-17: Maximum VIV Offset Curvature of SWIR Config. 11 v 11a
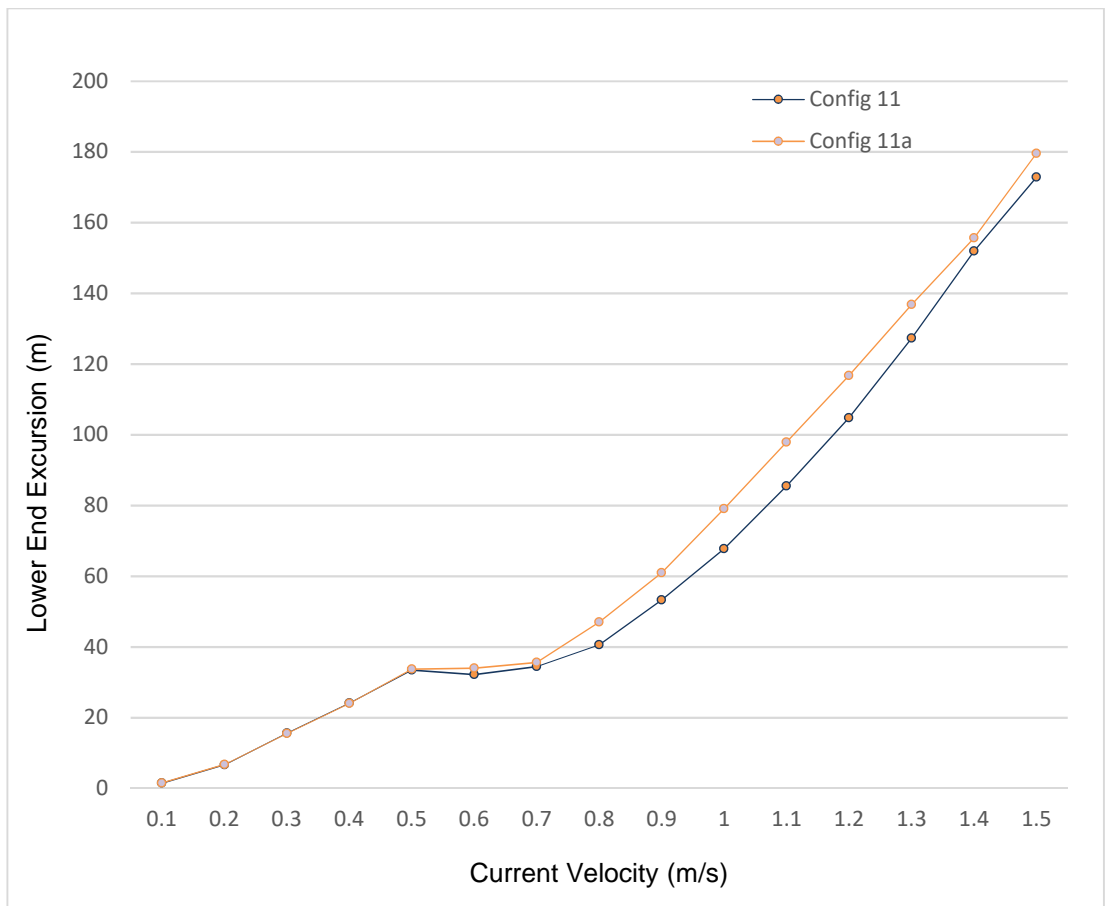
Fig.6-18: Maximum Lower End Excursion of SWIR Config. 11 v 11a
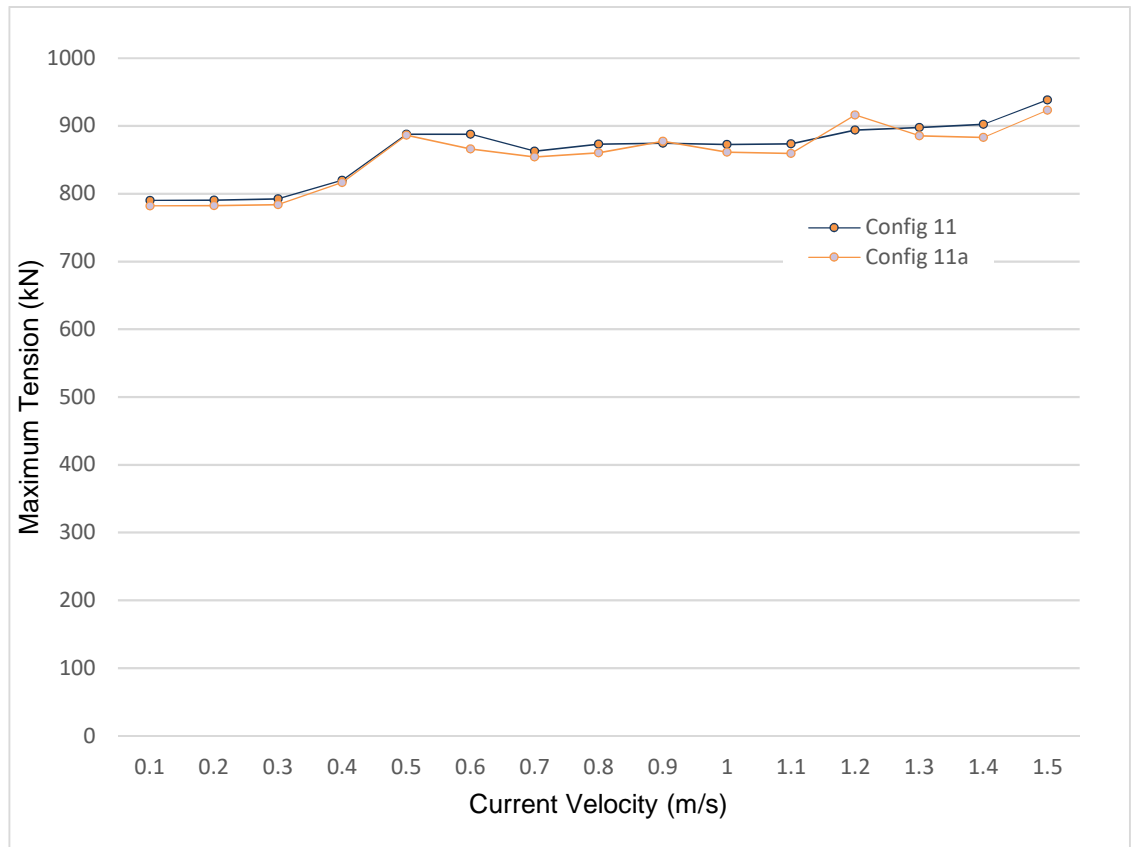
Fig.6-19:   Maximum End Tension of SWIR Config. 11 v 11a
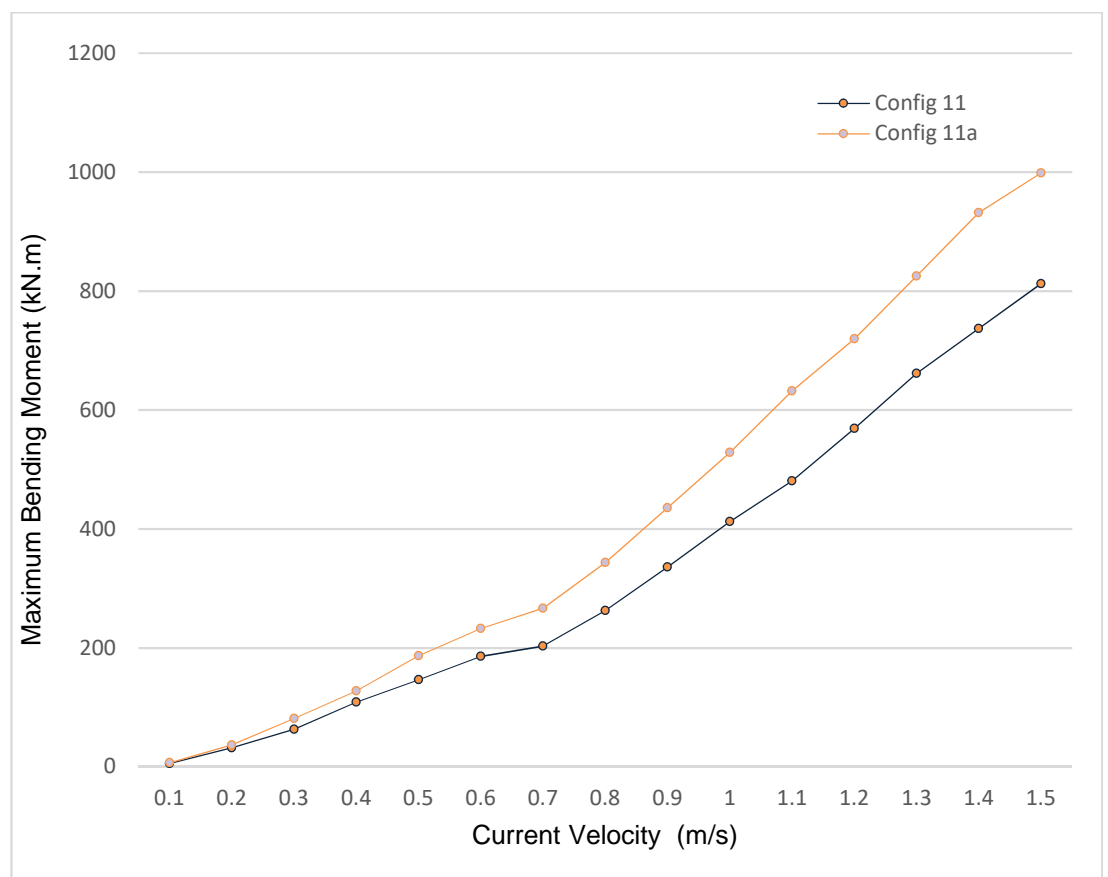
Fig.6-20:   Maximum Bending Moment of SWIR Config. 11 v 11a

It can be seen that the impact of the modification is slight with the exception the Bending Moment into the connection point which increases particularly at the higher current velocities. However, the VIV offset curvature is reduced and more consistent which is more desirable in terms of fatigue damage, therefore the original selection rationale remains valid.

The next section presents a more detailed analysis of configuration 11a.

6.2. Strength Analysis

To assess the strength of the proposed SWIR in service, a hydrodynamic analysis was performed using Orcaflex which considered the vessel and SWIR response to the environmental forces acting in the extreme conditions. Full details of the analysis are presented in the Portfolio [Section 8.0].

Response Amplitude Operator (RAO) data was used from a vessel representing a typical FLNG vessel in a turret moored configuration to which the SWIR were connected with a fixed connection.

A 40"NB x 500m and a 60"NB x 500m SWIR Riser were modelled as Configuration 11a (ref. Fig.6-14) using the physical and mechanical properties of the materials presented in Chapter 5 and as tabulated below in Table 6-1 and 6-2.

Component	Quantity	Length (m)	Mass in Air (kg)	Weight in Water (kg)
Steel Riser Head	1	-	2,500	2,175
Hose Section	10	115	64,000	22,000
HDPE Section	22	253	31,922	-2,354
Hose Section	2	23	12,800	4,400
Steel Pipe	9	103.5	48,474	42,147
Flange Connections	44	-	15,400	13,420
Steel Strainer	1	5.5	1,750	1,1061,520
TOTAL		500	176,846	83,308

Table 6-1: 40"NB SWIR Configuration

Component	Quantity	Length (m)	Mass in Air (kg)	Weight in Water (kg)
Steel Riser Head	1	-	3,500	3,043
Hose Section	10	115	119,900	41,450
HDPE Section	22	253	71,258	-5,214
Hose Section	2	23	23,980	8,290
Steel Pipe	9	103.5	73,170	63,630
Flange Connections	44	-	35,200	30,580
Steel Strainer	1	5.5	2,250	1,955
TOTAL		500	329,258	143,734

Table 6-2: 60"NB SWIR Configuration

The strainers were modelled as a section of straight pipe whereas the riser head and flange connections are modelled as clump weights of appropriate mass and volume.

The normal drag coefficient (Cd) were modelled as a variable of the Reynolds number using the technique provided within ESDU 80025 (ESDU, 2010), whereas the axial drag coefficient was set as a constant for plain pipe except for the flange connections which were modelled with a vertical drag area equal to the protruding flange and an axial drag coefficient in accordance with DNV-RP-C205 ((DNV, 2014) Table E11.9.
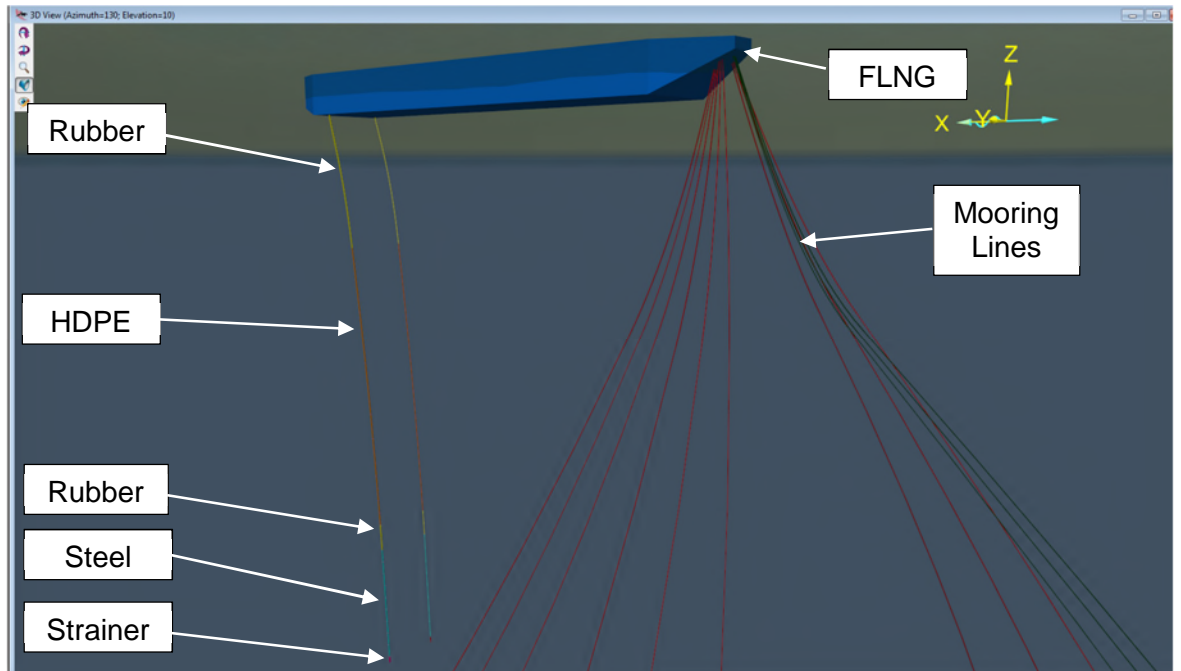
Fig.6-21:   Orcaflex Model of SWIR Arrangement
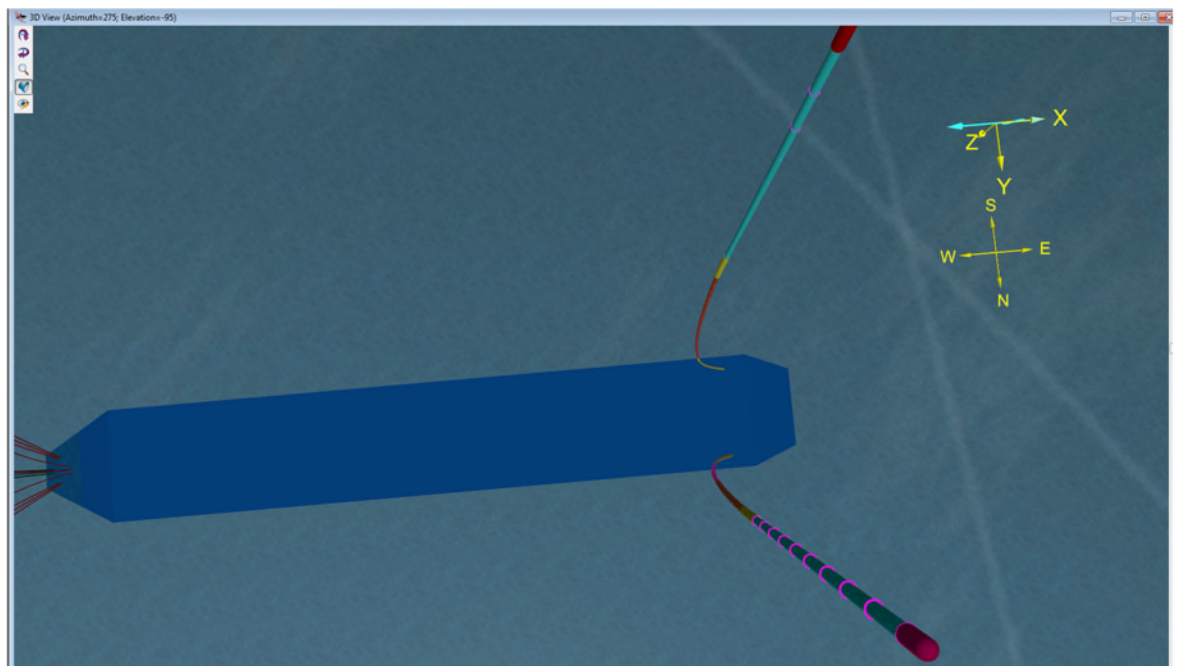
Fig.6-22:   Orcaflex Model of SWIR Arrangement (from below)

Environmental data from offshore Tanzania (Statoil, 2010), which is a location for the Coral South FLNG, was used for the analysis. For the design condition of the strength analysis, and as recommended API 17B (API, 2014) table 9, the 100 year return period data was considered and applied in a number of combinations to ensure that the most probable extreme event was captured.

The resulting analysis yielded the maximum values which are compared against the allowable values in Tables 6-3 & 6-4:

	Max	Allowable
Flexible Rubber Pipe Section		
• **Tension** (kN)	**808.0**	**3141**
• **Curvature** (Rad/m) *as MBR (m)*	**0.244** *4.1*	**0.25** *4.0*
HDPE Pipe Section		
• **Tensile Stress** (MPa)	**3.2**	**9**
• **Bending Stress** (MPa)	**0.7**	**9**
• **Von Mises Stress** (MPa)	**4.9**	**9**
• **Curvature** (Rad/m) *as MBR (m)*	**0.00168** *593.8*	**0.02756** *36.28*
Steel Pipe Section		
• **Tensile Stress** (MPa)	**4.0**	**137.9**
• **Bending Stress** (MPa)	**7.7**	**137.9**
• **Von Mises Stress** (MPa)	**12.8**	**137.9**
• **Curvature** (Rad/m) *as MBR (m)*	**0.00007445** *13431*	**0.001335** *749*

Table 6-3: 40"NB SWIR – Strength Analysis Results

	Max	Allowable
Flexible Rubber Pipe Section		
• **Tension** (kN)	**1451.0**	**7068.0**
• **Curvature** (Rad/m) *as MBR (m)*	**0.1429** *7.0*	**0.1666** *6.0*
HDPE Pipe Section		
• **Tensile Stress** (MPa)	**2.0**	**9**
• **Bending Stress** (MPa)	**0.8**	**9**
• **Von Mises Stress** (MPa)	**3.8**	**9**
• **Curvature** (Rad/m) *as MBR (m)*	**0.001244** *803.6*	**0.02756** *36.28*
Steel Pipe Section		
• **Tensile Stress** (MPa)	**4.2**	**137.9**
• **Bending Stress** (MPa)	**8.8**	**137.9**
• **Von Mises Stress** (MPa)	**14.2**	**137.9**
• **Curvature** (Rad/m) *as MBR (m)*	**0.00005697** *17554*	**0.001335** *749*

Table 6-4:   60"NB SWIR – Strength Analysis Results

6.2.1. Loads induced into Hull

The analysis strength analysis considers the extreme 100yr return period as the design condition. From this analysis, the loads induced into the connection point have been extracted and are presented below in Tables 6-5 and 6-6.

• *Maximum Values for 40"NB Hang-Off Design*

	Max.	Corresponding Maximum Value		
		End Force (kN)	**Bending Moment** (kNm)	**Shear Force** (kN)
End Force (kN)	**837.3**		644.6	321.1
Bending Moment (kNm)	**969.1**	697.4		422.0
Shear Force (kN)	**433.7**	704.4	968.76	

Table 6-5:   Maximum Values for 40"NB Hang Off Design

	Max.	Corresponding Maximum Value		
		End Force (kN)	Bending Moment (kNm)	Shear Force (kN)
End Force (kN)	**1508.9**		1473.7	502.2
Bending Moment (kNm)	**2141.8**	1317.7		677.9
Shear Force (kN)	**677.9**	1317.7	2141.8	

Table 6-6:   Maximum Values for 60"NB Hang Off Design

These values can be used as the input for the design of the hang-off arrangement and the hull structure in that area.

Previous work by the author presented in the Portfolio [Section 11.0] (Craig, 2014), included the FEA of a model of a standard hang off arrangement normally considered on FPSO vessels but scaled up to suit a 60"NB SWIR as shown in Fig. 6-23 below.
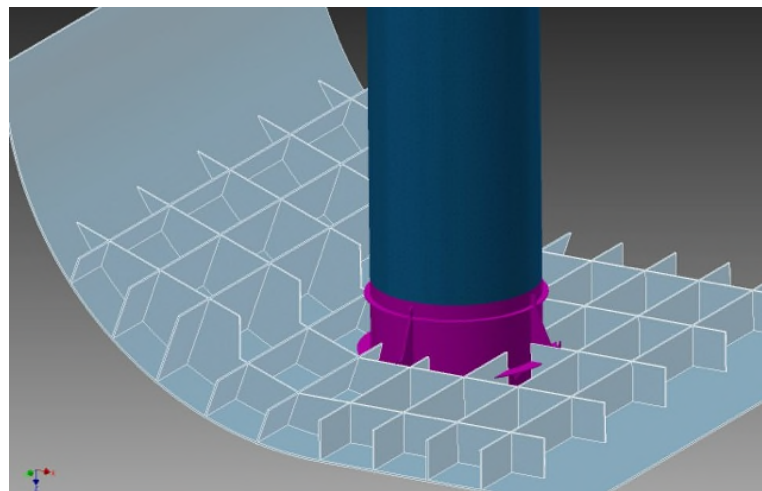
Fig.6-23:   Screenshots of Hang Off Structure

The input loads for this FEA were similar in magnitude to those presented in Table 6-6, which in the previous work by the author, reported maximum stresses in the region of 218N/mm^2, as shown in Fig.6-24, and which is within the allowable stress range for the steel grade S355 generally used in the construction of these components.
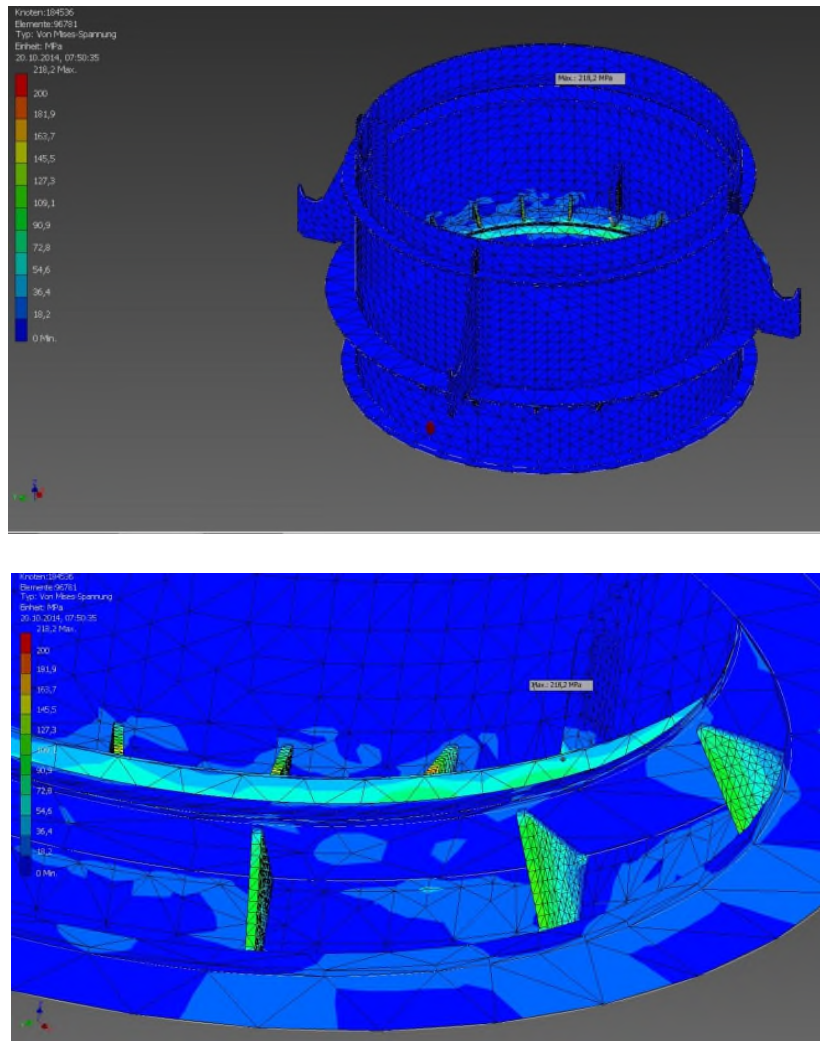
Fig.6-24:   Screenshots from Hang Off Structure FEA

This suggests that the arrangement currently installed on FPSO vessels can be scaled up and used in an FLNG application although a more detailed analysis would be required to verify the interface connections for a specific vessel.

6.3. Fatigue Analysis

To assess the predicted life of the proposed SWIR in service, the hydrodynamic analysis referenced Section 6.2 also investigated the fatigue capabilities of the two SWIR.

Two aspects were considered for the fatigue analysis, namely, fatigue due to waves and fatigue due to current. The fatigue due to waves primarily considered the effect of the vessel motion in a random sea whereas the fatigue due to current considered the effect of vortex induced vibration induced by the ocean current.

6.3.1. Fatigue Due to Waves

To predict the fatigue damage in the SWIR due to a random wave profile, the annual scatter data for significant wave height versus the wave period was used to determine the number of occurrences per annum. This data was then converted into a scatter table of regular waves using the Orcaflex 'Wave Scatter Conversion' tool which uses the formula of Longuet-Higgins (Longuet-Higgins, 1983) to give a probability density of individual wave in a random sea.

From this, a load case was generated for each wave condition and a simulation ran from which the fatigue results tool in Orcaflex was used to calculate the annual fatigue damage of each SWIR.

The SN data presented in Chapter 5 was input into Orcaflex and the 'regular' method selected, which uses the data from the last full cycle of each simulation and the number of annual occurrences to calculate the fatigue damage from the relevant SN curve.

The was performed for the SWIR in both the 'Clean' condition and with 'Marine Growth' from which the calculated fatigue damage was inverted to determine the predicted life of the SWIR in service as shown below in Figs.6-25 & 6-26.
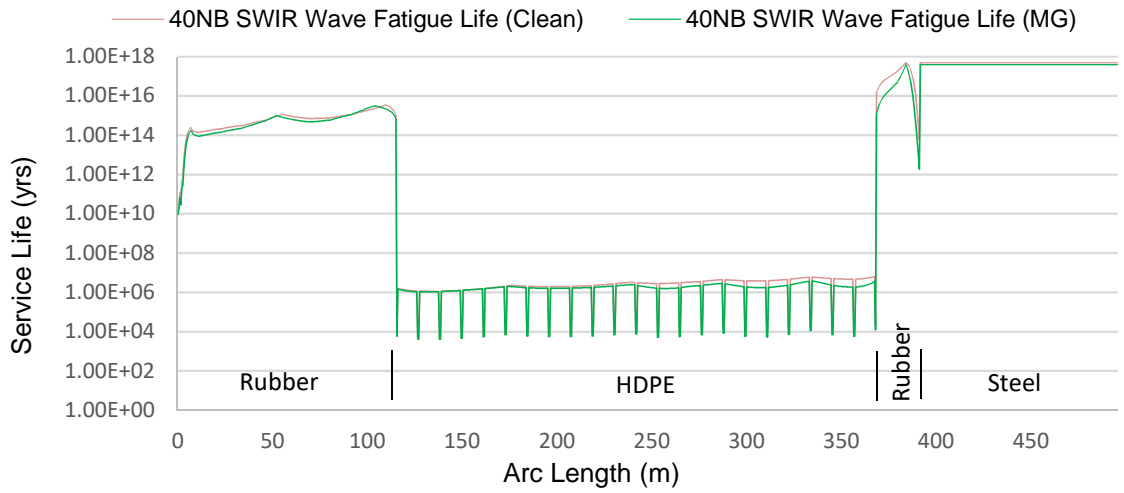
Fig.6-25: 40"NB SWIR – Fatigue Life Due to Waves
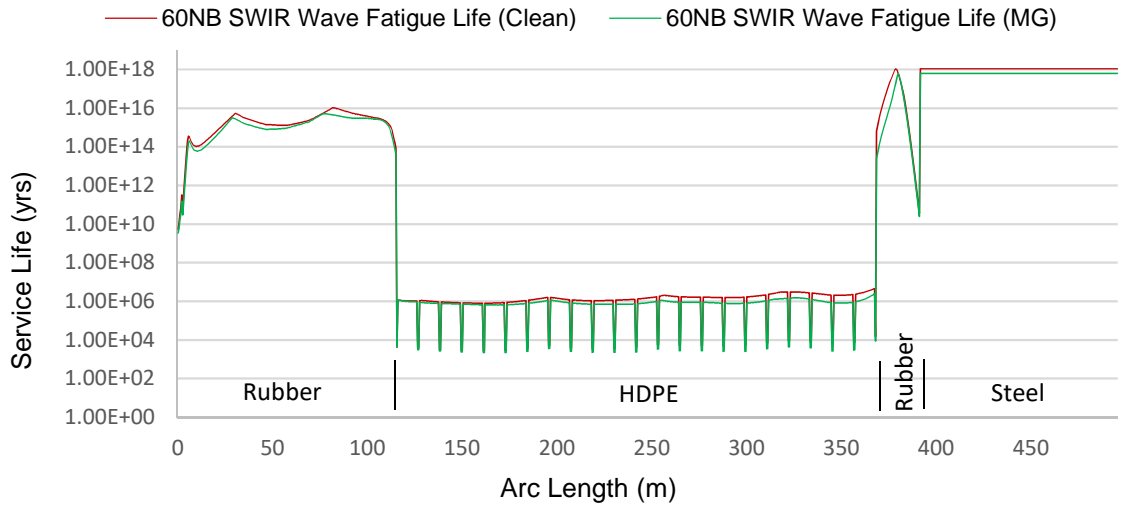
Fig.6-26: 60"NB SWIR – Fatigue Life Due to Waves

Note that the 'spikes' in the HDPE sections correspond to the locations of the butt fusion welds in the SWIR. Also, the steel sections report 'infinite' life in these conditions, however, for illustration purposes, where this is the case, the service life of the steel is set to correspond with the maximum life of the flexible rubber pipe sections.

6.3.2. Fatigue Due to Current

To predict the fatigue damage due to current, the 1 year return maximum current profile was factored in increments of 0.05 as shown in Fig.6-27 and the density of each factor determined using the Weibull shape factor for the most frequent current direction to give the current speed distribution as shown in Fig.6-28 from which the annual exposure hours can be determined.
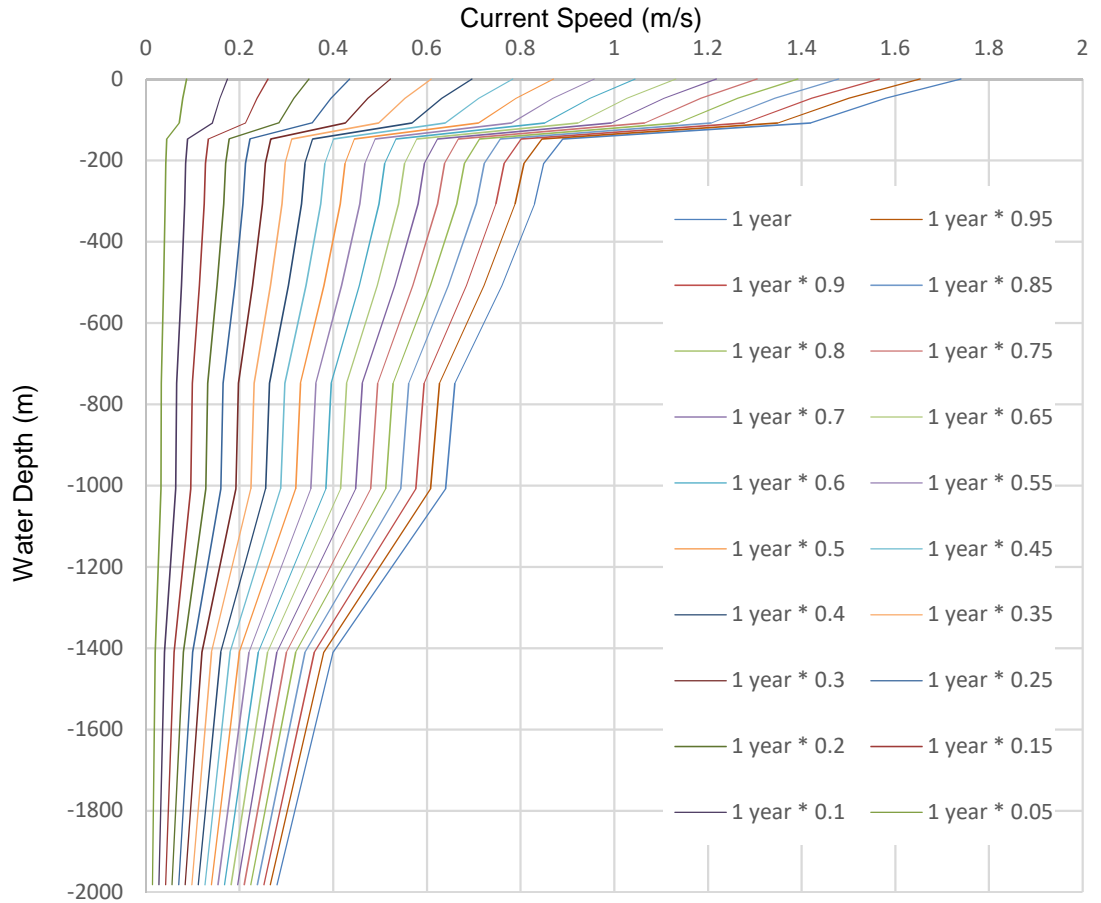
Fig.6-27:   1 year Return Maximum Current Profile (Factored)
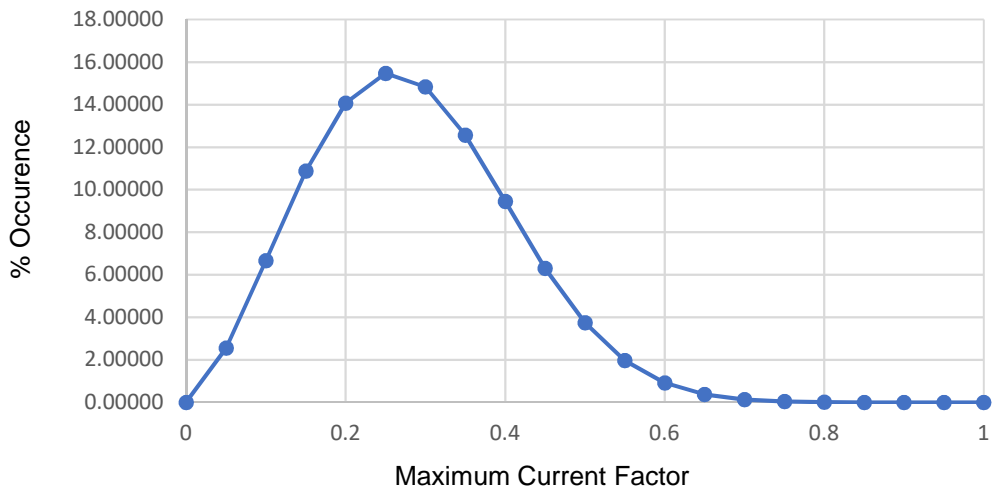
Fig.6-28:   Current Speed Distribution

With the Orcaflex 'Iwans and Blevins' vortex induced vibration model selected, a simulation was ran for each of the current velocity factors until the VIV response became settled from which the fatigue results tool in Orcaflex was used to calculate the annual fatigue damage of each SWIR.

The SN data presented in Chapter 5 was input into Orcaflex and the 'rainflow half cycle' method was selected using the annual exposure hours to calculate the fatigue damage from the relevant SN curve.

The was performed for the SWIR in both the 'Clean' condition and with 'Marine Growth' from which the calculated fatigue damage was inverted to determine the predicted life of the SWIR in service as shown below in Figs.6-29 & 6-30.
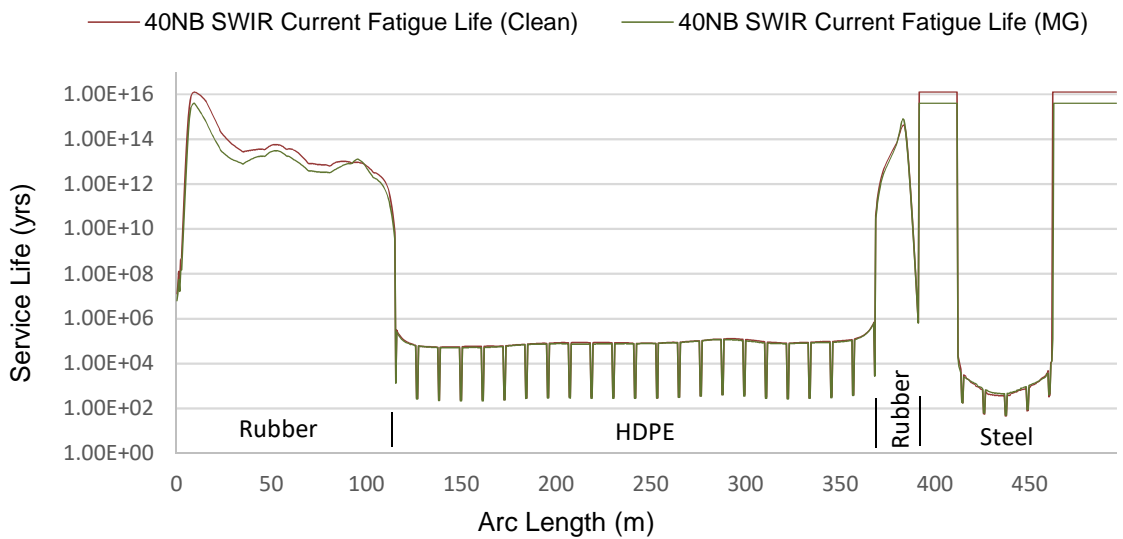
Fig.6-29:   40"NB SWIR – Fatigue Life Due to Current
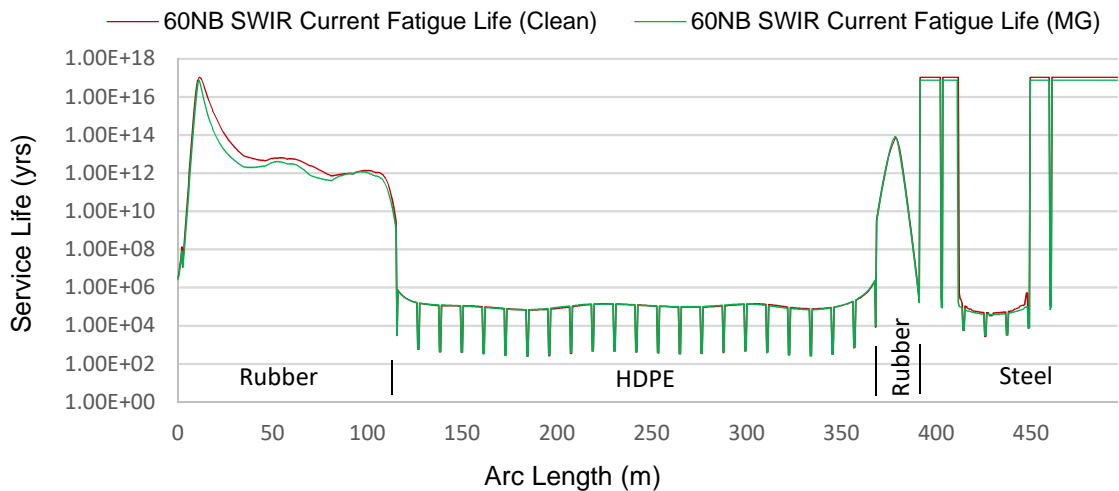
Fig.6-30:   60"NB SWIR – Fatigue Life Due to Current

Note that the 'spikes' in the HDPE and steel sections correspond to the locations of the welds in the SWIR. Also, some positions in the steel sections report 'infinite' life, however, for illustration purposes, where this is the case, the service life of the steel is set to correspond with the maximum life flexible rubber pipe sections.

6.3.3. Total Fatigue Damage

By summing the fatigue damage due to waves and the fatigue damage due to current, the total fatigue damage is inverted to predict the life of the SWIR in the field as shown in Figs. 6-31 and 6-32.
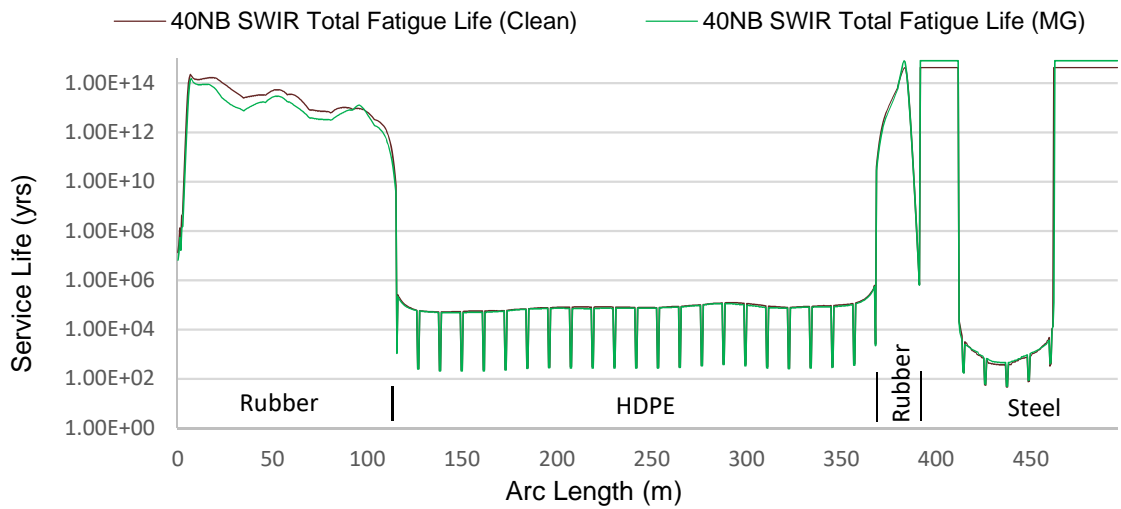
Fig.6-31:   40"NB SWIR – Total Fatigue Life
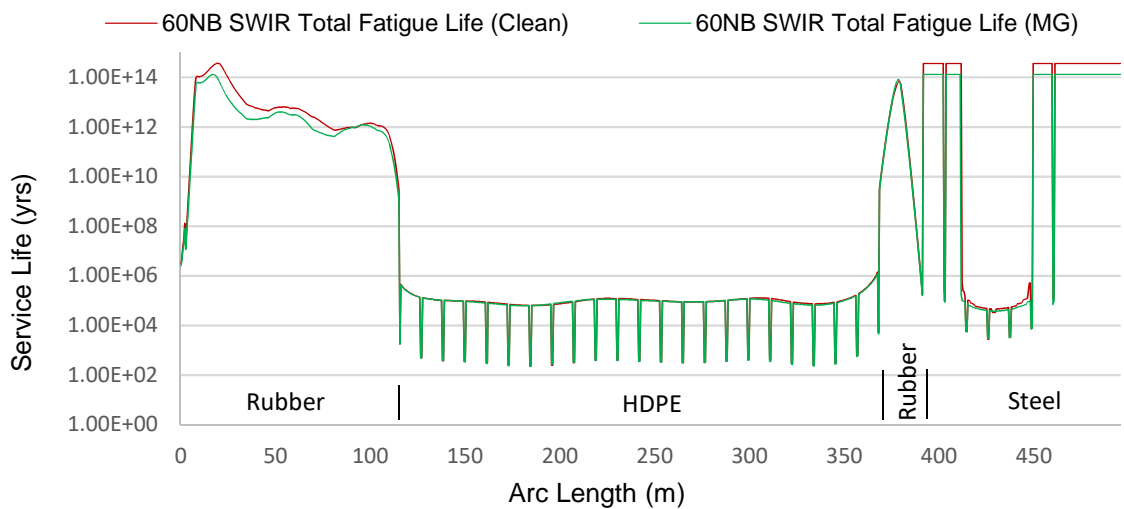
Fig.6-32:   60"NB SWIR – Total Fatigue Life

Note that the 'spikes' in the HDPE and steel sections correspond to the locations of the welds in the SWIR. Also, some positions in the steel sections report 'infinite' life, however, for illustration purposes, where this is the case, the service life of the steel is set to correspond with the maximum life of the flexible rubber pipe sections.

The fatigue results tool was used to calculate the fatigue damage to the connecting flange weld and studbolts due to waves and current but were reported to have infinite life, indicating that the stress levels fall within the fatigue endurance limit for these components.

6.3.4. Discussion

It can be seen from the predicted service life of the SWIR that generally the HDPE sections have the lowest predicted service life, and specifically at the butt fusion welds.

Interestingly however, for the 40"NB SWIR, it is the steel pipe sections which have the lowest expected fatigue life of approximately 50 years due to the VIV response. Further examination reveals that it is the 1 year current profiles with a factor of 0.5 - 0.6 which excites the steel pipe sections and causes the most fatigue damage within the SWIR. For these current profiles, the frequency of oscillation was found to be 0.07 and 0.09Hz for current profiles 0.5 and 0.6 respectively. Reference to Fig.6-15 and examination of the simulations indicates that within this frequency range, it is modes 5 and 6 which are excited. It is noted that the frequency of oscillation is below the test frequency of the SN data and close to the lower test frequency of 0.1Hz considered by Brogden (2000) and Channell & Cawood (1989), which indicates that the test data used is valid.

Using the techniques presented in DNV-RP-F204 (DNV, 2010), the effective velocity U_{eff} can be estimated as follows:

$$f_s = St * U_{eff} / D_h \qquad \text{(DNV, 2010) Eq. 4.4}$$

where: St = Strouhal Number

U_{eff} = Effective Velocity

D_h = Outside Diameter

Therefore: $U_{eff} = f_s * D_h / St$

and: St = ~0.20   (DNV, 2014) Fig 9-1

D_h = 1.067m (HDPE)

fs = 0.07 – 0.09 Hz

so: U_{eff} = |0.07:0.09| * 1.068 / 0.2

U_{eff} = 0.374 – 0.480 m/s

And then plotting this range on the current profile indicates the depth of the effective velocity as shown in Fig.6-33:
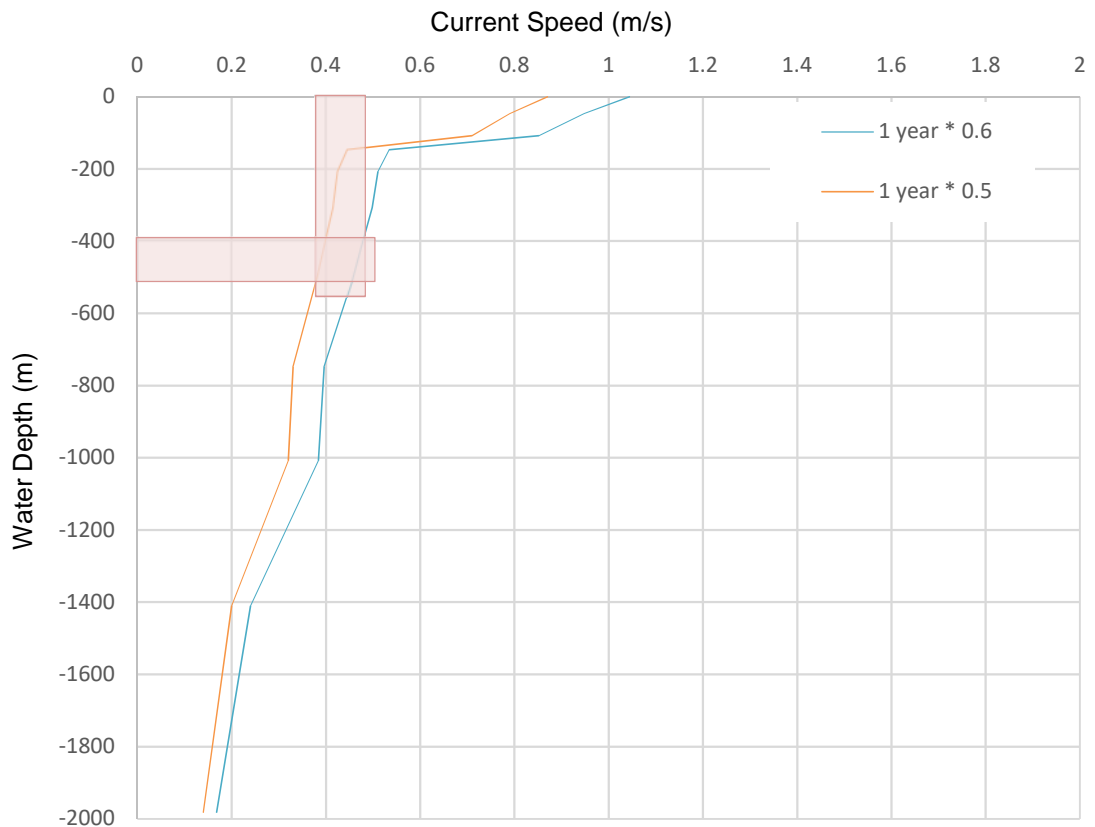
Fig.6-33:   40"NB SWIR – VIV Excitation Zone (Tanzania)

If this classic theory applies, it would suggest that the excitation zone is between 400-500m which is the lower region of the SWIR. This differs from that of a top tensioned riser where the excitation length is considered to be the part of the riser where the velocity is 2/3 of the maximum velocity (DNV, 2010) Sect 4.3, which would be the upper region of the riser.

Although the minimum service life is calculated at around 200 years for the HDPE butt fusion welds, which is a relatively small margin of safety, this is a conservative estimate in as much as the analysis assumes that the waves and current are unidirectional and therefore the fatigue damage will be concentrated in the same radial position on the SWIR. In practice, the waves and current will be multi-directional therefore the fatigue damage will be distributed radially around the SWIR which, theoretically, would increase the service life of the components. It is also assumed that vibration is always present in the SWIR whereas, it could be argued that, due to current speed and directional changes, VIV requires a period of time to become established during which time the fatigue damage is lower. Also, for the HDPE butt fusion joint, it should be noted that, for the SN data used, the low stress specimen test was still running which, depending on eventual failure point, may predict a higher service life of the SWIR. Additionally, and as discussed in section 5.2.5, tests in water by Takahara et al (1981) gave increased lifetimes which indicates that good heat transfer to the surroundings may also improve fatigue life.

Furthermore, if the loads induced into the HDPE butt fusion weld can be eliminated, then the service life of these sections would be as the parent pipe which is in the order of 100,000 years which provides a greater margin of safety.

One possible solution for this is to 'brace' the HDPE pipe sections at the flange connections so that the loads are transferred into the parent pipe. Fig. 6-34 shows a simple construction in this regard that utilises the existing backing ring. Clearly, any such design would need to be incorporate some element of flexibility so that the brace would act like a bend restrictor to ensure that a 'hard' spot was not created at the fixing positions.
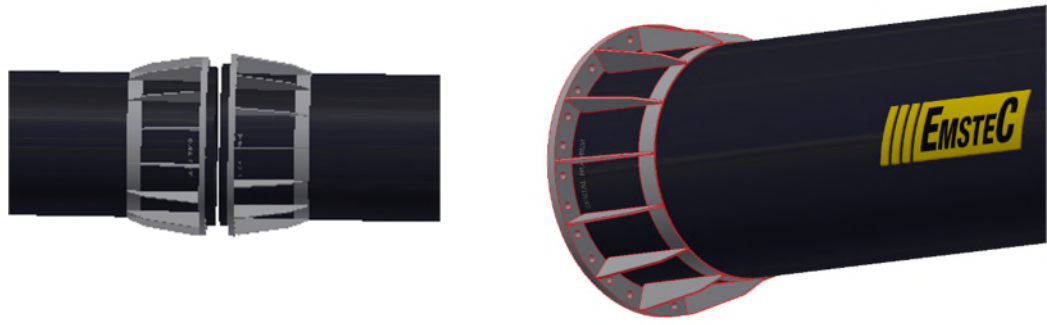
Fig.6-34:   HDPE Pipe Flange Brace

Similarly, if the excitation of the steel pipes can be avoided, this would increase the life of the steel section. The next section investigates damping of the SWIR to suppress the VIV of the steel section.

6.4. Riser Damping

VIV Suppression Strakes as shown in Fig. 6-35 below, are devices commonly used on structures in air and in water to suppress the effect of VIV by disturbing the vortices around the structure.
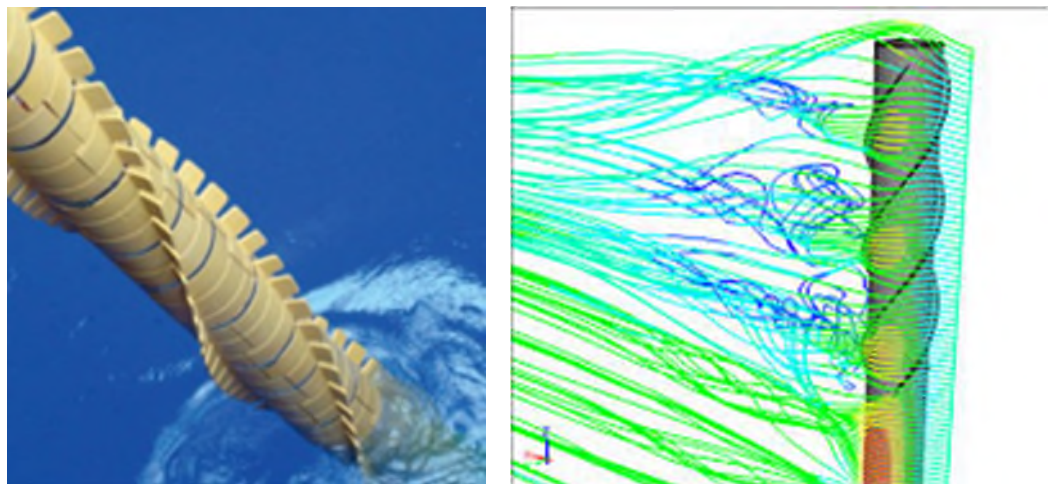
Fig.6-35:   VIV Suppression Strakes

Although there are a number of tools available to model VIV suppression strakes, for example SHEAR 7 and VIVA as discussed in section 2.7, Baarholm et al (2005) presents an empirical approach to model the effect of VIV suppression strakes based on the lift coefficient C_L, which if negative in the excitation zone, will have a damping contribution.

As an example, for the 40"NB steel pipe section excited by the most onerous current factor 0.6;

$$\hat{f} = \frac{f_{osc} * D}{U}$$

<div align="right">(Baarholm, et al., 2005)</div>

where: $\hat{f}$ =   Non-dimensional frequency:

f_{osc} =   Oscillating Frequency (Hz)

D =   Riser Diameter (m)

U =   Seawater Velocity (m/s)

and using values from the relevant Orcaflex simulation:

$$\hat{f} = \frac{0.09 * 1.016}{0.4713}$$

$$\hat{f} = 0.194$$

The Orcaflex simulation for this scenario reports an A/D value of between 0.3 – 0.4 for which the Lift Curves presented by Baarholm et al (2005) for the sample strakes at this non-dimensional frequency return a lift coefficient C_L = -0.5.

As the C_L is negative, this suggests that the installation of VIV suppression strakes will contribute to the damping of the steel sections in the SWIR. However, one of the disadvantages using strakes for this application is the increase in the drag coefficient C_D which will increase the lower end excursion of the SWIR. Another would be in relation to the deployment through the hang-off arrangement at the bottom of the caisson, the size of which would need to be increased accordingly to accommodate the strake dimensions.

Blevins (2001) indicates that damping can be increased by using materials with high internal damping such as rubber, therefore a further SWIR was modelled where two of the steel pipe sections were replaced by flexible rubber pipe sections as shown in Fig. 6-36.
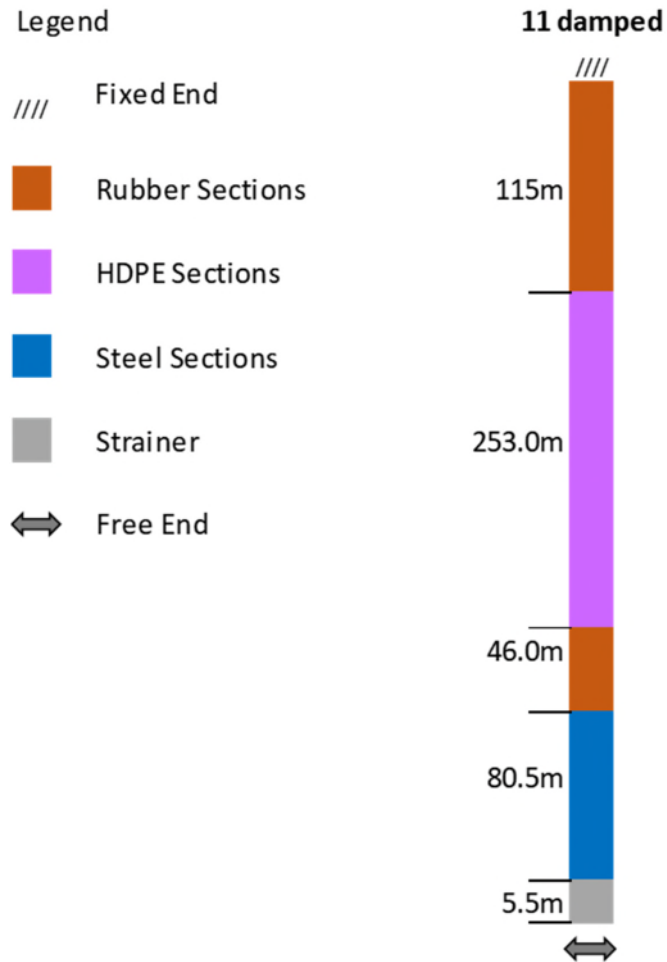
Fig.6-36:   Damped SWIR Configuration

The natural frequency of this configuration (referred to as damped SWIR) is lower than that of the original SWIR as shown in Fig.6-37.
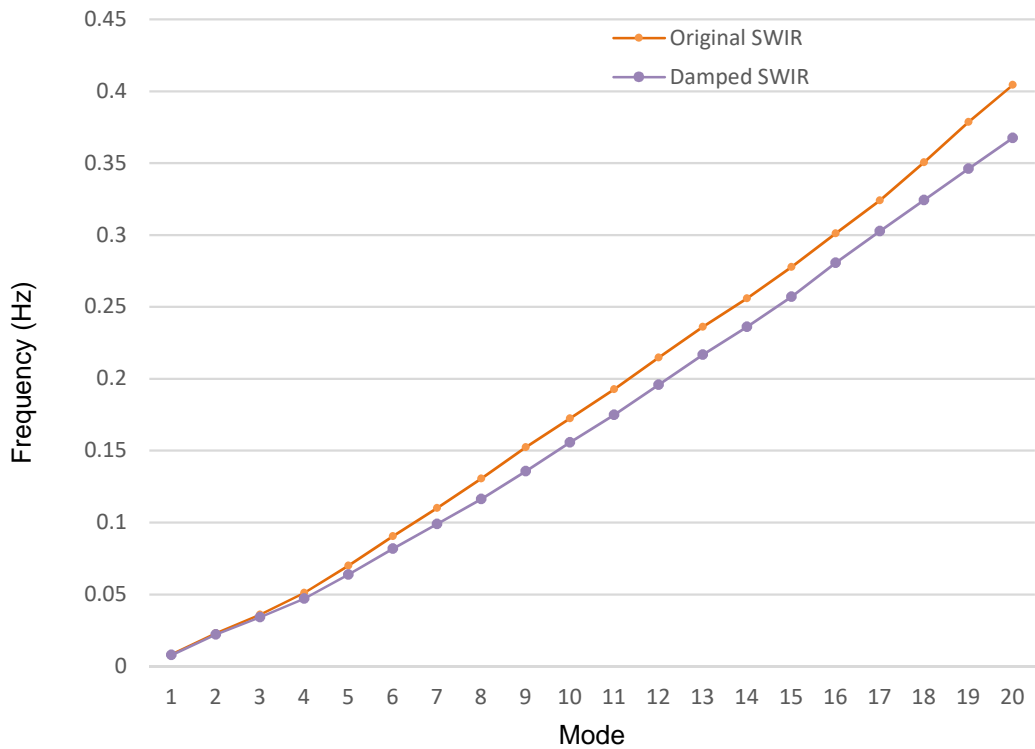
Fig.6-37:   Natural Frequency of 40"NB SWIR - Original v Damped

The damped SWIR was subjected to the same fatigue analysis as the original SWIR, ref. section 6.3, and the results extracted and compared as shown in Figs. 6-38 & 6-39 for the 40"NB & 60"NB SWIR respectively.
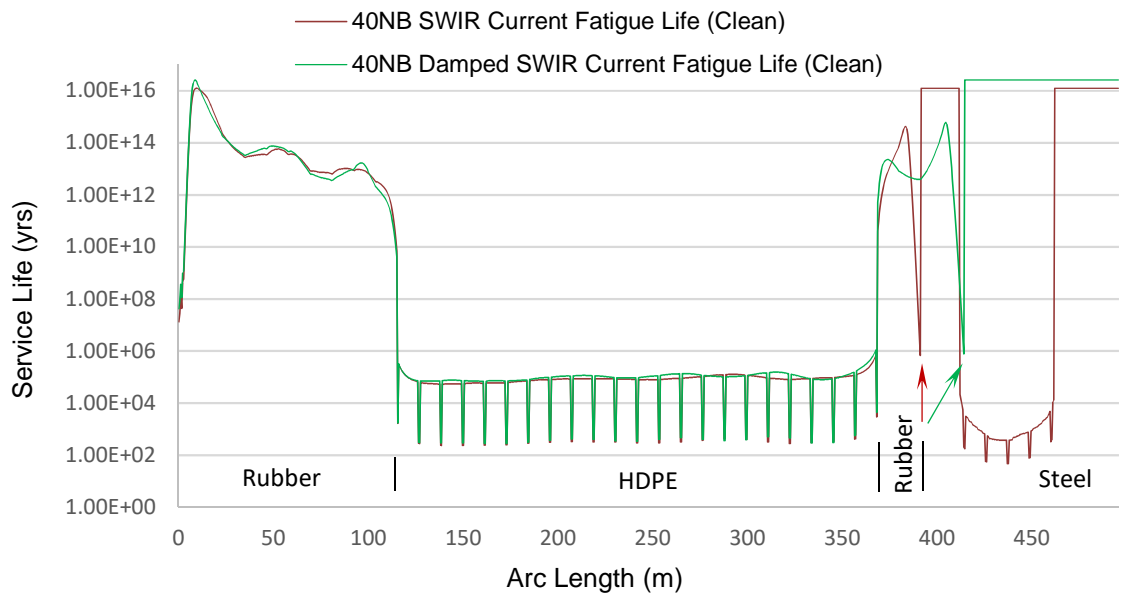
Fig.6-38:   40"NB SWIR Current Fatigue – Original v Damped
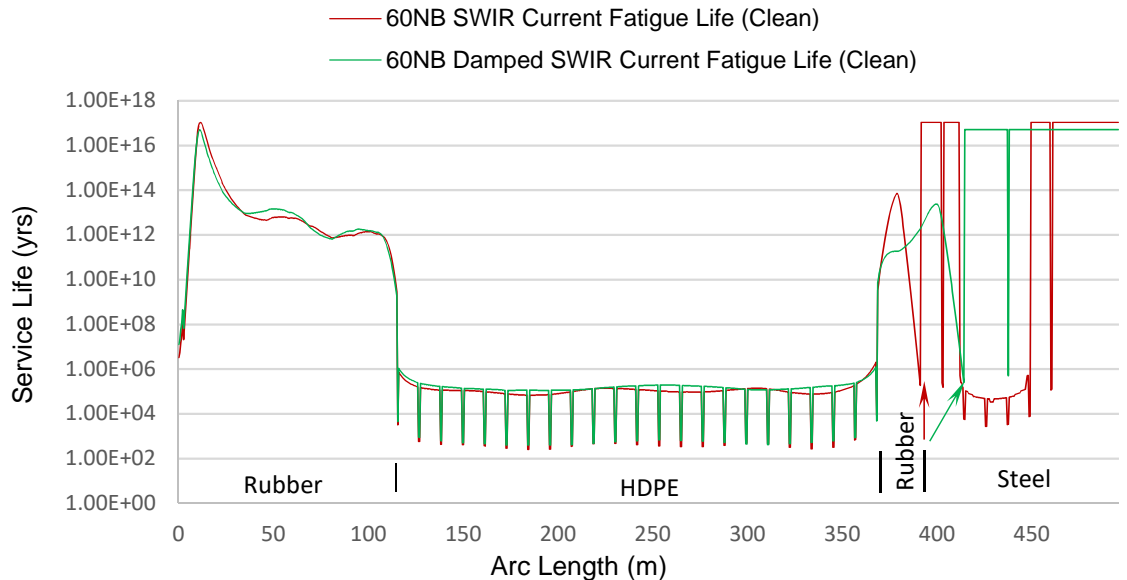
Fig.6-39: 60"NB SWIR Current Fatigue – Original v Damped

Fig.6-38 shows that the fatigue in the steel pipe sections is eliminated for the 40"NB damped SWIR, this is the same for the 60"NB damped SWIR with the exception of one reduced 'spike' as shown in Fig.6-39.

This suggests that by adjusting the number of flexible rubber sections and steel pipe sections, the SWIR damping can be 'tuned' to mitigate the VIV and therefore extend the fatigue life due to current.

The fatigue results tool was used to calculate the fatigue damage to the connecting flange weld and studbolts due to waves and current but were reported to have infinite life, indicating that the stress levels fall within the fatigue endurance limit for these components.

6.5. Riser Length

The above analysis considered a SWIR length of 500m, however, sensitivities were performed on both a shorter and longer variant of the damped SWIR to determine the effect that the length has on the fatigue life of the SWIR. For the shorter SWIR, 4-off x 11.5m HDPE sections were removed, giving a total SWIR length of 454m, and for the longer SWIR, 4-off x 11.5m HDPE pipe sections were added giving a total SWIR length of 546m.

A fatigue analysis as described in section 6.3 was performed for the shorter and longer damped SWIR and the results compared to the 500m damped SWIR as shown in Figs 6-40 & 6-41.
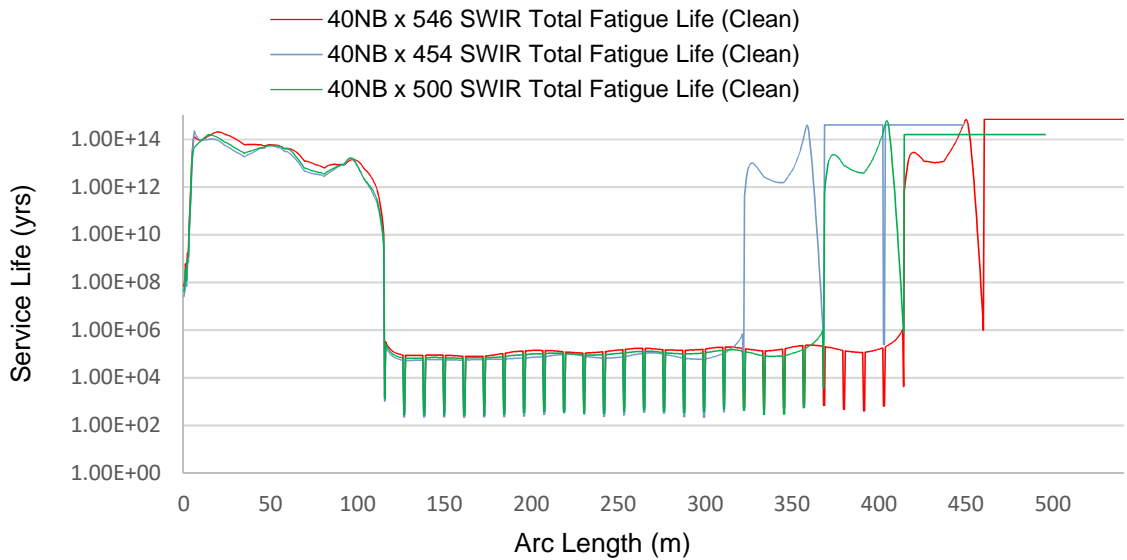
Fig.6-40: 40"NB SWIR Current Fatigue – 500m v 454m & 546m
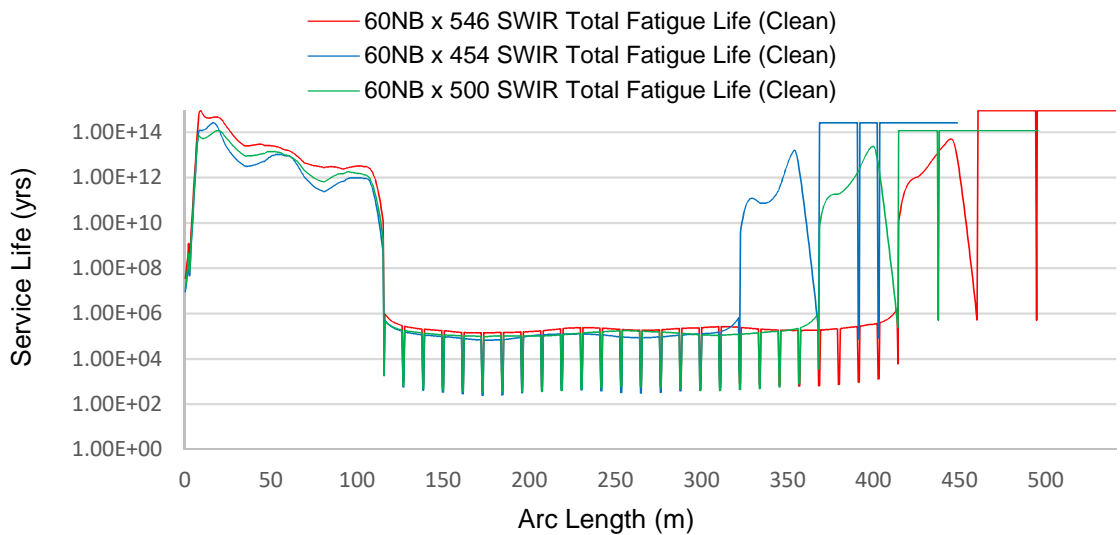
Fig.6-41: 60"NB SWIR Current Fatigue – 500m v 454m & 546m

It can be seen that varying the length of the SWIR has a small effect on its fatigue life in as much as the short SWIR fatigue life is reduced and the long SWIR fatigue life is increased as summarised in table 6-7.

SWIR Dia.	Minimum Fatigue Life (years)		
	SWIR Length (m)		
	454	500	546
40"NB	218	263	319
60"NB	247	346	515

Table 6-7: SWIR Length Variants– Min. Fatigue Life Strength

This is in line with the discussion in section 6.1.2 that by increasing the length of the riser reduces the natural frequency.

6.6. Geographical Locations

As shown in Fig.2-2, there are several geographical locations where offshore stranded gas is prevalent. One of the locations indicated is Africa, which has been considered for the above analysis, another is South America.

The environmental conditions for each of these regions is different, for example, the current velocities in Brazil are lower than those in Tanzania however, the distribution of current velocity is less concentrated as shown in Fig.6-42.

i) Distribution - Brazil

ii) Distribution - Tanzania

iii) 1 yr Current Profiles
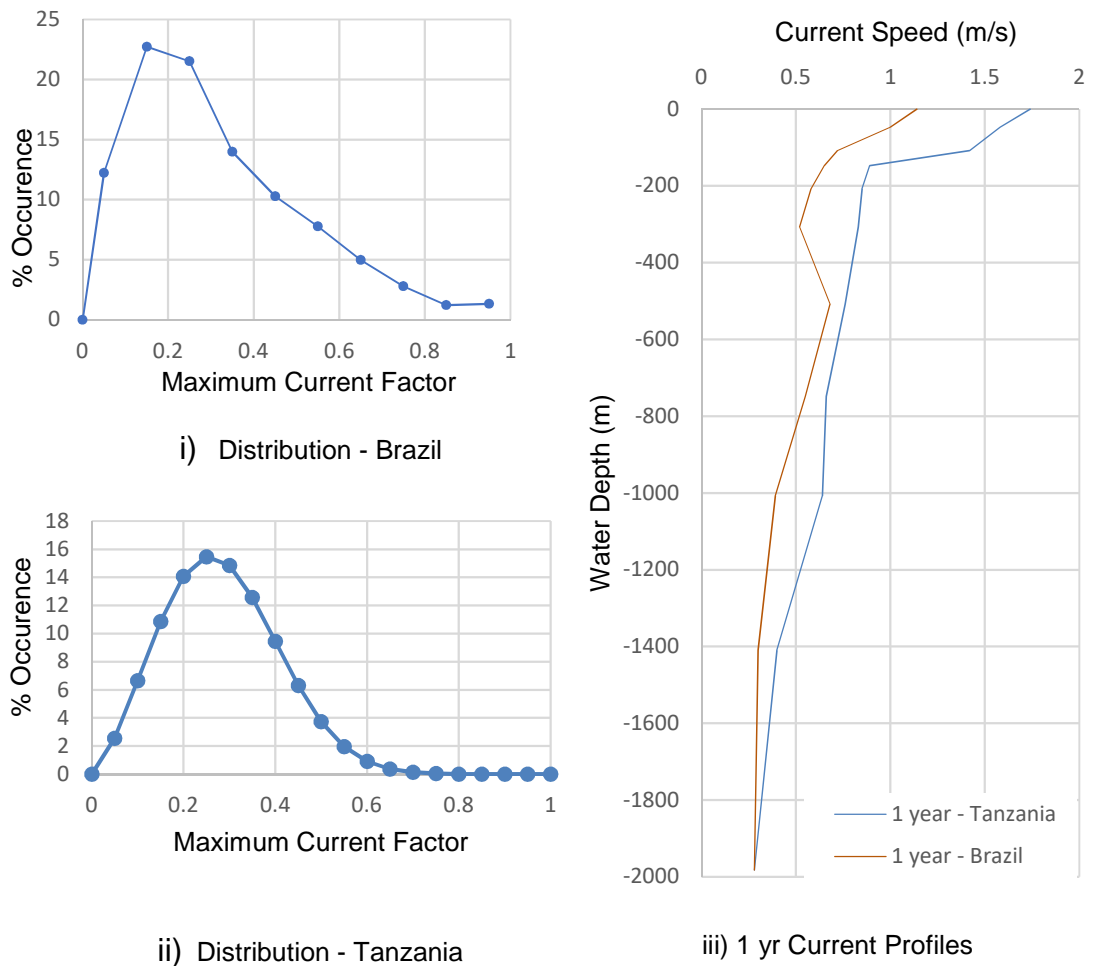
Fig.6-42:   Current Distribution & Profile Comparison

Therefore, to assess the impact, the damped SWIR was subject to the same fatigue analysis using metocean data from the Campos Basin in Brazil

(Petrobras, 2010) and compared to the damped SWIR in offshore Tanzania as shown in Figs 6-43 & 6-44 for the 40"NB & 60"NB SWIR respectively.
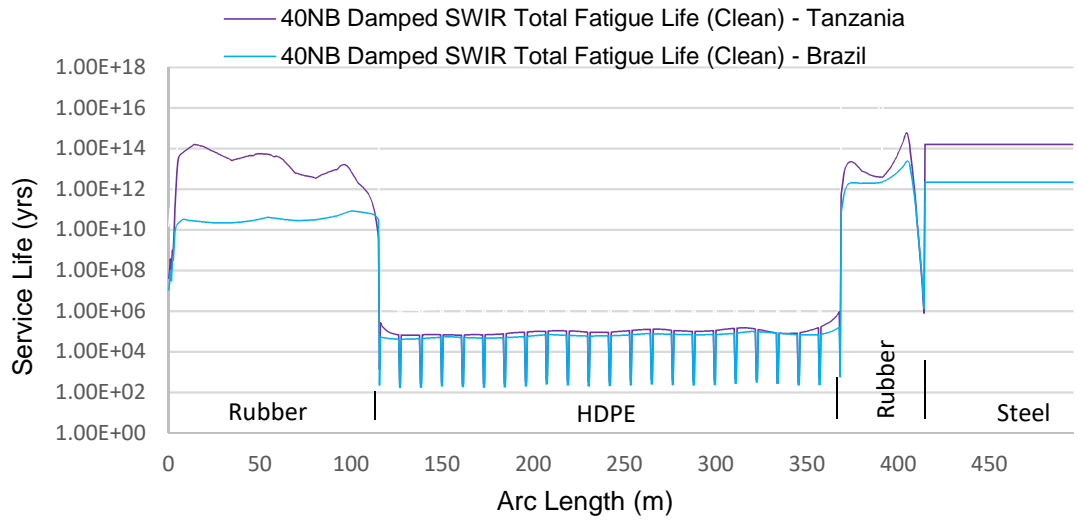
Fig.6-43:   40"NB SWIR Total Fatigue – Tanzania v Brazil
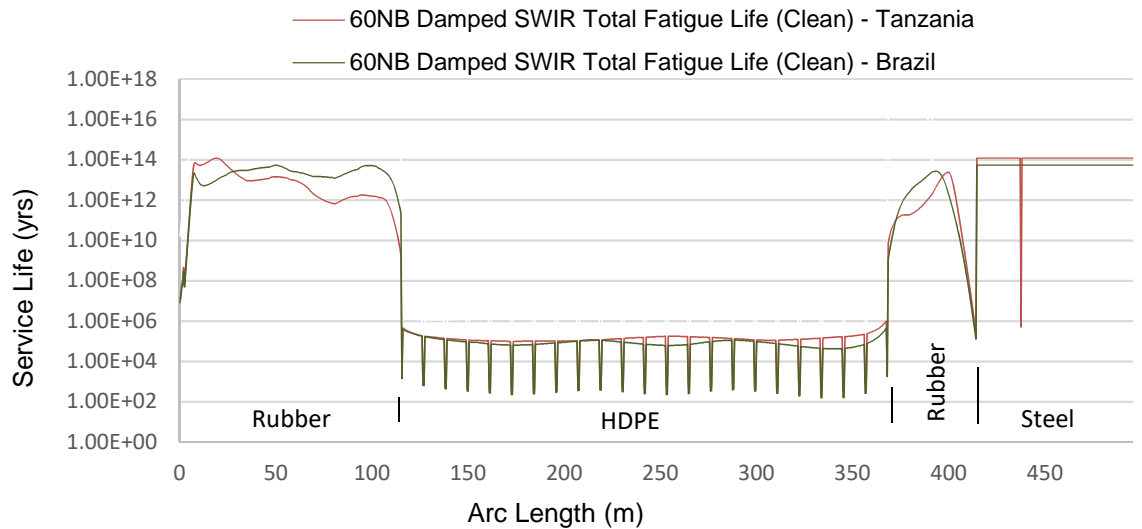
Fig.6-44:   60"NB SWIR Total Fatigue – Tanzania v Brazil

It can be seen from the above that although the maximum 1 year current speed is lower in Brazil, the current speed distribution is such that the fatigue life in both geographical locations is similar. It should be noted that, for the 60"NB SWIR, the VIV 'spike' in the steel pipe section is not present in the Brazil waters indicating that VIV in the SWIR is geographically sensitive.

Further examination reveals that it is the 1 year current profiles with a factor of 0.8 - 0.9 which causes the most fatigue damage within the SWIR. For these current profiles, the frequency of oscillation was found to be 0.08 and 0.1Hz

for current profiles 0.8 and 0.9 respectively. Reference to Fig.6-37 and examination of the simulations indicates that within this frequency range, it is modes 6 and 7 which are excited

Using the same theory discussed in section 6.3.4, the effective velocity was calculated as 0.425 – 0.530 m/s and is plotted on the current profiles in Fig.6-45.
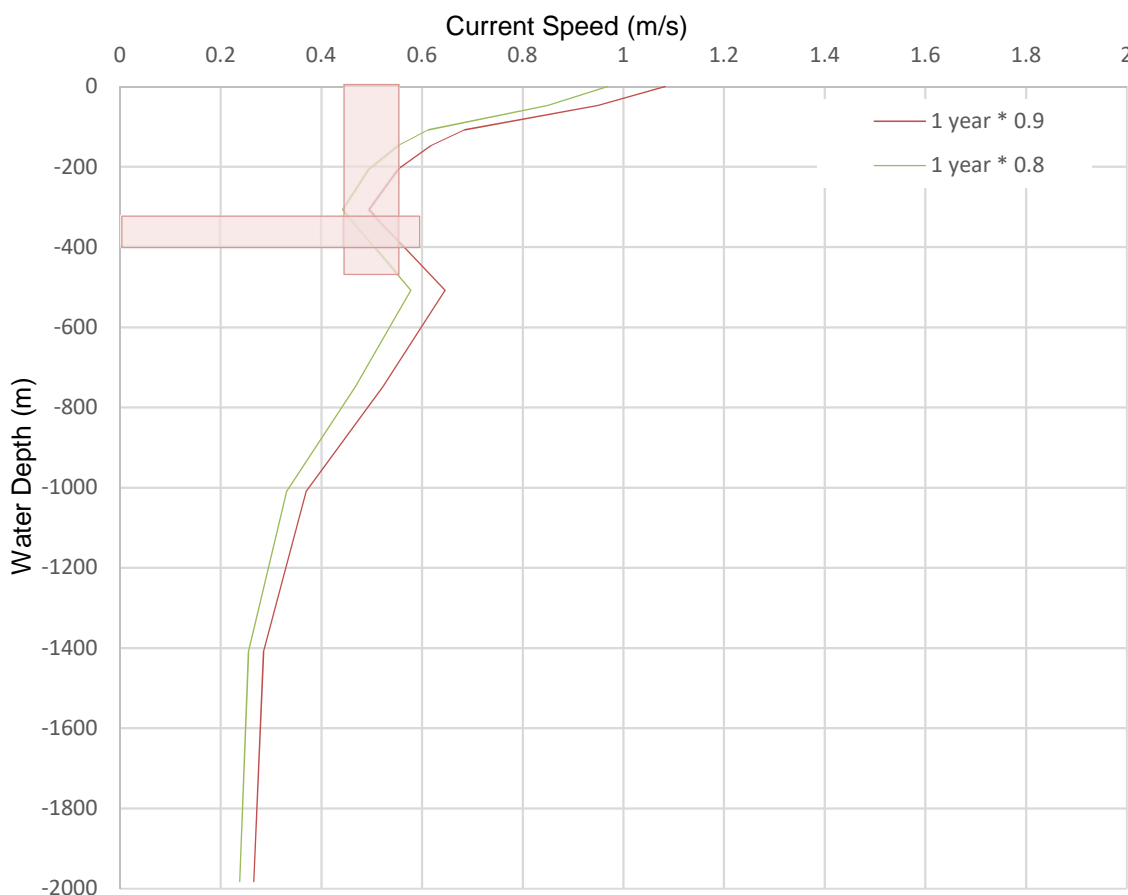
Fig.6-45:   40"NB Damped SWIR – VIV Excitation Zone (Brazil)

Although the Brazilian current profile is more irregular, it is feasible that this is in agreement with the earlier suggestion that the excitation zone is at the lower end of the SWIR.

The main contributor to fatigue damage in all the cases explored so far is the current and the subsequent VIV, the damage from waves is comparatively lower as the size of the FLNG is such that the vessel and SWIR response to waves is less acute. The next section investigates the effect the vessel size has on the proposed SWIR.

6.7. Vessel Characteristics

Due to the required processing facilities, the first generation of FLNG vessels currently under construction are dimensionally very large when compared to a typical FPSO, for example:

Petronas FLNG: L365m x W60m x D33m

Prelude FLNG: L488m x W74m x D42.5m

Coral South FLNG: L439m x W65m x D38.5m

Typical FPSO: L320m x W58m x D31m

A smaller vessel such as an FPSO may be more responsive to sea states and therefore the SWIR will be subject to increased loading. To assess the impact of installing the proposed SWIR onto a smaller vessel, the fatigue analysis due to waves for the damped SWIR was performed as per section 6.3.1 but using the RAO data from a typical FPSO. The resulting fatigue damage due to waves is extracted and compared against the fatigue damage on an FLNG vessel as shown in Figs.6-46 & 6-47.
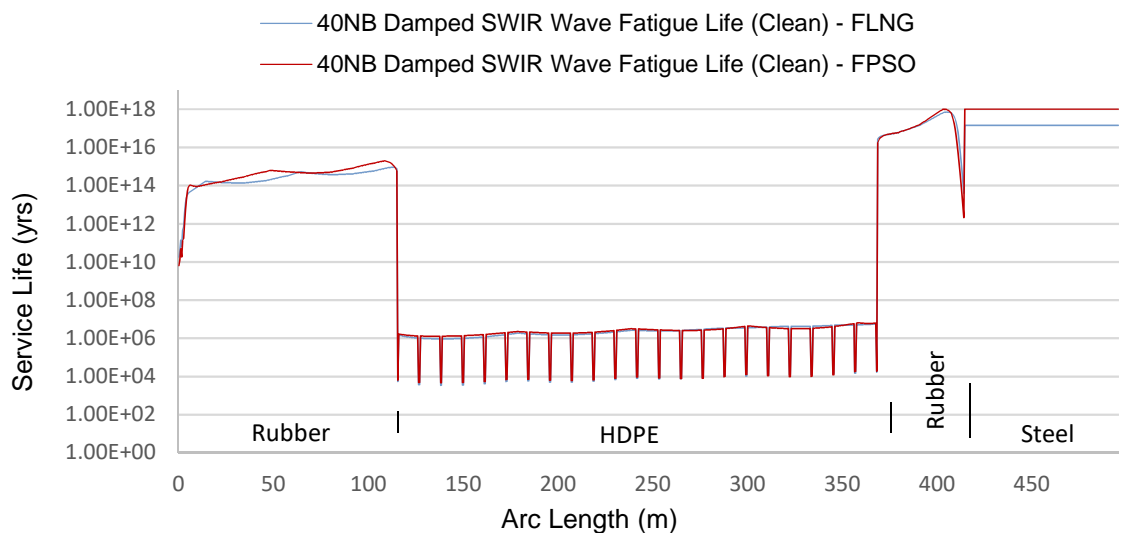
Fig.6-46:   40"NB SWIR Wave Fatigue – FLNG v FPSO
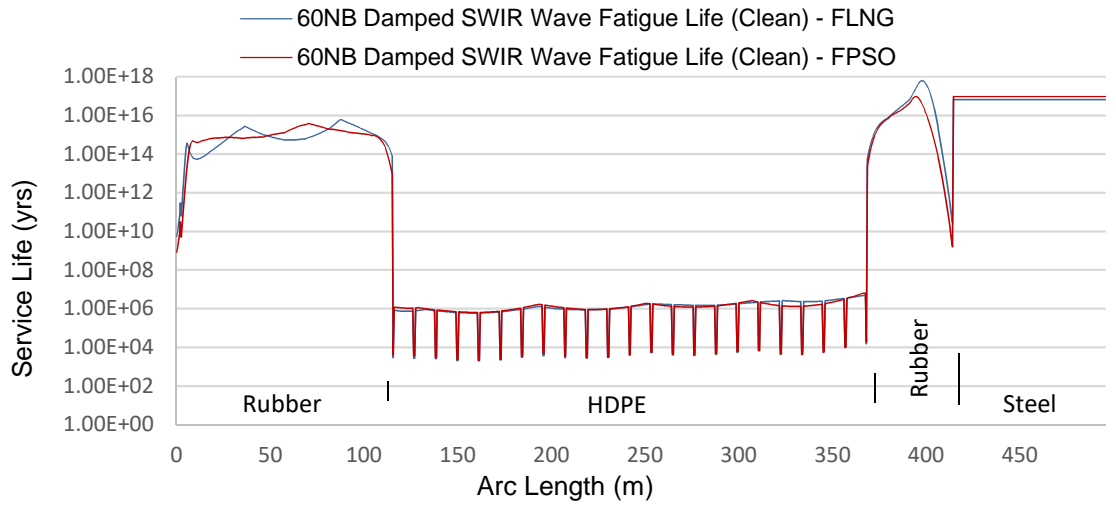
Fig.6-47:   60"NB SWIR Wave Fatigue – FLNG v FPSO

The effect on the total fatigue damage due to current and waves is shown in Figs.6-48 & 6-49.
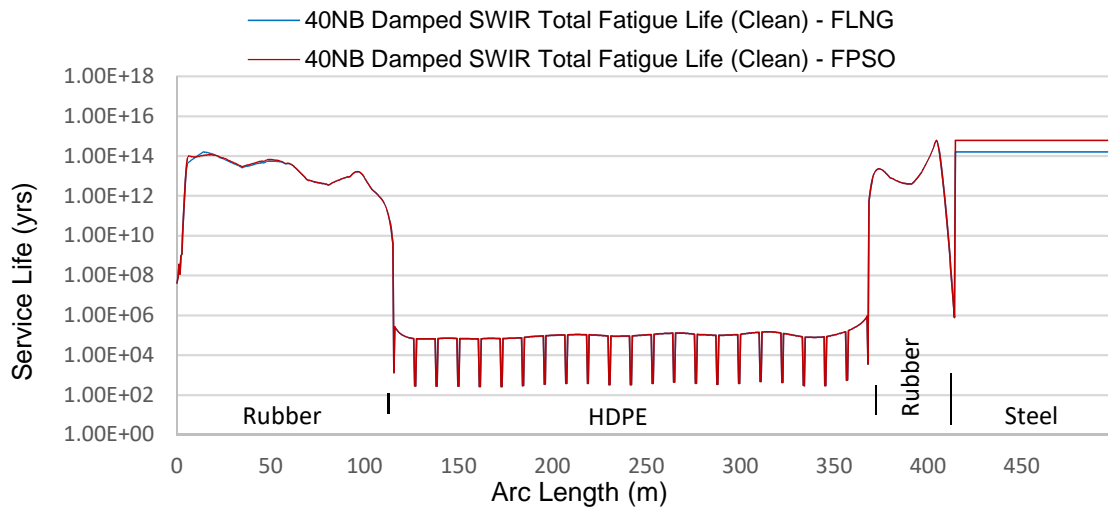
Fig.6-48:   40"NB SWIR Total Fatigue – FLNG v FPSO
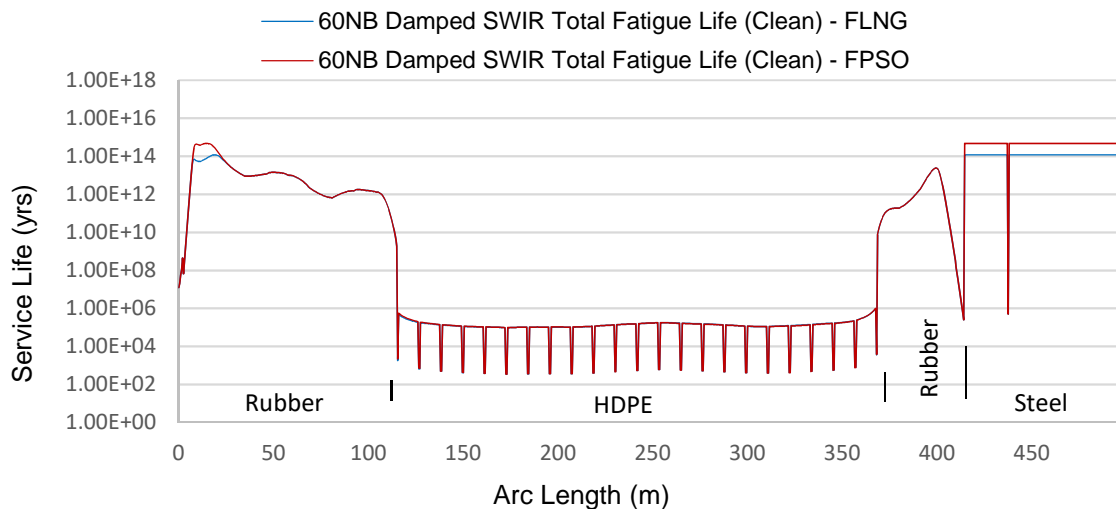
Fig.6-49:   60"NB SWIR Total Fatigue – FLNG v FPSO

A strength analysis was also performed as per section 6.2 to assess the impact the vessel response would have on the strength of the proposed SWIR and also the loads induced into the hull. The resulting analysis yielded the maximum values which are compared against the values reported for the FLNG vessel in Tables 6-8 & 6-9:

	Maximum Values	
	FLNG	**FPSO**
Flexible Rubber Pipe Section		
• **Tension** (kN)	**808.0**	**811.7**
• **Curvature** (Rad/m) *as MBR (m)*	**0.244** *4.1*	**0.242** *4.1*
HDPE Pipe Section		
• **Tensile Stress** (MPa)	**3.2**	**3.1**
• **Bending Stress** (MPa)	**0.7**	**0.7**
• **Von Mises Stress** (MPa)	**4.9**	**4.8**
• **Curvature** (Rad/m) *as MBR (m)*	**0.00168** *593.8*	**0.00165** *605.3*
Steel Pipe Section		
• **Tensile Stress** (MPa)	**4.0**	**4.0**
• **Bending Stress** (MPa)	**7.7**	**8.3**
• **Von Mises Stress** (MPa)	**12.8**	**13.3**
• **Curvature** (Rad/m) *as MBR (m)*	**0.00007445** *13431*	**0.00008** *12510*

Table 6-8: 40"NB SWIR Strength Analysis Results - FLNG v FPSO

	Maximum Values	
	FLNG	FPSO
Flexible Rubber Pipe Section		
• **Tension** (kN)	**1451.0**	**1487.6**
• **Curvature** (Rad/m) *as MBR (m)*	**0.1429** *7.0*	**0.1429** *7.0*
HDPE Pipe Section		
• **Tensile Stress** (MPa)	**2.0**	**2.0**
• **Bending Stress** (MPa)	**0.8**	**0.8**
• **Von Mises Stress** (MPa)	**3.8**	**3.9**
• **Curvature** (Rad/m) *as MBR (m)*	**0.001244** *803.6*	**0.00123** *815.3*
Steel Pipe Section		
• **Tensile Stress** (MPa)	**4.2**	**4.2**
• **Bending Stress** (MPa)	**8.8**	**9.7**
• **Von Mises Stress** (MPa)	**14.2**	**15.0**
• **Curvature** (Rad/m) *as MBR (m)*	**0.00005697** *17554*	**0.00006244** *16014*

Table 6-9: 60"NB SWIR Strength Analysis Results - FLNG v FPSO

The loads induced into the hull that can be used for the hang-off design are presented and compared against the values reported for the FLNG vessel in Tables 6-10& 6-11:

- *Maximum Values for 40"NB Hang-Off Design*

	Maximum Values	
	FLNG	FPSO
End Force (kN)	**837.3**	**843.1**
Bending Moment (kNm)	**969.1**	**966.7**
Shear Force (kN)	**433.7**	**427.2**

Table 6-10: Maximum Values for 40"NB Hang Off Design - FLNG v FPSO

- *Maximum Values for 60"NB Hang-Off Design*

	Maximum Values	
	FLNG	FPSO
End Force (kN)	1508.9	1545.1
Bending Moment (kNm)	2141.8	2144.0
Shear Force (kN)	677.9	672.2

Table 6-11:   Maximum Values for 60"NB Hang Off Design - FLNG v FPSO

It can be seen from the above that the total fatigue life of the SWIR and the loads induced into the SWIR from the FPSO vessel differ only slightly from those of the FLNG, the same can be seen for the loads induced into the hull of the vessel.

This suggests that the size of vessel, within the dimensions used within the industry, has a negligible effect on the strength and fatigue capabilities of the SWIR.

6.8. Stability due to Internal and External Flow

This section investigates the stability of the proposed Sea Water Intake Riser (SWIR) due to fluid flow, both internally and externally.

6.8.1. Internal fluid flow

As discussed in Section 2.6, the SWIR is in the form of a free hanging cantilever where the direction of flow is from the free end to the fixed end. In the research, this configuration is referred to as an aspirating cantilever. Although Paidoussis (2014) argues that instability does occur in aspirating pipes but the energy may be dissipated in the surrounding fluid making the critical flow velocity for the onset of flutter unattainable, he makes reference to research where attempts have been made to identify the critical flow velocity at which instability occurs. In the research, the flow velocity is generally expressed as the dimensionless flow velocity u which is defined as follows;

$$u = \left(\frac{M}{EI}\right)^{1/2} * U * L \qquad \text{(Giacobbi, et al., 2012) Eq.(30)}$$

where:
M = Mass of conveyed fluid per unit length
EI = Flexural Rigidity of the Pipe
U = Flow Velocity
L = Length of the Pipe

Giacobbi et al (2012) investigated the behaviour of cantilever pipes aspirating air using experimental numerical and analytical means and identified critical flow velocities in the range of:

u_{crit} = 2.0 - 4.0   (experimental)

u_{crit} = 2.0 - 3.5   (numerical)

u_{crit} = 4.0 − 6.0   (analytical)

Giacobbi et al (2012) also make reference to the unpublished results of experiments involving fully water-immersed aspirating cantilevers undertaken by Stephane Jamin at McGill University where:

$u_{crit} \approx 7.0$

Jamin (2010) performs experiments on a number of configurations for aspirating cantilever pipes immersed in water of which the reference configuration *3i* is most similar to the proposed SWIR configuration. The results show that the initial flow velocities of <3m/s actually have a stabilising effect on the pipe but it then starts to flutter at around 3.39m/s and increases more rapidly at 4.33m/s. For the pipe used in the experiments, this equates to a dimensionless critical flow velocity of:

$u_{crit} = 4.6 - 5.91$

Paidoussis (2014) makes reference to a 'lost' paper by Cui and Tani (1996) where theoretical and experimental analysis of a partly submerged water-aspirating cantilever, suggested flutter would not occur up to $u = 1000$ and was confirmed by experiment up to $u = 6.54$.

It should be noted that all of the above research is based on uniform cantilevers, with constant stiffness and mass, and that the surrounding medium is (or is assumed) to be still whereas the proposed SWIR under consideration is a non-uniform cantilever with varying stiffness and mass, and which is subject to external forces from ocean currents.

For a non-uniform aspirating cantilever like the proposed SWIR, the dimensionless flow velocity is more difficult to determine. However, as the research suggests that any instability originates at the intake of the aspirating cantilever, and as the proposed SWIR has steel pipe sections at the point of intake, to put the research into context, the following approximation is made.

If we assume that the lower section of the 40"NB damped SWIR is an 80.5m long uniform steel cantilever aspirating seawater at a velocity of 3m/s, the dimensionless fluid velocity can be calculated using:

$$u = \left(\frac{M}{EI}\right)^{1/2} * U * L \qquad \text{(Giacobbi, et al., 2012) Eq.(30)}$$

and where: M = 770 kg/m (assuming sea water density 1025kg/m³)

EI = 1.57E+09 N.m²

U = 3 m/s

L = 80.5 m

for Steel Pipe: OD   = 1.016 m

                    ID   = 0.978 m

                    E   = 212E+09 N/m^2

Therefore: $u = 0.169$

It can be seen that the dimensionless fluid velocity for this instance is significantly lower than the critical values of u = 2.0 - 7.0 referenced above. This is a broad assumption given that for the proposed SWIR, the top end of the steel pipe would not be clamped but instead connected to the flexible rubber pipe sections with six degrees of freedom. However, as the point of intake is the origin of the energy required to make the riser unstable, it could be argued that, as the steel pipe is below the critical velocities, then flutter would not be able to be established in the SWIR.

Additionally, and as discussed in Section 2.8, one of the general design parameters for the SWIR is a velocity of <3m/s and Jamin (2010) found that for velocities <3m/s the stability of aspirating cantilevers actually improved. Coupled with the conclusion made by Giacobbi et al (2012) that the forces are very weak and by Paidoussis (2014) that the energy may be dissipated into the surrounding fluid, it is assumed that instability due to aspiration of fluid is unlikely to occur and therefore will not be considered as a load case in this study.

Nonetheless, it is recommended that further research in this regard is undertaken with consideration for non-uniform cantilevers within external fluid flow.

6.8.2. External fluid flow

External fluid flow around the SWIR is caused by the ocean currents which vary in strength and profile depending upon the geographical location. One consequence of external fluid flow is the possibility of vortex induced vibration (VIV) and its contribution to fatigue damage which was investigated in Section 6.3.2. Another is the potential interference with other risers or mooring lines due to the excursion of the lower end of the SWIR.

Two approaches were used to evaluate the excursion of the proposed SWIR;

- *Lower End Excursion due to Extreme Current*

The simulations used in the strength analysis were interrogated to find the maximum lower end excursion due to the 100yr extreme current profile as shown in Fig.6-50 below.
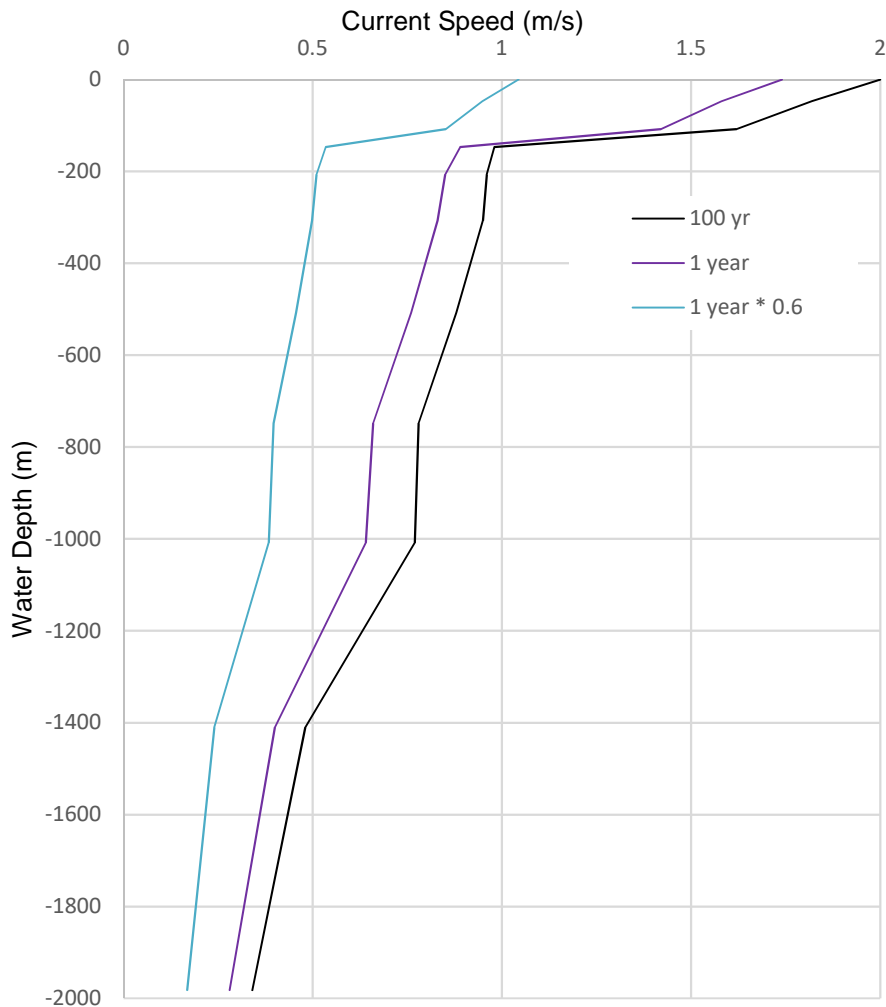
Fig.6-50:   Current Profiles

Is this scenario, the drag coefficients for the SWIR were established using the technique presented in ESDU (2010).

- *Lower End Excursion Due to VIV Drag Amplification*

Drag amplification occurs when VIV is established in a line and experiments by Vandiver (1983) gave good agreement with the following empirical formula;

$$C_D = C_{Do}[1 + 1.043\left(\frac{2*A_{rms}}{D}\right)^{0.65}]$$ (Vandiver, 1983)

where:

C_D	=	Drag Coefficient	
C_{Do}	=	Drag Coefficient for stationary cylinder	
A	=	Amplitude of cross flow vibration (m)	
D	=	Member Diameter (m)	

The Vandiver method, also presented in DNV-RP-C205 ((DNV, 2014) Sect 9.2.2.2, was used to determine the VIV Drag Amplification Factor (DAF) and applied to the simulations using the Iwans and Blevin Wake Oscillator model for the 1 year and the 1 year * 0.6 current profiles (as shown in Fig. 6-46) as these were found to have the largest VIV offsets and therefore, the largest VIV DAF.

The SWIR excursion profiles are presented below in Figs.6-51, 6-52 & 6-53.
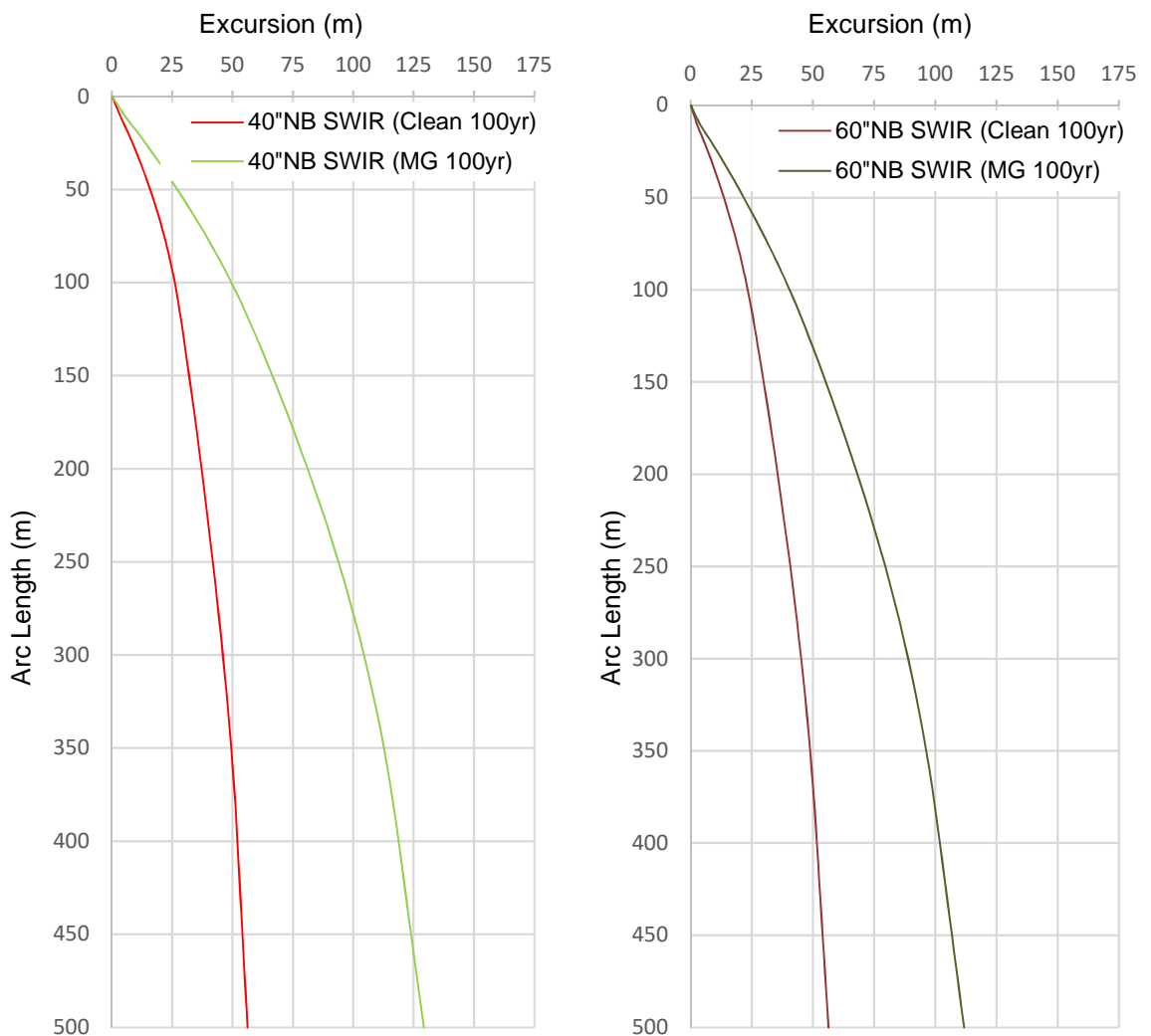
Fig.6-51:   Lower End Excursion – 100yr Current Profile
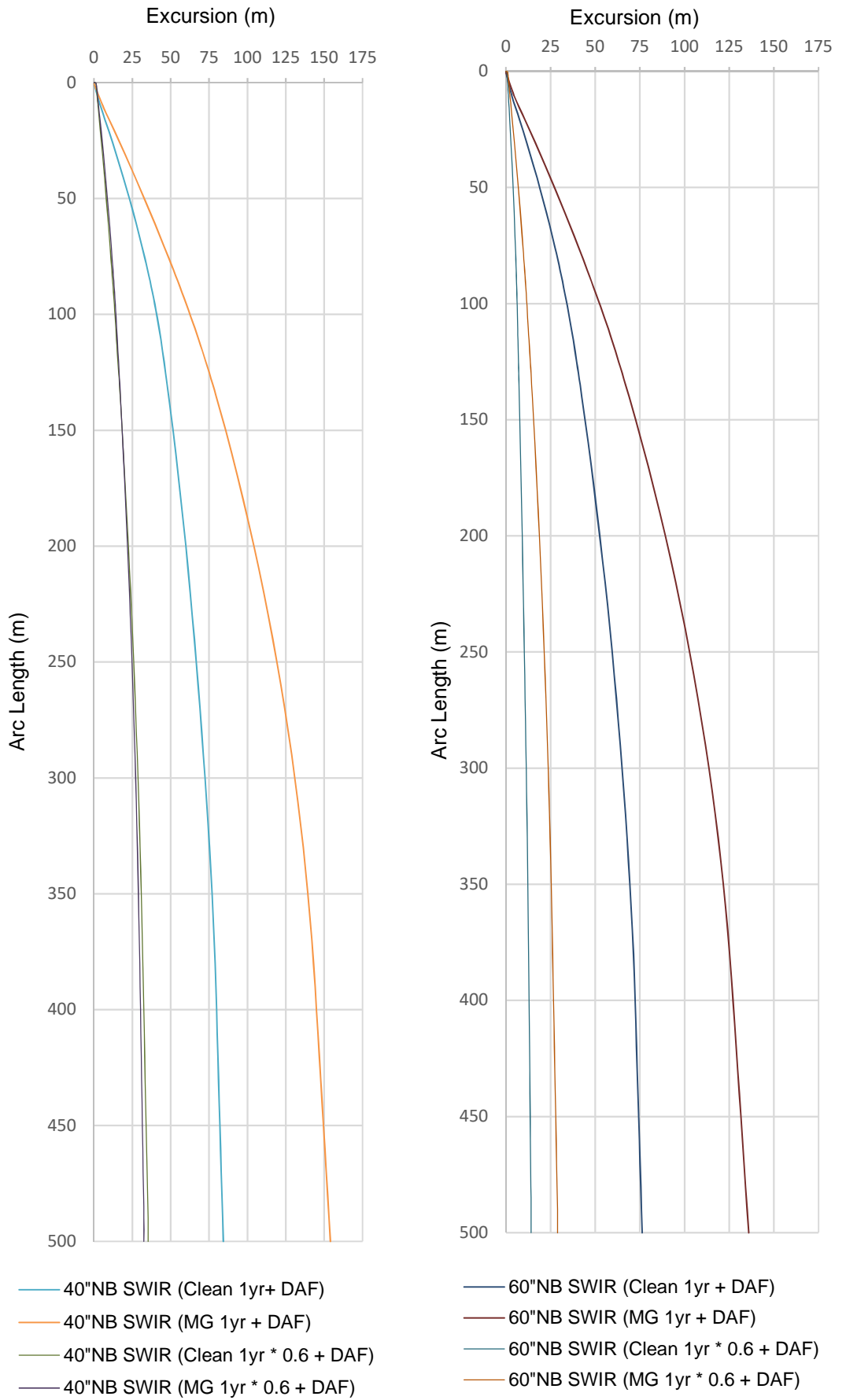
Fig.6-52:　　　Lower End Excursion – 1yr Current Profile + DAF
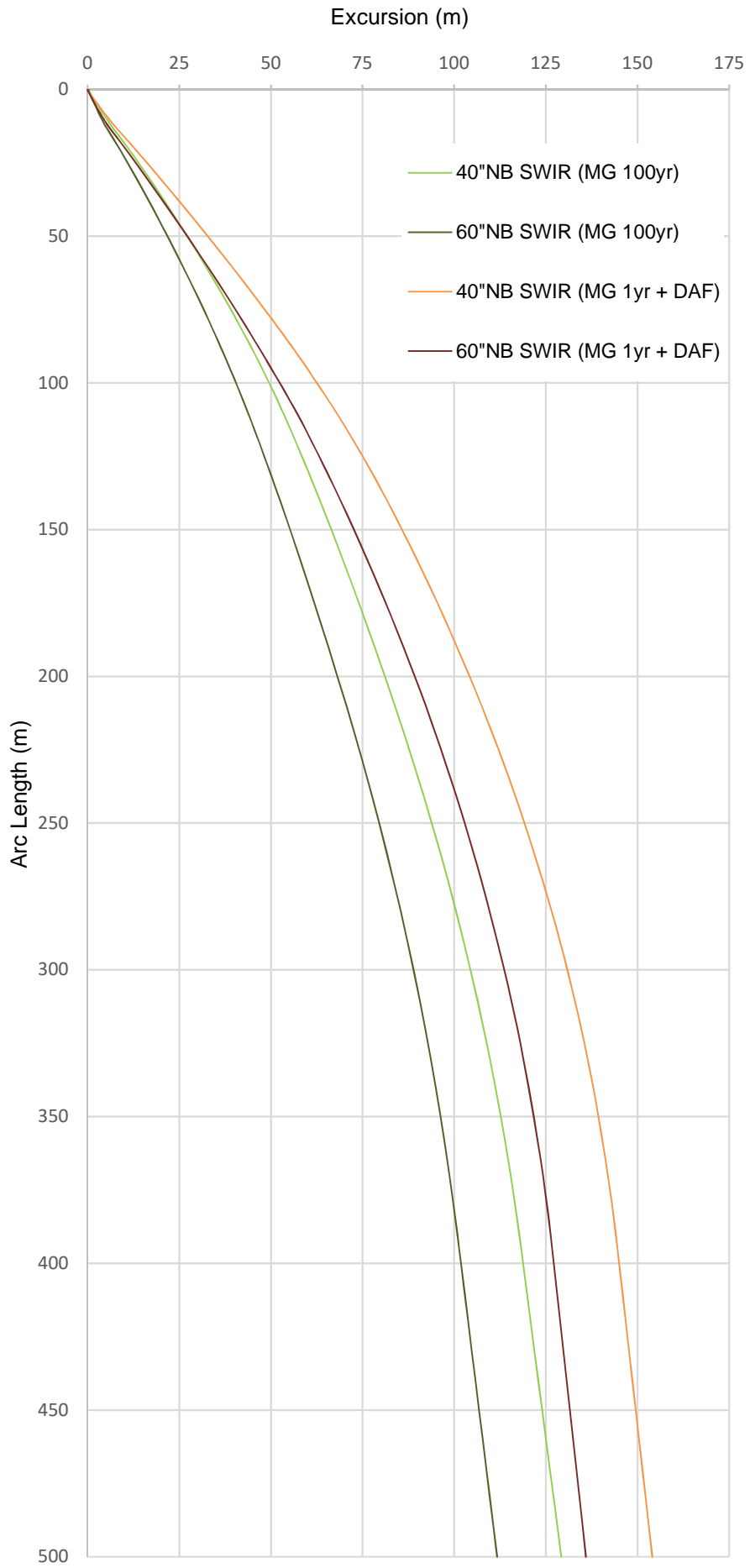
Fig.6-53:   Maximum Lower End Excursions

It can be seen from Fig.6.51 that the SWIR with marine growth attachment gives the largest excursion under the maximum 100yr current conditions. Similarly, in Fig.6-52 the SWIR with marine growth show the largest excursion under the maximum 1 year conditions with the DAF applied. Fig.6-53 compares the two approaches and shows that the 1 year current with a DAF applied has a greater excursion than the 100 yr return conditions. This suggests that the large excursions may occur frequently and should be assessed carefully in regard to interference with adjacent risers or structures.

- *Potential for adjacent SWIR Interference*

If more than one SWIR is installed on a vessel, there is a possibility that the current direction can be aligned with the two risers and if so, the upstream riser may create a wake and alter the behaviour of the downstream riser.

As stated in DNV-RP-F203 (DNV, 2009) Section 3.3, there is limited information available regarding VIV behaviour of a riser located in the wake of an upstream one, and that as a first estimate, no VIV response should be applied to the downstream riser. Therefore, to provide an indication of the behaviour of two SWIR in an aligned current, the maximum SWIR excursion determined from the 1yr return condition with the DAF applied is compared against the same without the DAF applied.

Fig. 6-54 shows the maximum excursion of each line and the approximate spacing required between the SWIR to avoid contact, which is approx. 57m and 52m for the 40NB SWIR and 60NB SWIR respectively.
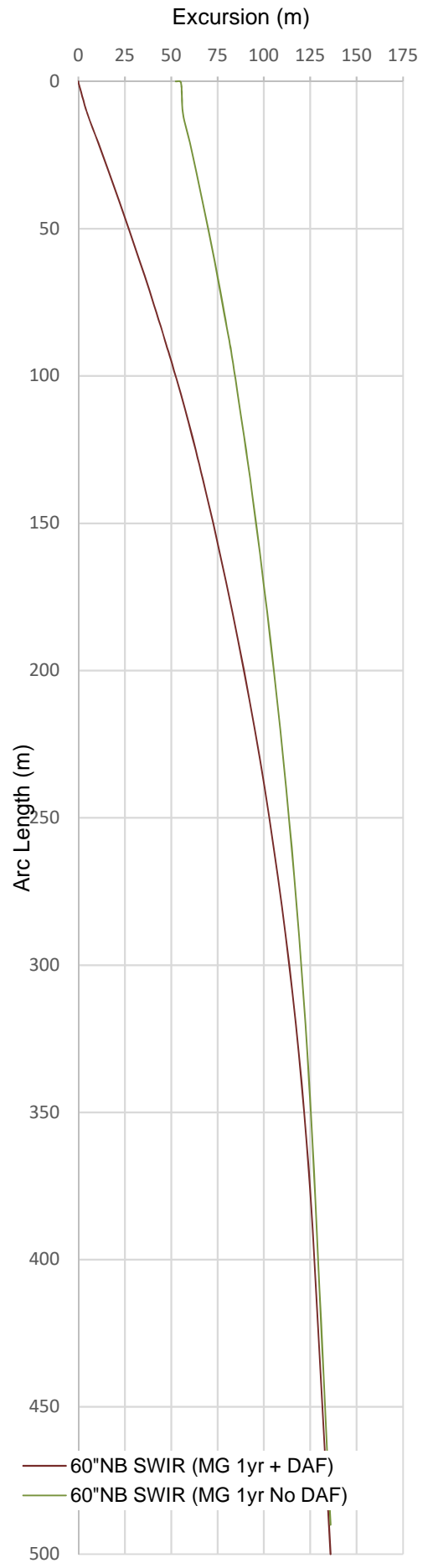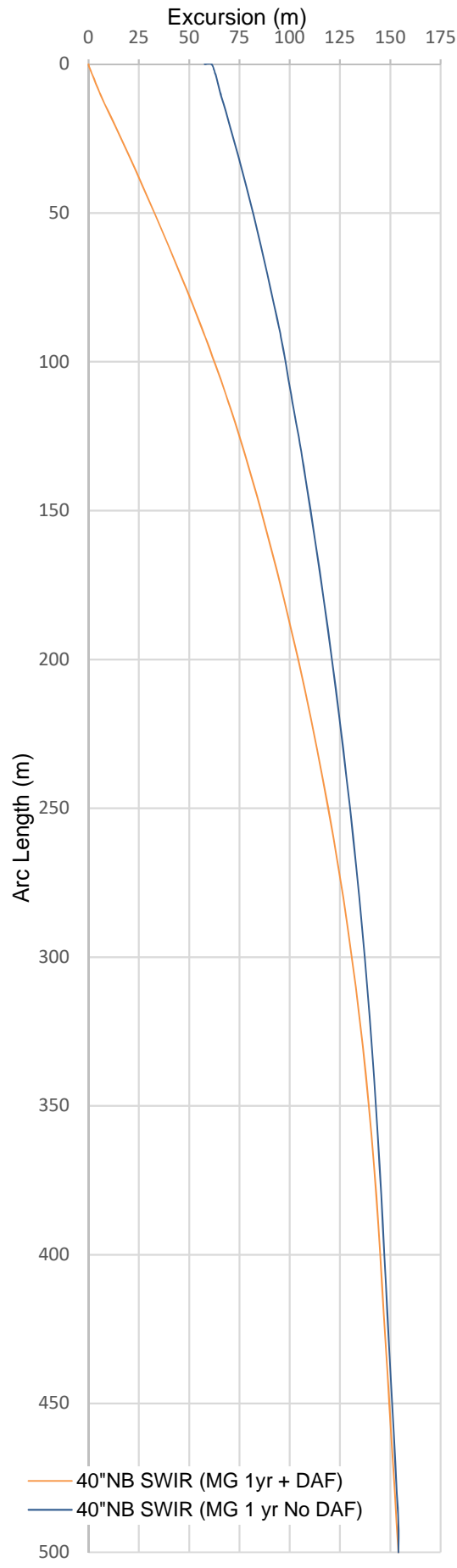
Fig.6-54:   SWIR Interference from Lower End Excursions

6.9. Flow Analysis

The function of the SWIR is to import cold seawater from below the surface of the ocean for use in the processing systems of the FLNG vessel. Of interest to the process engineers are the flow characteristics as seawater is imported through the Sea Water Intake Risers (SWIR), particularly the pressure loss characteristics and the temperature gain characteristics, therefore, a flow analysis of the SWIR in operation was performed, details of which are presented in the Portfolio [Section 9.0].

6.9.1. Pressure Losses

Pressure loss calculations for a range of flow rates were performed for both the 40"NB and 60"NB SWIR from which the pressure loss curves shown in Fig.6-55 and 6-56 were generated, showing the combined pressure loss through the strainer and the risers.
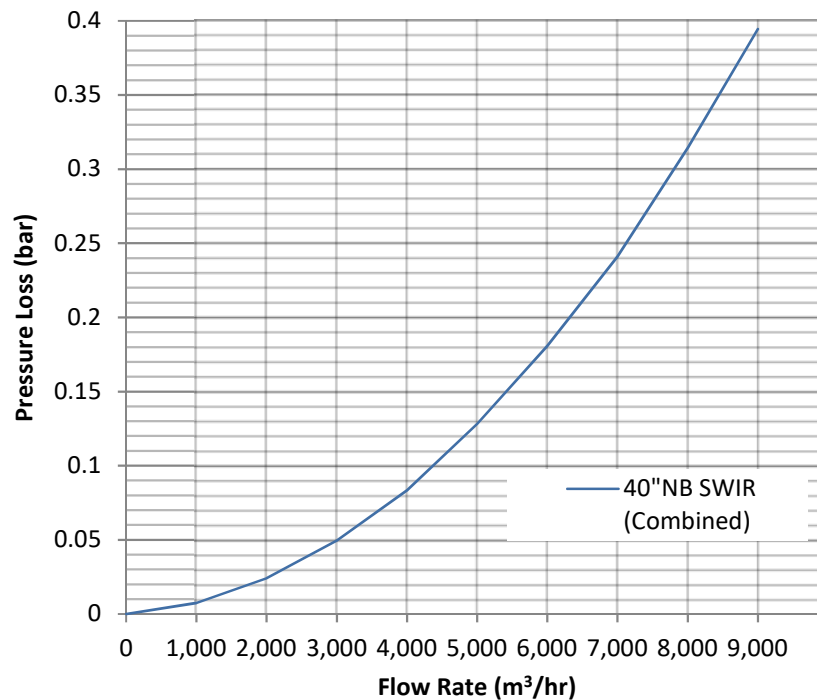
Fig.6-55:   Combined Pressure Losses through 40"NB SWIR
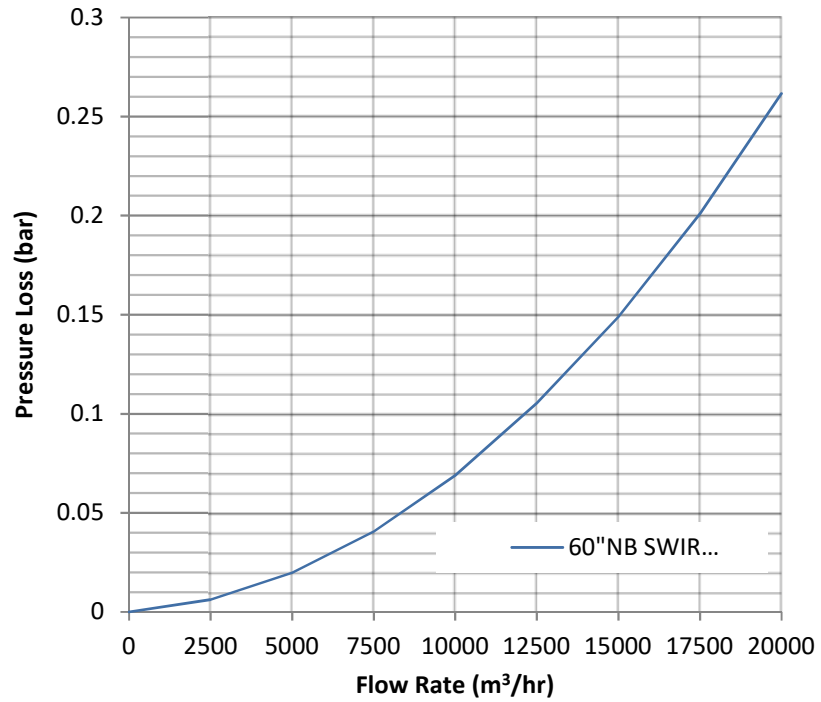
Fig.6-56:   Combined Pressure Losses through 60"NB SWIR

The curves shown above assume a 'clean' bore, that is without any wear or marine growth attachment.

- *Internal Roughness*

The pressure losses due to an increased internal roughness was evaluated to simulate the effect of marine growth or wear inside the SWIR.
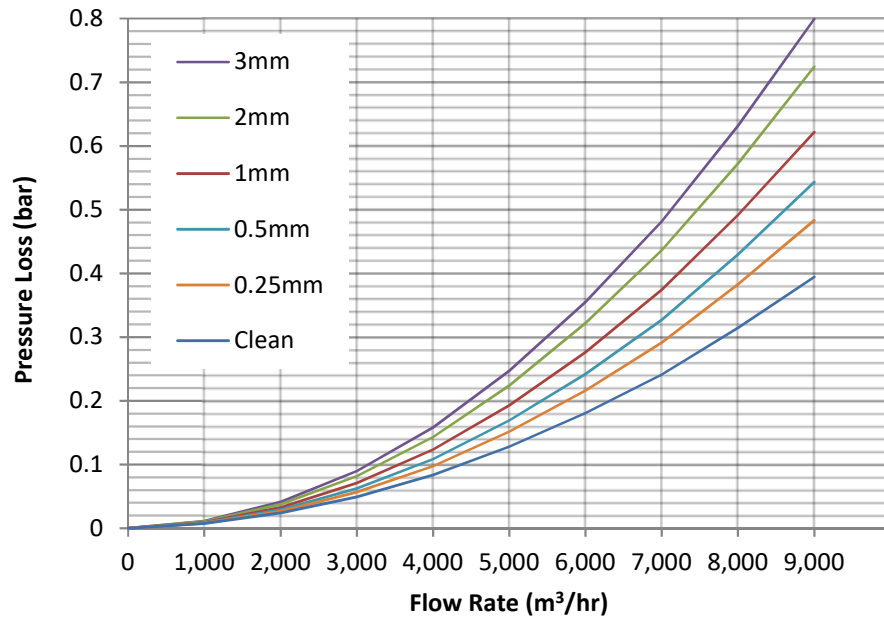
Fig.6-57:   Internal Roughness Effect on Pressure Losses (40"NB SWIR)
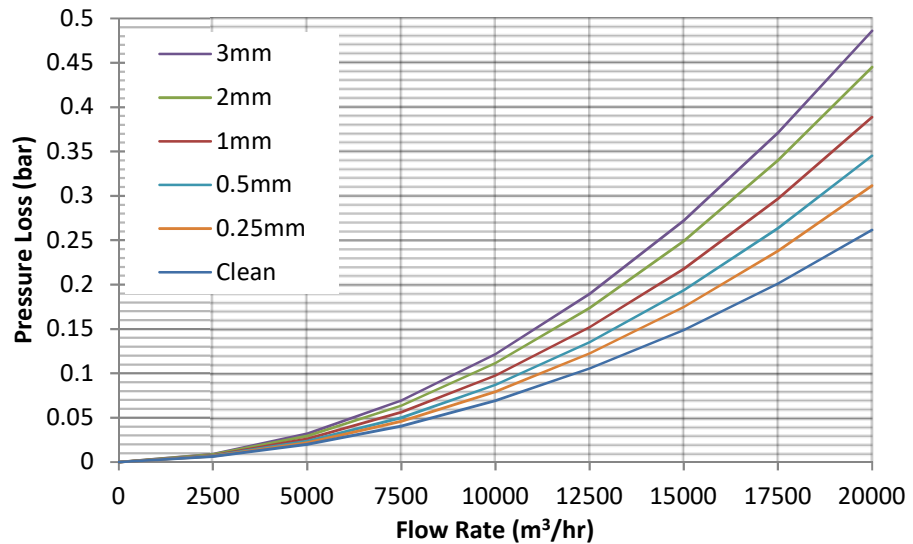
Fig.6-58:   Internal Roughness Effect on Pressure Losses (60"NB SWIR)

Figs. 6-57 and 6-58 show that the pressure losses can increase significantly due to the internal roughness of the SWIR, for the higher flow rates with a 3mm roughness, the pressure loss is approximately twice as that of a clean system. This effect should be taken into consideration during the design of the system and emphasises the advantages of an effective marine growth protection system.

- *Seawater Temperature*

The physical properties of seawater changes with temperature in as much as the colder the seawater, the higher the density and the greater the viscosity. Using the range of seawater temperatures and the corresponding properties shown in Table 6-12, a number of sensitivities were performed to quantify the effect of this on pressure loss through the system:

Seawater Properties (ITTC, 2011)		
Temp (°C)	**Density** (kg/m^3)	**Viscosity** (m^2/s)
22.9	1024	9.82E-07
21.1	1024.5	1.02E-06
19.3	1025	1.07E-06
17.3	1025.5	1.12E-06
15.1	1026	1.19E-06
12.7	1026.5	1.26E-06
10	1027	1.36E-06
6.7	1027.5	1.50E-06
2.2	1028	1.72E-06

Table 6-12:   Seawater Properties

The effect of seawater temperature on pressure loss through the system for a number of flow rates are shown in Figs 6-59 and Fig. 6-60 for the 40"NB SWIR and 60"NB SWIR respectively.
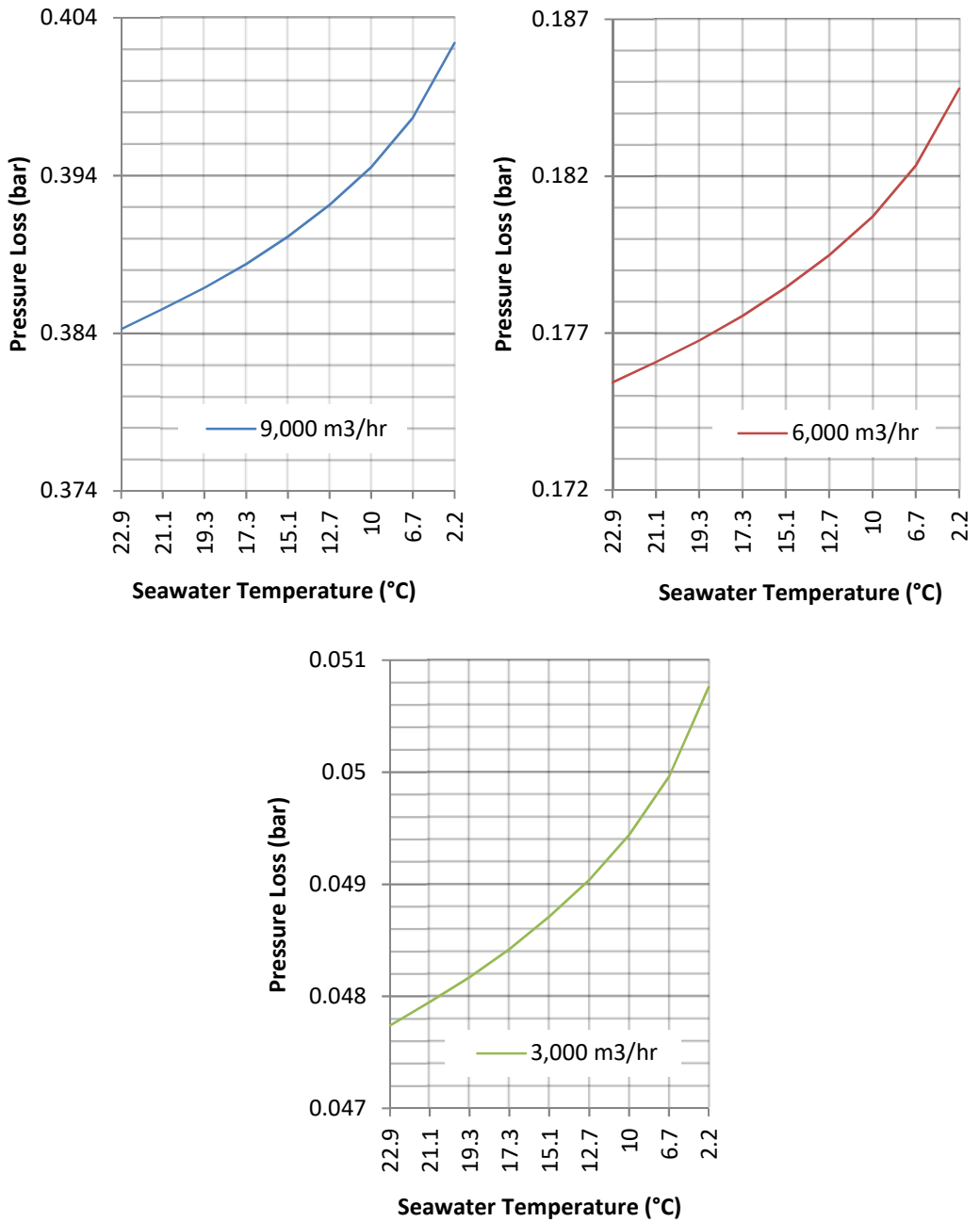
Fig.6-59:   Seawater Temperature effect on Pressure Losses (40"NB SWIR)
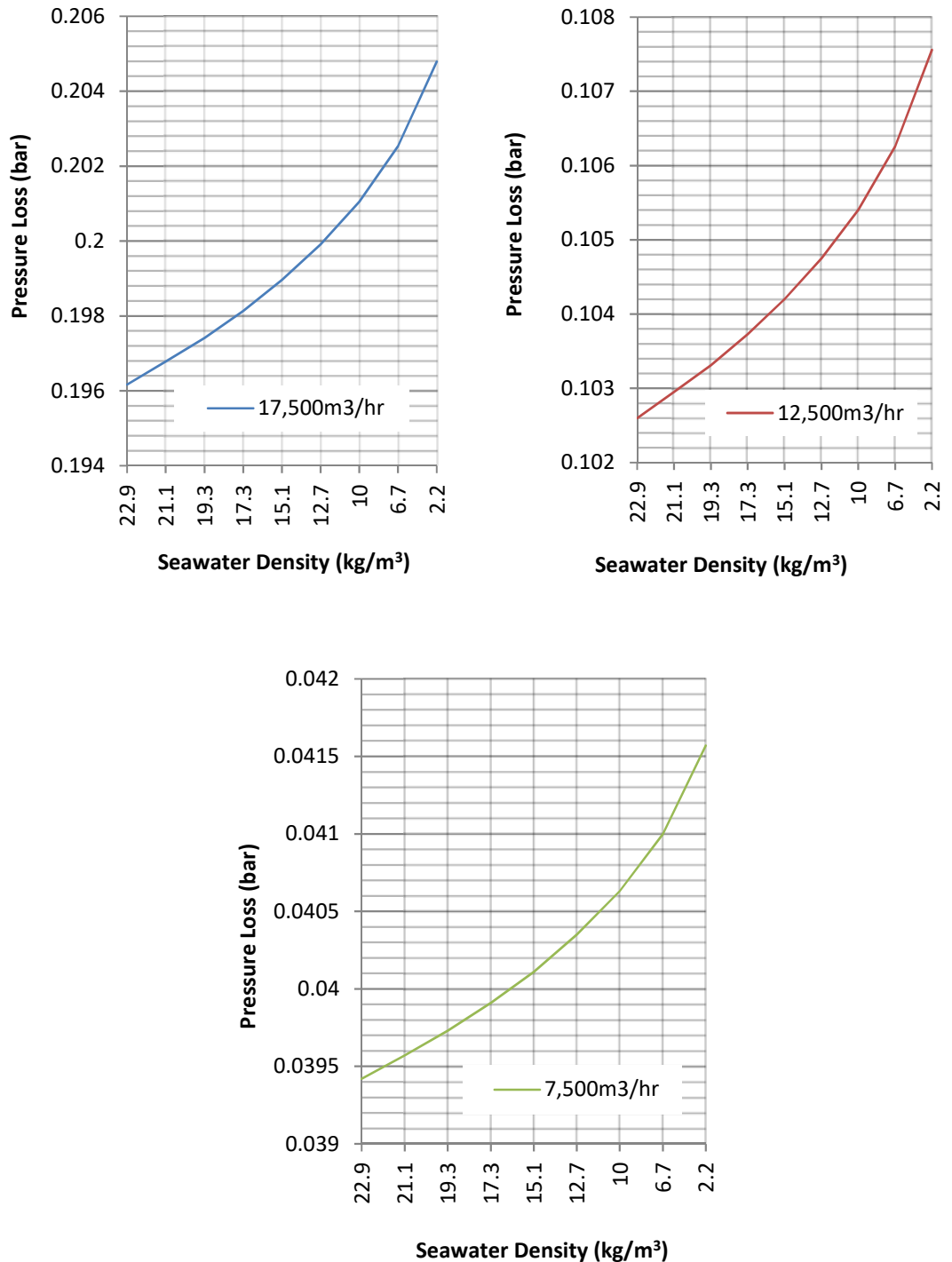
Fig.6-60:   Seawater Temperature effect on Pressure Losses (60"NB SWIR)

Figs. 6-59 and 6-60 show that the pressure losses do increase as the seawater temperature at the inlet point reduces however, these losses are in the order of 18mbar for the 40"NB SWIR at maximum flow rate to 2mbar for the 60"NB SWIR at reduced flow rate. Although these losses appear negligible, 18mbar represents approximately 9% of the generally accepted design parameter of 200mbar (0.2bar) so should be taken into consideration during the system design.

6.9.2. Temperature Gain

Temperature gain calculations for a range of flow rates were performed for both the 40"NB and 60"NB SWIR from which the Temperature Gain curves shown in:
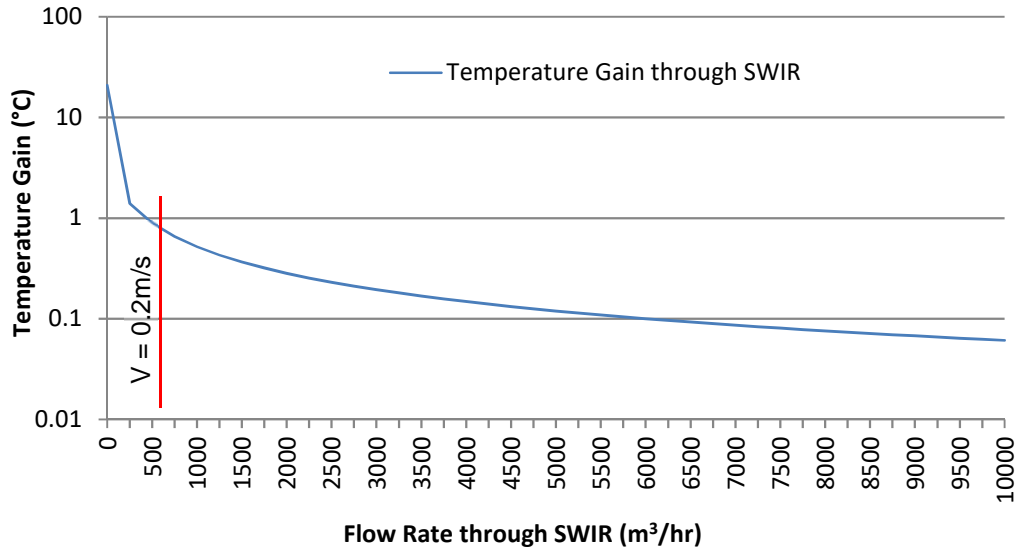
Fig.6-61:   Temperature Gain through 40"NB SWIR
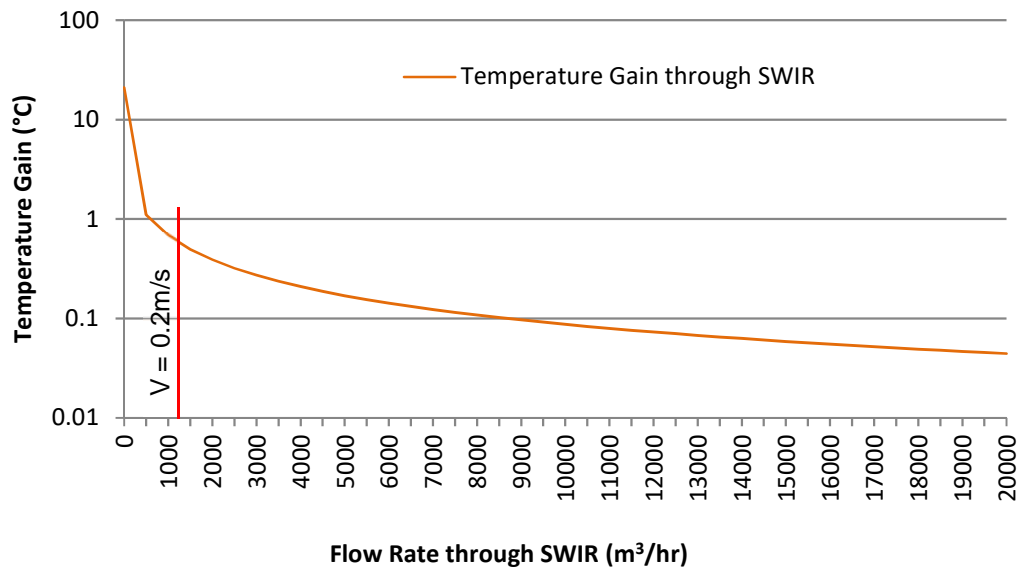
Fig.6-62:   Temperature Gain through 60"NB SWIR

It can be seen from Fig.6-61 and 6-62 that the temperature gain through the system is mostly negligible at around 0.1°C, however, when the flow rate is reduced so that the velocity of seawater through the SWIR is approximately 0.2m/s, the temperature gain starts to rise quite steeply.

6.10. Summary

This Chapter has investigated the mechanics of the proposed Seawater Intake Riser (SWIR) by performing preliminary analysis on a number of material configurations to determine which is the most optimum in terms of function, stability and loads induced into the vessel. It was found that a hybrid configuration of Rubber – HDPE – Rubber – Steel offered the most optimum solution and was subject to a more detailed analysis.

A strength analysis was undertaken to determine the most likely peak loads the system would encounter in service and a comparison made to the allowable loads. The strength analysis also reported the loads induced into the vessel hull at the connection point which were compared to previous work which indicated that the magnitude of these loads was within an acceptable range for the scaling up of the current and proven hang-off arrangement used on FPSO vessels.

A fatigue analysis was undertaken which investigated two contributors to fatigue damage, namely fatigue due to waves and fatigue due to current. For the fatigue due to waves, the energy from a random sea profile was converted into a regular sea profile and applied to the SWIR simulations and, using Miner's method and the SN data presented in Chapter 5.0, the fatigue damage was calculated. For the fatigue damage due to current, the annual current profile distribution was determined and the range of resulting current profiles applied to the SWIR simulations using a Wake Oscillator model to simulate vortex induced vibrations. Again, using Miner's method and the SN data presented in Chapter 5.0, the fatigue damage was calculated and added to the fatigue damage due to waves to determine the total fatigue damage, which was then inverted to predict the life of the SWIR in service. The results indicated that, although the SWIR would survive for the typical life of a vessel, there were some 'weak' points in the system that could be addressed to increase the safety margin. Interestingly, one of the weak points was in the steel pipe sections which became excited at a specific current speed. However, it was found that by damping the SWIR through replacing some of the steel sections with flexible rubber pipe sections mitigated the VIV response in the steel pipe sections and improved the fatigue life.

A number of sensitivities were performed on the proposed SWIR including increasing and decreasing the length of the SWIR. It was found that the fatigue life improved for the longer SWIR but was reduced for the shorter SWIR, albeit by small margins. A sensitivity on the geographical location indicated that a

reduced current velocity does not necessarily mean improved fatigue life, the distribution of the current velocity is just as important as the magnitude of the current velocity. A further sensitivity was performed on the vessel size and found that, in the locations considered, the typical vessel sizes used within the industry does not have a significant effect on the fatigue life of the proposed SWIR.

The stability of the SWIR was investigated in terms of internal and external fluid flow. For the internal fluid flow, a review of the literature around aspirating cantilever systems was undertaken and an assessment made as to whether this phenomenon would impact on the stability or induce fatigue of the system. From the research to date, the conclusion was made that, for the proposed SWIR, it was unlikely that internal fluid flow would affect the stability or life of the system. For the stability due to external flow, in addition to the effects of VIV determined from the fatigue analysis, the excursion distances for a range of current profiles were investigated and quantified. An assessment was made regarding the interaction between adjacent SWIR caused by wake and the spacing between required to avoid contact.

The flow of seawater through the SWIR was analysed and the expected pressure losses calculated for a range of flow rates. A number of sensitivities were run to determine the effects of water temperature on the pressure loss which appeared negligible but should be given consideration during system design. Similarly, the effect of internal roughness due to marine growth or wear was investigated and found to have a non-negligible effect pending the roughness value. The temperature gain of the seawater inside the SWIR was calculated for a range of flow rates and were found to be mostly negligible. However, once the flow rate was reduced to the point where the seawater velocity through the SWIR was <0.2m/s, the increase in temperature gain became very steep.

The next chapter addresses the seventh and final objective of this study which is to compare the system costs against the efficiency gains, so that an economic argument can be made for the proposed solution.

CHAPTER 7.0

ECONOMIC ARGUMENT

7. ECONOMIC ARGUMENT

7.1. Redundancy and Failure Mode Cost Impact

7.1.1. Redundancy

The two main components that provide the seawater intake capability on an FPSO or FLNG vessel are the Seawater Intake Risers (SWIR) and the Seawater Lift Pumps (SWLP) and, generally, there will be one SWIR for each SWLP. By comparison, the SWIR is a much less complex piece of equipment in as much as there are fewer components, no moving parts and no power demand, so consequently the maintenance requirements are minimal. The SWLP however is more complex piece of equipment will have a regular maintenance programme based on number of hours service and which would normally mean a redundancy requirement for the pump so that while one pump is being maintained, there is no loss of sea water capacity. According to Framo (2018), to achieve this the project would normally specify the required number of pumps as N+1 where N is the number of pumps required to deliver the design flow rate of seawater. The redundancy policy of the SWLP is in good agreement with the reliability of the SWIR in as much as, of the seawater intake systems supplied into the field to date, there have been no reported incidents of failure that have resulted in loss of seawater capacity and is thus the basis for minimal redundancy requirements. Also, a typical inspection and maintenance period for the SWLP is 5 years so the general recommendation is that the SWIR is recovered and inspected at the same time as the SWLP.

Therefore, the redundancy requirement for seawater intake capacity of the vessel is driven by the SWLP as opposed to the SWIR. Nonetheless as with any new or unproven system being introduced into the field, there is a level of risk involved. The next section investigates the potential risks and how these can be mitigated.

7.1.2. Failure Mode Analysis

DNV-RP-A203 (DNV, 2011) is a recommended practice with guidelines for the qualification of new technology ranging from Concept Evaluation through to Detailed Engineering. The main principle of the recommended practice is that the qualification process is a systematic, risk-based approach with specific attention on the novel elements of the technology and the potential failure modes. There are a number of publications in regard to failure mode analysis, for example BS5760 Part 5 (BSI, 1991) and the Siemens whitepaper

(Siemens, 2016), and which make use of a Risk Priority Number (RPN) to identify the most likely causes of failure.

To determine the RPN, each risk is ranked for its Severity (S), Occurrence (O) and Detection (D) as shown in Fig 7-1:

Severity

Rating	Meaning
1	No effect, no danger
2	Very minor – usually noticed only by discriminating or very observant users
3	Minor – only minor part of the system affected; noticed by average users
4-6	Moderate – most users are inconvenienced and/or annoyed
7-8	High – loss of primary function; users are dissatisfied
9-10	Very high – hazardous. Product becomes inoperative, customers angered. Failure constitutes a safety hazard and can cause injury or death.

Occurrence

Rating	Meaning
1	No documented failures on similar products/processes
2-3	Low – relatively few failures
4-6	Moderate – some occasional failures
7-8	High – repeated failures
9-10	Very high – failure is almost certain

Detection

Rating	Meaning
1	Fault is certain to be caught by testing
2	Fault almost certain to be caught by testing
3	High probability that tests will catch fault
4-6	Moderate probability that tests will catch fault
7-8	Low probability that tests will catch fault
9-10	Fault will be passed undetected to user/customer

(Siemens, 2016)

Fig.7-1: Severity, Occurrence and Detection Guideline

The product of S * O * D = RPN which can range from between 1 -1000 and the higher the RPN the greater the risk. Firstly though, the potential failure modes for the components within the system need to be identified.

API 17B (API, 2014) presents a list of potential failure modes for bonded rubber flexible pipes, most of which are primarily intended for high pressure discharge applications, however, they can be used as the basis for failure modes in a low pressure suction applications from which an RPN can be established as shown in Table 7-1.

Failure Mode	Failure Effect	Failure Mechanism	S	O	D	RPN
Collapse	-Restricted flow path	High tensile loads	8	1	1	**32**
Burst	-Leakage	High internal pressure	8	1	1	**8**
Tensile Failure	-Tensile reinforcement failure -Liner rupture -Leakage -Loss of system	High tensile loads	8	1	1	**8**
Compressive Failure	-Liner rupture -Leakage	Overbending	8	1	2	**16**
Overbending	-Leakage	High bending moments	8	2	8	**128**
Torsional Failure	-Leakage	High Torsional loads	8	1	2	**16**
Fatigue Failure	-Tensile reinforcement failure -Liner rupture -Leakage -Loss of system	High cyclic loads	8	2	8	**128**
Erosion	-Liner wear -Leakage	High solids content	8	1	8	**64**
Corrosion	-End fittings failure -Leakage -Loss of system	Exposure to seawater	8	1	8	**64**

Table 7-1:   Failure Modes of Bonded Flexible Pipes

As the medium is seawater, any potential failure of the SWIR will not have a catastrophic environmental impact, likewise, as the SWIR is located on the underside of the vessel, any potential failure is unlikely to cause injury to personnel, therefore, the Severity of a failure would be primarily the Dissatisfaction of the Customer. Occurrence can be based on the similarity of components currently operating in the field on FPSO vessels, where to date, there are no known failures of the SWIR elements, however for the time dependent modes, the ranking is higher. As the flexible rubber pipe is pressure tested and vacuum tested prior to delivery, the detection of manufacturing faults is high. Although Erosion may be difficult to detect, as the medium is raw seawater and the intake point above the seabed, the likelihood of sand or other solids being ingested is low. With reference to Section 4.2, there is a reported failure of the caisson itself resulting in the loss of a SWIR, however, as the failure cause is within the caisson, it will not be considered as a part of the FMEA for the SWIR.

The failure modes identified for the flexible rubber pipe can be adopted and amended for the HDPE pipe sections and the RPN established as shown in Table 7-2.

Failure Mode	Failure Effect	Failure Mechanism	S	O	D	RPN
Collapse	-Leakage	High tensile loads	8	1	8	**64**
Burst	-Leakage	High internal pressure	8	1	1	**8**
Ductile Failure	-Leakage -Loss of system	High tensile loads SCG	8	4	8	**256**
Brittle Failure	-Leakage -Loss of system	Creep SCG	8	4	8	**256**
Overbending	-Leakage -Loss of system	High bending moments SCG	8	4	8	**256**
Fatigue Failure	-Leakage -Loss of system	High cyclic loads	8	4	8	**256**
Erosion	-Wall thickness reduction -Leakage	High solids content	8	1	8	**64**
Chemical Degradation	-Wall thickness reduction -Leakage	Exposure to chemicals	8	1	8	**64**

Table 7-2: Failure Modes of HDPE Pipes

Connor (2015) identifies that Stress Crack Growth (SCG) is one of the major failure modes for PE piping systems and can result is ductile failure from overstressing or brittle failure from time dependent creep which is the general mode of field failure reported due to SCG in the butt fusion zone. This failure mode can be accelerated by temperature, stress concentrations, fatigue or the chemical environment. As the HPDE sections will be submerged in low temperature seawater, the effects of temperature and chemical environment can be discounted, however, fatigue and stress concentrations, particularly in the butt fusion zone are susceptible to SCG. Connor (2015) also highlights the difficulty in the detection of butt fusion welds flaws as traditional methods such as radiography and ultrasound are unreliable and new methods such as ultrasonic phase array and microwaves are not yet reliable or cost effective. As such the emphasis on butt fusion weld quality is prevention through quality control as opposed to detection. Based on this, the time dependent modes are ranked higher.

Sykes (2012) presents the major failure modes for metallic subsea pipelines in the Gulf of Mexico and the North Sea which are corrosion (internal and external), material failure (fatigue and localised buckling), storms and maritime activity. Maritime activity is a general reference to other activities along the length of a pipeline but as the SWIR is local to the vessel, this will be excluded as a potential failure mode whereas Storms can be related to high loadings

due to vessel motion and current strength. Although reported for a different application to the SWIR, these failure modes can be used as a basis for the steel sections in the SWIR and the RPN assigned as shown in Table 7-3.

Failure Mode	Failure Effect	Failure Mechanism	S	O	D	RPN
Corrosion	-Wall thickness reduction -Leakage	Exposure to seawater	8	1	1	**8**
Tensile Failure	-Leakage -Loss of system	High tensile loads	8	1	1	**8**
Fatigue Failure	-Leakage -Loss of system	High cyclic loads	8	1	8	**64**

Table 7-3:   Failure Modes of Steel Pipes

From the field data summarised in Section 4.4, the corrosion measures used for the steel strainer are proving to be satisfactory, therefore, if applied to the steel pipe sections, the occurrence of corrosion would be low, and as visual observation can be made by use of a boroscope or ROV, detection of corrosion would be high. The steel sections can also be pressure tested to verify the strength so detection of manufacturing faults is high. However, it is the cyclic loading in service that is difficult to detect and is predicted by numerical modelling and SN data, albeit, the SN data for steel is well established and proven.

The failure modes identified for the steel pipe sections can also be applied to the flange joint at the hang off connection. Again, using the corrosion measures currently in operation and inspection by ROV, the occurrence is low and the detection is high so the RPN for the hang off connection failure modes can be established as shown in Table 7-4.

Failure Mode	Failure Effect	Failure Mechanism	S	O	D	RPN
Corrosion	Wall thickness reduction Leakage	High solids content	8	1	1	**8**
Tensile Failure	Leakage Loss of system	High tensile loads SCG	8	1	1	**8**
Fatigue Failure	Leakage Loss of system	High cyclic loads	8	1	8	**64**

Table 7-4:   Failure Modes of Hang-off Connection

For the strainer, the main failure mode is blockage, either due to marine growth or else external debris. Detection of the blockage can be achieved

by visual means such as boroscope or ROV. It should also be noted that ROV can be equipped with jet wash equipment to clean the strainer as shown in Fig.7-2.

Fig.7-2: Jet Washing of Strainer

Consequently, the occurrence is moderate but the detection is high as shown by the RPN presented in Table 7-5

Failure Mode	Failure Effect	Failure Mechanism	S	O	D	RPN
Blockage	Restricted Flow Path	Marine Growth Formation	8	4	1	**32**

Table 7-5: Failure Modes of Strainer

It can be seen from Tables 7-1 thru' 7-5 that the potential failure modes with the highest risk are related to the time dependent mechanisms and the resulting damage due to fatigue. The next section looks at how these risks can be mitigated.

7.1.3. Mitigation & Cost Impact

These potential failure modes can be mitigated by a bespoke fatigue testing programme for the selected materials, with particular emphasis on the HDPE butt fusion welds performed on samples produced by the selected supplier/manufacturer for these components. Also, the numerical modelling of the system should ensure that comprehensive load cases are considered and that the field specific vessel details and environmental data are accurate. During manufacture of the system, the quality assurance and quality control measures must be validated and monitored and sufficient testing of the components undertaken

From the mitigation measures indicated above, the cost impact is primarily due to comprehensive fatigue testing of materials, extensive numerical modelling of the system and the implementation of strict quality control procedures. Although the magnitude of these measures will be specific to each project, and therefore difficult to quantify generically, an approximation can be made for inclusion into the overall economic argument for the proposed system.

For the costs associated with the long term fatigue testing of the materials, correspondence with a test facility by the Author (Craig & Hopley, 2016) suggested that to develop SN data for 6-8 specimens, cyclic testing at 5Hz in room temperature for up to one million cycles will cost approximately £1,200 per material. So, assuming that, for reliability data for a live project (ASTM, 2015), 24 specimens are required for each material (4-off specimens @ 6-off stress levels) and that 8 materials are to be tested (e.g. 2-off parent pipe, 2-off butt fusion welds, 2-off textile cords + 2-off contingency), this would give an estimated cost of approximately £28,800. With an allowance for preparation of samples, administration, logistics etc, this could be rounded up to £35,000.

To cover the required modelling and analysis of the system, we can assume employment of a dedicated analyst for one year at a cost to the project of say £60,000 per annum. Likewise, to ensure the Quality Control and Quality Assurance during material testing and manufacture, we can assume the employment of a dedicated Quality Engineer for two years, also at £60,000 per annum.

Based on this, the mitigation measures for the potential failure modes would equate to approximately £215,000, and with contingency allowance for, 3rd party involvement, travel, accommodation etc., could be assumed to be £250,000. Working in USD with an exchange rate of 1GBP = 1.4USD, this would equate to USD350,000, which will be considered for this study.

With regard to redundancy, as discussed in Section 7.1.1, the redundancy capacity will be in line with the SWLP which is N+1 and so one additional SWIR will be considered for this study.

7.2. FLNG Capital Costs

Due to confidentiality, differences in scope and the fact that most FLNG projects are still under construction, it is difficult to obtain accurate cost information (Songhurst, 2016), nonetheless, an estimate can be made based on various press releases and statements.

The production capacity of an FLNG vessel is generally stated in units of Million Tonnes per Annum (MTPA) and Duncan (2016) estimates the CAPEX cost of an FLNG vessel to be between USD 500-4,000 per Tonnes per Annum (TPA) of production capacity with the average being approximately USD 1,400 per TPA. Songhurst (2016) narrows this down to between USD 600-1000 per TPA, with the exception of the Shell Prelude project due to the complexity of the vessel compared to other projects.

To validate these unit costs, the production capacity of three of the first FLNG vessels, which are currently in various stages of development, are compared against the published CAPEX costs for the vessel, namely;

- *Petronas PFLNG1:*

Status: On station,1st Gas produced Nov. 2016 (Petronas, 2016)
Production Capacity: 1.2MTPA (Sakmar, 2016):
CAPEX: USD 1.16 Billion (Songhurst, 2016)

- *Shell Prelude:*

Status: In position, Hook-up & commissioning in hand (Shell Australia, 2017)
Production Capacity: 3.6MTPA (Sakmar, 2016):
CAPEX: USD 7.2 billion (Songhurst, 2016)

- *Total Coral South:*

Status: Financial Investment approved (Offshore Energy Today, 2017)
Production Capacity: 3.4MTPA (Offshore Energy Today, 2017)
CAPEX: USD 4.7 billion (Offshore Energy Today, 2017)

Petronas have not declared the CAPEX cost of the PFLNG1 other than to state that it is between USD 1-10 Billion (Chen, 2015) however Songhurst (2016) estimates the CAPEX as USD 1.16 Billion which equates to a unit cost of USD 967 per TPA. The unit cost for the Prelude equates to USD 2,000 per TPA, whereas the Coral South unit cost is USD 1,382.

For these three projects, the FLNG CAPEX costs are between USD 1000-2000 per TPA which are generally in line with the estimates by Duncan (2016) and Songhurst (2016) and will be used for this economic argument.

7.3. LNG Market Price

The market price for LNG is generally measured in units of US Dollars per million British Thermal Units (USD/mmBtu) and the price varies geographically as illustrated in the below image;
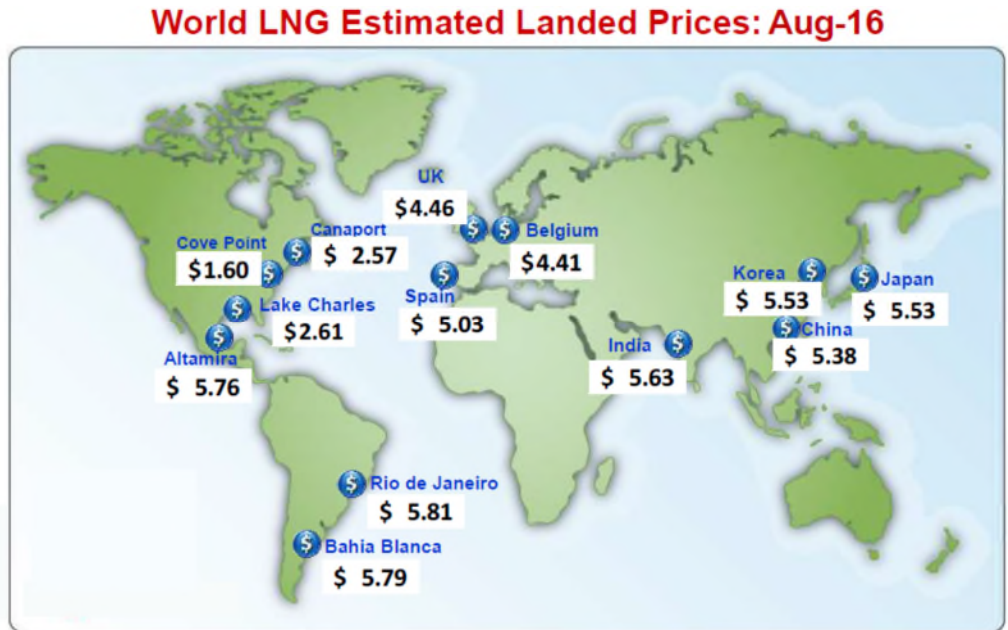
Fig.7-3: World LNG Estimated Landed Prices: Aug-16
(Waterstone Energy Inc, 2016)
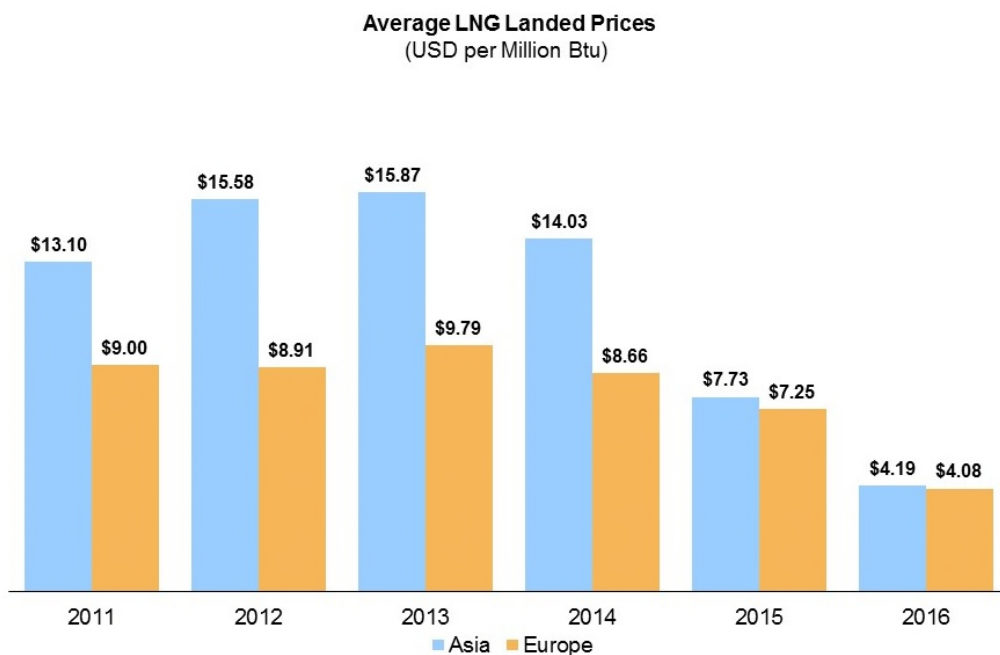
Fig.7-4: Average LNG Landed Prices
(Wilson & Turaga, 2016)

The above graph shows the average LNG landed prices by region for the last 6 years which shows that the current rates are the lowest in this period. For reference, 1 tonne of LNG equates to 53.38 mmBtu (IGU, 2012)

7.4. FLNG Cooling Water Requirements

Early reports estimated that for a FLNG vessel with a production capacity of 1.5MTPA, approximately 15,000m^3/hr of seawater would be required for cooling (Finn, 2009) which can be restated as 10,000m^3/hr/MPTA. However, for the three FLNG vessels considered in Section 7.2, the Shell Prelude flow rate requirement is 50,000m^3/hr which, for a production capacity of 3.6MTPA, gives a unit requirement of 13,888m^3/hr/MTPA. Likewise, the PFLNG1 flow rate requirement is 19,250m^3/hr which for a production capacity of 1.2MTPA gives a unit requirement of 16,040m^3/hr/MTPA, whereas the Total Coral South flow rate requirement of 22,200m^3/hr with a production capacity of 3.4MTPA gives a unit requirement of 6,530m^3/hr/MTPA. Although similar to the early estimates, these unit values do vary which are most likely due the cooling process adopted for each project and the redundancy capacity that may not have been considered initially.

7.5. SWIR Cost Advantage

7.5.1. Production Advantage

According to Pettersen et al (2013), a seawater temperature reduction of 15-20°C corresponds to an increase in the production capacity of the FLNG unit by 15-20%, i.e. -1°C = +1% MTPA. A further study (Corneliussen & Samnoy, 2015) indicated that for a 3°C decrease in seawater temperature, an increase of 1.8% in production capacity could be attained, i.e. -1°C = +0.6% MTPA.

7.5.2. SWIR CAPEX Costs

For the three live projects considered in Section 7.2, the SWIR lengths and the seawater import depths are known and the temperature differential can be estimated from the available environmental data. Additionally, from the Author's involvement with the tendering process for each of the above projects, the costs to supply the specified SWIR can be estimated, i.e.

- *Petronas PFLNG1:*   (Petronas, 2013)

SWIR Length: 37m

Seawater Import Depth: 50m

Mean Temperature Differential: 6°C

SWIR Package Cost: USD 1.35M[1]

- *Shell Prelude:*   (Kuiper, 2008)

SWIR Length: 132m

Seawater Import Depth: 150m

Mean Temperature Differential: 8°C

SWIR Package Cost: USD 12.5-25M[2]

- *Total Coral South:*   (Eni, 2017)

SWIR Length: 137m

Seawater Import Depth: 150m

Mean Temperature Differential: 8°C

SWIR Package Cost: USD 12.5-15M[3]

---

1) Author was Project Manager for Supply of Equipment
2) Author was involved with tender for supply of single pipe solution. Bundled pipe solution was selected at estimated cost of 1.5 x single pipe solution.
3) Author was involved with tender for Supply of Equipment

7.5.3. SWIR Installation Costs

The system installation costs are not included with the above, however, the Author has supervised the installation of several SWIR systems on FPSO's (and the PFLNG1) and estimates the time to install a SWIR as follows:

- Rig Up = 6 hours
- SWIR Assembly & Deployment = 2 hours per pipe section
- Rig Down = 6 hours

For example, the estimated time to install a SWIR with 6 hose sections would be 24 hours, i.e. 2 x 12-hour shifts.

From the Author's experience offshore, the personnel required to install a SWIR system consists of:

- 2-off Mechanical Fitters
- 4-off Riggers
- 1-off Crane Driver
- 1-off Supervisor
- 1-off Vendor Representative

Although the day rates (i.e. 12 hour shift) for each discipline can vary and are also sector specific, Songhurst (2016) estimates that the cost per person is USD 100,000 per annum which, assuming a 2-week on / 2-week off rotation, equates to USD 546 per 12 hour shift. If we assume that the Supervisor rate is approximately double at USD 1000 per 12 hour shift and the Vendor representative rate is USD 2000 per day, then the personnel costs for the installation team would be approximately USD 7,000 per 12-hour shift. With allowance for support functions and contingency this can be estimated at USD 10,000 per 12-hour shift which will be considered for this study.

7.5.4. SWIR Maintenance Costs

As discussed in section 7.1.1, the recommended inspection interval is in line with the Sea Water Lift Pump which is generally every 5 years so, for a service life in excess of 20 years, this would require a minimum of 4-off inspections. If we assume that the retrieval cost is the same as the installation cost, then the cost for each inspection would be double the installation cost plus say an estimated CAPEX x 3% for the spare parts. Using these figures, the lifetime maintenance costs for the system can also be estimated.

7.5.5. SWIR Costs for Live Projects

Using the data discussed in above, it is possible to evaluate the actual costs of the SWIR systems supplied for live projects and compare it against the production advantage gained from the temperature reduction.

	VESSEL			
FLNG Cost	PFLNG	Prelude	Coral	
FLNG Production Capacity	1.2	3.6	3.4	*MTPA*
Unit Cost of FLNG	967	2,000	1,382	*USD/TPA*
FLNG CAPEX	1.16	7.20	4.70	*B USD*
FLNG Revenue				
LNG Market Price	4.1	4.1	4.1	*USD/mmBTU*
LNG Revenue	242.3	727.0	686.7	*M USD/Annum*
FLNG CAPEX Recovery	4.8	9.9	6.8	*years*
Seawater Cooling				
No. Risers (N+1)	5	8	4	
Design Flow Requirement	19,250	50,000	22,200	m^3*/hour*
Flow Capability (N+1)	24,063	57,143	29,600	m^3*/hour*
Riser Length	37	132	137	*m*
SWIR CAPEX Cost	1.35	25.0	15.0	*M USD*
SWIR Unit Cost	1.52	3.31	3.70	*USD/m^3/hour/m*
SWIR Installation Costs	0.075	0.408	0.204	*M USD*
No SWIR Inspections	4	4	4	
SWIR Maintenance Costs	0.641	4.014	2.082	*M USD*
SWIR Lifetime costs	2.066	29.422	17.286	*M USD*
Advantage of SWIR				
Delta T	6	8	8	*°C*
Production Rate Advantage	0.6	0.6	0.6	*%/°C*
Total Production Advantage	3.6	4.8	4.8	*% MTPA*
Increased LNG Revenue	8.7	34.9	33.0	*M USD/Annum*
SWIR Cost Recovery	0.24	0.84	0.52	*years*

Fig.7-5: Estimated SWIR advantage for known FLNG Projects

To give the worst case scenario for the three live projects, the figures used for the evaluation in Fig. 7-5, consider the highest estimated SWIR costs, the lowest LNG Market Price and the lowest estimated Production Rate Advantage.

This evaluation suggests that the annual revenue increase from production will range from USD8.7M for PFLNG1 up to USD34.9M for the Prelude and that for all of the projects, the lifetime cost of the SWIR system will be recovered in less than 1 year of LNG production.

Also, by virtue of the fact that these three live projects have invested into SWIR systems, it suggests that the project process engineers have made a sound economic argument for the importation of colder seawater using SWIR.

7.5.6. Projected SWIR Costs for Proposed Solution

To make an economic argument for the installation of the proposed SWIR, the same data and assumptions are used for a 500m SWIR on these live projects.

	VESSEL			
FLNG Cost	**PFLNG**	**Prelude**	**Coral**	
FLNG Production Capacity	1.2	3.6	3.4	*MTPA*
Unit Cost of FLNG	967	2,000	1,382	*USD/TPA*
FLNG CAPEX	1.16	7.20	4.70	*B USD*
FLNG Revenue				
LNG Market Price	4.1	4.1	4.1	*USD/mmBTU*
LNG Revenue	242.3	727.0	686.7	*M USD/Annum*
FLNG CAPEX Recovery	4.8	9.9	6.8	*years*
Seawater Cooling				
No. Risers (N+1)	5	8	4	
Design Flow Requirement	19,250	50,000	22,200	$m^3/hour$
Flow Capability (N+1)	24,063	57,143	29,600	$m^3/hour$
Riser Length	500	500	500	*m*
SWIR Development Costs	0.35	0.35	0.35	
SWIR Unit Cost	1.52	3.31	3.70	$USD/m^3/hour/m$
SWIR CAPEX Cost	18.24	94.70	54.74	*M USD*
SWIR Installation Costs	0.075	0.408	0.204	*M USD*
No SWIR Inspections	4	4	4	
SWIR Maintenance Costs	1.147	6.105	3.274	*M USD*
SWIR Lifetime costs	19.816	101.560	58.573	*M USD*
Advantage of SWIR				
Delta T	17.6	20	17.6	*°C*
Production Rate Advantage	0.6	0.6	0.6	*%/°C*
Total Production Advantage	10.56	12	10.56	*% MTPA*
Increased LNG Revenue	25.6	87.2	72.5	*M USD/Annum*
SWIR Cost Recovery	0.77	1.16	0.81	*years*

Fig.7-6: Estimated advantage of 500m SWIR for known FLNG Projects

In the scenario presented in Fig.7-6, the same project data is used except the SWIR is increased to 500m, the development costs are added and the

seawater temperature differential adjusted accordingly. Note that for PFLNG, the water depth is only 77m so for this illustration, the temperature differential for 500m is based on the Coral South temperature profile.

It can be seen that the annual revenue increase from production will range from USD25.6M for PFLNG1 up to USD87.2M for the Prelude and that for all of the projects, the lifetime cost of the SWIR system will be recovered in less than 14 months of LNG production.

	VESSEL			
FLNG Cost	**PFLNG**	**Prelude**	**Coral**	
FLNG Production Capacity	1.2	3.6	3.4	*MTPA*
Unit Cost of FLNG	967	2,000	1,382	*USD/TPA*
FLNG CAPEX	1.16	7.20	4.70	*B USD*
FLNG Revenue				
LNG Market Price	4.1	4.1	4.1	*USD/mmBTU*
LNG Revenue	242.3	727.0	686.7	*M USD/Annum*
FLNG CAPEX Recovery	4.8	9.9	6.8	*years*
Seawater Cooling				
No. Risers (N+1)	5	8	4	
Design Flow Requirement	19,250	50,000	22,200	*m^3/hour*
Flow Capability (N+1)	24,063	57,143	29,600	*m^3/hour*
Riser Length	500	500	500	*m*
SWIR Development Costs	0.35	0.35	0.35	
SWIR Unit Cost	3.70	3.70	3.70	*USD/m^3/hour/m*
SWIR CAPEX Cost	44.50	105.68	54.74	*M USD*
SWIR Installation Costs	0.075	0.408	0.204	*M USD*
No SWIR Inspections	4	4	4	
SWIR Maintenance Costs	1.935	6.435	3.274	*M USD*
SWIR Lifetime costs	46.863	112.877	58.573	*M USD*
Advantage of SWIR				
Delta T	17.6	20	17.6	*°C*
Production Rate Advantage	0.6	0.6	0.6	*%/°C*
Total Production Advantage	10.56	12	10.56	*% MTPA*
Increased LNG Revenue	25.6	87.2	72.5	*M USD/Annum*
SWIR Cost Recovery	1.83	1.29	0.81	*years*

Fig.7-7: Worst Case advantage of 500m SWIR for known FLNG Projects

In the scenario presented in Fig.7-7, the same project data is used except the SWIR unit rate for all projects is increased to the maximum calculated for the known projects.

The impact of this is that the SWIR lifetime cost recovery is increased but remains less than 2 years of LNG production for all projects.

	VESSEL			
FLNG Cost	**PFLNG**	**Prelude**	**Coral**	
FLNG Production Capacity	1.2	3.6	3.4	*MTPA*
Unit Cost of FLNG	967	2,000	1,382	*USD/TPA*
FLNG CAPEX	1.16	7.20	4.70	*B USD*
FLNG Revenue				
LNG Market Price	8.2	8.2	8.2	*USD/mmBTU*
LNG Revenue	484.7	1,454.1	1,373.3	*M USD/Annum*
FLNG CAPEX Recovery	2.4	5.0	3.4	*years*
Seawater Cooling				
No. Risers (N+1)	5	8	4	
Design Flow Requirement	19,250	50,000	22,200	m^3*/hour*
Flow Capability (N+1)	24,063	57,143	29,600	m^3*/hour*
Riser Length	500	500	500	*m*
SWIR Development Costs	0.35	0.35	0.35	
SWIR Unit Cost	3.70	3.70	3.70	*USD/*m^3*/hour/m*
SWIR CAPEX Cost	44.50	105.68	54.74	*M USD*
SWIR Installation Costs	0.075	0.408	0.204	*M USD*
No SWIR Inspections	4	4	4	
SWIR Maintenance Costs	1.935	6.435	3.274	*M USD*
SWIR Lifetime costs	46.863	112.877	58.573	*M USD*
Advantage of SWIR				
Delta T	17.6	20	17.6	*°C*
Production Rate Advantage	1	1	1	*%/°C*
Total Production Advantage	17.6	20	17.6	*% MTPA*
Increased LNG Revenue	85.3	290.8	241.7	*M USD/Annum*
SWIR Cost Recovery	0.55	0.39	0.24	*years*

Fig.7-8: Best Case advantage of 500m SWIR for known FLNG Projects

The final scenario presented in Fig.7-8 represents the best outcome from the available data. The market price of LNG is doubled which is the approximate average price for the preceding 5 years and the Production Rate advantage is increased to 1% / 1°C.

It can be seen that the annual revenue increase from production will range from USD85.3M for PFLNG1 up to USD290.8M for the Prelude and that for all of the projects, the lifetime costs of the SWIR system will be recovered in less than 6 months of LNG production.

7.6. Summary

As with any equipment package, cost has to be a major consideration. A system where the cost outweighs the operational financial benefits of the system is not a realistic proposition. Similarly, during operation, it is desirable to recover the CAPEX of the system as quickly as possible.

The economic argument presented in this chapter is two-fold. Firstly, using known and published data for current FLNG vessels either in operation or under construction, the financial advantage of importing colder water from depth using the project specific SWIR is demonstrated. This is further validated by virtue of the fact that the three projects considered have all invested in sea water intake risers for this purpose.

Secondly, using the same data for each of the projects, the SWIR is extended to 500m and the associated installation and maintenance costs incorporated. The failure mitigation costs developed from an FMEA of the proposed solution are also incorporated and a number of scenarios explored.

The scenarios explored suggest that there is a definite economic advantage for the proposed solution in terms of increased production and therefore annual revenue from the FLNG and also demonstrate that the lifetime cost of the SWIR is recovered early.

It could be argued that each stranded gas reservoir only has a finite capacity therefore despite the rate of production, the total revenue from that reservoir will be constant. However, the increased production rate due to an SWIR would reduce the time the FLNG would need to be at the reservoir, thereby reducing the operating costs of the vessel. So, for example, if the production capacity advantage is 15%, this would mean a vessel to be on station 20 years instead of approx. 23 years, thus reducing the operating costs accordingly. Likewise, any arrangements made to finance the project can be settled earlier thus reducing the financing costs.

The following chapter summarises the findings and conclusions of the research, presents a statement of contribution made to the body of knowledge in the subject area and recommends further post-doctoral work. Finally, the fulfilment of the required learning outcomes is demonstrated by reference to the relevant areas of research and the professional career of the Author.

CHAPTER 8.0

CONCLUSIONS, CONTRIBUTION & RECOMMENDATIONS

8. CONCLUSIONS, CONTRIBUTION & RECOMMENDATIONS

8.1. Conclusions

"Can the concepts underpinning seawater intake systems on FPSO vessels be extended to the design of intake systems with the high volume and low temperature seawater requirements of FLNG vessels?"

The main conclusion from this research is that the concepts underpinning the field proven seawater intake systems on FPSO vessels can be extended to the design of seawater intake systems for the high volume and low temperature seawater requirements of an FLNG vessel.

By using field proven concepts, the risks associated with untested technological advancements in the field are mitigated. In effect, this also means that the proposed solution can be manufactured and installed, recovered and inspected using existing and proven techniques and, additionally, established logistics for handling and transportation can be adopted.

This conclusion has been reached by answering the research sub questions:

❖ *What are the additional seawater requirements of FLNG vessels?*

The literature review highlighted that high volumes of seawater were a key requirement for the cooling processes onboard an FLNG vessel with a volumetric requirement up to 50,000m^3/hr. It was found that for each degree centigrade cooler the seawater, the production capacity of the processing facilities improved by between 0.6-1.0%. A review of the ocean temperature profiles suggested that if seawater could be reached and imported from beyond the thermoclines at approximately 500m, the seawater temperature could be between 15-20°C cooler than the surface water which could provide an increase in production capacity of between 9-20%.

When compared to the seawater requirements of an FPSO vessel, which are typically 6,000m^3/hr from depths of up to 120m where the seawater is approximately 5-8°C cooler than the surface water, it was found that the additional seawater requirements of an FLNG in terms of increased volume and reduced temperature are significant.

Based on these findings, a large bore, deep seawater intake riser capable of reaching and importing seawater from depths of 500m was investigated further.

❖ *What is the optimum configuration for the proposed solution?*

A free-hanging cantilever riser is the most common method currently employed for importing seawater on FPSO vessels, albeit in lower volumes and from shallower depths. Using this same field proven concept, various configurations of material combinations were examined for a 40"NB x 500m free-hanging cantilever riser to determine the most suitable in terms of stability, functionality and loadings. By comparing a number of desirable parameters, the optimum configuration was identified which was a hybrid assembly consisting of (from the upper end):

- 115m x Rubber Flexible Pipe Sections
- 253m x HDPE Pipe Sections
- 23m x Rubber Flexible Pipe Sections
- 103.5m x Steel Pipe Sections.
- 5.5m x Strainer

Two diameters of the selected configuration, namely 40"NB & 60"NB were then subject to further analysis.

❖ *Does the proposed solution have sufficient strength and fatigue capabilities?*

Firstly, through documentary analysis, numerical modelling and material testing, the physical, mechanical and fatigue properties of the material elements under consideration were investigated which highlighted the following:

Flexible Rubber Pipe

- The tensile strength of the textile yarn used for the flexible pipe reinforcement is reduced during the vulcanisation process

- Usable SN curves were developed for the textile yarn (post vulcanisation) through a recognised statistical analysis of cyclic testing results

- Compression testing and tensile testing of the rubber compound indicated that the material stiffness was non-linear, which contradicts the linear model assumption suggested by ASTM D1415.

- Finite Element Analysis (FEA) software can be used to model the composite structure of a flexible rubber pipe section and tune it such that the physical

characteristics and behavioural response provide good correlation with the actual manufactured product.

- The FEA highlighted that the bending stiffness of the flexible rubber pipe was dominated by the rubber stiffness

- A flexible rubber pipe with textile yarn reinforcement has better fatigue characteristics than the same flexible rubber pipe reinforced with steel cord.

- A flexible rubber pipe with steel cord reinforcement requires less reinforcement material the same flexible rubber pipe reinforced with textile yarn resulting in a smaller outside diameter. It therefore has less rubber making is less stiff and, for the same reason, lighter than the textile reinforced flexible pipe.

- The FEA of the flexible rubber pipe provided stress factors for use in the fatigue analysis of the composite structure

HDPE Sections

- There is limited availability of fatigue data for HPDE PE100 parent pipe and more specifically for HDPE PE100 butt fusion welds

- The type of fatigue test method contributes to the fatigue life predictions of the HDPE parent pipe and HDPE butt fusion welds

- For the conditions under consideration, the test frequency, the R ratio and the test temperature of the HDPE fatigue testing has limited effect on the outcome of the test data

- The HDPE butt fusion weld has similar tensile strength as the HDPE parent pipe

- The HDPE butt fusion weld has a lower fatigue life than the HDPE parent pipe

- An attempt is made to determine the stress intensification factors associated with HDPE butt fusion welding versus HDPE parent pipe.

- At lower stress amplitudes, HDPE butt fusion welds subject to bending tend towards a similar fatigue life as parent pipe subject to bending

- At lower stress amplitudes, HDPE butt fusion welds subject to bending diverge from the fatigue life of parent pipe subject to axial loading

- Removal of the bead from the fusion butt weld increases the fatigue life of the joint

- Immersion in seawater improves the fatigue life of HDPE

Steel pipe

- It was found that recognised industry codes and guidelines provided comprehensive material and fatigue data.

Secondly, through documentary analysis and numerical modelling, the mechanics of the selected configuration was investigated which highlighted the following:

- The strength of the proposed solution is sufficient to accommodate the most likely peak loads the system would encounter during service

- The magnitude of the loads induced into the vessel hull at the connection point indicate that the field proven hang-off arrangement used on FPSO vessels can be scaled up accordingly

- The fatigue life of the proposed solution exceeded the typical service life of an FLNG vessel

- Vortex Induced Vibration due to ocean currents is a main contributor to fatigue damage within the system.

- The analysis suggests that the VIV excitation zone for the free-hanging cantilever is in the lower region of the riser.

- The VIV response frequency of the proposed solution is within the material cyclic test frequencies.

- At certain current speeds, the steel pipe sections become excited and exhibit the lowest fatigue life

- Replacing a number of steel sections with flexible rubber pipe sections dampens the riser and mitigates the fatigue damage in the steel pipe sections indicating that the proposed solution can be 'tuned'.

- By mitigating the VIV in the steel pipe sections, the HDPE butt fusion welds have the lowest fatigue life in the proposed solution

- A potential solution is provided to protect the HDPE butt fusion weld and thus increase the fatigue life of the system.

- Increasing the length of the proposed solution improves the fatigue life whereas shortening it reduces the fatigue life.

- Pending the current speed and distribution, the geographical location of the FLNG can affect the fatigue life of the proposed solution

- For the geographical locations considered, the size of the vessel typically used within the industry has limited influence on the strength of the system, the loads induced into the hull or the fatigue life.

- For the flow rates considered, it is unlikely that internal fluid flow of the aspirating cantilever will affect the stability or fatigue life of the system

- Dynamic amplification due to VIV and the wake effect of the system has been considered and estimate made of spacing to avoid interference between to risers in tandem.

❖ *Are the flow characteristics of the proposed solution fit for purpose?*

Analysis of the flow of seawater through the SWIR provided indicative pressure loss and temperature gain characteristics for the proposed solution, both of which were validated using two different techniques and found to provide close correlation.

Pressure losses were calculated for a range of flow rates, including a number of sensitivities with respect to water temperature and the effect of internal roughness due to marine growth or wear. The range of pressure losses were of an acceptable magnitude generally specified by the pump vendor and although the water temperature effect was negligible, the internal roughness was found to have a non-negligible effect pending the roughness value for which provision should be made during design and pump selection.

Similarly, the temperature gain of the seawater inside the SWIR was calculated for a range of flow rates and found to be mostly negligible. However, once the flow rate was reduced to the point where the seawater velocity through the SWIR was in the region of <0.2m/s, the increase in temperature gain became very steep, which should be given due consideration during process design scenarios.

The flow analysis demonstrates that the proposed solution can effectively import cold seawater.

❖ *Is the proposed solution economically viable?*

Using known and published data for current FLNG vessels either in operation or under construction, the financial advantage of importing colder water from depth using the project specific SWIR was demonstrated and which is further validated by virtue of the fact that the three projects considered have all invested in sea water intake risers for this purpose, albeit from shallower depths.

Using the same data for each of these projects, the SWIR was extended to 500m and the associated installation and maintenance costs incorporated, as were the failure mitigation costs developed from an FMEA.

A number of scenarios were explored which indicated that there is a definite economic advantage for the proposed solution in terms of increased production, and therefore annual revenue from the FLNG, which demonstrated that the lifetime cost of the SWIR would be recovered early in the production phase.

8.2. Contribution

The ethos of the Professional Doctorate is to make a research-based contribution to practice. As an experienced practitioner in the field, the authors wealth of knowledge that contributes to the research within this report, and to the existing body of knowledge, has been achieved through involvement with the community of practice in the subject area on a day to day basis over many years.

The contribution from this research is a solution that offers a significant technological advantage for free-hanging cantilever seawater intake systems in the field, enabling high volumes of seawater to be imported from depths not yet achieved whilst accommodating the loads induced by the environmental conditions and minimising the loads induced into the hull of the vessel.

Furthermore, the solution is based on the concepts of a field proven system, thereby limiting the risks associated with untested technological advancements.

The findings of this research enable the process efficiencies of FLNG vessels to be greatly enhanced thus contributing to the more efficient extraction of a cleaner fuel which, in a world with ever increasing energy demands, is critical to the global economy.

The novelty of the research is demonstrated by two successful patent applications, one in relation to the improved features of existing seawater intake riser systems and the other in relation to the use of multiple material elements for a hybrid seawater intake riser as is presented within this report. Both patents have been examined and granted in five jurisdictions, namely, Europe, Japan, China. South Korea and the USA.

8.3. Recommendations

Although this Doctoral Report has addressed the research question and sub-questions set out at the beginning of the project, it has also identified a number of areas where further work is recommended to strengthen the body of knowledge in this subject area, namely;

- **VIV**: The analysis undertaken suggested that, in a free hanging cantilever riser, the VIV excitation zone is at the lower region of the structure. It is recommended that more analysis is undertaken in relation to this as this may enable approximations of VIV response to be made.

- **Flexible Rubber Pipe**: It is recommended that further FEA is conducted on a range of diameters that may be considered for this application. This will provide the relevant data for the performance strength and fatigue calculations for this element. Although the research has focussed on the strength and fatigue capabilities of the textile reinforcement, it is recommended that the fatigue capabilities for the rubber compound under bending are further investigated.

- **HDPE**: A bespoke test programme is recommended for the HDPE pipe and butt fusion welds proposed for these applications. As a minimum, the test programme should consider fatigue testing, ageing tests, surface roughness measurement etc. to provide a reliable data set for the performance, strength and fatigue calculations for the system.

- **Textile Yarn**: It is recommended that more research is conducted into the degradation of the polyester textile yarn caused by the heat treatment process used during the manufactured of the flexible pipe. Although it is understood to be due to the degradation of the outer filament layers, further research may enable the mechanism to be identified and the decrease in strength predicted.

- **Rubber Compound**: Further stiffness testing of the rubber compound is recommended across a range of strains both in compression and tension. This will provide a more accurate data set for modelling and predicting the behaviour of the flexible rubber pipe in the application. Although the research has focussed on the strength and fatigue capabilities of the textile reinforcement, it is recommended that the fatigue capabilities for the rubber compound under bending are also investigated.

REFERENCES

Abdelghany, S. M., Ewis, K. M., Mahmoud, A. A. & Nassar, M. M., 2015. Vibration of a circular beam with variable cross sections using differential transformation method. *Journal of Basic and Applied Sciences,* Volume 4, pp. 185-191.

Adams, T. M., Munson, D., Nickholds, S. & Andrasik, J., 2014. *Determination of updated fatigue properties of PE4710 cell classification 445574C high density polyethylene.* Anaheim, ASME.

Al-Ansari, D. L. S., 2012. Calculating of Natrual Frequency of Stepping Cantilever Beam. *International Journal of Mechanical & Mechatronics Engineeirng,* Volume 12, pp. 59-68.

API, 2005. *Design and Analysis of Stationkeeping Systems for Floating Structures,* Washington: s.n.

API, 2013. *API 5L Specification for Line Pipe,* Washington: s.n.

API, 2014. *API RP 17B Recommended Practice for Flexible Pipe,* Washington: API.

API, 2017. *API 17J Specification for Unbonded Flexible Pipe,* Washington: API Publishing.

API, 2018. *API 17K Specification for Bonded Flexible Pipe,* Washington: API Publishing.

ASME, 2004. *ASME B36.10M-2004, Welded and Seamless Wrought Steel Pipe,* New York: s.n.

ASME, 2010. *Process Piping,* s.l.: s.n.

ASME, 2011. *ASME B16.47 Large Diameter Steel Flanges,* New York: s.n.

ASME, 2014. *ASME B31.3 Process Piping,* New York: s.n.

ASTM, 1999. *ASTM D1415-88; Standard Test Method for Rubber Property - International Hardness,* West Conshohocken: s.n.

ASTM, 2002. *ASTM A105 Standard Specification for Carbon Steel Forgings for Piping Applications,* West Conshohocken: s.n.

ASTM, 2013. *ASTM F714 Standard Specification for Polyethylene (PE) Plastic Pipe (SDR-PR) Based on Outside Diameter,* West Conshohocken: s.n.

ASTM, 2014. *ASTM Standard D3350 Standard Specification for Polyethylene Plastics Pipe and Fittings Materials.* West Conshohocken: s.n.

ASTM, 2015. *ASTM A106 Standard Specification for Seamless Steel Pipe for High-Temperature Service,* West Conshohocken: s.n.

ASTM, 2015. *ASTM E739 Standard Practice for Statisical Analysis of Linear or Linearised Stress-Life and Strain-Life Fatigue Data,* West Conshohocken: s.n.

Attanasi, E. D. & Freeman, P. A., 2013. *Role of Stranded Gas in Increasing Global Gas Supplies,* Reston: US Geological Survey.

Baarholm, G. S., Larsen, C. M. & Lie, H., 2005. Reduction of VIV using suppression devices - An empirical approach. *Marine Structures,* Volume 18, pp. 489-510.

Bahtui, A., 2008. *Development of a Constitutive Model to Simulate Unbonded Flexible Riser Elements,* London: Brunel University.

Baraniuk, C., 2018. *The battle of the gas-sucking mega giants is set to begin.*
[Online]
Available at: http://www.bbc.co.uk/news/business-44003521
[Accessed 22 May 2018].

Becetel, 2009. *Determination of the Notch and Fatigue Resisitance of PE100 HDPE Pipe,* Melle: (Commercially Sensitive - not publicly available).

Bergstrom, G., Nilsson, S. & Lindqvist, L., 2004. *The influence from pipe surface, weld beads and protective skins on long term failure times for PE butt fusion joints,* Sweden: SP Swedish National Testing and Research Institute.

Bharathan, D., 2011. *Staging Rankine Cycles Using Ammonia for OTEC Power Production,* Springfield: National Technical Information Service.

Billah, K. Y. & Scanian, R. H., 1991. Resonance, Tacoma Narrows bridge failure and undergraduate physics textbooks. *American Journal of Physics,* 59(2), pp. 118-124.

Blaxter, L., Hughes, C. & Tight, M., 2001. *How to Research.* 2nd ed. Buckingham: Open University Press.

Blevins, R. D., 2001. *Flow-Induced Vibration.* 2nd ed. Florida: Kreiger.

Bluewater, 2013. *What is an FPSO?.* [Online]
Available at: http://www.bluewater.com/fleet-operations/what-is-an-fpso/
[Accessed 13 August 2014].

Bourner, T., Bowden, R. & Laing, S., 2001. Professional Doctorates in England. *Sudies in Higher Education,* 26(1), pp. 65-83.

Bourrieres, F.-J., 1939. *Sur un phenomene d'oscillation auto-entretenue en mecanique des fluides reels,* Paris: Publications Scientifiques et Techniques du Ministere de l'Air.

Boyatzis, R. E., 1998. *Transforming qualitative information: Thematic analysis and code development.* London: SAGE Publications.

Brandt, D. M., Morooka, C. K. & Guilherme, I. R., 2008. *Automated System for the Study of Environmental Loads Applied to Production RIsers.* Rio de Janeiro, Internaional Conference of Engineering Optimzation.

Brogden, S., 2000. *The effects of fatigue loading on polyvinylchloride and polyethylene materials for use in pipeline systems,* Manchester: The Manchester Metropolitan University.

Brown, M. G., 1998. *FPSO Technology Applied to OTEC.* [Online]
Available at: http://www.clubdesargonautes.org/otec/vol/vol9-2-1.htm
[Accessed 28 December 2017].

BSI, 1991. *BS5760-5: 1991 Reliability of systems, equipment and components - Part 5: Guide to failure modes, effects and criticality analysis (FMEA and FMECA),* London: BSI.

BSO, 2017. *Professional Doctorate in Osteopathy,* s.l.: The British School of Osteopathy.

Burgess, R. G., 1990. *In the Field; An Introduction to Field Research.* 4th ed. London: Routledge.

Cao, P. et al., 2015. *OTC-25917-MS: Advancing Cold Water Intake Riser Design through Model Test.* Houston, Offshore Technology Conference.

Channell, A. D. & Cawood, M. J., 1989. *Fatigue in PC 002-50,* Grangemouth: BP Chemicals International.

Chaudhury, G. & Chakkarapani, V., 2014. *Innovative Caisson Type Seawater Intake Riser Design Concept for FLNG.* Houston, Society of Naval Architects and Marine Engineers, pp. 1-10.

Chen, H., 2015. *Petronas outlines its FLNG strategy.* [Online]
Available at: http://www.lngworldshipping.com/news/view,petronas-outlines-its-flng-strategy_38997.htm
[Accessed 3 Oct 2016].

Connor, C. O., 2015. *Polyethylene Pipeline Systems - Avoiding the Pitfalls of Fusion Welding,* Loughborough: DNVGL.

Corneliussen, M. & Samnoy, E., 2015. *Near Shore FLNG Concept Evaluation,* Trondheim: NTNU.

Craig, I., 2014. *Feasibility Study of 500m Seawater Intake System,* Hamburg: s.n.

Craig, I., 2016. *Review of Bonded Rubber Flexible Hose Design Codes and Guidelines in Relation to Sea Water Intake Risers on FPSO Vessels.* Kuala Lumpur, Offshore Technology Conference.

Craig, I. & Hopley, M., 2016. *e-mail 15.04.16.* Middlesbrough: Intertek.

Cui, H. & Tani, J., 1996. Effect of boundary conditions on the stability of a cantilever pipe discharging and aspirating fluid. *JSME International Journal,* Volume 39, pp. 20-24.

Davies, P., Bunsell, A. R. & Chailleux, E., 2010. Tensile fatigue behaviour of PBO fibres. *Journal of Materials Science,* 45(23), pp. 6395-6400.

Delft University of Technology, 2014. *Mooring of a Floating Container Terminal.* [Online]
Available at:
http://www.offshoremoorings.org/moorings/2007/Group%20A/Group%20A%20-%20Floating%20Container%20Terminal/pages/concepts.html
[Accessed 3 August 2014].

DIN, 2012. *DIN 8075 Polyethylene (PE) pipes; General quality requirements and testing,* Berlin: s.n.

Djelbi, A. et al., 2014. Uniaxial Fatigue of HDPE-100 Pipe. *Engineering, Technology & Applied Science Research,* 4(2), pp. 600-604.

Djelbi, A. et al., 2015. Fatigue life prediction and damage modelling of High-density polyethylene under constant two-block loading. *Procedia Engineering,* Volume 101, pp. 2-9.

DNV, 2009. *DNV-RP-F203; Riser Interference,* Oslo: s.n.

DNV, 2010. *DNV-RP-F204; Riser Fatigue,* Oslo: Det Norske Veritas.

DNV, 2011. *DNVRP-A203 Qualification of New Technology,* Oslo: Det Norske Veritas.

DNV, 2014. *DNV-RP-C205; Environmental Conditions and Environmental Loads,* Oslo: s.n.

DNVGL, 2016. *DNVGL-RP-C203: Fatigue Design of Offshore Steel Structures,* Oslo: s.n.

Duncan, A., 2016. *FLNG: Costs and cost drivers.* [Online]
Available at: http://www.gastechnews.com/lng/flng-costs-and-cost-drivers/
[Accessed 03 Oct 2016].

DVS, 2015. *DVS 2205-1; Design calculations for containers and apparatus made from thermoplastics; Characteristic Values,* Dusseldorf: s.n.

Earthguide, 2013. *General Circulation of the Sea.* [Online]
Available at:
http://earthguide.ucsd.edu/virtualmuseum/Glossary_Climate/gencircocean.html
[Accessed 05 September 2014].

EIA, 2016. *World energy demand and economic outlook.* [Online]
Available at: https://www.eia.gov/forecasts/ieo/world.cfm
[Accessed 8 October 2016].

Emstec, 2013. *Data Book: FPSO Cidade de Ilhabela,* Oststeinbek: (Commercially Sensitive - not publicly available).

Emstec, 2014. *Hose Data,* Oststeinbek: (Commercially Sensitive - not publicly available).

Energy Information Administration, 1999. *Natural Gas 1998 : Issues and Trends,* Washington: Energy Information Administration.

Eni, 2017. *Job Specification for Design - Sea Water Intake Risers Package,* Rome: Eni S.p.A.

ESDU, 2010. *ESDU 80025 Mean forces, pressure and flow field velocities for circular cylindrical strucures: single cylinder with two dimensional flow,* s.l.: IHS Global Ltd..

Excelplas, 2015. *Butt Fusion Welds.* [Online]
Available at: www.polypipetesting.com.au/butt-fusion-welds/
[Accessed 10 Feb 2018].

Falco, M., Fossati, F. & Resta, F., 1999. *On the vortex induced vibration of submarine cables: Design optimisation of wrapped cable for controlling vibrations.* Trondheim, 3rd International Symposium on Cable Dynamics.

Finn, A. J., 2009. Are Floating LNG Facilities Viable Options. *Hydrocarbon Processing,* Volume July 2009, pp. 31-38.

FRAMO, 2018. *Framo oil and gas pumping systems.* [Online]
Available at: https://www.framo.com/globalassets/pdf-files/fra_010_oil__gas_pumping_systems_korr193.pdf
[Accessed 13 March 2018].

Fujarra, A. L. C., Pesce, C. P., Flemming, F. & Williamson, C. H. K., 2001. Vortex Induced Vibration of a Flexible Cantilever. *Journal of Fluids and Structures,* Volume 15, pp. 651-658.

Giacobbi, D. B., 2007. *A numerical and experimental study of the dynamics of aspirating cantilever pipes: BEng(Hons) Thesis.* Montreal: McGill University.

Giacobbi, D. B., 2010. *The dynamics of aspirating cantilevered pipes and pipes conveying variable fluid density: M.Eng Thesis.* Montreal: McGill University.

Giacobbi, D. B., Rinaldi, S., Semler, C. & Paidoussis, M. P., 2012. The dynamics of a cantilevered pipe aspirating fluid studied by experimental, numerical and analytical methods. *Journal of Fluids and Structures,* Volume 30, pp. 73-96.

Giacobbi, D. B., Semler, C. & Paidoussis, M. P., 2008. *Numerical fluid-structure interaction study of a cantilevered pipe discharging or aspirating fluid via a computational fluid dynamics and finite elements model.* Stirlingshire, Scotland, Civil Comp Press, p. 48.

Harder, T. & Lee, L. H., 2009. Bacterial Adhesion and marine fouling. In: C. Hellio & D. Yebra, eds. *Advances in marine antifouling coatings and technologies.* Cambridge: Woodhead Publishing Ltd, pp. 113-131.

Heselmans, J., Buijs, N. W. & Isaac, E., 2011. *Sacrificial anodes for protection of seawater pump caissons against galvanic corrosion.* Houston, NACE.

Hill, D. J., Wilson, K. A. & Headford, A. L., 2001. *Butt Fusion Welding of Large Diameter / Thick Walled Pipes.* Munich, Proceeding of Plastic Pipes XI.

Howell, G. B., Duggal, A. S., Heyl, C. & Ihonde, O., 2006. *Spread Moored or Turret Moored FPSO's for Deepwater Field Developments.* Houston, Offshore West Africa.

Ibrahim, R., 2010. Overview of Mechanics of Pipes Conveying Fluids - Part I: Fundamental Studies. *Journal of Pressure Vessel Technology,* Volume 132, pp. 034001-1 : 034001-32.

Ice Engineering, 2009. *Spread Mooring.* [Online]
Available at:
http://www.offshoremoorings.org/Moorings/2009/Group02_Prabhakar/OffshoreMooringsWEBSITE25sept2009/Spread_Mooring.htm
[Accessed 13 August 2014].

IGU, 2012. *Natural Gas Conversion Pocket Book,* Oslo: IGU.

Intec Engineering BV, 2008. *TRNC Drinking Water Supply Project: Design Basis Final Report,* Delft: Intec (Commercially Sensitive - not publicly available).

Intec Engineering BV, 2010. *TRNC Drinking Water Supply Project : HDPE Pipe Specification,* Delft: Intec (Commercially Sensitive - not publicly available).

Interesting Engineering, 2014. *Prelude FLNG: Largest Ship Hull in the World.* [Online]
Available at: http://interestingengineering.com/worlds-largest-ship-hull-to-be-created/
[Accessed 05 September 2014].

International Paint Ltd, 2010. *Intersleek: Better for the environment. Better for your business,* Gateshead: International Paint Ltd.

International Paint Ltd, 2014. *Intersleek 970: Foul Release Technology,* s.l.: International Paint Ltd.

Intertek, 2015. *Characterisation of a Reinforcing Yarn by Tensile Fatigue Analysis,* Redcar: s.n.

ISO, 2009. *ISO 12162:2009 Thermoplastics materials for pipes and fittings for pressure applications - Classification, designation and design coefficient.* s.l.:International Organization for Standardization.

ITTC, 2011. *Fresh Water and Seawater Properties,* Kgs. Lyngby: ITTC.

Iwan, W. D. & Blevins, R. D., 1974. A model for Vortex Induced Oscillation of Structures. *Journal of Applied Mechanics,* pp. 581-586.

Jahanshahi, E., 2013. *Control solutions for Multiphase Flow: Linear and nonlinear approaches to anti-slug control,* Trondheim: Norwegian University of Science and Technology.

Jamin, S., 2010. *Stability of Thick and Thin Flexible Pipes Subject to Axial Flow: MEng Thesis,* Montreal: McGill University.

Jenkins, A., 2011. Sprinkler Head Revisited: Momentum, Forces and Flows in Machian Propulsion. *European Journal of Physics,* 32(5), pp. 1213-1226.

Jung, D.-h., Kim, H.-j. & Moon, D.-s., 2010. *Dynamics of Large Diameter Riser.* Beijing, Thie International Society of Offshore and Polar Engineers, pp. 240-247.

Kalyanam, S. et al., 2016. *Slow crack growth fracture resistance parameter evaluation for parent and joint HDPE materials.* Indianapolis, SPE ANTEC.

Kalyanam, S. et al., 2015. *A Fracture Mechanics Approach to Service Life Prediction of HDPE Fusion Joints in Nuclear Applications.* Orlando, ANTEC.

Krishnaswamy, P., 2007. *Review of Literature on the use of Polyethylene (PE) Piping in Nuclear Power Plant Safety Releated Class 3 Service Water Systems,* Ohio: Engineering Mechanics Corporation of Columbus.

Kuiper, G., 2008. *Generic Floating LNG: Basic Design Package Sect IV Ch 4 Water Intake Risers,* The Hague: Shell Global Solutions.

Kuiper, G. L. & Metrikine, A. V., 2005. Dynamic stability of submerged, free hanging riser conveying fluid. *Journal of Sound and Vibration,* Volume 280, pp. 1051-1065.

Kuiper, G. L. & Metrikine, A. V., 2008. Experimental investigation of dynamic stability of a cantilever pipe aspirating fluid. *Journal of Fluids and Structures,* Volume 24, pp. 541-558.

Kuiper, G. L., Metrikine, A. V. & Efthymiou, M., 2007. *Experimental investigation of the dynamci behaviour of a water intake riser.* San Diego, OMAE.

Lebret, K., Thabard, M. & Hellio, C., 2009. Algae as marine fouling organisms: adhesion damage and prevention. In: C. Hellio & D. Yebra, eds. *Advances in marine antifouling coating and technologies.* Cambridge: Woodhead Publishing Ltd, pp. 80-112.

Lechat, C., Bunsell, A. R., Davies, P. & Burgoyne, C. J., 2010. *Characterisation of long term behaviour of polyester fibres and fibre assemblies for offshore mooring lines,* Leatherhead: s.n.

Lee, M. et al., 2012. Metamodel-Based Multidisciplinary Design Optimization of a Deep-Sea Manganese Nodules Test Miner. *Journal of Applied Mathematics,* Volume 2012, p. 18.

Lester, S., 2004. Conceptualizing the practitioner doctorate. *Studies in Higher Education,* 29(6), pp. 757-770.

Li, C., 2015. *Dynamic Stress Behavior of Bonded Pipes and Umbilicals,* Trondheim: Norwegian University of Science and Technology.

Lines, C., 2012. *Solving the problem of adhesionto plastics and rubber.* [Online] Available at: http://www.dynetechnology.co.uk/pdfs/bondingtoplasticandrubber.pdf [Accessed 11 Nov 2014].

Lloyd's Register, 2014. *Studying the finite elements of flexible pipe.* [Online] Available at: http://www.lr.org/en/news-and-insight/articles/studying-the-finite-

elements-of-flexible-pipe.aspx
[Accessed 08 01 2018].

Longuet-Higgins, M. S., 1983. On the joint distribution of wave periods and amplitudes in a random wave field. *Mathematical and Physical Sciences,* Volume 389, pp. 241-258.

Lowe, D., Powell, T. & Starkey, P., 2006. *Optimisation of Butt Fusion Welding (and Testing) of Thick Walled PE100,* UK: Bodycote PDL.

Luppi, A., Saunier, C. & Mayau, D., 2014. *FLNG Cold Sea Water Intake Risers.* Kuala Lumpur, Offshore Technology Conference, pp. 1-22.

Marczyk, G., DeMatteo, D. & Festinger, D., 2005. *Essentials of Research Design and Methodology.* Hoboken: John Wiley & Sons.

Marley, 2010. *HDPE Buttwelding Principles,* Nigel: Marley Pipe Systems.

Marley, 2016. *Joining HDPE Pipe: Traditional & Modern Methods.* [Online]
Available at: http://marleypipesystems.co.za/marley-pipe-news/457-joining-hdpe-pipe-traditional-modern-methods
[Accessed 10 Feb 2018].

Maxwell, T. W., 2008. *Presentation at UK DBA Conference.* Bradford, s.n.

Maxwell, T. W., Hickey, C. & Evans, T., 2004. *Professional Doctorates: Working Towards Impact: Proceeding of the 5th Professional Doctorates Conference.* Geelong, Research Institute for Professional & Vocational Education & Training, Deakin University.

McIver, D. B., 1995. A method of modelling the detailed component and overall structural behaviour of flexible pipe sections. *Engineering Structures,* 17(4), pp. 254-266.

Meng, S. & Kajiwara, H., 2013. *VIV Analysis of a Cantilevered Pipe Discharging Fluid with a Nozzle in the Sea.* Osaka, The International Federation of Automatic Control.

NORSOK, 2006. *NORSOK standard P-001,* Lysaker: Standard Norge.

NORSOK, 2007. *N-003 Actions and action effects,* Lysaker: s.n.

Nutter, T., 2014. *Storage and Offloading (FPSO) Units,* Houston: Offshore Magazine.

OE, 2014. 2014 FLNG market worth $12bn. *Offshore Engineer*, 23 May, pp. 178-180.

OE, 2014. Douglas-Westwood looks at FLNG market. *Offshore Engineer*, 8 January.

Office of Science and Technology (OST), 1993. *Realising our potential: A Strategy for Science, Engineering and Technology,* London: Command 2250, HMSO.

Offshore Energy Today, 2017. *Eni Close $4.7 billion Coral South FLNG project financing.* [Online]
Available at: https://www.offshoreenergytoday.com/eni-closes-4-7-billion-coral-south-flng-project-financing/
[Accessed 18 March 2018].

Open Seas Instrumentation, 2014. *STABS - Sidescan Towed Acoustic Body System.* [Online]
Available at: http://openseas.com/portfolio/stabs-sidescan-towed-acoustic-body-

system/
[Accessed 28 December 2017].

Orcina, 2014. *Orcina... home of Orcaflex.* [Online]
Available at: http://www.orcina.com/
[Accessed 15 March 2014].

Paidoussis, M., 1998. *Fluid-Structure Interactions: Slender Strucures and Axial Flow (Volume 1).* 1st ed. London: Academic Press Ltd.

Paidoussis, M., 2005. Some unresolved issues in fluid-strucure interactions. *Journal of Fluids and Structures,* Volume 20, pp. 871-890.

Paidoussis, M. P., 1999. Aspirating pipes do not flutter at infinitesimally small flow. *Journal of Fluids and Structures,* Volume 13, pp. 419-425.

Paidoussis, M. P., 2014. *Fluid-Structure Interactions: Slender Structures and Axial Flow (Volume 1).* 2nd ed. Oxford: Academic Press.

Paidoussis, M. P. & Luu, T. P., 1985. Dynamics of a pipe aspirating fluid such as might be used in ocean mining. *ASME Journal of Energy Resources and Technology,* Volume 107, pp. 250-255.

Paidoussis, M. & Tetreault-Friend, M., 2009. Aspirating Cantilevers and Reverse Sprinklers. *American Journal of Physics,* Volume 77, pp. 349-353.

PDL, 667-002:2015. *40" Suction Hose Fatigue Assessment; Global Analysis,* Hexham: s.n.

PDL, 667-003:2015. *40" Suction Hose Fatigue Assessment; Local Analysis,* Hexham: s.n.

PDL, 727-001:2015. *40" Suction Hose with Steel Reinforcement Fatigue Analysis; Local Analysis,* Hexham: PDL Solutions (Europe) Ltd.

PDL, 727-002:2015. *40" Suction Hose with Steel Reinforcement Fatigue Assessment; Global Analysis,* Hexham: PDL Solutions (Europe) Ltd.

Petrobras, 2010. *Campos Basin : Metocean Data,* Rio de Janeiro: Petrobras.

Petronas, 2013. *Seawater Hose Basis of Design,* Kuala Lumpur: Petronas.

Petronas, 2016. *First Gas for Petronas First FLoating LNG Facility, PFLNG Satu.* [Online]
Available at: http://www.petronas.com.my/media-relations/media-releases/Pages/article/FIRST-GAS-FOR-PETRONAS'-FIRST-FLOATING-LNG-FACILITY,-PFLNG-SATU.aspx
[Accessed 18 March 2018].

Pettersen, J. et al., 2013. *Technical and Operational Innovation for Onshore and Offshore Floating LNG.* Houston, Gas Technlogy Institute, pp. 1-12.

Pipeline & Gas Journal, 2014. Shell's First FLNG Readied for Western Australia Operations. *Pipeline & Gas Journal,* Issue April 2014, p. 96.

Powell, 2002. *Sodium Hypochlorite General Information Handbook,* St Louis: Powell.

Powell, C. & Webster, P., 2012. *Copper Alloys for Marine Environments,* Hemel Hempstead: s.n.

PPI, 2000. *TR-14 2000 Water Flow Characterisitcs of Thermoplastic Pipe,* Wayne, NJ: PPI.

PPI, 2004. *Engineering Properties of Polyethylene.* Wayne, NJ: Plastics Pipe Institute.

PPI, 2008. *Handbook of Polyethylene Pipe.* 2nd ed. Irving: Plastics Pipe Institute.

PPI, 2009. *TN-27: Frequently Asked Questions HDPE Pipe for Water Distribution and Transmission Applications,* Wayne, NJ: s.n.

PPI, 2014. *TN-28/2014 Guide to Differences in Pressure Rating PE Water Pipe using the ASTM/PPI and ISO Methods,* Irving TX: s.n.

Prastianto, R. W., 2009. Hydrodynamic Forces acting on Two Flexible Free-hanging Cantilevers in Tandem Configurations due to Cross-flows. *The Journal of Technology and Science,* 20(4), pp. 162-168.

Prastianto, R. W., Otsuka, K. & Ikeda, Y., 2009. Vortex Induced Vibration of a Flexible Free Hanging Circular Cantilever. *ITB Journal of Engineering Science,* 41(2), pp. 111-125.

Project Connect, 2011. *Project Packages.* [Online]
Available at: http://www.projectconnect.com.au/uploads/671673369379.pdf
[Accessed 11 August 2014].

Rahmati, M. T., Norouzi, S., Bahai, H. & Alfano, G., 2017. Experimental and numerical study of structural behavior of a flexible riser model. *Applied Ocean Research,* Volume 67, pp. 162-168.

Rangel, L., 2016. Floating prospects. *Offshore Engineer*, June, pp. 24-26.

Rinaldi, S., 2009. *Experiments on the dynamics of cantilevered pipes subjected to internal and/or external flow: M.Eng Thesis,* Montreal: McGill University.

Robinson, C., Steinberg, D. K. & Anderson, T. R., 2010. Mesopelagic zone ecology and biochemistry - a synthesis. *Deep-Sea Research,* II(57), pp. 1504-1518.

Robson, C., 2002. *Real World Research.* 2nd ed. Oxford: Blackwell Publishing.

Rogez, F., 2012. *Deep large seawater intakes: a common soution for Floating LNG in oil & gas industry and OTEC in marine renewable energy.* Dublin, Geocean, pp. 1-6.

Saevik, S., 2011. Theoretical and experimental studies of stresses in flexible pipes. *Computers and Structures,* Volume 89, pp. 2273-2291.

Sakmar, S. L., 2016. *FLNG: Looking ot the future.* [Online]
Available at: http://www.gastechnews.com/processing-technology/flng-looking-to-the-future/
[Accessed 3 Oct 2016].

Schatzman, L. & Strauss, A. L., 1973. *Field Research: Strategies for a Natural Sociology.* Englewood Cliffs, NJ: Prentice-Hall.

SGS, 2015. *Compressive Test; Report No: SHIN1509042854MR,* Shanghai: s.n.

Shell Australia, 2017. *Prelude in Position.* [Online]
Available at: http://www.shell.com.au/about-us/projects-and-locations/prelude-flng/prelude-e-news/prelude-in-position.html
[Accessed 18 March 2018].

Shell Global, 2014. *Shaping the energy future through innovation.* [Online]
Available at: http://www.shell.com/global/future-energy/shaping-future.html
[Accessed 05 September 2014].

Siemens, 2016. *How to conduct a failure modes and effects analysis (FMEA),* Plano: Siemens.

Songhurst, B., 2016. *Floating Liquefaction (FLNG): Potential for Wider Deployment,* Oxford: The Oxford Institute for Energy Studies.

Sparks, C. P., 2007. *Fundementals of Marine Riser Mechanics.* 1st ed. Oklahoma: Penwell Books.

Stanczak, M., 2004. *Biofouling: It's not just barnacles anymore.* [Online]
Available at: http://www.csa.com/discoveryguides/biofoul/overview.php
[Accessed 23 October 2014].

Statoil, 2010. *Tanzania Block 2 Metocean Design Basis: Metocean RE2010-12,* Stavanger: Statoil ASA (Commercially Sensitive - not publicly available).

Stephens, R. I., Fatemi, A., Stephens, R. R. & Fuchs, H. O., 2001. *Metal Fatigue in Engineering.* 2nd ed. New York: Wiley-Interscience.

Sykes, J., 2012. *Metallurgical Failures in Oil and Gas Pipelines.* Jimbaran, Asia Offshore Energy Conference.

Takahara, A., Yamada, K., Kajiyama, T. & Takayanagi, M., 1981. Analysis of fatigue behavior of high-density polyethylene based on dynamic viscoelastic measurements during the fatigue process. *Journal of Aplied Polymer Science,* 26(4), pp. 1085-1104.

Thilmany, J., 2009. Amazing Analyses. *Mechanical Engineering*, May, pp. 24-27.

Tonatto, M. L. P. et al., 2017. Parametric Analysis of an offloading hose under internal pressure via computational modeling. *Marine Structures,* Volume 51, pp. 174-187.

University of Sunderland, 2015. *AQH-L8 Professional Doctorate Programme Specification.* Sunderland: UOS.

Vance, A., 2013. Ansys is out to simulate the world. *Bloomberg Businessweek*, 11-17 March, pp. 32-34.

Vandiver, J. K., 1983. *OTC 4490 Drag Coefficients of Long flexible Cylinders.* Houston, Offshore Technology Conference.

Wang, Y., Gao, D. & Fang, J., 2016. Longitudinal Vibration Analysis of Marine Riser During Installation and Hangoff in Ultra Deepwater. *CMES,* 111(4), pp. 357-373.

Water UK, 1994. *WIS 4-32-08: Specification for the Site Fusion Jointing of PE80 and PE100 Pipe and Fittings,* London: Water UK.

Water UK, 2016. *WIS 4-32-08: Specification for the Fusion Jointing of Polyethylene Pressure Pipeline Systems using PE80 and PE100 Materials.* London: Water UK.

Waterstone Energy Inc, 2016. *World LNG Estimated Landed Prices: Aug-16.* [Online]
Available at: http://www.ferc.gov/market-oversight/mkt-gas/overview/ngas-ovr-lng-wld-pr-est.pdf
[Accessed 3 Oct 2016].

Websters New World College Dictionaries, 2014. *Websters New World College Dictionary.* 5th ed. Boston: Houghton Miffin Harcourt.

Wilson, K. A., 1995. *Verification of butt fusion weld quality in large diameter PE100 water pipes.* Plastic Pipes IX, Edinburgh, The Institute of Materials.

Wilson, T. & Turaga, U., 2016. *Petronas Starts-Up While Other FLNG Projects Struggle.* [Online]
Available at: http://adi-analytics.com/2016/05/26/petronas-commences-operations-of-worlds-first-flng-while-other-operators-struggle/
[Accessed 3 Oct 2016].

Young, W. C., 1989. *Roark's Formulas for Stress & Strain.* 6th ed. Singapore: McGraw-Hill.

APPENDICES

APPENDIX A – FULFILMENT OF LEARNING OUTCOMES

APPENDIX A – FULFILMENT OF LEARNING OUTCOMES

	Learning Outcomes	How this was achieved	Reference
K1	Deep understanding of the recent developments in their profession nationally and internationally	Literature Review	Chapter 2.0
		Voluntary work as an Assessor with the Institute of Engineering & Technology (IET)	Portfolio [Section 2.0]
		Received a commendation from a Client whilst working as an active practitioner in the field (Project Manager) for the supply of these systems.	Portfolio [Section 2.0]
		Named as an inventor on patents granted in five jurisdictions relating to improvements and development of the research subject.	Portfolio [Section 10.0]
		Publication and presentation of a research paper at an internationally recognised industry conference.	Portfolio [Section 10.0]
		Formation of company and tenure as Technical Director (+6 years) of internationally renowned company supplying these systems into the field.	Portfolio [Section 12.0]
		Formation of company, tenure as Director and independent provider of project management and technical support (+7 years) for these systems into the field	Portfolio [Section 12.0]
K2	Deep understanding of current theoretical frameworks and approaches which have direct relevance to their own professional context	Literature Review	Chapter 2.0
		Understanding and application of Riser Mechanics to research subject.	Chapter 6.0
		Achieved Chartered Engineer status with the Engineering Council	Portfolio [Section 2.0]
		Named as an inventor on patents granted in five jurisdictions relating to improvements and development of the research subject.	Portfolio [Section 10.0]

	Learning Outcomes	How this was achieved	Reference
K2		Publication and presentation of a research paper at an internationally recognised industry conference.	Portfolio [Section 10.0]
		Performing technical analyses and submitting reports for peer review for systems supplied to live projects in the field	Portfolio [Section 11.0]
S1	Make a significant contribution to practice within their chosen field	Development of system, based on proven concepts, for reaching and importing cold seawater from depths not yet achieved for use with next generation of energy recovery vessels (FLNG)	Doctoral Report
		Obtain, collate and analyse field data from systems operating in the field and propose a marine growth mitigation philosophy for use within these systems.	Chapter 4.0
		Review, analysis, establishment and synthesis of properties and characteristics for materials used within these systems.	Chapter 5.0
		Use of empirical, theoretical and numerical modelling techniques to present a novel hybrid intake riser for the importation of high volumes of cold seawater.	Chapter 6.0
		Establishment and grant of two patents relating to the improvement and development of the research subject.	Portfolio [Section 10.0]

	Learning Outcomes	How this was achieved	Reference
S2	Apply theory and research methodology within the workplace, and feel comfortable in integrating different approaches to address "messy" multidisciplinary problems in a rigorous yet practical manner	Development of Research Methodology to align with the Research Aims & Objectives.	Chapter 3.0
		Collate existing data, review test methodology and use numerical modelling techniques to analyse, synthesise and establish material characteristics for use in the research.	Chapter 5.0
		Use empirical, theoretical and numerical modelling techniques to analyse capabilities and functionality of research subject.	Chapter 6.0
S3	Recognise budgetary, political, strategic, ethical and social issues when addressing issues within the workplace	Investigate system redundancy and failure modes and monetarise implications.	Chapter 7.0
		Review costing data from live projects in the field and apply to research subject to present economic argument for the systems.	Chapter 7.0
		Voluntary work as an Assessor with the Institute of Engineering & Technology (IET)	Portfolio [Section 2.0]
		Formation of company and tenure as Technical Director (+6 years) of internationally renowned company supplying these systems into the field.	Portfolio [Section 12.0]
S4	Reflect of their own work, and on themselves, and thus operate as a truly reflective independent practitioner	Relevance of DProf to research subject	Foreword
		Reflective Account of DProf	Portfolio [Section 1.0]
		Formation of company, tenure as Director and independent provider of project management and technical support consultancy (+7 years) for these systems into the field	Portfolio [Section 12.0]

	Learning Outcomes	How this was achieved	Reference
S5	Present and defend an original and coherent body of work which demonstrates, reflects upon, and evaluates the impact upon practice which they have personally made	Doctoral Report Portfolio VIVA	Doctoral Report Portfolio VIVA